Final Technical Report

GRANT # : N00014-00-1-0609
PRINCIPAL INVESTIGATOR : Professor Bruce W. Fouke
INSTITUTION : University of Illinois Urbana-Champaign
GRANT TITLE : The Role of Shipyard Pollutants in Structuring Coral Reef Microbial Communities: Monitoring Environmental Change and the Potential Causes of Coral Disease
AWARD PERIOD : April 15, 2000 – March 31, 2006

OBJECTIVE : The United States Navy operates many military bases in tropical and sub-tropical seas, most of which are surrounded by living coral reefs. Therefore, the long-term effects of naval activity on the health of these reef ecosystems needs to be monitored and evaluated. Our research shows that microbes inhabiting the tissues of healthy and diseased coral are diverse and highly sensitive to environmental change caused by harbor and near-shore naval activity. Our integrated optical, biochemical, molecular, and ecological analyses indicate that: (1) coral tissue $\delta^{34}N$ content is the most sensitive ecological indicator to quantify average sewage concentration with the human enteric bacteria found in the BBD microbial consortium; (2) quantitative correlation of seawater (depth, temperature, pollution, light intensity), coral health (physiology, mucus chemistry, symbiotic zooxanthellae diversity), and coral microbial communities indicate that environmental impact exerts the strongest influence on coral microbes. The long-term goal of this study has been to further develop methods to monitor the diversity and function of coral microbes, quantify the concentration of shipyard pollutants in overlying seawater, and determine their cause-and-effect linkage. Results have permitted the development of microbial screening to permit identification of threatened reef ecosystems impacted by harbor and near-shore activity. This can be used in preservation efforts to quantitatively gauge and mitigate naval impact.

APPROACH: Black band disease (BBD) is one of the most destructive and widespread of the coral diseases. It is manifested as a narrow 0.1 to 1.5-cm wide bacterial mat that migrates as quickly as 1 cm/day from top-to-bottom across infected corals, killing healthy tissue and leaving behind dead skeletal surfaces (Fig. 1A).

A. 

B. 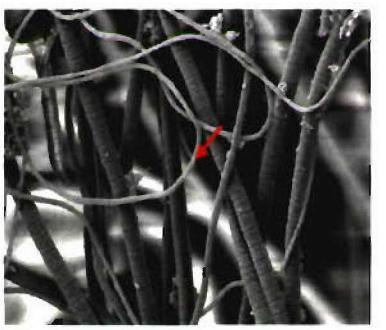

Figure 1. A. *In situ* photograph of BBD on the brain coral *D. strigosa* (0.5 m diameter). B. ESEM of the BBD mat showing the dominant filamentous cyanobacteria (clone CD1C11, putative *Phormidium corallyticum*) and putative *Beggiatoa* (arrow). Modified from Frais-Lopez et al. (2002, 2004a).

Because BBD preferentially infects massive framework building corals, the aftermath of the disease has a profound influence on coral reef ecosystems. The BBD microbial mat is dominated by a large filamentous cyanobacterium (Fig. 1B) that structurally supports the BBD mat and houses a complex, high-diversity community of bacteria. The approach of this study has been to: (1) apply optical analyses, standard culturing techniques, and new culture-independent molecular techniques to determine the phylogenetic and functional diversity of microbial communities inhabiting healthy, diseased, and dead scleractinian corals; (2) create an ecological context for these studies, by conducting the work in specific pristine, at risk, and heavily impacted portions of a reef ecosystem; (3) quantitatively correlate results with chemical analyses of seawater immediately overlying coral colonies and coral health and physiology; and (4) conduct multivariate statistical analyses of these microbial, chemical, and ecological data sets to identify linkages between harbor activity, microbial ecology and coral disease.

ACCOMPLISHMENTS: This ONR grant has resulted in 10 published manuscripts in top tier internationally peer-reviewed research journals, including *Applied and Environmental Microbiology*, *Coral Reefs*, *Bulletin of Marine Science*, and *Environmental Microbiology*. In addition, seven B.Sc. undergraduate students, four M.Sc. graduate students, one Ph.D. graduate students, and three postdoctoral researchers have been supported to work on this project. Research results were presented at 7 international coral research meetings (including the International Coral Reef Congress), as well as in 35 invited lectures at universities around the world (including M.I.T., U.C. Berkeley, Columbia, and Texas).

Our studies of the microbial ecology and distribution of coral BBD have been centered on the reefs of the Caribbean island of Curaçao, Netherlands Antilles (Fig. 3A), and the Indo-Pacific island of New Britain, Papua New Guinea. Our experimental results have lead us to develop the working hypothesis that anthropogenic mucolytic bacteria derived from sewage and bilge dumping: (1) alter coral mucus; (2) facilitate polymicrobial coral disease infections; and (3) impact energy and nutrient cycling of the entire coral reef ecosystem. The consistent spatial advance of a moving "front" of BBD mat created a geometric frame of reference within which to analyse infection development according to: (1) cm-to-meter scale stages of pre-infection, early infection, middle infection, late infection, and post-infection events (Fig. 2A); and (2) micron-to-millimeter scale structure and microorganism distributions across the leading edge of the BBD mat (Fig. 2B). Furthermore, this top-to-side context allowed km-scale comparisons of coral heads living in different sites along a given reef track (i.e. corals from different geographic sites were categorized according to the stage of BBD progression).

A.

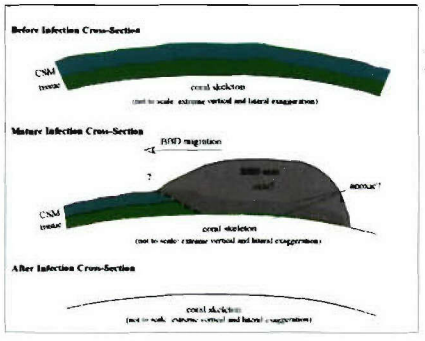

B.

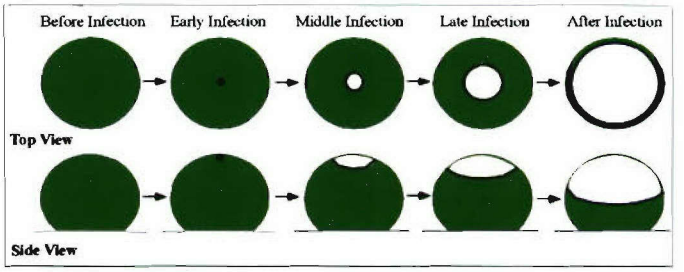

Figure 2. Theoretical sketches of the BBD mat "front" in cross-section (A) top and (B) side.

REPORT DOCUMENTATION PAGE

Form Approved
OMB No. 0704-0188

The public reporting burden for this collection of information is estimated to average 1 hour per response, including the time for reviewing instructions, searching existing data sources, gathering and maintaining the data needed, and completing and reviewing the collection of information. Send comments regarding this burden estimate or any other aspect of this collection of information, including suggestions for reducing the burden, to Department of Defense, Washington Headquarters Services, Directorate for Information Operations and Reports (0704-0188), 1215 Jefferson Davis Highway, Suite 1204, Arlington, VA 22202-4302. Respondents should be aware that notwithstanding any other provision of law, no person shall be subject to any penalty for failing to comply with a collection of information if it does not display a currently valid OMB control number.
PLEASE DO NOT RETURN YOUR FORM TO THE ABOVE ADDRESS.

1. REPORT DATE *(DD-MM-YYYY)*	2. REPORT TYPE	3. DATES COVERED *(From - To)*
June 31, 2006	Final Technical Report ONR 341	April 15, 2000 - March 31, 2006

4. TITLE AND SUBTITLE
The Role of Shipyard Pollutants in Structuring Coral Reef Microbial Communities: Monitoring Environmental Change and the Potential Causes of Coral Disease

5a. CONTRACT NUMBER

5b. GRANT NUMBER
N00014-00-1-0609

5c. PROGRAM ELEMENT NUMBER

6. AUTHOR(S)
(PI) Bruce W. Fouke

5d. PROJECT NUMBER

5e. TASK NUMBER

5f. WORK UNIT NUMBER

7. PERFORMING ORGANIZATION NAME(S) AND ADDRESS(ES)
Department of Gelogy University of Illinois Urbana-Champaign 1301 W. Green Street Urbana, IL 61801

8. PERFORMING ORGANIZATION REPORT NUMBER

9. SPONSORING/MONITORING AGENCY NAME(S) AND ADDRESS(ES)

10. SPONSOR/MONITOR'S ACRONYM(S)

11. SPONSOR/MONITOR'S REPORT NUMBER(S)

12. DISTRIBUTION/AVAILABILITY STATEMENT

DISTRIBUTION STATEMENT A
Approved for Public Release
Distribution Unlimited

13. SUPPLEMENTARY NOTES

14. ABSTRACT
The US Navy operates military bases in tropical and sub-tropical seas that are surrounded by coral reefs. Therefore, the goal of this work has been to develop methods for long-term monitoring of the effects of naval activity on the health of these reef ecosystems. Our research shows that microbes inhabiting the tissues of healthy and diseased coral are sensitive indicators of environmental change associated with harbor and near-shore naval activity. Our integrated analyses indicate that: (1) coral tissue d34N content is the most sensitive ecological indicator to quantify average sewage concentration with the human enteric bacteria found in the BBD microbial consortium; (2) quantitative correlation of seawater (depth, temperature, pollution, light intensity), coral health (physiology, mucus chemistry, symbiotic zooxanthellae diversity), and coral microbial communities indicate that environmental impact exerts the strongest influence on coral microbes. Results have permitted the development of microbial screening to permit identification of threatened reef ecosystems impacted by harbor and near-shore activity.

15. SUBJECT TERMS
harbor and near-shore naval activity, coral disease, coral reef ecosystems, marine microbiology, pollution, sewage

16. SECURITY CLASSIFICATION OF:			17. LIMITATION OF ABSTRACT	18. NUMBER OF PAGES	19a. NAME OF RESPONSIBLE PERSON
a. REPORT	b. ABSTRACT	c. THIS PAGE		9	Linda Chrisey, Program Officer
					19b. TELEPHONE NUMBER *(Include area code)* (703) 696-4504

We have collected several lines of evidence that suggest human mucolytic bacteria may be associated with the development of coral BBD, including: (1) bacterial 16S rRNA gene sequences were detected in BBD mats that exhibited more than 97% similarity with human gastrointestinal bacteria, including *Campylobacter*, *Clostridium*, *Cytophaga*, and *Argobacter*; (2) the greatest incidence of BBD disease occurs just down-current from the harbor at St. Annabaai, which releases sewage into the uni-directional longshore current (Fig. 3A; we mapped the frequency of BBD at 36 sites on the island; Fortwengler 2003); (3) more than 95% of the observed cases of BBD occur in the back reef ecological environment, which is where the sewage discharge pipes and maximum ship bilge dumping are located; (4) the $\delta^{15}N$ composition of tissue from apparently healthy and infected heads of the coral *Monastraea cavernosa* was significantly elevated directly offshore from the sewage effluent at St. Annabaai (Boca Simon) and decreases down current (Fig. 3A), which indicates that sewage-derived N is being incorporated into infected coral tissues (this is consistent with previously reported eutrophication trends on Curaçao; and (5) average k-dominance curves of bacterial 16S rRNA gene sequence fragment abundance (T-RFLP) indicate that just 2 or 3 types of microorganisms dominate apparently healthy coral tissue bacterial communities at sewage-impacted sites while consortia inhabiting corals in less-impacted down current sites are more diverse (Fig. 3B; Table 1).

Table 1. Frequencies of the different bacteria identified as present in high numbers in BBD mats[a]

Clone	Division	Number of Bacteria[b]		No of positives in healthy samples (n=3)
		BBD mat (n=4)	Healthy coral (n=3)	
Universal Primers		100	100	**3**
CD1C11	Cyanobacteria	44.40 ± 41.92 [c]	<0.0001 ± 0	**0**
CD22E1	CFB	22.12 ± 20.56 [c]	0.75 ± 0.36	**3**
CD22E6	Firmicute	16.84 ± 28.72	0.75 ± 0.36	**3**
R3-M4	CFB	14.21 ± 8.69 [c]	0.64 ± 0.55	**2**
CD22D5	δ-Proteobacteria	9.05 ± 4.54	9.70 ± 8.40	**3**

[a] Results were obtained by MPN-PCR and refer to the total number of bacteria obtained using universal primers.
[b] Average (percent respect to the total DNA) ± standard deviation.
[c] Significantly different ($P < 0.05$) from the value for healthy coral sample as determined by the Mann-Whitney U test.

A brief summary of our analyses of the ecological and environmental conditions associated with BBD development is as follows. In addition to the possible influence of sewage (described above), we believe the combined effects of seawater warming and cyanobacterial activity are central to BBD development. The greatest annual incidence of BBD on Curacao is in August and September when sea surface temperatures reach 31° C, which is 4° C higher than the annual average wintertime low of 27° C. This elevated seawater temperature may weaken the corals, and/or it may increase the viability of the BBD microbial consortium (which includes at least 65 unique bacteria). BBD is consistently observed to start at the top of massive (hemispherical) coral colonies and later stop halfway down the side, implying that light intensity is also influential. In addition, BBD is infectious based on our *in situ* inoculation experiments of healthy corals with detached portions of active BBD mat.

Multiple strains of photosynthetic cyanobacteria are an essential structural component of the polymicrobial BBD infection, based on: (1) optical analyses; (2) molecular analyses; and (3) *in situ* experiments showing that BBD is stopped when shaded from sunlight for 48 hours (Fig. 4).

In addition, our application of RNA-arbitrarily primed PCR techniques has identified three genes that are up-regulated during infection, which have homology with transporter, photosynthesis, and N fixation pathways.

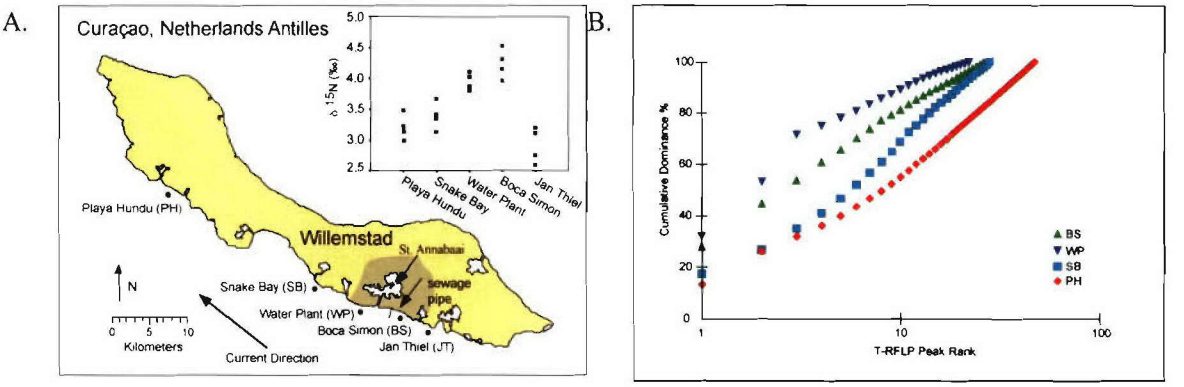

Figure 3. (A). Map of Curaçao showing study sites. Boca Simon (BS) and Water Plant (WP) are heavily sewage impacted (highest coral tissue $\delta^{15}N$). Snake Bay (SB) and Playa Hundu (PH) are less-impacted (moderate coral tissue $\delta^{15}N$), and the up-current site of Jan Thiel is the least sewage impacted site (lowest coral tissue $\delta^{15}N$). (B). Average k-dominance curves of bacterial 16S rRNA gene sequence T-RFLP fragment abundance peaks obtained from the tissues of 4 colonies of non-infected *D. strigosa* corals. Note that the highly sewage impacted sites of BS and WP have 75% of their microbial communities composed of 3 to 7 unique types of bacteria. Conversely, the less-impacted sites of SB and PH have 75% of their microbial communities made up of 13 to 30 unique types of bacteria.

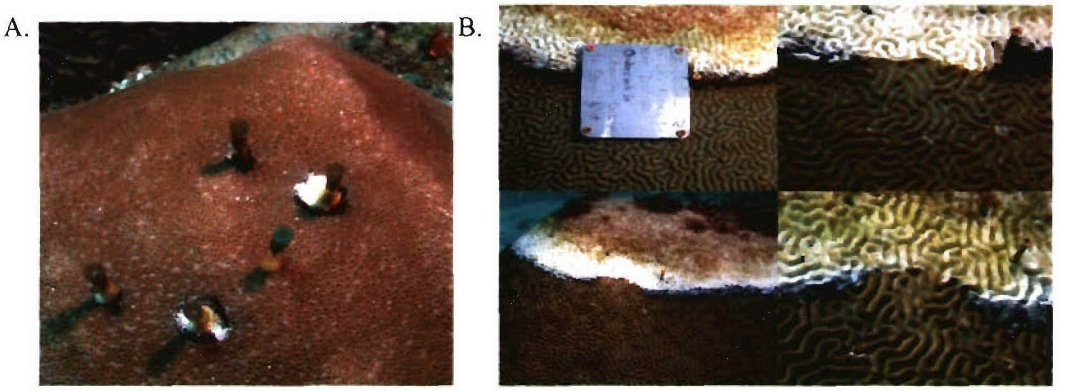

Figure 4. Results of *in situ* shading experiment. (A). Transplant experiment showing BBD development at each site where the coral was innoculated (brown needle). Note no BBD development at the control point (blue needle). B. Shading experiment with shade in place (upper left), shade removed after 5 days (upper right), 3 days after the shade was removed (lower left), and 9 days after the shade was removed (lower right).

We have developed a surgical method to recover single coral polyps from a colony with minimal damage to neighboring individuals (Fig. 5). The histomorphometric, histopathologic and proteomic features of individual coral polyps will be used in conjunction with gross morphology of the experimental coral colony in order to provide a more accurate view of the host response to systemic covariations centered around polymicrobial disease. This approach will markedly improve the current standard of gross morphology to determine coral health and

provide clearly defined parameters for covariate analysis. In addition to improved statistical power, surgical reovery of individual animals will be less damaging to endangered reef systems than the current practice of fragmentation.

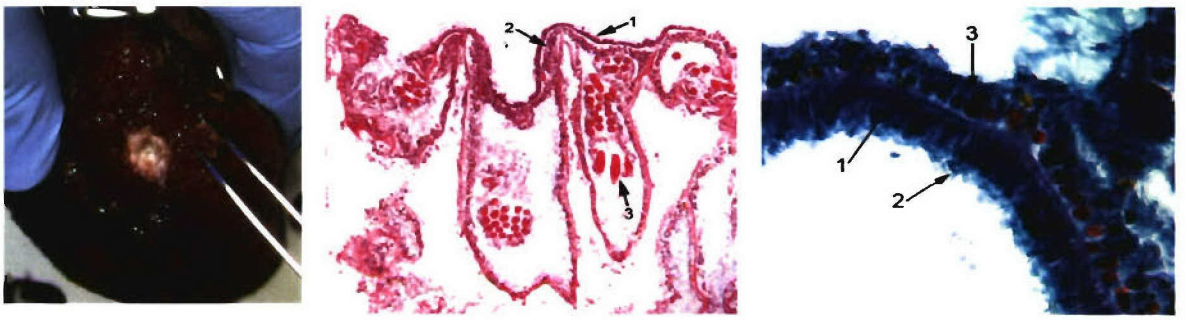

Figure 6. (Left panel). Surgical removal of an individual polyp from a small colony of G*oniastrea retiformis*. Note recovery of single polyp (held by forceps) and the minimal disruption of surrounding individuals in the colony. (Middle panel). Digital Image of an H&E Stain from the Oral Disk Area of an Individual Coral Polyp. This is a longitudinal cross section of a coral polyp processed as described below. Arrow 1= epidermal layer. Arrow 2=gastrodermal layer with zooxanthellae. Arrow 3= aggregate of nematocysts contained within a tentacle. Original magnification=63x. (Right panel). Digital Image of Oral Disk Region from Coral Polyp Stained with Alcian Blue-Periodic Acid Shiff Stain. Arrow 1 shows basal orientation of epidermal nuclei. Several cells (mucocytes) show prominent apical vacuoles containing alcian blue positive mucins. Arrow 2 shows intact surface mucus layer covering the epidermal cells. Arrow 3 shows zooxanthellae in gastrodermis. Although not reported in the literature, the ABPAS stain appears to differentially stain the zooxanthellae in the gastrodermis. We currently do not know the significance of this finding, however, we plan to incorporate differential zooxanthellae staining as a variable in our covariate analyses. Original magnification= 400x.

We conducted a pilot analysis the mucus composition of *M cavernosa* and its zooxanthellae from Curacao. The mucus carbohydrates were dominated by fucose and N-acetyl glucosamine (Table 2), and appeared to contain significant quantities of the alcohol sugar inositol, which had not been detected in mucus before. The composition was very different from the profiles previously described, which confirms the existence of species-specific mucus composition. The carbohydrate composition of a *Symbiodinium l*aboratory culture was completely different, indicating a significant contribution by corals to the excreted carbon fixed by zooxanthellae

To determine the influence of symbiotic algal communities (*Symbiodinium sp.*) on bacterial communities, *Symbiodinium* communities were characterized by T-RFLP analysis of 28S rRNA genes and sequencing of clone libraries. Furthermore, the $\delta^{13}C$ value, and C:N ratio of coral tissues was used to determine differences in the relative proportion of autotrophic (*Symbiodinium*) versus heterotrophic modes of coral nutrition and analyses of amino acid and monosaccharide composition were used to determine how coral mucus varied among the sampled coral colonies. The $\delta^{15}N$ value of coral tissue was used to quantify the relative impact of pollution at the different reef sites. Results of Spearman rank correlation tests among the different datasets suggest the variation observed in bacterial community structure along the sampled gradients is primarily controlled by the external environment, including anthropogenic

pollution, with little influence due to changes in the composition of coral mucus, the structure of *Symbiodinium* communities or changes in the host coral physiologic state.

Carbohydrates	*Montastrea annularis*	*Symbiodinium culture*	*Fungia fungites (Meikle et al 1988)*	*Acropora Formosa (Meikle et al 1988)*
inositol	2.6	24.6	nd	nd
fucose	38	0.5	41	2
arabinose	1	4.0	2	47
rhamnose	0	9.6	nd	nd
galactose	6.8	10.6	4	2
glucose	12.4	35.4	3	1
Glucosamine	2.6	0	nd	nd
xylose	0.4	8.9	2	nd
N-acetyl glucosamine	34.9	3.5	22	29
N-acetyl galactosamine	0	0	7	1
mannose	0.1	0.2	19	18
fructose	0	2.7	nd	nd
Glucuronic acid	2.4	0	nd	nd

Table 2. Comparison of chemical composition of *M. annularis* mucus (our research group) with mucus from zooxanthellae and two other coral species.

Bacterial communities sampled at 5, 10 and 20 m at three sites along a pollution gradient were characterized by T-RFLP analysis of 16S rRNA genes for bacteria and sequencing of clone libraries. Analysis of T-RFLP profiles using nonmetic multidimensional scaling (NMDS), and one-way analysis of similarity (ANOSIM) indicate distinct differences in bacterial community structure with depth. By comparing T-RFLP peaks to sequenced clone libraries we found the black band disease microbe *Phormidium coralyticum* (CD1C11) to be most abundant on corals in less than 10 m water depth. Similarly, we identified sequences belonging to a putative new division (CAP-I) that is also more common in shallow water. Differences in bacterial communities at polluted and control localities were only recognized at the shallowest water depth. Bacterial communities of the most polluted localities showed very little similarity among replicates and could not be characterized by a specific microbial fauna.

An extract from the BBD mat was found to have toxic effects on the growth and viability of the symbiotic dinoflagellate *Symbiodinium* sp. Nonetheless, neither the pellet recovered from the extraction nor extracts from other bacteria have such an effect, suggesting that neither LPS nor membrane proteins are involved in BBD toxicity. Moreover, this compound has a molecular weight lower than 10,000 Da and is heat stable. All these results indicate that there is a toxic compound possibly involved in the mechanism of pathogenesis of BBD in corals. Further studies will involve the isolation and characterization of such compound.

A series of experiments was conducted to determine the role of cyanobacteria in the etiology of BBD. We established that small 3-5 mm pieces of BBD mat could be transplanted and start an infection when it was placed on a healthy coral colony using sterile syringe needles. BBD mat pieces were also placed within polyp them between the coral 'valleys' of D. strigosa where they were held in place by a mesh net attached to fish line, which allows innolcution withot the injury caused by the syringe needles. In all cases, both with and without the needle, the area where the piece of BBD was placed on healthy corals became the site of full-scale BBD infection within 2 to 6 days. The surface under control nets remained healthy and was not visibly damaged. To

investigate the coral species specificity of BBD microbes, we performed *in situ* infection experiments by collecting BBD mat from 4 species of corals and using these to infect healthy specimens of the same 4 species.

To investigate a possible role for cyanobacterial ecotypes in infection, we studied the fine-scale sequence heterogeneity and distribution of BBD cyanobacteria. To this end we focused on a fraction of the rRNA gene spanning the 3' end of the 16S and the full internal transcribed spacer (rRNA-ITS). ITS sequences are known to be more heterogeneous than 16S sequences and thus have a higher potential to discriminate between closely related organisms or ecotypes. Cyanobacteria-specific primers were used to amplify the rRNA-ITS and TRFLP profiles were generated with 7 four-basepair recognizing enzymes (AluI, CfoI, DpnII, TaqI, MspI, RsaI and HaeIII). Based on these TRFLPs, the BBD communities infecting the different cortals were identical, with the exception of the seafan BBD which showed a different microbial community composition. These findings were confirmed by using denaturing gradient gel electrophoresis (DGGE).

Full 16S+ITS sequences showed a sequence difference between clones in a 6 bp rRNA-ITS sequence. Based on this sequence difference we selected an enzyme (EarI) that allowed differentiation of the ecotypes. Application of this fine-scale community analysis to the BBD mats infecting different corals revealed that one ecotype is limited to *D. strigosa* and *C. natans*, as well as *M. myandrina*, *M. annularis*, *M. faveolata* and *M. cavernosa*.
To move beyond merely detecting the community structure of microorganisms that are present in healthy and diseased coral samples, we made an effort to identify the active members of the microbial communities. To this end, we extracted RNA, and generated and amplified the cDNA from several samples. BBD mat samples yielded abundant cDNA from the rRNA gene (crDNA). Since the crDNA T-RFLP profiles were very similar to the DNA T-RFLP profiles, it was concluded that the microorganisms that comprise the major part of the BBD community are also the most active members of the community.

CONCLUSIONS : Our work provides evidence that multiple anthropogenic bacteria are associated with coral BBD, and that apparently healthy corals in sewage impacted areas of the Curacao reef tract have a unique microbial communities from apparently healthy corals in less-impacted sites (see below). Our data suggests that bacteria derived from human sewage and ship bilge are compromising the mucus that coats coral tissue, which is a coral's primary protective barrier against environmental insults. These results do not suggest that human waste is the source of a single pathogen, but instead that the activity of anthropogenic mucolytic bacteria is associated with a variety of possible mechanisms that compromise the integrity of the coral mucus. This mucus alteration predisposes the coral to what may be a polymicrobial infection that ultimately results in BBD. In this context, the actual organisms that *cause* disease (the pathogens) may or may not be derived from sewage.

SIGNIFICANCE : The US Navy can use the results of this study to monitor the effects of harbor and near shore human activity on the health of coral reef ecosystems surrounding each of its bases. Efforts hould move forward to take the results of our study to create practical microbial environmental screening tool for use by Naval personnel to assess reef health and impact. To permit accurate microbial molecular screens, we have begun to develop and experiment with

modified protocols for fluorescent *in situ* hybridization developed from the 16S rRNA gene sequences detected in our study (customized in our lab for a variety of taxonomic levels), that could be modified into standard shipboard or shipyard analyses. Simultaneously, we have been establishing techniques by which analysis of $\delta^{18}O$ and $\delta^{35}N$ could be analyzed in water samples to track the source and concentration of sewage pollution. By normalizing the isotopic ratio at each measured site to the isotopic ratio of samples taken from the putative source of the pollution, a quantitative measure can be made of the relative concentration of sewage in the seawater from the N- and O-isotope covariation. By synthesizing this microbiological information with basic analyses of seawater sewage and ordinance-derived chemicals, a numerical scale could be established to define thresholds of microbiological and chemical composition that could be used to identify pristine, at risk, and heavily impacted coral reef ecosystems.

PATENT INFORMATION : No patents.

AWARD INFORMATION : Fellow in the University of Illinois Center for Advanced Study; Professor in the University of Illinois Institute for Genomic Biology

PUBLICATIONS and ABSTRACTS (for total period of grant) :

1) Klaus, J., Janse, I., Sandford, R., and Fouke, B.W., 2006. Coral microbial communities, zooxanthellae, and mucus along gradients of seawater depth and coastal pollution. *Environmental Microbiology*, submitted.

2) Klaus, J., Budd, A., and Fouke, B.W., 2006. Environmental controls on corallite morphology in the reef coral *Montastrea annularis*. *Bulletin of Marine Science*, submitted.

3) Janse, I., Klaus, J., Fouke, B.W.. 2006. Characterization and host specificity of the microbial communities associated with healthy and black band disease infected corals. *Environmental Microbiology*, submitted.

4) Frias-Lopez, J., Klaus, J.S., Fouke, B.W., 2006. Cytoxic activity of Black Band Disease (BBD) extracts against the symbiotic dinoflagellate *Symbiodinium sp.*, Proceedings of the International Coral Reef Symposium, Okinawa, p. 785-788.

5) Klaus, J.S., Frias-Lopez, J., Fouke, B.W., 2006. The effect of temperature on bacterial communities inhabiting healthy tissues of *Diploria strigosa*, Proceedings of the International Coral Reef Symposium, Okinawa, p. 794-799.

6) Klaus, J.S., Frias-Lopez, J., Bonheyo, G.T., Heikoop, J.M., and Fouke, B.W., 2005, Bacterial communities inhabiting the healthy tissues of two Caribbean reef corals: interspecific and spatial variation: *Coral Reefs*, Vol. 24, p. 129-137.

7) Frias-Lopez, J., Klaus, J., Bonheyo, G.T., and Fouke, B.W., 2004, The bacterial community associated with black band disease in corals: *Applied and Environmental Microbiology*. Vol. 70, p. 5055-5062.

8) Frias-Lopez, J., Bonheyo, G.T., and Fouke, B.W., 2004, Identification of differential gene expression in bacteria associated with coral black band disease using RNA-arbitrarily primed PCR: *Applied and Environmental Microbiology*. Vol. 70, p. 3687-3694.

9) Frias-Lopez, J., Bonheyo, G.T., Jin, Q., and Fouke, B.W., 2003, Cyanobacteria associated with coral black band disease in Caribbean and Indo-Pacific reefs: Applied and Environmental Microbiology, v. 69, p. 2409-2413.

10) Frias-Lopez, J., Zerkle, A.L., Bonheyo, G.T., and Fouke, B.W., 2002, Partitioning of bacterial communities between seawater and healthy, black band diseased, and dead coral surfaces. *Applied and Environmental Microbiology*, Vol. 68, No. 5, p. 2214-2228.

APPLIED AND ENVIRONMENTAL MICROBIOLOGY, May 2002, p. 2214–2228 Vol. 68, No. 5
0099-2240/02/$04.00+0 DOI: 10.1128/AEM.68.5.2214–2228.2002

Partitioning of Bacterial Communities between Seawater and Healthy, Black Band Diseased, and Dead Coral Surfaces

Jorge Frias-Lopez, Aubrey L. Zerkle, George T. Bonheyo, and Bruce W. Fouke*

Department of Geology, University of Illinois, Urbana, Illinois 61801

Received 21 December 2001/Accepted 25 February 2002

Distinct partitioning has been observed in the composition and diversity of bacterial communities inhabiting the surface and overlying seawater of three coral species infected with black band disease (BBD) on the southern Caribbean island of Curaçao, Netherlands Antilles. PCR amplification and sequencing of bacterial 16S rRNA genes (rDNA) with universally conserved primers have identified over 524 unique bacterial sequences affiliated with 12 bacterial divisions. The molecular sequences exhibited less than 5% similarity in bacterial community composition between seawater and the healthy, black band diseased, and dead coral surfaces. The BBD bacterial mat rapidly migrates across and kills the coral tissue. Clone libraries constructed from the BBD mat were comprised of eight bacterial divisions and 13% unknowns. Several sequences representing bacteria previously found in other marine and terrestrial organisms (including humans) were isolated from the infected coral surfaces, including *Clostridium* spp., *Arcobacter* spp., *Campylobacter* spp., *Cytophaga fermentans*, *Cytophaga columnaris*, and *Trichodesmium tenue*.

Infectious disease in scleractinian corals has emerged as one of the primary causes of the accelerating global destruction of coral reef ecosystems (22, 25, 27, 56, 74). Black band disease (BBD) is one of the most widespread and destructive of these coral infections (see review in reference 50). The diagnostic symptom of BBD is the development of a narrow 0.1- to 7-cm-wide ring-shaped black to red microbial mat that migrates from top to bottom across massive coral colonies, killing healthy coral tissue at rates of as much as 1 cm per day (47, 53). BBD preferentially affects corals such as *Montastrea annularis*, *Montastrea cavernosa*, and *Diploria strigosa* (6, 15, 53). These species, known as framework building corals, form large structures that become the dominant physical elements of reefs. As a result, coral mortality caused by BBD is a potent force in restructuring coral reef ecosystems (15, 36).

There is considerable controversy as to whether BBD is caused by physical and chemical environmental stresses or is an infectious disease or both (50, 56). However, an impediment to determining the cause of BBD has been the lack of information about the diversity and distribution of microbial populations that inhabit normal healthy coral tissue and the BBD bacterial mat. It is known from studies of infectious disease in marine and terrestrial invertebrates, fish, and mammals (including humans) that pathogens are most effectively studied within an ecological context of interactions among microbes, their hosts, and the environmental conditions in which they live (25, 54). Accurate diagnosis and eventual treatment and prevention of BBD will therefore require a basic knowledge of the composition and distribution of the microbial communities associated with healthy as well as diseased organisms. This type of community-based comparative analysis of the microorganisms associated with infectious diseases in corals has not previously been completed.

* Corresponding author. Mailing address: Department of Geology, University of Illinois, 1301 W. Green St., Urbana, IL 61801. Phone: (217) 244-5431. Fax: (217) 244-4996. E-mail: fouke@uiuc.edu.

The purpose of the present report was to complete the first culture-independent 16S rRNA phylogenetic survey of the bacterial communities inhabiting seawater and healthy, BBD-infected, and dead coral surfaces. The coral reef chosen for analysis was on the leeward reef tract of Curaçao, Netherlands Antilles (Fig. 1). A factor that may contribute to BBD is the daily dumping of sewage and other pollutants directly onto the reef from the major commercial, municipal, and military harbor of St. Annabaai (Fig. 1). The following three fundamental questions have been addressed: (i) is there a coral-specific microbial population that is different from that of the bacterioplankton community in the overlying seawater column; (ii) are the microbial communities comprising the BBD mat and the dead coral surfaces distinct from each other; and (iii) have sewage microbes colonized the diseased coral, as might be expected if sewage microbes were contributing to the disease process? Results are presented that indicate the healthy coral tissue is colonized by a microbial population that is unique and distinct from that found in the water column and the BBD mat and dead coral surfaces. Also, bacteria associated with sewage were detected only in the BBD bacterial mat.

MATERIALS AND METHODS

Field work and sample collection. Field sampling using standard scuba techniques was conducted in August 2000 on the leeward reef tract of Curaçao, Netherlands Antilles (Fig. 1). Diseased corals were studied at the Playa Kalki and Water Plant sites in back reef environments approximately 0.5 km offshore (33). These included BBD-infected colonies of *M. annularis* (Fig. 2A and B) and *M. cavernosa* (Fig. 2C and D) at Playa Kalki at a 5-m water depth, as well as a colony of *D. strigosa* (Fig. 2E and F) at Water Plant at a 4-m water depth. Three individual BBD-infected coral heads, one each of *M. annularis*, *M. cavernosa*, and *D. strigosa*, were analyzed. From each coral head, four individual samples were collected in situ from the following environments: the overlying seawater, the healthy coral surface, the black band diseased coral surface, and the dead coral surface. Seawater was sampled by collecting 2 liters of seawater in cleaned 1-liter Nalgene high-density polyethylene bottles from directly above the coral colonies. The water was pumped through a sterile 0.45-μm-filter-loaded cup (Pall/Gelman) when brought on shore. All filters and centrifuge tubes were then immediately frozen at −20°C, transported to Illinois on dry ice, and stored at −40 to −80°C. The coral surface samples were collected by removing a 2-cm by

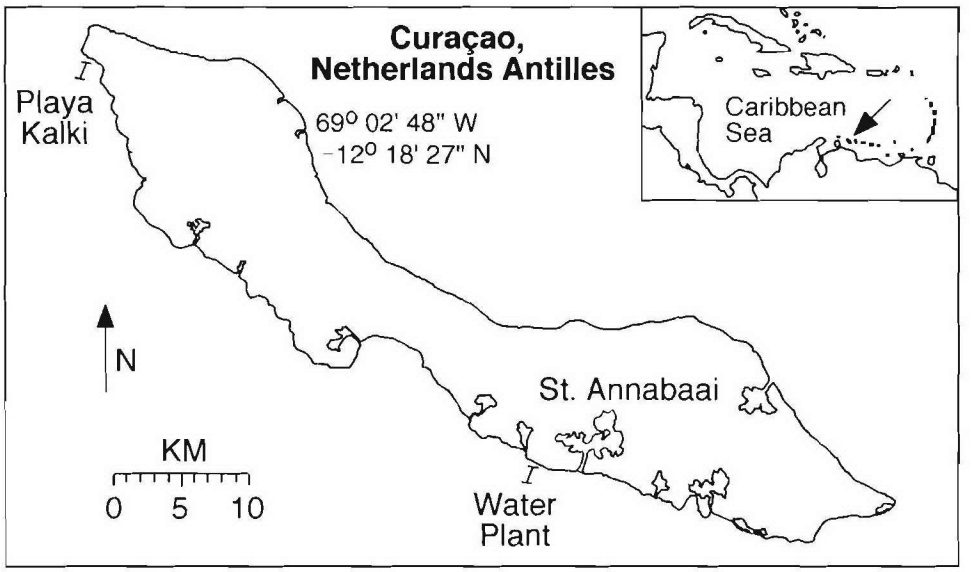

FIG. 1. Map of Curaçao, Netherlands Antilles, in the southern Caribbean Sea. The regional location of the island is shown with an arrow on the inset map. Study sites were on the leeward reef tract at Water Plant and Playa Kalki. Also shown is the location of the St. Annabaai seaport.

1-cm portion of the uppermost 1 cm of the coral colonies with a chisel and placing the sample in a sterile disposable 50-ml polypropylene centrifuge tube. Furthermore, portions of some BBD microbial mats were physically peeled off the coral surface with forceps and placed in sterile 15-ml polypropylene centrifuge tubes. Immediately upon the return to shore, the seawater within each tube was decanted and coral samples were immersed in either of the following solutions: (i) 80% ethanol for molecular analyses or (ii) Karnovsky's aldehyde fixative (2.0% paraformaldehyde and 2.5% glutaraldehyde in 0.1 M sodium phosphate buffer [pH 7.2]) for scanning electron microscopy (SEM) analyses. Coral samples preserved in 80% ethanol were crushed and homogenized in the tube, creating a slurry of coral tissue, zooxanthellae, mucus, microorganisms, and skeletal material.

SEM analyses. The Karnovsky's aldehyde fixative was removed and replaced with buffered 0.1 M sodium phosphate (pH 7.2). The samples were dehydrated by stepwise immersion in 33, 67, and 95% ethanol for 1 h each and in 100% ethanol for 3 h. The ethanol was then removed and the samples were soaked in hexamethyldisilazane for 2 h, after which they were air dried in a laminar flow hood and placed in a desiccator. Small 0.25-cm-diameter pieces of each specimen were mounted on a 2-cm-diameter aluminum stub using double-stick carbon tabs. Samples were grounded with colloidal silver paint and covered with a 90- to 100-nm-thick gold-palladium coating using a Denton Desk II Turbo sputter coater. Imaging was done on a Phillips XL30 ESEM-FEG apparatus, which is housed at the University of Illinois Urbana-Champaign Beckman Institute, in high-vacuum mode with an accelerating voltage of 15 kV.

DNA extraction. Several methods of DNA extraction were utilized with each sample to increase the likelihood that no microorganism would escape detection. Filters were sectioned into quarters with flame-sterilized scissors and forceps and placed in a sterile disposable 50-ml polypropylene centrifuge tube with 3 ml of sterile ultrapure water. Cells were then washed off the filter during 3 min of vigorous agitation on a vortexing apparatus and stored frozen at −80°C.

Bead beating (32), freeze-thaw cycling, and chemical lysis protocols (55) were used to extract genomic DNA from the cells collected on the filters, the crushed coral slurries, and the BBD mat samples. For bead beating, 300 μl of sample material was added to a 2-ml O-ring-equipped screw-cap microcentrifuge tube containing 600 μl of sterile ultrapure water and 800 μl of 0.1-mm zirconia-silica beads (BioSpec Products, Bartlesville, Okla.). The beads were cleaned and sterilized beforehand with a series of HCl acid and bleach washes. The tube was then filled to capacity with sterile ultrapure water and shaken on a reciprocating Mini-BeadBeater-8 (BioSpec Products) for 2.5 min at the homogenize (highest) speed setting. This protocol has been optimized by using several samples and *Escherichia coli*-positive controls. For the freeze-thaw procedure, samples were added to sterile 2-ml O-ring-equipped screw-cap microcentrifuge tubes containing 1 ml of sterile ultrapure water. The tubes were frozen at −80°C and rapidly thawed by plunging the tubes into a 65°C water bath. The freeze-thaw cycle was repeated three times, with the tubes vigorously agitated on a vortex apparatus for approximately 1 min after each thaw cycle. In some instances, samples were treated with an alkaline lysis step by using NaOH (0.13 M final concentration), sodium dodecyl sulfate (SDS; 0.3%) and incubation at 25°C (55).

For both the bead beating and freeze-thaw techniques, 400 μl of the lysate was used for DNA extraction. Standard phenol DNA extraction procedures were used (55). The ethanol-precipitated lysate, phenol-extracted lysate, and untreated lysate were used in subsequent PCRs. This entire protocol was tested with 300 μl of the sterile ultrapure water as both a negative control and contamination screen and with 50 μl of an overnight Luria broth *E. coli* culture as a positive control. The control preparations were included with their simultaneously prepared environmental samples each time a PCR was performed. In no case were nucleic acids detected in the negative controls.

PCR amplification. Total DNA was amplified with a Mastercycler gradient thermocycler (Eppendorf, Westbury, N.Y.) by PCR using specific 16S rRNA primers for bacteria. Primers used in the PCR amplifications were obtained from Operon Technologies, Inc. (Alameda, Calif.). B. Paster (personal communication) provided the sequence of each primer as follows: forward primer, 28F (5′-GAGTTTGATYMTGGCTC); reverse primer, 1492R (5′-GYTACCTTGTT ACGACTT). Reaction mixtures included a final concentration of 1× TaqMaster buffer (Eppendorf), 1.5 mM $MgCl_2$ (Eppendorf), a 0.2 mM concentration of each deoxynucleoside triphosphate (Gibco/BRL, Rockville, Md.), 200 ng each of the forward and reverse primers, 5 to 30 μl of the sample preparation, and water to bring the total volume to 49.5 or 99.5 μl. Reaction mixtures were layered beneath 50 μl of mineral oil (Sigma, St. Louis, Mo.). An initial denaturation-hot start of 5 min at 95°C was followed by the addition of 0.5 μl (approximately 2 U) of MasterTaq polymerase (Eppendorf) or *Taq* DNA polymerase (Gibco/BRL). The hot start was followed by 30 cycles of the following incubation pattern: 94°C for 1 min, 55°C for 1 min, and 72°C for 2 min. A final soak at 72°C for 5 min concluded the reaction.

Cloning and sequencing. PCR products were purified by electrophoresis through a 1.0% low-melting-point agarose gel (SeaPlaque GTG; BioWhittaker Molecular Applications, Rockland, Maine), stained with ethidium bromide, and visualized on a UV transilluminator. The approximately 1,500-bp heterologous ribosomal DNA (rDNA) product was excised from the gel, and the DNA was purified from the gel slice by using the Wizard PCR Prep kit (Promega, Madison, Wis.). The gel-purified PCR product was cloned into the pGEM-T Easy vector (Promega) and transformed into calcium chloride-competent DH5αMCR *E. coli* cells according to manufacturers' instructions and standard techniques (55). Plasmid DNA was isolated from individual clones (QIAprep Spin Miniprep kit; Qiagen, Inc., Valencia, Calif.). Restriction fragment length polymorphism (RFLP) analysis was used in some samples to verify the presence of an appropriately sized insert and to select unique clones for sequencing. Aliquots from a subset of the samples of purified plasmid DNA were digested with 1 U of the

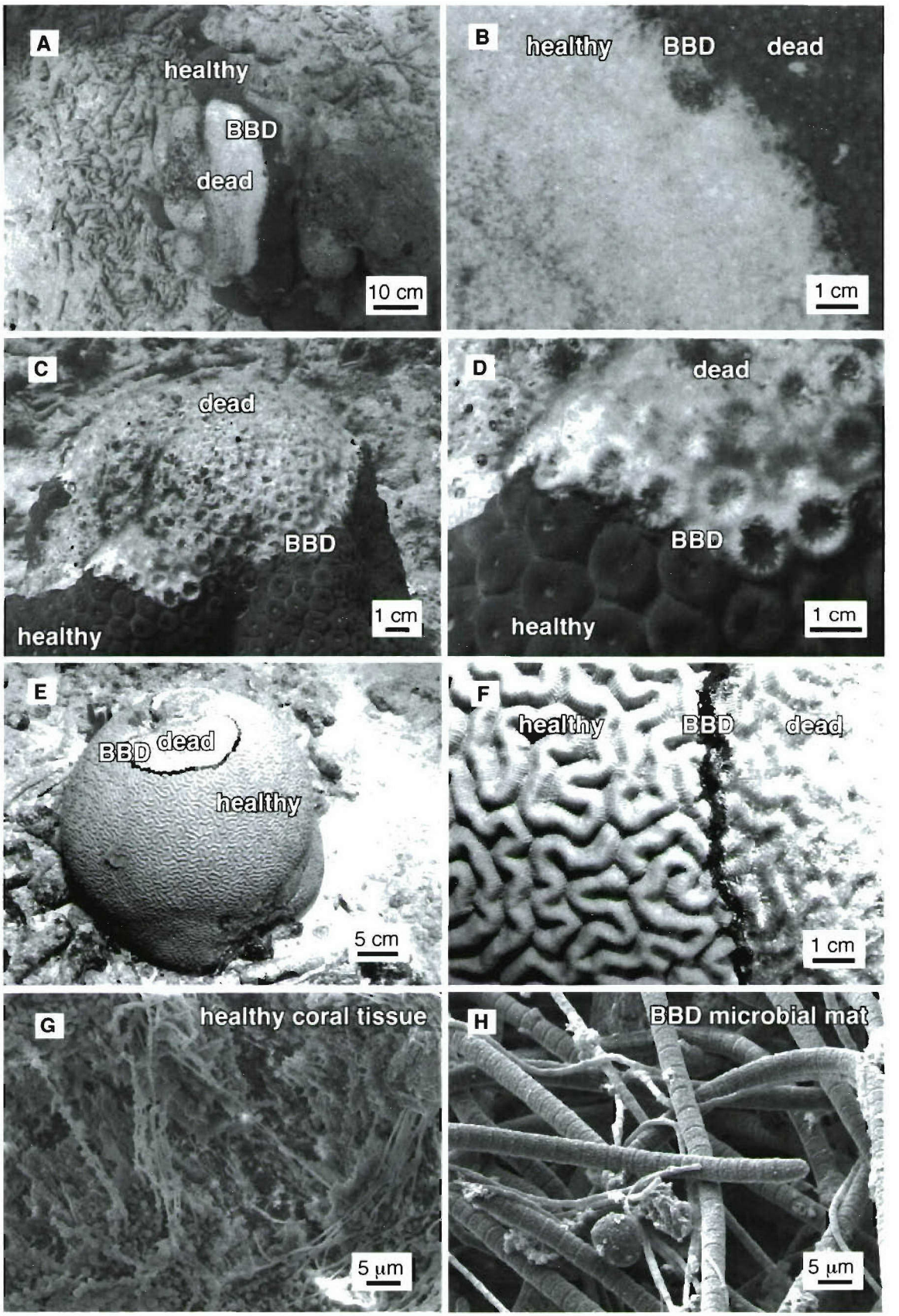

FIG. 2. Underwater photographs of BBD infection in colonies of *M. annularis* (panels A and B), *M. cavernosa* (panels C and D), and *D. strigosa* (panels E and F). (G) SEM image of healthy tissue from the infected colony of *D. strigosa* shown in panels E and F. (H) SEM image of the BBD mat from the infected colony of *D. strigosa* shown in panels E and F.

restriction enzyme *Eco*RI in 1× REact 3 buffer (Gibco/BRL) for more than 3 h at 37°C, and the digested product was separated by electrophoresis on a 0.8% agarose gel (SeaKem LE; BioWhittaker Molecular Applications). After staining with ethidium bromide, the bands were visualized on a UV transilluminator and the RFLP patterns were analyzed to select clones containing the appropriately sized insert. Plasmid DNA from these clones was then digested with the four-base recognition site enzymes *Msp*I and *Hin*P1I in 1× NEB buffer 2 (New England Biolabs, Beverly, Mass.) under the conditions described above. The digest products were then separated by electrophoresis on a 3.0% agarose gel (MetaPhor; BioWhittaker Molecular Applications) and stained with ethidium bromide, and the RFLP patterns were used to identify unique clones to be submitted for sequence analysis. Multiple samples with seemingly identical RFLP patterns were selected for sequence analysis in an effort to capture different sequences with similar RFLP patterns. Clones selected for sequence analysis were patched onto Luria broth agar petri dishes supplemented with 100 μg of ampicillin/ml (Roche Molecular Biochemicals, Indianapolis, Ind.) and incubated overnight at 37°C.

Inoculation, cell culturing, template preparation, and sequencing were performed in the high-throughput laboratory of the W. M. Keck Center for Comparative and Functional Genomics of the University of Illinois at Urbana-Champaign. The plates were used to inoculate 2-ml 96-well culture blocks containing Circle Grow medium (Bio100) supplemented with ampicillin (100 μm/ml). Plasmid template DNA was purified from the cultures by using an automated system and a QIAwell 96 Turbo Prep BioRobot kit (Qiagen). Sequencing was completed by using T7(−26) primer, which was synthesized in house (63). Sequence reactions were performed on the plasmid templates by using a Qiagen Bio Robot 9600 and Big Dye Terminator chemistry apparatus (v.2.0) from ABI. Sequencing was performed on an ABI 3700 capillary sequencer, and then the results were processed in the Bioinformatics Unit of the W. M. Keck Center.

Sequence analyses. The rDNA sequences were first compared with those in the GenBank database with the basic local alignment search tool (BLAST) network service (4). From the alignments created by this search, the orientation of each cloned 16S rRNA gene could be determined and a rough phylogenetic association was established. Each sequence was analyzed using the CHIMERA_CHECK program (version 2.7) available at the Ribosomal Database Project web site (39). Those sequences deemed to be chimeric were culled from the data set. A 97 to 100% match of the unknown clone with the GenBank dataset was considered an accurate identification to the species level, 93 to 96% similarity was accepted as a genus-level identification, and a 86 to 92% match was considered an accurate identification of a related organism (21).

Nucleotide sequence accession numbers. The GenBank accession numbers for the 16S rRNA sequences generated in this study are AY037873 through AY038581 and AF441866 through AF442078.

RESULTS

Optical and SEM analyses. Visual assessment of the surface of infected *M. annularis*, *M. cavernosa*, and *D. strigosa* colonies indicate that healthy coral tissues contain microbes with different morphologies than those of the microbes inhabiting the BBD microbial mats. Bacteria inhabiting healthy coral tissue occurred within a stringy exopolymer matrix. In contrast, the BBD mat is dominated by large (2- to 5-μm by 0.5- to 2-mm) filamentous nonheterocystous cyanobacteria that have previously been optically identified as *Phormidium corallyticum* (52). A smaller filamentous bacterium that has previously been optically identified as a member of the *Beggiatoa* spp. (14, 53) occurs intertwined with *P. corallyticum*. Rare 0.5-mm-diameter bundles of *P. corallyticum* and *Beggiatoa* spp. were sometimes observed on healthy coral tissue within a few centimeters of the leading edge of the migrating BBD mat, which is consistent with previous observations (48).

16S rRNA clone library diversity. High-diversity assemblages of bacterial sequences were detected in seawater and healthy, BBD-infected, and dead coral surfaces in *M. annularis*, *M. cavernosa*, and *D. strigosa* colonies (Tables 1, 2, and 3, respectively). A total of 295 partial 16S rRNA gene sequences were identified: 65 bacterial sequences in seawater directly overlying the coral colonies and a total of 230 sequences from healthy (64 sequences), BBD-infected (64 sequences), and dead (102 sequences) coral surfaces. Microorganism identifications were based on comparison of these sequences with the GenBank database. Division-level microbial diversity in each sample was estimated by dividing the number of clones representing each division by the total number of clones in the seawater and healthy, BBD diseased, and dead coral surface libraries associated with *M. annularis*, *M. cavernosa*, and *D. strigosa* (shown as pie diagrams in Fig. 3, 4, and 5, respectively).

Microbial communities inhabiting overlying seawater. Bacterioplankton clone libraries were constructed from samples of seawater collected at 10 cm immediately above the surfaces of BBD-infected *M. annularis*, *M. cavernosa*, and *D. strigosa* colonies (Fig. 3A, 4A, and 5A, respectively). The most abundant sequences in the seawater clone libraries at both locations represented cyanobacteria (30 to 43%). The next most abundant clones in the seawater libraries represented the γ-proteobacteria (6 to 38%) and α-proteobacteria (6 to 31%) divisions. Chloroplast sequences, which comprised 3 to 8% of the libraries, were likely derived from the rDNA of chlorophyll-containing organelles in planktonic algae and free-living zooxanthellae just above the coral colony surfaces (45). Only two sequences were common to all three seawater clone libraries: those which represented the genera *Prochlorococcus* and *Synechococcus* (Tables 1, 2, and 3).

Microbial communities inhabiting healthy coral tissue. Clone libraries from healthy tissues indicated that each of the three coral species contained a significantly different assemblage of bacterial sequences (Fig. 3B, 4B, and 5B). A maximum of only 5% of the sequences were representative of cyanobacteria, in contrast to the dominance of cyanobacteria sequences in the overlying seawater clone libraries (Fig. 3A and B, 4A and B, and 5A and B). Chloroplasts in these libraries were most likely derived from zooxanthellae inhabiting the coral tissues. *M. annularis* sequences (Fig. 3B) exhibited significantly more microbial diversity than those of either *M. cavernosa* or *D. strigosa*. (Fig. 4B and 5B, respectively) and were dominated by green sulfur bacteria (19%), α-proteobacteria (16%), firmicutes (16%), and planctomycetales (13%). Healthy tissue libraries from *M. cavernosa* and *D. strigosa* contained sequences representing only three and five divisions, respectively, both of which were dominated by γ-proteobacteria (62 to 81%). None of the same bacterial sequences were detected in all three of the healthy coral species (Tables 1, 2, and 3).

Microbial communities inhabiting the BBD microbial mat. Clone libraries constructed from the BBD microbial mat on *M. annularis*, *M. cavernosa*, and *D. strigosa* colonies consistently exhibit high division-level diversity (Fig. 3C, 4C, and 5C, respectively). Sequences were dominated by firmicutes (5 to 26%), Cytophaga-Flavobacterium-Bacteroides group (CFB) (9 to 29%), γ-proteobacteria (17 to 35%), and δ-proteobacteria (2 to 15%). The chloroplasts (4 to 7%) were most likely derived from coral zooxanthellae. These results indicate that the BBD microbial communities are completely distinct from those inhabiting healthy coral tissue, sharing no common 16S rRNA sequences on any individual coral colony (Tables 1, 2, and 3). These clone libraries also confirm that the BBD mats contain significantly more microbial diversity than that suggested by optical analyses (Fig. 2D). Sequences representing

TABLE 1. 16S rRNA sequencing results for *Montastrea annularis* from the back reef at Playa Kalki[a]

ID%	No. of similar clones	No. of base pairs sequenced	Best-matched organism	Accession no.	Division	Location of clone[b]			
						SW	HC	BBD	DC
98–99	3	389	Uncultured marine bacterium ZD0409	AJ400350	α-Proteobacteria	×			
93–97	3	450	Uncultured bacterium OCS 126	AF001638	α-Proteobacteria	×			
99	1	594	Marine bacterioplankton clone SAR102	L35460	α-Proteobacteria	×			
91	1	568	*Magnetospirillum* sp. strain MSM-6	Y17391	α-Proteobacteria	×			
90	1	571	Uncultured bacterium MND8	AF292999	α-Proteobacteria	×			
99	1	622	Uncultured *Roseobacter* sp. strain NAC11-1	AF245630	α-Proteobacteria	×			
98	1	283	Unidentified alpha proteobacterium	U78945	α-Proteobacteria	×			
99	3	483	*Pseudoalteromonas* sp. strain A28	AF227238	γ-Proteobacteria	×			
94–96	3	601	Uncultured marine eubacterium HstpL49	AF159675	γ-Proteobacteria	×			
99	2	567	*Pseudoalteromonas* sp. strain PRLIST2	Y15323	γ-Proteobacteria	×			
97	1	567	*Alteromonas macleodii* strain CH-518	Y18232	γ-Proteobacteria	×			
95	1	640	Uncultured bacterium CHAB-I-7	AJ240911	γ-Proteobacteria	×			
99	6	589	*Prochlorococcus* sp. strain MIT9202	AF115269	Cyanobacteria	×			
99	2	597	*Prochlorococcus* sp. strain MIT9312	AF053398	Cyanobacteria	×			
98	2	605	Marine bacterioplankton clone SAR7	X52171	Cyanobacteria	×			
99	1	480	*Prochlorococcus marinus* subsp. *pastoris*	AF180967	Cyanobacteria	×			
97	1	406	*Synechococcus* sp. strain WR8101	AJ292905	Cyanobacteria	×			
91	1	621	*Cytophaga* sp. strain JTB250	AB015264	CFB	×			
96	1	619	Unidentified eukaryote OM8 1	U70717	Chloroplasts	×			
94	1	542	Magnetite-containing magnetic *Vibrio* sp.	L06455	α-Proteobacteria		×		
94	1	432	*Magnetospirillum* sp. strain MSM-6	Y17391	α-Proteobacteria		×		
95	2	302	*Rhodothalassium salexigens*	M59070	α-Proteobacteria		×		
95	2	285	Unknown proteobacterium clone JAP553	U09830	α-Proteobacteria		×		×
98–99	3	337	Uncultured bacterium SUR-FREE-32	AF114653	α-Proteobacteria		×		×
98	1	340	Uncultured bacterium BURTON-9	AF142829	α-Proteobacteria		×		
96	1	594	Unidentified bacterium isolate HNSS21	Z88572	α-Proteobacteria		×		
92–95	2	516	Unidentified alpha proteobacterium OM65	U70682	α-Proteobacteria		×		×
98	1	443	Unidentified beta proteobacterium	AB015567	β-Proteobacteria		×		
94	1	609	Uncultured bacterium S2551	AF177428	δ-Proteobacteria		×		
90–92	3	382	Agricultural soil bacterium clone SC-I-15	AJ252618	δ-Proteobacteria		×		
94	1	587	*Legionella feeleii* sgp2 (ATCC 35849)	X73406	γ-Proteobacteria		×		
94	1	595	*Legionella londiniensis*	AF129525	γ-Proteobacteria		×		
90	1	321	Unidentified eubacterium, clone LRE18	AJ232879	γ-Proteobacteria		×		
92	1	310	*Ornithodoros moubata* symbiote A	AB001521	γ-Proteobacteria		×		
89	1	563	Uncultured bacterium strain JTB256	AB015255	γ-Proteobacteria		×		
94–95	11	548	*Chlorobium vibrioforme*	Y10648	Green sulfur bacteria		×		
91	1	609	*Planctomyces brasiliensis*	X85247	Planctomycetales		×		
86	2	648	Uncultured bacterium ACE-29	AF142804	Planctomycetales		×		×
94	1	566	Uncultured marine eubacterium HstpL64	AF159640	Planctomycetales		×		
90	1	297	Bacterium 2-400 C2.5	Z77532	Planctomycetales		×		
95	1	448	Uncultured bacterium 03 19-7F4	AF234144	Planctomycetales		×		
88	1	509	Unidentified bacterium, strain BD2-16	AB015544	Unknown		×		
89	2	607	Uncultured bacterium ACE-29	AF142804	Planctomycetales		×		×
91	1	446	Thermophilic bacterium MV 1087	AJ272422	Firmicutes		×		
90	1	610	*Clostridium aldrichii*	X71846	Firmicutes		×		
87	2	497	*Moorella thermoacetica*	AJ242494	Firmicutes		×	×	
91	1	325	Unidentified eubacterium clone BSV72	AJ229216	Firmicutes		×		
89–91	3	559–613	Unidentified soil bacterium clone BSV73	AJ229217	Firmicutes		×		
91	1	223	*Dietzia* sp. strain CIP104293	Y08313	Firmicutes		×		
90	1	564	*Cytophaga diffluens*	M58765	CFB		×		
96	1	365	*Leptolyngbya* sp. strain PCC7375	AB039011	Cyanobacteria		×		
89–92	2	398	*Mesostigma viride*	L49152	Chloroplasts		×		
86	1	500	*Astasia longa*	AJ294725	Chloroplasts		×		
92	1	326	*Codium fragile*	U08345	Chloroplasts		×		
84	1	307	*Prototheca wickerhamii*	AJ245645	Chloroplasts		×		
99	1	417	Rape rhizosphere bacterium tsb088	AJ295458	Unknown		×		
96	1	462	Uncultured sponge symbiont PAWS51	AF186441	Unknown		×		
86	1	453	Unidentified bacterium, strain BD2-3	AB015533	Unknown		×		
96–97	3	501	*Desulfovibrio salexigens*	M34401	δ-Proteobacteria			×	
97	1	617	Unidentified bacterium isolate Aspo3	X95231	δ-Proteobacteria			×	
93	1	502	Uncultured epsilon proteobacterium KTc1160	AF235116	ε-Proteobacteria			×	
92	1	644	Uncultured epsilon proteobacterium 1065	AB030598	ε-Proteobacteria			×	
92	1	589	Uncultured epsilon proteobacterium	AF246706	ε-Proteobacteria			×	
92	1	604	*Arcobacter* sp. clone D1a1	AJ271654	ε-Proteobacteria			×	

Continued on following page

TABLE 1—*Continued*

ID%	No. of similar clones	No. of base pairs sequenced	Best-matched organism	Accession no.	Division	Location of clone[b]			
						SW	HC	BBD	DC
91–94	7	551	*Cytophaga fermentans*	M58766	CFB			×	×
92–93	3	430	Uncultured *Cytophaga* kps30	AF195441	CFB			×	
92	1	601	*Cytophaga* sp. strain BD1-16	AB015525	CFB			×	
93	1	595	*Trichodesmium tenue*	AF013029	Cyanobacteria			×	
92	3	441	Bacterium strain 77003	AF227847	Unknown			×	
91	1	594	*Clostridium fimetarium*	AF126687	Firmicutes			×	
91	1	637	*Clostridium paradoxum* clone para99	Z69939	Firmicutes			×	
89	1	349	Uncultured marine bacterium 90d10	AF295117	Firmicutes			×	
90–91	2	487	*Guillardia theta*	AF041468	Chloroplasts			×	
87	1	318	Unidentified eubacterium clone BSV85	AJ229229	Unknown			×	
97	1	496	*Roseobacter* sp. (*P. decipiens* symbiont)	AF107210	α-Proteobacteria				×
96	1	568	*Roseobacter* sp. (*P. filiformis* symbiont)	AF107209	α-Proteobacteria				×
95	1	626	*Sulfitobacter pontiacus*	AF182018	α-Proteobacteria				×
96	1	507	Uncultured *Agrobacterium* sp. strain kpc102rc	AF194391	α-Proteobacteria				×
99	1	515	Uncultured marine eubacterium HstpL78	AF159652	α-Proteobacteria				×
86–93	9	454	*Desulfocella halophila*	AF022936	δ-Proteobacteria				×
96–98	4	487	*Desulforhopalus singaporensis*	AF118453	δ-Proteobacteria				×
97–98	4	549	*Desulfobotulus* sp. strain BG14	U85470	δ-Proteobacteria				×
91	2	483	*Desulfofrigus fragile*	AF099065	δ-Proteobacteria				×
98	1	524	*Desulfobacterium catecholicum*	AJ237602	δ-Proteobacteria				×
94	1	218	Uncultured bacterium ODPB-B3	AF121088	δ-Proteobacteria				×
94	1	612	Unidentified bacterium clone NB1-k	AB013832	δ-Proteobacteria				×
91	1	587	*Plesiomonas shigelloides*	X60418	γ-Proteobacteria				×
93	1	583	Uncultured bacterium strain BD1-7	AB015519	γ-Proteobacteria				×
92	1	564	*Pseudoalteromonas* sp. strain A25	AF227237	γ-Proteobacteria				×
98	1	652	*Vibrio alginolyticus* (ATCC 17749T)	X56576	γ-Proteobacteria				×
89	1	582	Unidentified bacterium, clone NB1-o	AB013836	γ-Proteobacteria				×
94	1	398	Uncultured bacterium adhufec29.25	AF153855	γ-Proteobacteria				×
91	1	571	*Cytophaga* sp. strain JTB244	AB015262	CFB				×
86	1	325	*Flexibacter tractuosus*	M58789	CFB				×
94	1	487	*Microscilla furvescens*	M58792	CFB				×
91	1	331	*Psychroserpens burtonensis* ACAM188	U62913	CFB				×
96	1	503	Uncultured bacterium KC305	AB022513	CFB				×
92	1	589	Uncultured cytophagales QSSC9L-1	AF170779	CFB				×
96	1	602	*Clostridium halophilum* DSM 5387	X77837	Firmicutes				×
89	1	411	Uncultured soil bacterium clone K20-71	AF145861	Firmicutes				×
87	1	415	Uncultured bacterium Sva0855	AJ240981	Firmicutes				×
87	1	566	Uncultured eubacterium clone vadinBB35	U81761	Unknown				×

[a] Listed are the percent identities (ID%) to previously identified sequences, the numbers of similar clones, the numbers of base pairs sequenced (bp), and the accession numbers and divisions of the best s-matched organism in GenBank.

[b] × signs indicate whether the clone occurred in the overlying seawater (SW), healthy coral tissues (HC), black band diseased coral tissue (BBD), or dead coral skeleton surfaces (DC).

Desulfovibrio and the associated genus *Desulfobotulus* were detected in clone libraries from all three coral species (Tables 1, 2, and 3). Sequences associated with *Trichodesmium* and *Clostridium* occurred in BBD mat clone libraries from *M. annularis* and *D. strigosa* (Tables 1 and 3, respectively).

Microbial communities inhabiting dead coral surfaces. Clone libraries from dead surfaces of the *M. annularis*, *M. cavernosa*, and *D. strigosa* colonies also contained a high diversity of sequences, representing 6 to 9 microbial divisions (Fig. 3D, 4D, and 5D, respectively). However, the relative proportions of sequences representing each division varied significantly between species. In general, clone libraries were dominated by δ-proteobacteria (0 to 42%), α-proteobacteria (5 to 17%), γ-proteobacteria (0 to 28%), and CFB (0 to 17%). Sequences detected on dead coral surfaces were 95% distinct from those detected in the overlying seawater, healthy coral tissues, and the BBD microbial mats.

DISCUSSION

The optical and molecular analyses completed in this study of corals infected with BBD on Curaçao indicate that bacterial communities are distinctly partitioned between overlying seawater and healthy, diseased, and dead coral surfaces. The following discussion evaluates the implications of this partitioning with respect to the proportion of cyanobacterium-related sequences in reef tract seawater clone libraries, the possibility of coral species-specific microbial communities, and the microbial ecology of BBD in *M. annularis*, *M. cavernosa*, and *D. strigosa* colonies.

Reef tract bacterioplankton. Sequences affiliated with two globally distributed bacterioplankton were detected in all seawater clone libraries collected from the Curaçao reef tract. The most common was *Prochlorococcus*, which is the smallest yet most abundant oxygenic photoautotroph in tropical and sub-

TABLE 2. 16S rRNA sequencing results for a *Montastrea cavernosa* colony from the back reef at Playa Kalki[a]

ID%	No. of similar clones	No. of base pairs sequenced	Best-matched organism	Accession no.	Division	Location of Clone[b]			
						SW	HC	BBD	DC
98	2	594	Uncultured bacterium SAR102	L35460	α-Proteobacteria	×			
94–98	2	534	Uncultured bacterium OCS126	AF001638	α-Proteobacteria	×			
91	1	543	*Caedibacter caryophilus*	AJ238683	α-Proteobacteria	×			
92	1	573	*Olavius loisae* endosymbiont 2	AF104473	α-Proteobacteria	×			
99	1	596	Uncultured *Roseobacter* NAC11-1	AF245630	α-Proteobacteria	×			
98	1	610	Uncultured bacterium EBAC31A08	AF268219	δ-Proteobacteria	×			
92	1	334	Uncultured bacterium CHAB-II-49	AJ240909	δ-Proteobacteria	×			
98–99	2	546	Unknown marine bacterioplankton SAR7	X52171	δ-Proteobacteria	×			
94	2	587	Unidentified marine bacterium OM60	U70696	γ-Proteobacteria	×			
98–99	9	587	*Prochlorococcus* sp. strain MIT9202	AF115269	Cyanobacteria	×			
98	3	546	Uncultured *Synechococcus* sp. strain NAC1-5	AF245618	Cyanobacteria	×			
96	1	454	*Prochlorococcus marinus pastori*	AF180967	Cyanobacteria	×			
99	1	603	*Prochlorococcus* sp. strain MIT9312	AF053398	Cyanobacteria	×			
99	1	602	*Synechococcus* WH8101	AF001480	Cyanobacteria	×			
92	2	675	Uncultured *Cytophagales* CRE-FL75	AF141488	CFB	×			
93	1	688	Marine psychrophile sp. SW17	AF001368	CFB	×			
93	1	645	Uncultured marine bacterium ZD0403	AJ400347	CFB	×			
99	1	588	Unidentified cytophagales OM188	U70687	CFB	×			
94	1	601	Unidentified planctomycete OM190	U70712	Planctomycetales	×			
98	1	567	Unidentified bacterium isolate HRV16	Z88588	Unknown	×			
95	12	564	Unidentified beta proteobacterium OPB30	AF026979	β-Proteobacteria		×		
94	6	558	*Hydrogenophilus thermoluteolus* TH-4	AB009829	β-Proteobacteria		×		
95	1	478	Unidentified beta proteobacterium OPS140	AF026983	β-Proteobacteria		×		
95–96	2	664	Uncultured epsilon proteobacterium KTc1160	AF235116	ε-Proteobacteria		×		
98–99	34	539	Chromatium sp. RW	AF384210	γ-Proteobacteria		×		
99	1	406	*Escherichia coli* K12 MG1655	AE000345	γ-Proteobacteria		×		
95	1	527	Uncultured alpha proteobacterium SIC.926	AF277517	α-Proteobacteria			×	
99	1	583	Uncultured proteobacterium clone CD5H5	AY038412	α-Proteobacteria			×	
93	1	588	*Maricaulis* sp. strain MCS18	AJ227806	α-Proteobacteria			×	
94	1	607	Uncultured alpha proteobacterium KTc0993	AF235129	α-Proteobacteria			×	
95	1	583	Uncultured proteobacterium clone CD4D6	AY038529	δ-Proteobacteria			×	
99	2	515	*Desulfovibrio* sp. strain TBP-1	AF090830	δ-Proteobacteria			×	×
98	1	582	Uncultured proteobacterium clone CD5B11	AY038410	ε-Proteobacteria			×	
96	1	321	*Shewanella* sp. clone NB65-G	AB013842	γ-Proteobacteria			×	
93	1	606	*Marinobacter hydrocarbonoclasticus*	Y18240	γ-Proteobacteria			×	
99	1	566	*Pseudomonas stutzeri*	AY017341	γ-Proteobacteria			×	
93–94	2	443	Uncultured gamma proteobacterium clone 26	AF369718	γ-Proteobacteria			×	
96	1	542	Unidentified proteobacterium strain NKB4	AB013256	γ-Proteobacteria			×	
92	2	616	*Oceanospirillum linum*	M22365	γ-Proteobacteria			×	
88	1	530	Marine bacterium BBFL7	AY028207	CFB			×	
99	1	630	Uncultured *Cytophagales* clone CD4B12	AY038511	CFB			×	
92	1	597	*Parasporobacterium paucivorans* sp. SYR1	AJ272036	Firmicutes			×	
92–95	2	478	*Spirochaeta litoralis*	M88723	Spirochaetales			×	×
91	1	220	Uncultured rumen bacterium 4C3d-12	AB034093	Unknown			×	
91	1	612	Unidentified butyrate-producing L1-92	AJ270487	Unknown			×	
97	1	613	Uncultured Crater Lake bacterium CL0-45	AF316686	Unknown			×	
98	2	435	*Silicibacter lacuscaerulensis*	U77644	α-Proteobacteria				×
97	1	489	Alpha proteobacterium MBIc1876	AB026194	α-Proteobacteria				×
88	1	489	Uncultured alpha proteobacterium MB13E08	AY033327	α-Proteobacteria				×
95	2	497	*Caulobacter* sp. strain MCS33	AJ227811	α-Proteobacteria				×
96	1	341	Uncultured *Rhodobacter* CtaxPhil-16	AF259624	α-Proteobacteria				×
97	1	477	*Agrobacterium gelatinovorum*	D88523	α-Proteobacteria				×
95	1	342	Uncultured alpha proteobacterium CHAB-I-5	AJ240910	α-Proteobacteria				×
97	1	373	*Sulfitobacter pontiacus*	AF182018	α-Proteobacteria				×
90	1	399	Uncultured ferromanganous bacterium MND	AF292999	α-Proteobacteria				×
99	1	333	Beta proteobacterium OS-ac-15	U46749	β-Proteobacteria				×
87	1	296	*Desulfovibrio zosterae*	Y18049	δ-Proteobacteria				×
90–91	2	555	*Desulfocella halophila*	AF022936	δ-Proteobacteria				×
91	1	425	Delta proteobacterium S2551	AF177428	δ-Proteobacteria				×
89	1	302	*Desulfovibrio alaskensis* NCIMB13491	Y11984	δ-Proteobacteria				×
87	1	462	Uncultured delta proteobacterium Sva0447	AJ240999	δ-Proteobacteria				×
92	1	535	*Desulfofrigus oceanense* strain ASv26	AF099064	δ-Proteobacteria				×
96	1	371	*Desulfobotulus* sp. strain BG14	U85470	δ-Proteobacteria				×

Continued on following page

TABLE 2—*Continued*

ID%	No. of similar clones	No. of base pairs sequenced	Best-matched organism	Accession no.	Division	Location of Clone[b]			
						SW	HC	BBD	DC
95	1	459	Uncultured epsilon proteobacterium 1006	AB030592	ε-Proteobacteria				×
92	1	512	Uncultured epsilon proteobacterium 1065	AB030598	ε-Proteobacteria				×
93	1	454	*Campylobacter* sp. strain DSM806	AF144694	ε-Proteobacteria				×
96	1	351	*Arcobacter* sp. clone A3b2	AJ271655	ε-Proteobacteria				×
96	1	421	Uncultured epsilon proteobacterium KTc116	AF235116	ε-Proteobacteria				×
99	1	470	*Vibrio* sp. strain Lu1	AF094701	γ-Proteobacteria				×
90–91	2	406	*Vibrio proteolyticus* (ATCC 15338T)	X74723	γ-Proteobacteria				×
96	1	335	*Photobacterium damselae* subsp. *damselae*	AB032015	γ-Proteobacteria				×
93–94	2	367	Uncultured gamma proteobacterium EC-B3	AF287041	γ-Proteobacteria				×
89	1	408	*Halomonas* sp. strain Eplume3.D3	AF212203	γ-Proteobacteria				×
89	1	447	*Pseudoalteromonas aurantia*	AF025570	γ-Proteobacteria				×
99	1	428	*Alteromonas macleodii* strain DSM 6062	Y18228	γ-Proteobacteria				×
95	2	535	*Pseudoalteromonas* sp. strain A25	AF227237	γ-Proteobacteria				×
95	1	472	Uncultured proteobacterium TIHP368-52	AB031651	γ-Proteobacteria				×
94	1	489	Uncultured proteobacterium CHAB-IV-34	AJ240917	γ-Proteobacteria				×
90	1	366	*Vibrio halioticoli* strain 1AM14599	AB000393	γ-Proteobacteria				×
90	1	344	*Vibrio rumoiensis*	AB013297	γ-Proteobacteria				×
94	1	459	Unclassified *Pseudomonas* group	AF102866	γ-Proteobacteria				×
98	1	453	*Eubacterium tenue*	M59118	Firmicutes				×
91	3	414	Uncultured low-G+C gram-positive MT35	AF211297	Firmicutes				×
91	2	431	Uncultured low-G+C gram-positive 36-3	AF351218	Firmicutes				×
86	1	560	*Clostridium estertheticum* (NCIMB12511)	X68181	Firmicutes				×
99	1	464	*Propionibacterium acnes* isolate 8261	AB042291	Firmicutes				×
89	1	522	*Paenibacillus* sp. strain EE17	AF306538	Firmicutes				×
91	1	472	*Sporocytophaga myxococcoides*	AJ310654	CFB				×
86–87	3	392	*Cytophaga* sp. strain JTB250	AB015264	CFB				×
86	1	475	Uncultured bacterium BS5	AF087089	CFB				×
93	1	501	Bacterium SB12	AF367851	CFB				×
93	1	517	*Cytophaga* sp. strain BD1-27	AB015528	CFB				×
91	2	486	*Flavobacteriaceae* SA-0082	AB057592	CFB				×
91–92	2	591	*Cytophaga fermentans*	M58766	CFB				×
93	1	549	*Cytophaga* sp. strain JTB132	AB015260	CFB				×
91	1	474	Uncultured bacterium TX2	AF298764	CFB				×
93	1	485	*Symploca* sp. strain VP642c	AY032934	Cyanobacteria				×
73	1	371	Bacterium 2-400 C2.5	Z77637	Planctomycetales				×
98	1	475	Unidentified marine eubacterium Hstp14	U41090	Unknown				×
91	1	475	Uncultured Crater Lake bacterium CL0-6	AF316682	Unknown				×
97	1	377	Uncultured eubacterium CHA3-30	AJ132732	Unknown				×
90	1	361	*Oleiphilus messinensis* isolate ME102	AJ295154	Unknown				×
92	1	414	Rhizosphere soil bacterium isolate RSI-28	AJ252595	Unknown				×
91	3	378	Uncultured bacterium clone Car68rc	AF224865	Unknown				×
94	1	576	Uncultured eubacterium CHA3-437	AJ132728	Unknown				×
90–91	3	409	Uncultured bacterium CHAB-II-49	AJ240909	Unknown				×
98	1	552	Uncultured Crater Lake bacterium CL120-63	AF316691	Unknown				×
88	1	372	*Codium fragile*	U08345	Chloroplast				×
85	1	318	*Chondrus crispus*	Z29521	Chloroplast				×

[a] Abbreviations are as defined in footnote *a* to Table 1.

[b] × signs indicate whether the clone occurred in the overlying seawater (SW), healthy coral tissue (HC), black band diseased coral tissue (BBD), or dead coral skeleton surfaces (DC).

tropical seas (16, 44). The second cyanobacterium was *Synechococcus*, a genus which has been combined with that of *Prochlorococcus* into a single clade called the picophytoplankton (69). The phenomenon of the large proportion of cyanobacterium sequences detected in the Curaçao seawater clone library is somewhat unique with respect to bacterioplankton found in open ocean surface seawater. Sequences affiliated with cyanobacteria from the Mediterranean Sea comprised only 6 to 8% of the clone libraries from offshore surface waters (1, 2, 3). Similarly low proportions of cyanobacteria have also been detected in surface waters of the Pacific and North Atlantic oceans and the North Sea (12, 19, 20, 24, 41, 44, 46, 64, 65, 66).

The relatively large proportion of sequences affiliated with cyanobacteria in Curaçao seawater relative to those reported in rDNA surveys from other locations may reflect the ecological differences between near-shore and offshore marine environments. The near-shore reef tract setting on Curaçao is strongly influenced by the physical and chemical effects of terrestrial runoff, which include coastal pollution and organic as well as inorganic sedimentation (37). It is therefore not unexpected that the composition of bacterioplankton communities in near-shore and offshore environments would track these environmental differences (66). Another possibility is that this discrepancy in the proportions of cyanobacteria may result from methodological differences. The bead beating used

TABLE 3. 16S rRNA sequencing results for a *Diploria strigosa* colony from the back reef at Water Plant[a]

ID%	No. of similar clones	No. of base pairs sequenced	Best-matched organism	Accession no.	Division	Location of clone[b]			
						SW	HC	BBD	DC
98	1	567	Uncultured marine bacterium ZD0409	AJ400350	α-Proteobacteria	×			
96	1	568	Uncultured marine eubacterium HstpL28	AF159650	α-Proteobacteria	×			
99	3	604	*Pseudoalteromonas* sp. isolate PRLIST2	Y15323	γ-Proteobacteria	×			
99	2	610	*Pseudomonas* sp. strain MBIC2027	AB030085	γ-Proteobacteria	×			
97	1	622	*Alteromonas macleodii* strain CH-518	Y18232	γ-Proteobacteria	×			
99	1	423	*Alteromonas macleodii* strain DSM 6062	Y18228	γ-Proteobacteria	×			
99	1	444	*Pseudoalteromonas* sp. strain A28	AF227238	γ-Proteobacteria	×			
99	1	572	Uncultured bacterium Car164	AF285610	γ-Proteobacteria	×			
98	1	560	Uncultured CHAB-I-7	AJ240911	γ-Proteobacteria	×			
91	1	619	Uncultured KTc0924	AF235121	γ-Proteobacteria	×			
97	1	511	Uncultured marine eubacterium HstpL66	AF159670	γ-Proteobacteria	×			
97	1	598	Uncultured OCS44	AF001650	γ-Proteobacteria	×			
99	1	611	Unidentified bacterium	Z93992	γ-Proteobacteria	×			
98–99	6	593	*Prochlorococcus* sp. strain MIT9202	AF115269	Cyanobacteria	×			
99	3	531	*Prochlorococcus marinus* subsp. *pastoris*	AF180967	Cyanobacteria	×			
99	1	603	*Prochlorococcus* sp. strain MIT9312	AF053398	Cyanobacteria	×			
98	1	603	*Synechococcus* WH8101	AF397728	Cyanobacteria	×			
98–99	3	513	*Cyanophora paradoxa cyanelle*	M19493	Chloroplasts	×			×
97	1	603	*Guillardia theta*	AF041468	Chloroplasts	×			
91	2	638	*Cyanophora paradoxa cyanelle*	M19493	Chloroplasts	×			×
92	1	659	Marine psychrophile SW17	AF001368	CFB	×			
92	1	419	*Fusibacter paucivorans*	AF050099	Firmicutes	×			
98	1	594	Unidentified eubacterium clone SAR276	U65915	Planctomycetales	×			
98	1	532	Unidentified planctomycete OM55	U70681	Planctomycetales	×			
96	1	548	Uncultured eubacterium TRA2-10	AF047642	Unknown	×			
100	1	554	Unidentified bacterium isolate HRV39	Z88591	Unknown	×			
95–96	3	347	Uncultured marine eubacterium HstpL93	AF159684	γ-Proteobacteria		×		
96	7	389	Uncultured marine eubacterium HstpL43	AF159674	γ-Proteobacteria		×		
93–96	4	466	Unidentified strain NKB4	AB013256	γ-Proteobacteria		×		
93	13	542	Uncultured gamma proteobacterium clone 26	AF369718	γ-Proteobacteria		×		
92	13	698	*Oceanospirillum linum*	AF260752	γ-Proteobacteria		×		
92	1	567	*Pseudomonas* sp. strain IMT40	AF302796	γ-Proteobacteria		×		
92	1	471	*Pseudomonas denitrificans* IAM 12023	AB021419	γ-Proteobacteria		×		
93	1	541	Uncultured proteobacterium MBIC3958	AB020600	γ-Proteobacteria		×		
97	1	385	*Haemophilus paraphrophilus*	M75042	γ-Proteobacteria		×		
92	1	613	*Oceanospirillum maris williamsae* IFO15468	AB006763	γ-Proteobacteria		×		
99–100	4	604	*Propionibacterium acnes*	AF154832	Firmicutes		×		
97	1	373	Uncultured *Cytophagales* clone CRE-PA10	AF141499	CFB		×		
91	1	576	*Flexibacter aggregans*	M64628	CFB		×		
98	1	590	Uncultured *Cytophagales* clone CD4E12	AY038534	CFB		×		
91	1	635	*Planktothrix* sp. strain FPI	AF212922	Cyanobacteria		×		
93	2	588	*Xenococcus* PCC7305	AF132783	Cyanobacteria		×		
92	1	546	Arctic seawater bacterium R7366	AJ293826	Unknown		×		
89–98	8	471	*Clostridium halophilum* DSM 5387	X77837	Firmicutes			×	×
88	1	370	*Eubacterium oxidoreducens* strain G2-2	AF202259	Firmicutes			×	
96	1	605	Uncultured *Cytophaga* kps30	AF195441	Firmicutes			×	
89–94	5	470	*Cytophaga* sp. strain JTB132	AB015260	CFB			×	
87–93	3	535	*Cytophaga fermentans*	M58766	CFB			×	
89	1	433	*Flavobacterium columnare*	AB023660	CFB			×	
90	1	348	*Flavobacterium* sp. strain A43	AB008043	CFB			×	
97	1	480	*Roseobacter* sp. (*Prionitis* symbiont)	AF107210	α-Proteobacteria			×	
91	1	596	Unidentified proteobacterium strain BD7-3	AB015579	α-Proteobacteria			×	
96	1	440	*Desulfobotulus* sp. strain BG14	U85470	δ-Proteobacteria			×	
96	3	512–607	Uncultured epsilon proteobacterium KTc1160	AF235116	ε-Proteobacteria			×	×
91–92	2	624	Uncultured proteobacterium strain BD1-29	AB015529	ε-Proteobacteria			×	
94–99	3	557	*Alteromonas macleodii*	AF025957	γ-Proteobacteria			×	
94–95	2	462	*Oceanospirillum* sp. strain ME113	AJ302700	γ-Proteobacteria			×	
92	2	499	*Neptunomonas naphthovorans*	AF053734	γ-Proteobacteria			×	
95	1	489	Unclassified *Pseudomonas* group	AF102866	γ-Proteobacteria			×	
99	1	565	*Vibrio campbelli* ATCC 25920T	X74692	γ-Proteobacteria			×	
82	1	547	*Spinacia oleracea*	M21453	Chloroplasts			×	
89	1	473	*Nephroselmis olivacea*	X74754	Chloroplasts			×	
93	1	577	*Spirochaeta litoralis*	M88723	Spirochaetales			×	
93	1	532	*Trichodesmium tenue*	AF013029	Cyanobacteria			×	
89	1	491	Uncultured bacterium TIHP302-14	AB031600	Unknown			×	

Continued on following page

TABLE 3—*Continued*

ID%	No. of similar clones	No. of base pairs sequenced	Best-matched organism	Accession no.	Division	Location of clone[b]			
						SW	HC	BBD	DC
94	2	525–567	*Desulfovibrio aespoeensis* (isolate Aspo2)	X95230	δ-Proteobacteria			×	×
95	1	546	North Sea bacterium H120	AF069667	Unknown			×	
88	1	626	Unidentified bacterium strain BD2-14	AB015542	Unknown			×	
93	1	544	Bacterium strain 77003	AF227847	Unknown			×	
90	1	356	Marine snow bacterium Adriatic87	AF030773	Unknown			×	
94	1	568	Uncultured bacterium PENDANT-24	AF142936	α-Proteobacteria				×
99	1	338	*Escherichia coli* K12 MG1655	AE000345	γ-Proteobacteria				×
91	1	768	Uncultured gamma proteobacterium CHAB-IV-34	AJ240917	γ-Proteobacteria				×
93	1	297	Uncultured gamma proteobacterium DSS65	AJ401386	γ-Proteobacteria				×
94	1	355	Uncultured gamma proteobacterium KTc119	AF235120	γ-Proteobacteria				×
94	4	612	*Chlorobium vibrioforme*	Y08103	Green Sulfur Bacteria				×
96	1	622	*Prosthecochloris aestuarii*	AJ291826	Green Sulfur Bacteria				×
96	1	505	Uncultured bacillariophyte AWS98-19b	AF327029	Chloroplasts				×
91	1	614	*Epulopiscium* sp. morphotype B	M99574	Firmicutes				×
97–98	2	576	Uncultured marine eubacterium HstpL78	AF159652	Unknown				×

[a] Abbreviations are as defined in footnote *a* to Table 1.
[b] × signs indicate whether the clone occurred in the overlying seawater (SW), healthy coral tissue (HC), black band diseased coral tissue (BBD), or dead coral skeleton surfaces (DC).

in the present study may have more effectively lysed the tough cyanobacterial cell walls than the techniques used for the offshore studies, none of which applied bead beating. Furthermore, the consistently high proportion of cyanobacteria in all three of the seawater samples analyzed from Curaçao (Fig. 3A, 4A, and 5A) suggests that this is an accurate representation of the reef tract bacterioplankton clone library.

Healthy coral microbial communities. Sequencing results in the present study indicate that the microbial communities inhabiting healthy coral tissue have the following characteristics: (i) they are unique in that they are distinct from the bacterioplankton in overlying seawater, especially with respect to cyanobacteria sequences; and (ii) they are markedly different among the three coral species. Significant reductions in the proportion of cyanobacterium-affiliated sequences from the seawater clone libraries (30 to 43%) to those from the healthy coral tissue clone libraries (0 to 5%) (Fig. 3A and B, 4A and B, and 5A and B, respectively) are likely to be the result of chemical defense mechanisms that inhibit coral tissue colonization by cyanobacteria (35). This partitioning is also consistent with the results of previous optical and culture-based studies of the mucus-rich biofilm covering coral tissue, which is called the coral surface microlayer (CSM) (13, 14, 38, and 45). Expelled and free-living zooxanthellae are prominent components of the CSM, which protects coral from light, exposure, and sedimentation and is the first line of defense against disease infection (11, 38, 45, 56).

Inferred metabolisms from the *M. annularis* clone library sequences suggest that mixtures of aerobic and anaerobic microbes inhabit the healthy coral tissue (Tables 1, 2, and 3). This type of mixed metabolic assemblage is similar to those of the diverse microbial communities detected in the tissues of marine sponges, where low-oxygen microniches occur in the pores of well-oxygenated sponge surfaces (73). In addition, several other bacteria inhabiting healthy *M. annularis* tissue have not previously been observed in marine environments. Specifically, sequences of several microbial strains, which comprise 3% of the *M. annularis* healthy tissue clone library, were previously isolated exclusively from terrestrial soils (e.g., agricultural soil bacterium SC-I-iS and unidentified soil bacterium clones BSV72 and BSV73; Tables 1, 2, and 3).

Sequences from clone libraries constructed from healthy *M. annularis* tissue exhibit significantly higher bacterial diversity (10 divisions) than those from clone libraries constructed from healthy *M. cavernosa* and *D. strigosa* tissue (3 and 4 divisions, respectively; Fig. 3B, 4B, and 5B, respectively). These preliminary results imply that scleractinian corals may contain species-specific microbial communities. The abundance of γ-proteobacteria and β-proteobacteria and the low overall sequence diversity levels observed in *M. cavernosa* and *D. strigosa* (Fig. 4B and 5B) are somewhat similar to those of the microbial communities detected with molecular screening of healthy tissues from a single *Montastrea franksi* colony in Panama (4 divisions) (51). Sequences affiliated with *Silicibacter lacuscaerulensis* were also detected in several other healthy *M. franksi* colonies by using denaturing gradient gel electrophoresis techniques (51). However, *S. lacuscaerulensis* sequences were only detected in the present study on Curaçao in the dead coral surface clone library of *M. cavernosa* (Table 2). This further supports the possibility that individual coral species contain unique microbial consortia. An important difference from the Curaçao corals is that *M. franksi* healthy tissue clone libraries from Panama were dominated by cyanobacteria (51), which is surprising given the chemical mechanisms inhibiting cyanobacterial settlement on healthy coral tissues (35). In addition, *M. franski* did not contain chloroplast-affiliated sequences in the healthy tissue clone libraries (51), which was unexpected given the abundance of zooxanthellae in the coral tissue and the CSM (45) and their use of primers similar to those applied in the present study.

Microbes associated with BBD. The BBD microbial mat is dominated by large filamentous cyanobacteria originally identified as *Oscillatoria submembranaceae* (A. Antonius, Abstr. 10th Meet. Assoc. Isl. Mar. Lab. Caribb., p. 3, 1973 [abstr.]) and

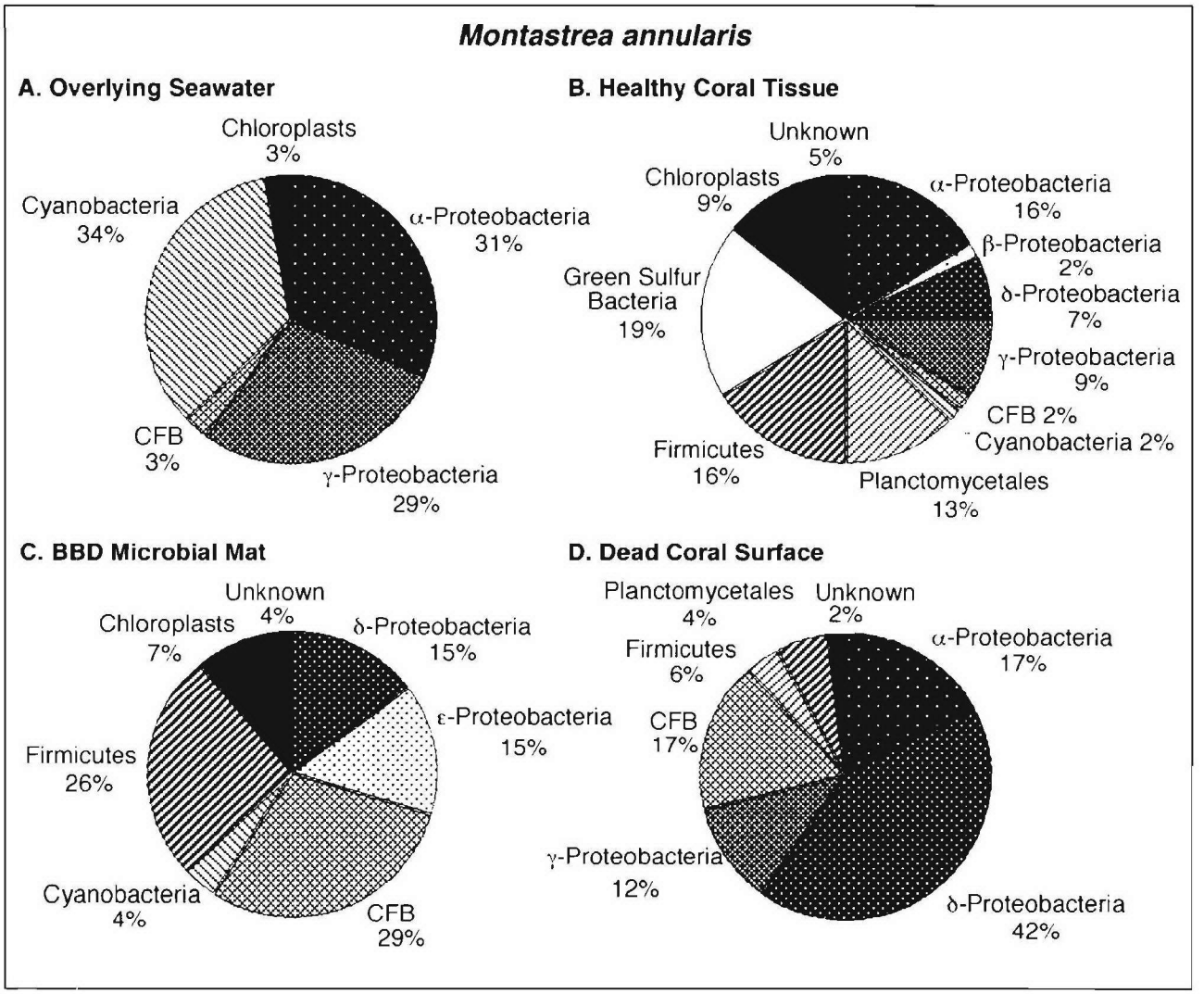

FIG. 3. Pie diagrams illustrating the division-level diversity of the partial 16S rRNA bacterial sequences comprising the clone libraries associated with *M. annularis*. The colony was growing in the back reef environment at Playa Kalki at a 5-m water depth. The seawater at the time and location of sampling in August 2000 was at a temperature of 27.5°C.

later systematically reclassified as *Phormidium corallyticum* (52). Other bacteria previously identified in the BBD mat include motile, nonphotosynthetic sulfide-oxidizing *Beggiatoa* spp. (optically identified) (14, 18, and 52) and the sulfate-reducing *Desulfovibrio* spp. (identified optically and with 16S rRNA oligonucleotide probes) (18 and 53 and S. Schnell, B. Assmus, and L. L. Richardson, abstract from the Annual Meeting of the VAAM [Vereinigung fuer Allgemeine und Angewandte Mikrobiologie] and GBCH [Gesellschaft fuer Biologische Chemie], Biospecktrum, p. 116, 1996 [abstr.]). Although SEM imaging for the present report indicated that the BBD microbial mat was predominantly composed of filamentous cyanobacteria (Fig. 2G and H), cyanobacterial sequences represented only 0 to 4% of the BBD mat clone libraries (Table 1). Furthermore, neither *P. corallyticum* or *Beggiatoa* sp. sequences were detected in the BBD mat (Tables 1, 2, and 3).

One explanation for these discrepancies may be that *P. corallyticum* has not been previously sequenced. While several species of terrestrial *Phormidium* have been detected in desert soil crusts (17), no marine species have previously been reported in GenBank. Similarly, multiple *Beggiatoa* species have been sequenced from other marine environments (3) but their sequences were not similar to those in the BBD mat clone library. Another explanation could be that *P. corallyticum* and *Beggiatoa* spp. were represented by one of the unknown bacterial sequences in the BBD mat clone library (Fig. 3, 4, and 5). Other possibilities are that they are present in the BBD mat but their rDNA was not extracted, amplified, and sequenced and they are not present in the BBD mat. It is important to note that sequences affiliated with the filamentous cyanobacterium *Trichodesmium tenue* were found in the BBD mats (Tables 1, 2, and 3). Members of the family *Trichodesmium* (formerly *Oscillatoria*) are nonheterocystous nitrogen-fixing (diazotrophic) cyanobacteria that are a globally abundant com-

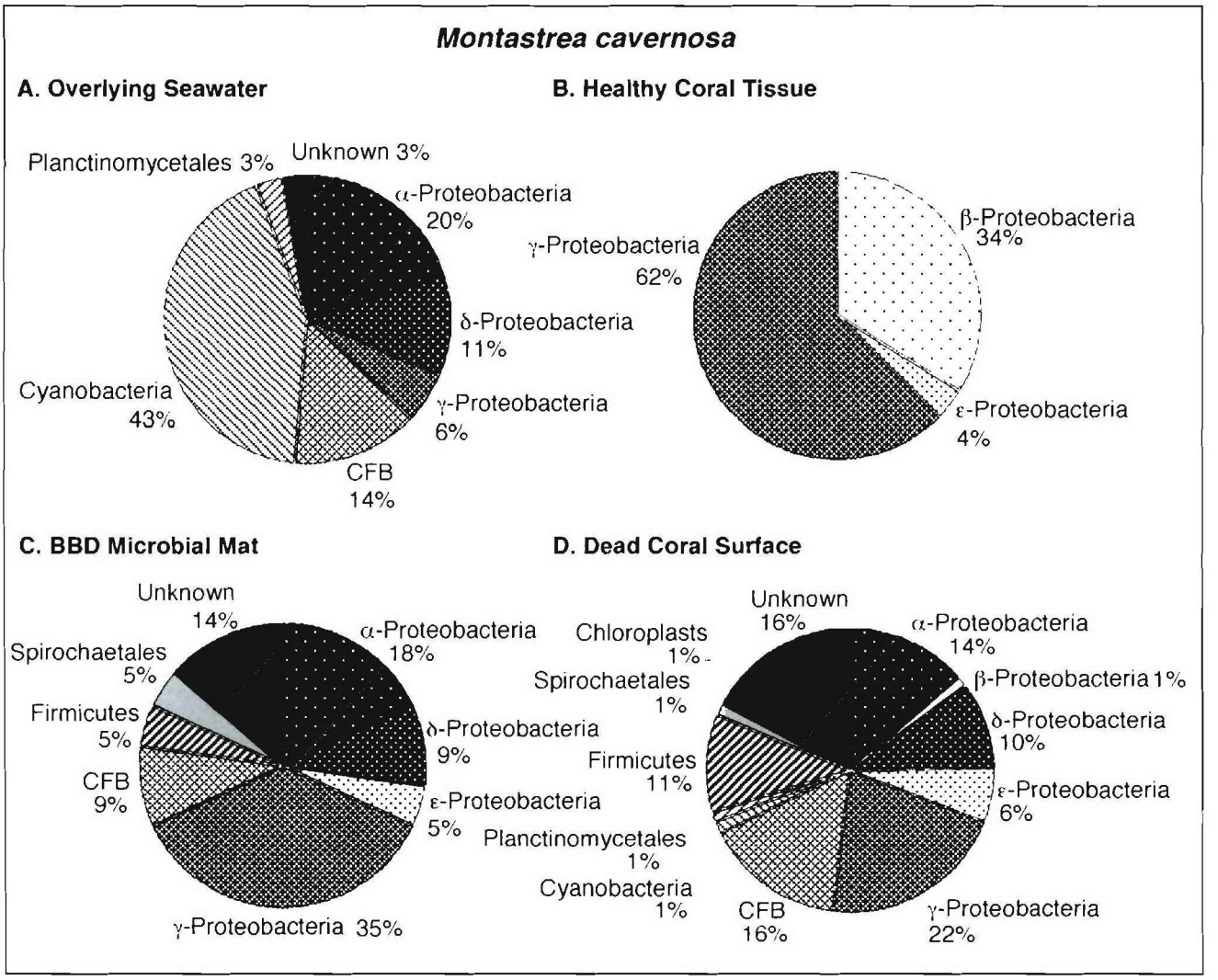

FIG. 4. Pie diagrams illustrating the division-level diversity of the partial 16S rRNA bacterial sequences comprising the clone libraries associated with *M. cavernosa*. The colony was growing in the back reef environment at Playa Kalki at a 5-m water depth. The seawater at the time and location of sampling in August 2000 was at a temperature of 27.5°C.

ponent of bacterioplankton in tropical and subtropical oceans (9, 34).

Implications for the microbial ecology of BBD. Several of the microbial sequences detected in the seawater and healthy, BBD-infected, and dead coral surface clone libraries (Tables 1, 2, and 3) are affiliated with microbes with one or more of the following characteristics: (i) they have previously been reported in humans, some commonly occurring in human sewage; (ii) they are known pathogens in other marine and terrestrial organisms; or (iii) they were derived from terrestrial soils. The following discussion summarizes what is known of the ecologies and pathogenicities of the microorganisms whose affiliated sequences have been found in the BBD mat.

Several of the sequences detected on the coral surfaces are affiliated with microbes that are known pathogens in humans. Sequences affiliated with the genus *Clostridium*, which occur in the BBD mat clone library of *M. annularis* (Table 1), are commonly part of mixed-pathogen infections in a variety of terrestrial organisms, including humans and birds (61, 62). The presence of clostridial spores is commonly used as an indication of fecal contamination in drinking water. Pathogenic clostridia, which are gram-positive obligatory anaerobes incapable of dissimilatory reduction of sulfate, produce toxins that necrotize body tissues or interfere with nerve transmission (31, 60). Sequences affiliated with the genera *Campylobacter* and *Arcobacter* were also detected in the BBD and dead coral surface clone libraries (Tables 1, 2, and 3). These ε-proteobacteria have been grouped into the bacterial family *Campylobacteraceae*, a diverse group of gram-negative commensal and pathogenic bacteria that colonize the mucosal surfaces of the intestinal tracts, oral cavities, or urogenital tracts in humans and other animal hosts (68, 70). *Arcobacter* spp. are known enteropathogens that cause abdominal cramps in children (71, 72). *Campylobacter* spp. are a major cause of bacterial enteritis in humans and are commonly found in polluted seawater contaminated with sewage (28, 29). The absence of

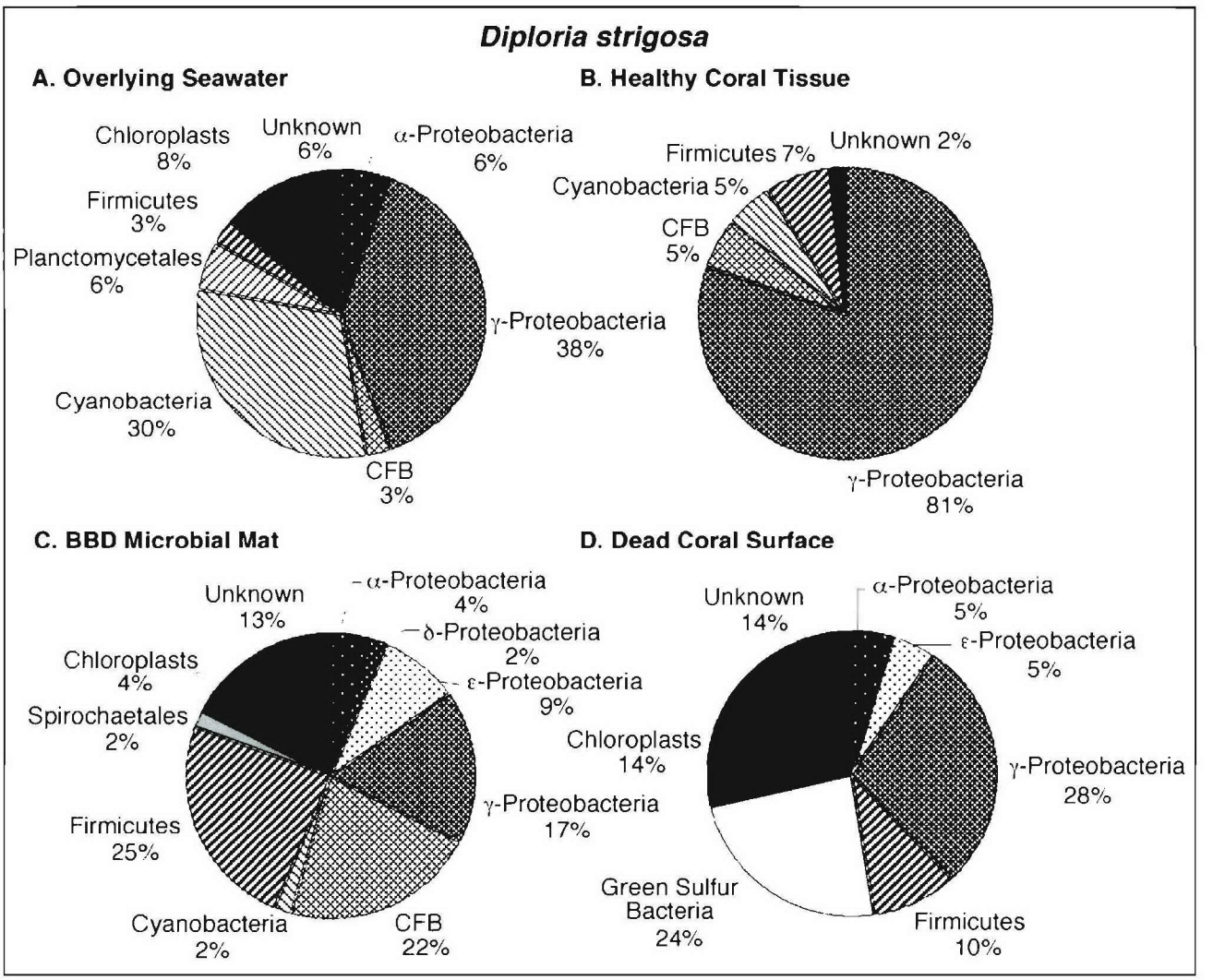

FIG. 5. Pie diagrams illustrating the division-level diversity of the partial 16S rRNA bacterial sequences comprising the clone libraries associated with *D. strigosa*. The colony was growing in the back reef environment at Water Plant at a 4-m water depth. The seawater at the time and location of sampling in August 2000 was at a temperature of 27.5°C.

these bacteria on the dead coral surfaces suggests that none of the BBD bacteria remain behind as the BBD mat migrates. Thus the mat itself could be a requirement for the survival of these bacteria. Therefore, the BBD bacterial community has specificity for the living and dying coral tissues but not for the dead skeletal surface of the coral. One possible source for these bacteria could be human sewage.

It is also possible that BBD has been transmitted by infected fish that bite, eat, defecate upon, or otherwise come in contact with healthy corals. *Cytophaga fermentans*, detected in the BBD mats of *M. annularis* and *D. strigosa*, is thought to be responsible for a number of illnesses in freshwater and saltwater fish, including eroded mouth, columnaris, cotton wool, cold water, hemorrhagic gill, saddle back, and branchionephritis diseases and ulcers, tail and fin rot, and black patch necrosis (5, 7, 30). Although the precise etiology of each of these diseases is not well understood, environmental factors correlated with the onset of infection include extremely high or low temperatures, low oxygen levels, and reduced availability of dissolved Fe^{3+} (8, 40). Another possibility is that *T. tenue* may have carried out the pathogenic functions previously ascribed to *P. corallyticum* (49, 53, 67). *T. tenue* produces intracellular biotoxins that have proven to be toxic to zooplankton and other higher animals, such as the copepod *Acartia tonsa* (23, 26, 58). If present in the BBD mat, *T. tenue* would primarily utilize nitrogenase linked to O_2-depleted microzones within aggregated filaments to carry out highly efficient nitrogen fixation during oxygenic photosynthesis (42, 43). These nutrient and oxygen regimes are similar to those of the microenvironments in the BBD mat (10, 49).

An additional possibility raised by the results in this report is that bacteria derived from terrestrial soils may have played a role in the development of BBD infections on the Curaçao reef tract. This conjecture is based on the detection of a large number of sequences affiliated with terrestrial soil bacteria on the healthy, BBD-infected, and dead coral surfaces (Tables 1,

2, and 3). It is possible that these soil bacteria were attached to soil-derived particles that were transported via terrestrial runoff onto the reef tract, settled onto coral colonies, and inoculated healthy coral tissues. However, it is unknown if these bacteria were alive or dead at the time that they were collected. The feasibility of this mechanism is exemplified by the results of studies of the terrestrial fungus *Aspergillus sydowii*, an organism that was derived from terrestrial runoff, which has been identified as a pathogen in marine sea fans (59; G. W. Smith, L. D. Ives, I. A. Nagelkerken, and K. B. Ritchie, Letter, Nature **383**:487, 1996). It has been further hypothesized that *A. sydowii* can be attached to dust particles and can thus cause coral disease, as aerosols settle on the sea surface and become suspended sediment (57).

In summary, the culture-independent molecular methods applied in this study indicate that microbiota are distinctly partitioned between seawater and the surface of BBD-infected corals. Sequences affiliated with known pathogens in humans and other organisms detected in the BBD mat suggest that human sewage, infection from other marine organisms, and terrestrial runoff may all have contributed to the development of the disease. Further advances in understanding BBD etiology will require tracking variations in these microbial communities, as the host corals and zooxanthellae respond to environmental changes in seawater temperature and pollution chemistry.

ACKNOWLEDGMENTS

This work was supported by research grants from the Office of Naval Research (N00014-00-1-0609), the Petroleum Research Fund of the American Chemical Society (34549-G2), and the Geological Society of America (7058-01).

Ongoing discussions with A. Salyers and C. Woese throughout the project significantly added to all aspects of the data collection and interpretation. Reviews by A. Salyers and A. Murray significantly improved the manuscript. S. Schaffers and M. Fortwengler are thanked for taking the underwater photographs.

REFERENCES

1. **Acinas, S. G., F. Rodriguez-Valera, and C. Pedros-Alio.** 1997. Spatial and temporal variation in marine bacterioplankton diversity as shown by RFLP fingerprinting of PCR amplified 16S rRNA. FEMS Microb. Ecol. **24**:27–40.
2. **Acinas, S. G., J. Anton, and F. Rodriguez-Valera.** 1999. Diversity of free-living and attached bacteria in offshore western Mediterranean waters as depicted by analysis of genes encoding 16S rRNA. Appl. Environ. Microbiol. **65**:514–522.
3. **Ahmad, A., J. P. Barry, and D. C. Nelson.** 1999. Phylogenetic affinity of a wide, vacuolate, nitrate-accumulating *Beggiatoa* sp. from Monterey Canyon, California, with *Thioploca* spp. Appl. Environ. Microbiol. **65**:270–277.
4. **Altschul, S. F., W. Gish, W. Miller, E. W. Meyers, and D. J. Lipman.** 1990. Basic local alignment search tool. J. Mol. Biol. **59**:143–169.
5. **Anderson, J. I. W., and D. A. Conroy.** 1969. The pathogenic myxobacteria with special reference to fish diseases. J. Appl. Bacteriol. **32**:30–39.
6. **Antonius, A.** 1981. The "band" diseases in coral reefs. p. 7–14. Fourth International Coral Reef Symposium, vol. 2. Manila, Philippines.
7. **Becker, C. D., and M. P. Fujihara.** 1978. The bacterial pathogen *Flexibacter columnaris* and its epizootiology among Columbia River fish. Monograph No. 2. American Fishery Society, Washington, D.C.
8. **Campbell, A. C., and J. A. Buswell.** 1982. An investigation into the bacterial etiology of "black patch necrosis" in Dover sole, *Solea solea*. J. Fish Dis. **5**:495–508.
9. **Capone, D. G., J. P. Zehr, H. W. Paerl, B. Bergman, and E. J. Carpenter.** 1997. Trichodesmium, a globally significant marine cyanobacterium. Science **276**:1221–1229.
10. **Carlton, R. G., and L. L. Richardson.** 1995. Oxygen and sulfide dynamics in a horizontally migrating cyanobacterial mat: black band disease of corals. FEMS Microbiol. Ecol. **18**:155–162.
11. **Coffroth, M. A.** 1990. Mucous sheet formation on poritid corals: an evaluation of coral mucous as an energy source on reefs. Mar. Biol. **105**:39–49.
12. **Cottrell, M. T., and D. L. Kirchman.** 2000. Natural assemblages of marine proteobacteria and members of the *Cytophaga-Flavobacter* cluster consuming low- and high-molecular-weight dissolved organic matter. Appl. Environ. Microbiol. **66**:1692–1697.
13. **Ducklow, H. W., and D. Mitchell.** 1979. Composition of mucus released by coral coelenterates. Limnol. Oceanogr. **24**:706–714.
14. **Ducklow, H. W., and R. Mitchell.** 1979. Bacterial populations and adaptations in the mucus layers on living corals. Limnol. Oceanogr. **24**:715–725.
15. **Edmunds, P. J.** 1991. Extent and effect of black band disease on Caribbean reefs. Coral Reefs **10**:161–165.
16. **Fuhrman, J. A., and L. Campbell.** 1998. Marine ecology: microbial diversity. Nature **393**:410–411.
17. **Garcia-Pichel, F., and O. Pringault.** 2001. Cyanobacteria track water in desert soils. Nature **413**:380–381.
18. **Garrett, P., and P. Ducklow.** 1975. Coral disease in Bermuda. Nature **253**: 349–350.
19. **Giovannoni, S., and M. S. Rappé.** 2000. Evolution, diversity, and molecular ecology of marine prokaryotes. p. 47–84. *In* D. L. Kirchman (ed.), Microbial ecology of the oceans. Wiley-Liss, Inc., New York, N.Y.
20. **Glöckner, F. O., B. M. Fuchs, and R. Amann.** 1999. Bacterioplankton compositions of lakes and oceans: a first comparison based on fluorescence in situ hybridization. Appl. Environ. Microbiol. **65**:3721–3726.
21. **Goebel, B. M., and E. Stackebrandt.** 1994. Cultural and phylogenetic analysis of mixed microbial populations found in natural and commercial bioleaching environments. Appl. Environ. Microbiol. **60**:1614–1621.
22. **Goreau, T. J., J. Cervino, M. Goreau, R. Hayes, M. Hayes, L. Richardson, G. Smith, K. DeMeyer, I. Nagelkerken, F. J. Garzon, D. Gil, G. Garrison, E. H. Williams, W. L. Bunkley, C. Quirolo, K. Patterson, J. W. Porter, and K. Porter.** 1998. Rapid spread of diseases in Caribbean coral reefs. Rev. Biol. Trop. **46**:157–171.
23. **Guo, C., and P. A. Tester.** 1994. Toxic effect of the bloom-forming *Trichodesmium* sp. (Cyanophyta) to the copepod *Acartia tonsa*. Nat. Tox. **2**:222–227.
24. **Hagström, A., J. Pinhassi, and U. L. Zweifel.** 2000. Biogeographical diversity among marine bacterioplankton. Aquat. Microb. Ecol. **21**: 231–244.
25. **Harvell, C. D., K. Kim, J. M. Burkholder, R. R. Colwell, P. R. Epstein, D. J. Grimes, E. E. Hofmann, E. K. Lipp, A. D. M. E. Osterhause, R. M. Overstreet, J. W. Porter, G. W. Smith, and G. R. Vasta.** 1999. Emerging marine diseases—climate links and anthropomorphic factors. Science **285**:1505–1510.
26. **Hawser, S. P., J. M. O'Neil, M. R. Roman, and G. A. Codd.** 1992. Toxicity of blooms of the cyanobacterium *Trichodesmium* to zooplankton. J. Appl. Phycol. **4**:79–86.
27. **Hayes, R. L., and N. I. Goreau.** 1998. The significance of emerging diseases in the tropical coral reef ecosystem. Rev. Biol. Trop. **46**:173–185.
28. **Healing, T. D., M. H. Greenwood, and A. D. Pearson.** 1992. Campylobacters and enteritis. Rev. Med. Microbiol. **3**:159–167.
29. **Hernandez, J., A. Fayos, J. L. Alonso, and R. J. Rowen.** 1996. Ribotypes and AP-PCR fingerprints of thermophilic campylobacters from marine recreational waters. J. Appl. Bacteriol. **80**:157–164.
30. **Hikida, M., H. Wakabayashi, S. Egusa, and S. Masumura.** 1979. Flexibacter sp., a gliding bacterium pathogenic to some marine fishes in Japan. Bull. Jpn. Soc. Sci. Fish. **45**:421–428.
31. **Hippe, H., J. R. Andreesen, and G. Gottschalk.** 2001. The genus *Clostridium*. *In* The Prokaryotes. Springer-Verlag, New York, N.Y.
32. **Huggenholtz, P., C. Pitulle, K. L. Hershberger, and N. R. Pace.** 1998. Novel division level bacterial diversity in a Yellowstone hot spring. J. Bacteriol. **180**:366–376.
33. **James, N. P., and P. A. Bourque.** 1992. Reefs and Mounds. p. 323–348. *In* R. G. Walker and N. P. James (ed.), Facies models: response to sea level change. Geological Association of Canada, St. John's, Canada.
34. **Janson, S., B. Bergman, E. J. Carpenter, S. J. Giovannoni, and K. Vergin.** 1999. Genetic analysis of natural populations of the marine diazotrophic cyanobacterium *Trichodesmium*. FEMS Microbiol. Ecol. **30**:57–65.
35. **Koh, E. G. L.** 1997. Do scleractinian corals engage in chemical warfare against microbes? J. Chem. Ecol. **23**:379–398.
36. **Kuta, K. G., and L. L. Richardson.** 1997. Black band disease and the fate of diseased coral colonies in the Florida Keys. p. 601–606. Eighth International Coral Reef Symposium, vol. 1. Balboa, Republic of Panama.
37. **Laws, E. A.** 2000. Aquatic pollution. John Wiley and Sons. New York, N.Y.
38. **Lyons, M. M., P. Aas, J. D. Pakulski, L. Van Waasbergen, R. V. Miller, D. L. Mitchell, and W. H. Jeffrey.** 1998. DNA damage induced by ultraviolet radiation in coral-reef microbial communities. Mar. Biol. **130**:537–543.
39. **Maidik, B. L., G. J. Olsen, N. Larsen, R. Overbeek, M. J. McCaughey, and C. R. Woese.** 1997. The RDP (Ribosomal Database Project). Nucleic Acids Res. **25**:109–110.
40. **McVicar, A. H., and P. G. White.** 1982. The prevention and cure of an infectious disease in cultivated juvenile Dover sole, *Solea solea*. Aquaculture **26**:213–222.
41. **Olson, R. J., S. W. Chisholm, E. R. Zettler, and E. V. Armburst.** 1990. Pigments, size and distribution of *Synechococcus* in the North Atlantic and Pacific Oceans. Limnol. Oceanogr. **35**:45–58.
42. **Paerl, H. W., B. M. Bebout, and L. E. Prufert.** 1989. Bacterial associations

with marine *Oscillatoria* sp. (*Trichodesmium* sp.) populations: ecophysiological implications. J. Phycol. **25**:773–784.
43. **Paerl, H. W., B. M. Bebout, and L. E. Prufert.** 1989. Naturally occurring patterns of oxygenic photosynthesis and N_2 fixation in a marine microbial mat, p. 326–341. *In* Y. Cohen and E. Rosenberg (ed.), Microbial mats: physiological ecology of benthic microbial communities. American Society for Microbiology, Washington, D.C.
44. **Partensky, F., W. R. Hess, and D. Vaulot.** 1999. *Prochlorococcus*, a marine photosynthetic prokaryote of global significance. Microbiol. Mol. Biol. Rev. **63**:106–127.
45. **Paul, J. H., M. F. DePlaun, and W. H. Jeffrey.** 1986. Elevated levels of microbial activity in the coral surface microlayer. Mar. Ecol. Prog. Ser. **33**:29–40.
46. **Rappé, M. S., K. Vergin, and S. Giovannoni.** 2000. Phylogenetic comparisons of a coastal bacterioplankton community with its counterparts in open ocean and freshwater systems. FEMS Microbiol. Ecol. **33**:219–232.
47. **Richardson, L. L.** 1996. Horizontal and vertical migration patterns of *Phormidium corallyticum* and *Beggiatoa* spp. associated with black-band disease of corals. Microb. Ecol. **32**:323–335.
48. **Richardson, L. L.** 1997. Occurrence of the black band disease cyanobacterium on healthy corals of the Florida Keys. Bull. Mar. Sci. **61**:485–490.
49. **Richardson, L. L., K. G. Kuta, S. Schnell, and R. G. Carlton.** 1997. Ecology of the black band disease microbial consortium, p. 597–600. Eighth International Coral Reef Symposium, vol. 1, Balboa, Panama.
50. **Richardson, L. L.** 1998. Coral disease: what is really known? Trends Ecol. Evol. **13**:438–443.
51. **Rohwer, F., M. Breitbart, J. Jara, F. Azam, and N. Knowlton.** 2001. Diversity of bacteria associated with the Caribbean coral *Montastrea franksi*. Coral Reefs **20**:85–91.
52. **Rützler, K., and D. L. Santavy.** 1983. The black band disease of Atlantic reef corals. I. Description of the cyanophyte pathogen. Mar. Ecol. **4**:301–319.
53. **Rützler, K., D. L. Santavy, and A. Antonius.** 1983. The black band disease of Atlantic reef corals. III. Distribution, ecology, and development. Mar. Ecol. **4**:329–358.
54. **Salyers, A. A., and D. D. Whitt.** 1994. Regulation of virulence genes. *In* A. A. Salyers and D. D. Whitt (ed.), Bacterial pathogenesis: a molecular approach. ASM Press, Washington, D.C.
55. **Sambrook, J., E. F. Fritsch, and T. Maniatis.** 1989. Molecular cloning: a laboratory manual, 2nd ed. Cold Spring Harbor Laboratory Press, Cold Spring Harbor, N.Y.
56. **Santavy, D. L., and E. C. Peters.** 1997. Microbial pests: coral disease in the Western Atlantic, p. 607–612. Eighth International Coral Reef Symposium, vol. 1, Balboa, Panama.
57. **Shinn, E. A., G. W. Smith, J. M. Prospero, P. Betzer, M. L. Hayes, V. Garrison, and R. T. Barber.** 2000. African dust and the demise of Caribbean coral reefs. Geophys. Res. Lett. **27**:3029–3032.
58. **Skulberg, O. M., B. Underdal, and H. Utkilen.** 1994. Toxic waterblooms with cyanophytes in Norway—current knowledge. Archiv Hydrobiol. Suppl. **105**: 279–289.
59. **Smith, G. W.** 1998. Response of sea fans to *Aspergillus* sp. Rev. Biol. Mar. **46**:205–208.
60. **Smith, L. D. S.** 2001. The genus *Clostridium*—medical. *In* The Prokaryotes. Springer-Verlag, New York, N.Y.
61. **Smith, L. D. S., and B. L. Williams.** 1984. The pathogenic anaerobic bacteria. Charles C Thomas Publishers, Springfield, Mass.
62. **Sterne, M., and I. Batty.** 1975. Pathogenic clostridia. Butterworths, London, England.
63. **Studier, W. F., and J. J. Dunn.** 1983. Complete nucleotide sequence of bacteriophage T7 DNA and the location of T7 genetic elements. J. Mol. Biol. **166**:477–535.
64. **Suzuki, M., M. S. Rappé, Z. W. Haimberger, H. Winfield, N. Adair, J. Strobel, and S. Giovannoni.** 1997. Bacterial diversity among small-subunit rRNA gene clones and cellular isolates from the same seawater sample. Appl. Environ. Microbiol. **63**:983–989.
65. **Suzuki, M., M. S. Rappé, and S. Giovannoni.** 1998. Kinetic bias in estimates of coastal picroplankton community structure obtained by measurements of small-subunit rRNA gene PCR amplicon length heterogeneity. Appl. Environ. Microbiol. **64**:4522–4529.
66. **Suzuki, M. T., O. Beja, L. T. Taylor, and E. F. Delong.** 2001. Phylogenetic analysis of ribosomal RNA operons from uncultivated coastal marine bacterioplankton. Environ. Microbiol. **3**:323–331.
67. **Taylor, D. L.** 1983. The black band disease of Atlantic reef corals. II. Isolation, cultivation, and growth of *Phormidium corallyticum*. Mar. Ecol. **4**:320–328.
68. **Trust, T. J., S. M. Logan, C. E. Gustafson, P. J. Romaniuk, N. W. Kim, V. L. Chan, M. A. Ragan, P. Guerry, and R. R. Gutell.** 1994. Phylogenetic and molecular characterization of a 23S rRNA gene positions the genus *Campylobacter* in the epsilon subdivision of the *Proteobacteria* and shows that the presence of transcribed spacers is common in *Campylobacter* spp. J. Bacteriol. **176**:4597–4609.
69. **Urbach, E., D. J. Scanlan, D. L. Distel, J. B. Waterbury, and S. W. Chisholm.** 1998. Rapid diversification of marine picophytoplankton with dissimilar light harvesting structures inferred from sequences of *Prochlorococcus* and *Synechococcus*. J. Mol. Evol. **46**:188–201.
70. **VanDamme, P., and J. De Ley.** 1991. Proposal for a new family, *Campylobacteraceae*. Int. J. Syst. Bacteriol. **41**:451–455.
71. **Vandamme, P., P. Pugina, G. Benzi, R. Van Etterijck, L. Vlaes, K. Kersters, J. P. Butzler, H. Lior, and S. Lauwers.** 1992. Outbreak of recurrent abdominal cramps associated with *Arcobacter butzleri* in an Italian school. J. Clin. Microbiol. **30**:2335–2337.
72. **Wassenaar, T. M., and D. G. Newell.** 2001. The genus *Campylobacter*. *In* The Prokaryotes. Springer-Verlag, New York, N.Y.
73. **Webster, N. S., K. J. Wilson, L. L. Blackall, and R. T. Hill.** 2001. Phylogenetic diversity of bacteria associated with the marine sponge *Rhopaloeides odorabile*. Appl. Environ. Microbiol. **67**:434–444.
74. **Williams, E. H., and L. Bunkley-Williams.** 1990. The world-wide coral reef bleaching cycle and related sources of coral mortality. Atoll Res. Bull. **335**: 1–71.

APPLIED AND ENVIRONMENTAL MICROBIOLOGY, Apr. 2003, p. 2409–2413 Vol. 69, No. 4
0099-2240/03/$08.00+0 DOI: 10.1128/AEM.69.4.2409–2413.2003
Copyright © 2003, American Society for Microbiology. All Rights Reserved.

Cyanobacteria Associated with Coral Black Band Disease in Caribbean and Indo-Pacific Reefs

Jorge Frias-Lopez, George T. Bonheyo, Qusheng Jin, and Bruce W. Fouke*

Department of Geology, University of Illinois, Urbana, Illinois 61801

Received 22 August 2002/Accepted 9 January 2003

For 30 years it has been assumed that a single species of cyanobacteria, *Phormidium corallyticum*, is the volumetrically dominant component of all cases of black band disease (BBD) in coral. Cyanobacterium-specific 16S rRNA gene primers and terminal restriction fragment length polymorphism analyses were used to determine the phylogenetic diversity of these BBD cyanobacteria on coral reefs in the Caribbean and Indo-Pacific Seas. These analyses indicate that the cyanobacteria that inhabit BBD bacterial mats collected from the Caribbean and Indo-Pacific Seas belong to at least three different taxa, despite the fact that the corals in each case exhibit similar signs and patterns of BBD mat development.

Black band disease (BBD) is a globally distributed coral disease that affects a variety of different coral species (3, 16). It is manifested as a bacterial mat, ranging from 0.1 mm to a few centimeters wide, that migrates across infected corals at a rate as high as 1 cm/day from top to bottom, killing healthy tissue and leaving behind dead skeletal surfaces stripped clean of tissue (3, 13, 15). Because BBD preferentially infects massive framework-building corals (3, 6), the aftermath of the disease has a profound influence on the ecological and geological structures of coral reef ecosystems (6, 9). Since BBD was first reported in the 1970s, it has been known that the BBD microbial mat is dominated by a filamentous cyanobacterium (2, 3) that was originally optically identified as *Oscillatoria submembranaceae* (3) and later reclassified as *Phormidium corallyticum* (16). *P. corallyticum* has been the focus of many BBD studies (9, 13, 14, 15) and has also been proposed to be the disease pathogen (16). However, it has not yet been proven by a systematic fulfillment of Koch's postulates that *P. corallyticum* is a BBD pathogen. *P. corallyticum* cyanobacteria create a ropy network that structurally supports the BBD mat and houses a complex, phylogenetically diverse community of at least 40 species of bacteria (8). Moreover, the microbial consortium of the BBD mat is 92% distinct from the microbial communities that inhabit overlying seawater, healthy coral tissue, and dead coral surfaces (8). Cyanobacteria produce low-molecular-weight toxins that can kill fish and other animals during bacterial blooms (4). However, as a group, cyanobacteria have not generally been considered to be associated with the infection of eukaryotic tissue. Prior to the present study, culture-independent molecular techniques have not specifically targeted the filamentous cyanobacteria associated with BBD. Therefore, it is unknown whether BBD mats growing on infected coral surfaces in different ocean basins actually contain the same species of cyanobacteria. Difficulties in growing pure cultures of BBD cyanobacteria have proven to be a significant obstacle to completing the 16S rRNA gene sequence for identification purposes. The goal of the present study was to determine the phylogenetic identity of the cyanobacteria that volumetrically dominate BBD mats and to determine whether a single species occurs on the coral reefs within an ocean basin and on those in different ocean basins.

Phylogenetic diversity of cyanobacteria present in BBD. Comparative analyses were performed on BBD mat samples collected from infected corals at three different locations along the southwestern coast of Curaçao, Netherlands Antilles, in the Caribbean Sea, and at two different locations on the northern coast of New Britain, Papua New Guinea, in the Indo-Pacific Sea. On Curaçao, samples were collected from three back reef sites at water depths of 4 to 5 m along the southern coast of the island in August 2000 and in January and August 2001. These sites included the sea aquarium, the water plant, and Playa Kalki (Fig. 1). On New Britain, BBD mat samples were collected from an equivalent back reef environment off the northern coast at Father's Reef (Fig. 1) at a water depth of 5 m in August 2000. A natural segregation of coral species exists between the Caribbean and Indo-Pacific Seas; the framework-building corals of the Caribbean belong to the family *Faviidae*, and those in the Indo-Pacific belong to the family *Poritidae* (17). Samples were taken from actively migrating BBD mats on 12 different coral colonies representing four different coral species. These included three coral species from Curaçao (six colonies of *Diploria strigosa*, two colonies of *Montastrea cavernosa*, and one colony of *Montastrea annularis*) and one coral species from New Britain (two colonies of *Porites lutea*). Only two cases of BBD were observed on New Britain corals along almost 1,200 km of coastline, while over 50 cases of BBD were observed on Curaçao corals along only 50 km of coastline (7). In addition, a nonaxenic culture of *P. corallyticum* provided by L. Richardson (Florida International University, Miami) and collected in the Florida Keys was analyzed. Finally, data from samples taken from two other locations each in the Caribbean, Barbados, and the U.S. Virgin Islands (5) were compared with the results obtained in the present work.

Visual analyses of our samples by fluorescence and scanning electron microscopies confirmed the dominance of a filamentous cyanobacterium in each BBD mat sample (16). Although the bacterium thought responsible for BBD had been optically identified previously as *P. corallyticum* (16), recent 16S rRNA

* Corresponding author. Mailing address: Department of Geology, University of Illinois, 1301 W. Green St., Urbana, IL 61801. Phone: (217) 244-5431. Fax: (217) 244-4996. E-mail: fouke@uiuc.edu.

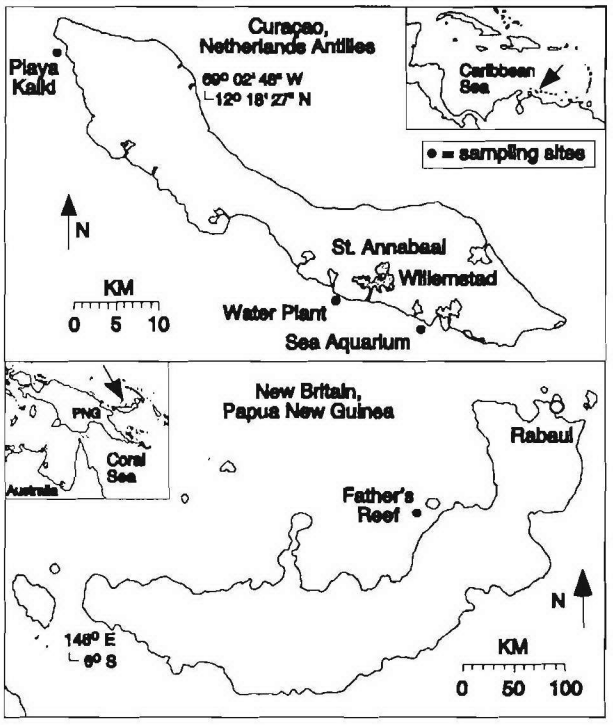

FIG. 1. Map of sampling sites on the islands of Curaçao, Netherlands Antilles, and New Britain, Papua New Guinea.

gene analyses of BBD mats did not detect the genus *Phormidium* in either healthy or BBD-infected coral tissues (5, 8). The molecular sampling, extraction, cloning, and sequencing techniques used in this study have been presented previously (8). In the present study, two sets of primers specific for the cyanobacterial 16S rRNA gene (11) were used on environmental BBD mat samples that contained complex microbial communities. In addition, terminal restriction fragment length polymorphism (T-RFLP) analyses of PCR products obtained by using one set (CYA106) of cyanobacterium-specific primers used previously (10) provided relative estimates of the most abundant cyanobacterium present in selected samples of the BBD mat.

A total of 31 clones from the six colonies of *D. strigosa*, 8 clones from the two colonies of *M. cavernosa*, and 8 clones from the one colony of *M. annularis* yielded identical 16S rRNA gene sequences, regardless of the coral species sampled and its location. Sequences ranging from 300 to 600 bp were used for the analysis. A partial gene sequence for this cyanobacterium had previously been reported and designated CD1C11 (8) (Fig. 2). A new sequence has been identified in the present study from both of the cases of BBD observed in New Britain, and this clone is herein designated PNG-50. The relative abundance of cyanobacterium CD1C11 and PNG-50 in each BBD mat was determined by T-RFLP analyses as described previously (10). T-RFLP analyses were applied in this study to assess the relative abundance of microorganisms. The results indicate that the sequences obtained for the cyanobacterial clones CD1C11 and PNG-50 are the most abundant in the BBD mats. The use of cyanobacterium-specific primers proves that this result is not the product of random amplification of some other cyanobacterial 16S rRNA genes. The forward primer was labeled at the 5′ end with 6-carboxyfluorescein. Aliquots of amplified 16S rRNA genes were digested with *Hha*I, *Rsa*I, and *Msp*I. The actual sizes of the peaks obtained by T-RFLP were compared with the expected sizes generated by a theoretical digest of the previously obtained sequences from CD1C11 and PNG-50. These analyses document that with respect to the cyanobacterial portion of the community, CD1C11 and PNG-50 were the most abundant (10) cyanobacteria found in the BBD mats collected from the Caribbean and Indo-Pacific reefs, respectively (Fig. 3). Furthermore, samples from the Caribbean showed the presence of at least four additional types of cyanobacteria at much lower concentrations than that of CD1C11. Samples from the Indo-Pacific showed the presence of at least six other types of cyanobacteria, and two of these were present in high concentrations.

Phylogenetic analysis of the samples was performed by using the program CLUSTALX to align the sequences. Phylogenetic analysis and trees were generated by using the program PAUP. Trees were constructed by parsimony analysis by bootstrapping 10,000 trees from resampled data. Results of the phylogenetic analyses showed that the 16S rRNA gene sequence from clone CD1C11 was 98% similar to cyanobacterial sequence 128-56. This uncultured cyanobacterium has been reported to be present in BBD mats on *D. strigosa* and *M. annularis* in other Caribbean sites, including Barbados and the U.S. Virgin Islands (5). This relationship is supported by a 100% bootstrap correlation of the phylogenetic trees. In addition, cyanobacterium CD1C11 and cyanobacterium 128-56 form a cluster with *Oscillatoria corallinae*, a marine benthic strain isolated from the surface of a worm tube whose sequence was supported in only 60% of the bootstrap trees. Importantly, sequences from two marine *Phormidium* species appear to be more distantly related to this *Oscillatoria* strain than to each other (Fig. 2), which suggests the need for future reclassification of *P. corallyticum* as a member of the genus *Oscillatoria*.

In addition, the 14 clones obtained from the nonaxenic culture of *P. corallyticum*, herein called cyanobacterium LR-3L (5), yielded unique sequences that were not affiliated with cyanobacteria detected at other sites in the Caribbean and Indo-Pacific Seas. However, the bootstrap values supporting the separation of these branch points were only 9 and 24% (Fig. 2). The closest related genus to cyanobacterium LR-3L was *Geitlerinema*, which also belongs to the order *Oscillatoriales*, in which *P. corallyticum* has been grouped. Identical phylogenetic relationships for cyanobacterium LR-3L have previously been reported (5). Eleven clones generated from BBD mats collected in the Indo-Pacific Sea yielded gene sequences, herein designated PNG-50, that are affiliated with a different genus of filamentous cyanobacterium which is closely related to *Trichodesmium* spp. These results indicate that at least three taxonomically distinct filamentous cyanobacteria—two taxa from the Caribbean Sea and one taxon from the Indo-Pacific Sea—are associated with the BBD mats that were analyzed.

Cyanobacterium CD1C11 was the most common cyanobacterium detected in Caribbean corals in this study, occurring in three of the four sample sites analyzed. The presence or absence of this cyanobacterium does not appear to be coral species specific. The absence of CD1C11 sequences in the

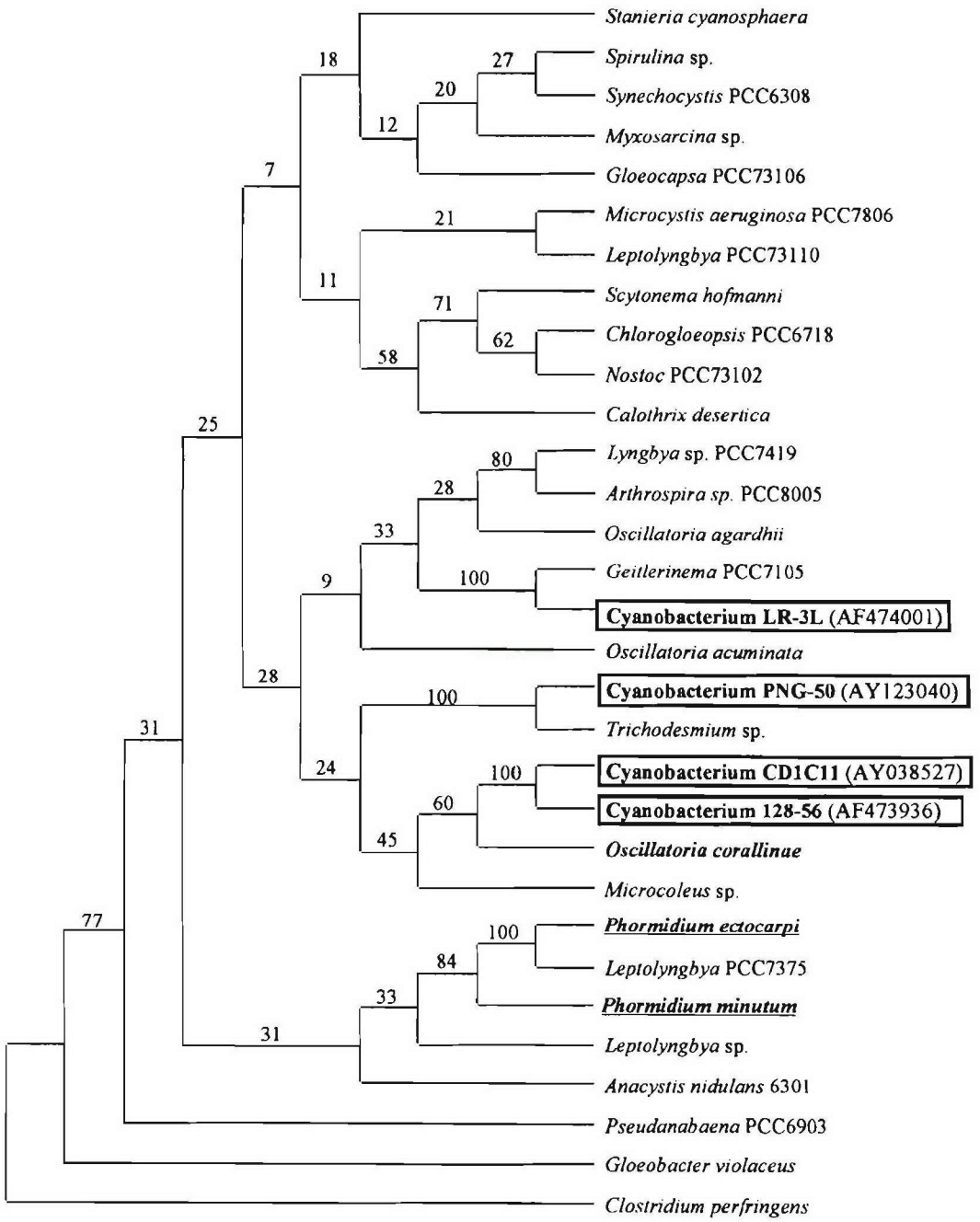

FIG. 2. Phylogenetic consensus tree based on parsimony analysis of 16S rRNA gene sequences of BBD cyanobacteria and other cyanobacteria. The tree is based on sequences of 300 to 600 bp in length. These represent a total of 31 clones from six colonies of *D. strigosa*, 8 clones from two colonies of *M. cavernosa*, and 8 clones from one colony of *M. annularis*. The numbers at the nodes are the bootstrap values based on a total of 10,000 replicate resamplings. GenBank accession numbers are included. The underlined strains represent marine *Phormidium* spp.

BBD mat samples from New Britain, as well as its presence in all but one sample from the Caribbean, suggests that the cyanobacteria associated with BBD may have distinct geographic distributions. If that is the case, this biogeographic distribution is significantly different from that observed for *Trichodesmium*, one of the most abundant genera of filamentous cyanobacteria in the world's oceans. *Trichodesmium* spp. from the Indian Ocean, the Caribbean Sea, and the Indo-Pacific Sea exhibit essentially identical 16S rRNA gene sequences (12). The phylogenetic diversity of cyanobacteria associated with BBD may therefore at least partially explain the variable environmental conditions in which BBD has been observed (1). Little is known about the environmental factors that lead to the development of BBD. The genetic diversity among the cyanobacte-

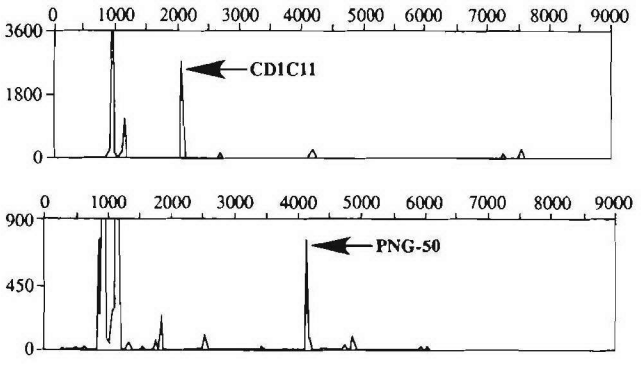

FIG. 3. Results of T-RLFP analysis of BBD samples from Curaçao (top) and New Britain (bottom) by using specific primers for the cyanobacterial 16S rRNA gene. PCR analyses of products from the BBD mats were obtained by using the primers indicated in the text for amplifying cyanobacterial 16S rRNA genes.

TABLE 1. Occurrence of cyanobacterium CD1C11 in different coral samples and seawater

Coral and condition or seawater	No. of samples	Positivity for CD1C11	
		No. of samples	Frequency (%)
Montastrea cavernosa, BBD infected	2	2	100
Montastrea annularis, BBD infected	1	1	100
Diploria strigosa, BBD infected	6	6	100
Porites lutea, BBD infected	1	0	0
Montastrea cavernosa, BBD infected, healthy	1	0	0
Montastrea annularis, healthy	3	0	0
Diploria strigosa, healthy	3	0	0
Porites lutea, healthy	3	0	0
Porites furcata, healthy	2	0	0
Porites astreoides, healthy	1	0	0
Montastrea annularis, dead	1	1	100
Montastrea cavernosa, dead	1	1	100
Diploria strigosa, dead	3	1	33
Porites astreoides, dead	1	0	0
Seawater	4	0	0

ria that are part of the BBD mat is a new discovery that may help explain why BBD has been observed under many different environmental conditions (1, 7, 14). BBD may be a consequence of combined coral and microbial responses to environmental stress. Each of the different cyanobacteria that we have detected may have a different environmental tolerance with regard to temperature, heavy metal contamination, organic pollution, and other factors.

Occurrence of cyanobacterium CD1D11 on healthy coral tissues, BBD mats, dead coral surfaces, and overlying seawater. Questions about how BBD is transmitted and what the natural habitat for cyanobacterium CD1D11 is remain unanswered. One previous study that used microscopy to detect *P. corallyticum* showed that this cyanobacterium is present in healthy corals, although at a low frequency (14). The sequence for CD1C11 was used in the present study as a template for designing primers to make PCR a more sensitive method to detect the presence of this cyanobacterium in different marine subenvironments (including overlying seawater, healthy coral tissues, BBD mats, and dead coral surfaces) and therefore better elucidate its potential source (8). We chose this sequence because it was detected in all of our BBD samples from the Caribbean Sea and because its presence has now been reported in two other Caribbean locations (5). The specific primers used for detecting *P. corallyticum* were PhcF (5′-CTG TAGGTGGCCAGCT-3′) and PhcR (5′-TTCCCTTCGCAG GTTCGCTGC-3′). The specificity of these primers was tested by comparing them to a clone library of several representative cyanobacterial 16S rRNA gene sequences, including clones CD1C11, PNG-50, and LR-3L (Fig. 2). Results indicated that the primers amplified DNA exclusively from clone CD1C11. The conditions for PCR have been described previously (8). A total of 33 different samples were analyzed. All BBD mat samples except for the New Britain samples were positive for the presence of clone CD1C11 (Table 1). In the case of the dead zone left behind by the BBD mat, half of the samples analyzed were positive for the presence of clone CD1C11. However, none of the healthy coral species or the seawater analyzed gave a positive result. This low frequency of occurrence of CD1C11 agreed with previous results (14). Whatever the natural habitat for CD1C11 might be, its presence in the different marine environments sampled appeared to be at low concentrations except when growing in the BBD mat.

Conclusion. It had previously been hypothesized that a single cyanobacterial species was the primary microbial constituent of BBD mats. The present work shows that more than one species of cyanobacteria constitute BBD mats and that these species differ not only between the Caribbean and Indo-Pacific Seas but also within the Caribbean Sea. In the Caribbean, each of the cyanobacteria is present on multiple coral species of the family *Faviidae* that are infected with BBD. These results provide the microbial baseline needed for future studies that will attempt to identify environmental controls of BBD transmission through seawater and the resulting initiation and development of infection on healthy corals.

This work was supported by a research grant from the Office of Naval Research.

The invitation of P. Cruz and his research team to join their Natural Products expedition to Papua New Guinea was greatly appreciated. We thank J. Klaus for his review of the manuscript.

The conclusions in this report are those of the authors and do not necessarily reflect those of the funding agencies.

REFERENCES

1. **Al-Moghrabi, S. M.** 2001. Unusual black band disease (BBD) outbreak in the northern tip of the Gulf of Aqaba (Jordan). Coral Reefs **19**:330–331.
2. **Antonius, A.** 1981. Coral reef pathology—a review. p. 3–6. *In* E. D. Gomez et al. (ed.). The reef and man. Proceedings of the Fourth International Coral Reef Symposium. vol. 2. Marine Sciences Center. University of the Philippines. Quezon City.
3. **Antonius, A.** 1981. The 'band' diseases in coral reefs. p. 7–14. *In* E. D. Gomez et al. (ed.). The reef and man. Proceedings of the Fourth International Coral Reef Symposium. vol. 2. Marine Sciences Center. University of the Philippines. Quezon City.
4. **Codd, G. A., C. J. Ward, and S. G. Bell.** 1997. Cyanobacterial toxins: occurrence, modes of action, health effects and exposure route. Arch. Toxicol. Suppl. **19**:399–410.
5. **Cooney, R. P., O. Pantos, M. D. A. Le Tissier, M. R. Barer, A. G. O'Donell, and J. C. Bythell.** 2002. Characterization of the bacterial consortium associated with black band disease in coral using molecular microbiological techniques. Environ. Microbiol. **4**:401–413.
6. **Edmunds, P. J.** 1991. Extent and effect of black band disease on a Caribbean reef. Coral Reefs **10**:161–165.
7. **Fortwengler, M. R.** 2002. Distribution and frequency of black band disease

and partial mortality of *Diploria strigosa* on Curaçao, Netherland Antilles. M.S. thesis. University of Illinois Urbana-Champaign, Urbana.

8. **Frias-Lopez, J., A. L. Zerkle, G. T. Bonheyo, and B. W. Fouke.** 2002. Partitioning of bacterial communities between seawater and healthy, black band diseased, and dead coral surfaces. Appl. Environ. Microbiol. **68:**2214–2228.
9. **Kuta, K., and L. L. Richardson.** 1996. Abundance and distribution of black band disease of corals in the northern Florida Keys. Coral Reefs **15:**219–223.
10. **Liu, W.-T., T. L. Marsh, H. Cheng, and L. J. Forney.** 1997. Characterization of microbial diversity by determining terminal restriction fragment length polymorphisms of genes encoding 16S rRNA. Appl. Environ. Microbiol. **63:**4516–4522.
11. **Nübel, U., F. Garcia-Pichel, and G. Muyzer.** 1997. PCR primers to amplify 16S rRNA genes from cyanobacteria. Appl. Environ. Microbiol. **63:**3327–3332.
12. **Orcutt, K. M., U. Rasmussen, E. A. Webb, J. B. Waterbury, K. Gundersen, and B. Bergman.** 2002. Characterization of *Trichodesmium* spp. by genetic techniques. Appl. Environ. Microbiol. **68:**2236–2245.
13. **Richardson, L. L.** 1996. Motility patterns of *Phormidium corallyticum* and *Beggiatoa* spp. associated with black band disease of corals. Microb. Ecol. **32:**323–335.
14. **Richardson, L. L.** 1997. Occurrence of the black-band disease cyanobacterium on healthy corals of the Florida Keys. Bull. Mar. Sci. **61:**485–490.
15. **Richardson, L. L.** 1998. Coral diseases: what is really known? Trends Ecol. Evol. **13:**438–443.
16. **Rutzler, K., and D. Santavy.** 1983. The black band disease of Atlantic reef corals. I. Description of a cyanophyte pathogen. Mar. Ecol. **4:**301–319.
17. **Veron, J. E. N.** 2000. Corals of the world. Odyssey Publishing, El Cajon, Calif.

APPLIED AND ENVIRONMENTAL MICROBIOLOGY, June 2004, p. 3687–3694 Vol. 70, No. 6
0099-2240/04/$08.00+0 DOI: 10.1128/AEM.70.6.3687–3694.2004
Copyright © 2004, American Society for Microbiology. All Rights Reserved.

Identification of Differential Gene Expression in Bacteria Associated with Coral Black Band Disease by Using RNA-Arbitrarily Primed PCR

Jorge Frias-Lopez,* George T. Bonheyo, and Bruce W. Fouke

Department of Geology, University of Illinois at Urbana-Champaign, Urbana, Illinois 61801

Received 12 February 2004/Accepted 19 February 2004

RNA-arbitrarily primed PCR techniques have been applied for the first time to identify differential gene expression in black band disease (BBD), a virulent coral infection that affects reef ecosystems worldwide. The gene activity for the BBD mat on infected surfaces of the brain coral *Diploria strigosa* was compared with that for portions of the BBD mat that were removed from the coral and suspended nearby in the seawater column. The results obtained indicate that three genes (DD 95-2, DD 95-4, and DD 99-9) were up-regulated in the BBD bacterial mat on the coral surface compared to the transcript base levels observed in the BBD mat suspended in seawater. Clone DD 95-4 has homology with known amino acid ABC transporter systems in bacteria, while clone DD 99-9 exhibits homology with chlorophyll A apoprotein A1 in cyanobacteria. This protein is essential in the final conformation of photosystem I P700. DD 95-2, the only gene that was fully repressed in the BBD mat samples suspended in seawater, exhibited homology with the AraC-type DNA binding domain-containing proteins. These transcriptional activators coordinate the expression of genes essential for virulence in many species of gram-negative bacteria.

Coral reefs are important reservoirs of biodiversity in oceanic environments and thus are used as a sensitive indicator of environmental change (23, 39). The number and incidence of diseases that affect corals around the world have dramatically increased over the last four decades (21). As evidence of this worldwide degradation of coral reef ecosystems mounts, interest in identifying the etiological agents of infectious disease in scleractinian corals continues to intensify (21, 39)

Black band disease (BBD) is among the most important of the globally distributed coral diseases known today, yet the environmental conditions leading to BBD infection are still not well understood (34). BBD results from the rapid migration of a complex mat of microorganisms across the surface of scleractinian coral colonies; this mat lyses healthy coral tissue and leaves dead coral skeleton behind (2, 34). BBD preferentially affects massive-framework-building coral species that serve as the ecological cornerstone of reefs. Therefore, BBD is an important agent in altering coral reef ecosystems.

Although BBD is a polymicrobial disease (34, 35), the population of bacteria growing in the BBD biofilm is composed primarily of large filamentous cyanobacteria previously optically identified as the single species *Phormidium corallyticum* and recently identified as multiple species by molecular techniques (14, 18). Several previous studies have suggested that these cyanobacteria are the BBD pathogens (40). However, the culturing of these cyanobacteria has proved difficult (23, 33), thus preventing tests to fulfill Koch's postulates to determine BBD pathogenicity (34).

The aim of the present study was to better understand BBD pathogenesis by analyzing bacterial gene expression in the BBD mat consortia by RNA-arbitrarily primed PCR (RAP-PCR) (5, 9, 16, 43). This analysis was done by characterizing abundant mRNAs expressed by bacteria inhabiting the BBD mat on infected surfaces of the brain coral *Diploria strigosa* and comparing the resulting expression profile with that for samples of the BBD mat that were removed from the infected coral and suspended nearby in the open seawater column. These results demonstrate the great potential of the use of mRNA methodologies, typically reserved for pure cultures, to unravel differential gene expression in complex mixed bacterial communities and to identify differentially expressed genes under different environmental conditions. At least three genes were up-regulated in the BBD bacterial mat on the coral surface compared to the transcript base levels observed in the BBD mat suspended in seawater.

MATERIALS AND METHODS

Sample collection. Sampling was conducted by using standard scuba techniques on the leeward coral reefs of the island of Curaçao, Netherlands Antilles. Colonies of *D. strigosa* exhibiting the distinct BBD ring were sampled at water depths of approximately 3 m in the back reef facies of the water plant reef (17, 18). Portions of active BBD mats were physically peeled off the infected coral surfaces with forceps and placed in 50-ml Falcon tubes filled with seawater. An additional sample of BBD mat was then placed into either a 50-ml perforated polypropylene centrifuge tube or a 18-cm-long polyvinyl chloride pipe (inside diameter, 5.2 cm) with a solid cap at one end and a 20-μm-mesh screen at the other end to allow the free flow of water. The tube was suspended in seawater 30 cm to 1 m from the coral head from which samples were taken and oriented with the transparent screen facing slayward to allow light into the tube. This sample tube was left suspended for 3 days. Immediately upon reaching the surface, the in situ and seawater-suspended BBD mat samples were decanted to remove the seawater and the mat samples were immersed in RNAlater (Ambion, Austin, Tex.). For each pairing of samples, the exposure was carried out simultaneously. All samples were then immediately frozen at −20°C. Subsamples of the bacterial mats growing on corals and suspended in seawater were preserved in 80% ethanol at −20°C for use in the analysis of bacterial communities.

Analysis of bacterial communities during infection and after suspension in

* Corresponding author. Mailing address: Department of Geology, University of Illinois, 1301 W. Green St., Urbana, IL 61801. Phone: (217) 333-0672. Fax: (217) 244-4996. E-mail: friaslop@uiuc.edu.

TABLE 1. Random primers used for RAP-PCR analysis of BBD samples

Sequence	Primer name	Reference
CTGCTTGATGAAA	R1	J. T. Flemming, personal communication
CTGCTTGATGAAC	R2	J. T. Flemming, personal communication
CTGCTTGATGAAG	R3	J. T. Flemming, personal communication
TGAGCGGACA	Lnr81	38
TCGCCGCAAA	Lnr97	38
CAGCCCAGAG	Lnr95	38
TCGTGCGGGT	Lnr99	38
AAGCTTTGGTCAG	H-AP3	7
AAGCTTAGTAGGC	H-AP5	7
GCCGGAGCTCNNNN	RP-1	This study, based on reference 20
GCCGGAGCTCNNN	RP-2	This study, based on reference 20
GCCGGAGCTCNN	RP-3	This study, based on reference 20

seawater. Differences found in the mRNA profiles of two complex microbial communities could arise either from changes in gene expression levels or from differences in community compositions. To characterize and compare the composition of bacteria inhabiting BBD infectious in situ mat communities with that of suspended BBD mat communities, we used terminal-restriction fragment length polymorphism (T-RFLP) analysis. The DNA extraction and T-RFLP protocols, according to those presented by Frias-Lopez et al. (18, 19), are briefly described here. The universal bacterial oligonucleotide primers used in the PCR amplifications were obtained from Integrated DNA Technologies (Coralville, Iowa). These primers were Univ9F (5′-GAGTTTGATYMTGGCTC) and the reverse primer Univ1509R (5′-GYTACCTTGTTACGACTT). Reaction mixtures included 20 μl of TaqMaster buffer (an agent which improves the thermostability and processivity of the polymerase), 10 μl of *Taq* Reaction buffer containing 15 mM $MgCl_2$ (Eppendorf, Westbury, N.Y.), 8 μl of deoxynucleoside triphosphate (dNTP) mix (each dNTP at 2.5 mM; Gibco/BRL, Rockville, Md.), 1 μl each of forward and reverse primers (200 ng each), 5 to 30 μl of the sample preparation, and water to bring the total volume to 99.5 μl. Some reactions were layered beneath 50 μl of mineral oil (Sigma, St. Louis, Mo.). An initial denaturation-hot start of 5 min at 95°C was followed by the addition of 0.5 μl (approximately 2 U) of MasterTaq polymerase (Eppendorf) or *Taq* DNA polymerase (Gibco/BRL). The hot start was followed by 30 or 35 cycles of 94°C for 1 min, 55°C for 1 min, and 72°C for 2 min. A final soak at 72°C for 5 min concluded the reaction.

PCR products were cleaned up with the Wizard PCR Prep kit (Promega, Madison, Wis.) and eluted with 30 μl of water. Ten microliters of clean DNA was aliquoted into each of three tubes, and restriction digests were performed with RsaI, HhaI, or MspI. The final volume of each digest mixture was 20 μl. At least 300 ng of total DNA per digestion was used. Tubes were incubated overnight at 37°C and then covered with aluminum foil and kept at −20°C.

Prior to loading on an acrylamide gel, 1 μl of sample was added to a loading cocktail (1.25 μl of deionized formamide, 0.25 μl of blue loading dye, 0.3 μl of size standard TAMRA 2500). This procedure was repeated for each sample in separate tubes. These preparations were mixed and then denatured at 95°C for 3 min. Samples where then loaded onto a 5% Long Ranger (proprietary acrylamide formula from BioWhittaker) and 7 M urea gel and separated by electrophoresis by using an Applied Biosystems, Inc. (ABI), 377-XL sequencer and a run time of 5 h. Results were analyzed with the ABI GeneScan software.

RNA isolation. BBD mat samples initially preserved in RNA were later transferred to a 2-ml screw-cap tube containing 1 ml of Trizol reagent (Invitrogen, Carlsbad, Calif.) and 300 μl of 0.1-mm-diameter zirconia-silica beads. The samples were kept on ice during the entire procedure to prevent RNA degradation. Samples were mechanically disrupted in a Mini Beadbeater-8 (Biospec Products, Bartlesville, Okla.) at maximum speed for 30 s, followed by three cycles of freezing and thawing at −80 and 65°C, respectively.

After disruption, samples were vortexed and incubated on ice for 5 min. Two hundred microliters of chloroform was added to the homogenate, and the tubes were shaken vigorously for 15 s and then incubated on ice for 3 min. Samples next underwent centrifugation at 14,000 × *g* for 15 min at 4°C. The aqueous phase was transferred to a new tube, and the same volume of isopropanol was added. Samples were incubated for 1 h at room temperature, then centrifuged at 14,000 × *g* for 15 min at 4°C, and then washed once with 75% ethanol. Total RNA was resuspended in diethyl pyrocarbonate water and RNA*secure* reagent (Ambion). The isolate total RNA was treated with the DNA*free* kit according to the manufacturer's instructions (Ambion) and checked for the presence of remaining DNA. RNA samples were run in a formaldehyde gel to check the integrity of the RNA. Samples with DNA or degraded RNA were excluded from further analysis.

Arbitrarily primed PCR. cDNA synthesis was carried out immediately after RNA isolation. First-strand synthesis was performed by using ImPromII (Promega), random hexamers (Promega), and random decamers RETROscript (Ambion) as primers. The protocol was performed according to the manufacturer's instructions. Between 500 ng and 2 μg of sample was used, depending on the experiment. Primers (random hexamers or random decamers) were added at 0.5 μg up to a final volume of 5 μl. Samples were incubated in a Mastercycler gradient thermocycler (Eppendorf) at 70°C for 5 min followed by a quick chill at 4°C for 5 min. This 5-μl reaction mixture was used in a 20-μl (total volume) cDNA synthesis reaction mixture comprising 4 μl of Improm-II 5X reaction buffer (Promega), 2.4 μl $MgCl_2$ at 25 mM (final concentration, 3 mM), 1 μl of dNTP mix (each dNTP at 10 mM; final concentration, 0.5 mM), 0.5 μl of Rnasin RNase inhibitor (Promega), 0.5 μl of DNA*secure* reagent (Ambion), and 1 μl of Improm-II reverse transcriptase (Promega). The synthesis reactions were performed with a Mastercycler gradient thermocycler (Eppendorf) by using annealing at 25°C for 5 min and extension of the first strand for 60 min at 37°C. Parallel negative controls consisted of exactly the same mix except that water was substituted for the RNA sample. One microliter of the first-strand cDNA was then used to perform the PCR amplification. Oligonucleotides were obtained from Integrated DNA Technologies (Table 1). Reaction mixtures included 5 μl of *Taq* reaction buffer, 1.5 μl of 25 mM magnesium acetate (Eppendorf), 4 μl of dNTP mix (each dNTP at 2.5 mM; Gibco/BRL), 2 μl of the random primer (200 ng), 1 μl of the cDNA sample, and water to bring the total volume to 50 μl. The hot start was followed by between 45 and 50 cycles of 94°C for 1 min, 40°C for 1 min, and 72°C for 2 min. A final soak at 72°C for 5 min concluded the reaction. In all cases, reactions were performed in duplicate.

Identification of differentially expressed genes. Differences in gene expression for in situ and suspended samples of BBD mats were detected by comparing side-by-side samples of RAP-PCR products. These products were electrophoresed either in 2.0% high-resolution agarose Agarose-HR (Ambion) or in a 6% polyacrylamide gel under native conditions. Only bands present in two separate RAP-PCRs were analyzed. Bands obtained from agarose gels were passed through a 250- to 300-μm-diameter glass bead (Sigma) column and purified by using the PCR Prep kit (QIAGEN, Alameda, Calif.). DNA from bands excised from the polyacrylamide gel was eluted as follows. Two hundred microliters of crush-and-soak solution (0.5 M ammonium acetate, 0.1% sodium dodecyl sulfate, 0.1 mM EDTA) was added, and the acrylamide was crushed and incubated overnight at 37°C. The following day, tubes were spun down for 10 min at 14,000 rpm. The supernatant was removed, another 200 μl of crush-and-soak solution was added, the spin was repeated, and the recovered supernatant was pooled with the initial supernatant fraction. DNA was then precipitated and recovered. In order to clone the eluted bands into the pGEM-T vector, the DNA was incubated for 10 min at 72°C in the presence of *Taq* polymerase and dATP (2.5 mM). The gel-purified PCR product was cloned into the pGEM-T vector (Promega) and transformed into calcium chloride-competent DH5αMCR *Escherichia coli* cells by using the manufacturer's instructions and standard techniques (41). Clones were checked for the presence of the insert by PCR with the universal primers M13 (position −21) and T7 (position −26). An (RFLP) analysis of the products was performed to determine identical patterns. PCR products were digested with MspI and HinP1 enzymes and analyzed in a 1.6% Metaphor agarose gel. Clones selected for sequence analysis were patched onto

Luria broth agar petri dishes supplemented with 100 μg of ampicillin/ml (Roche Molecular Biochemicals, Indianapolis, Ind.) and incubated overnight at 37°C.

Inoculations, cultures, DNA preparations, and sequence reactions were performed in the High Throughput Laboratory of the University of Illinois W. M. Keck Center for Comparative and Functional Genomics. Plates were used to inoculate 2-ml 96-well culture blocks containing Circle Grow media (Bio100) supplemented with ampicillin. Plasmid template DNA was purified from the cultures by using an automated system and the QIAwell 96 Turbo prep BioRobot kit (QIAGEN, Valencia, Calif.). The first round of sequencing was completed by using the T7 (position −26) primer. Plasmid templates were prepped on a QIAGEN Bio Robot 9600, and Big Dye Terminator Chemistry (version 2.0) from ABI was used for sequencing reactions. Sequencing was performed with an ABI 3700 capillary sequencer, followed by processing at the Bioinformatics Unit of the W. M. Keck Center.

Confirmation of differential gene expression by semiquantitative RT-PCR. In order to verify the differences in gene expression of the genes identified by RAP-PCR, we performed reverse transcription-PCR (RT-PCR) with the original samples of RNA used for RAP-PCR. First-strand cDNA was obtained as described above by using random primers (Promega) and 1 μg of total RNA. One microliter of cDNA was used as a template for the PCR, with specific primers being used for each target gene. Different numbers of cycles were used to avoid saturation of the PCR products. Only products obtained in a number of cycles below the saturation point were used for relative quantification analysis. Analysis of the relative levels of expression of each of the bands obtained for the different genes was performed by using the program ImageJ 1.30v (Wayne Rasband, National Institutes of Health, Bethesda, Md.), obtained in the public domain (http://rsb.info.nih.gov/ij/Java 1.3.1). Analyses were performed in three different independent experiments and in triplicate RAP-PCRs.

Nucleotide sequence accession numbers. The GenBank accession numbers for the sequences generated in this study are AY494600 through AY494604.

RESULTS

Bacterial community analysis. Prior to the evaluation of differential gene expression, the compositions of the microbial consortia comprising the in situ coral surface and water column-suspended samples of the BBD bacterial mats were determined. This was an important starting point, since BBD is a polymicrobial disease, and therefore RNA was extracted from a mixed population of bacteria. In both the in situ and the suspended samples of BBD mats, we obtained the same T-RFLP profile. This finding indicates that the most abundant bacteria in both types of BBD mat samples were the same (Fig. 1). Therefore, the differences between RAP-PCR fingerprinting profiles may be attributable to a change in gene expression rather than to changes in the composition of the bacterial communities comprising each BBD mat sample in our controlled experiment.

RAP-PCR fingerprinting of RNA. Different authors have recently used RAP-PCR to analyze differences in gene expression in prokaryotes. However, all of those experiments used cultures grown under laboratory conditions (5, 9, 16, 43). Because our samples were collected directly from the ocean environment, we had to use RNAlater to preserve them before analysis. The RNA obtained from the environmental samples was of good quality, as shown in Fig. 2. The first cDNA strand was obtained by using either random hexamers or random decamers as primers. In all cases, the shorter random primers provided cDNA for a larger number of different genes. In combination with the cDNA products, a total of 12 different random primers were used (Table 1). Preliminary results showed that the use of primers Lnr95 and Lnr99 provided a larger number of DNA bands as well as a more consistent pattern, and therefore these primers were used in subsequent experiments.

Nonradioactive methods have previously been used successfully to analyze differences in gene expression (1, 6, 10, 38). Both a high-resolution agarose and a 6% polyacrylamide gel were used with good results to analyze RAP-PCR fingerprinting results for our samples (Fig. 3). Nevertheless, polyacrylamide gels were more sensitive, showing a larger number of different bands. All sequences analyzed except one came from bands obtained from BBD mats growing on the coral during infection. The number of genes up-regulated during infection was always higher than the number of genes down-regulated, and a total of seven bands were finally chosen for subsequent analysis. These bands were cloned into the pGEM-T vector and sequenced. BLASTX analysis for the fragments of DNA sequenced gave significant hits for five out of six sequences. One of the bands was excluded from further analysis because it was too short and did not give any significant hits in the database. The results obtained are shown in Table 2. Two of the bands (clones DD 95-4 and DD 99-8) had homology with proteins involved in amino acid transporters. DD 95-4 had 51% identity (68% positives) with a hypothetical amino acid ABC transporter from *Shewanella oneidensis*, while DD 99-8 had 46% homology (70% positives) with a glutamine-binding protein of a member of *Archaea*, *Methanosarcina mazei*. Nonetheless, the rest of the hits for DD 99-8 had homology with amino acid ABC transporters in bacteria with homologies higher than 35%. Another clone, DD 95-1, had 47% homology (64% positives) with a hypothetical protein from *Vibrio parahaemolyticus*. Clone DD 99-9 had 93% homology (97% positives) with a protein that is part of photosystem I in cyanobacteria. Since the filamentous cyanobacteria are the most abundant microorganisms present in the infectious mat, the sequence from clone DD 99-9 is probably derived from these cyanobacteria. Finally, the best hit for clone DD 95-2 was an AraC-type DNA-binding domain protein with a homology of 25% (68% positives). Finally, the best hit for clone DD 95-2 was an AraC-type DNA-binding domain protein with a homology of 25% (68% positives).

Semiquantitative RT-PCR analysis. The final step was to verify that the characterized genes were actually differentially expressed during infection of the coral. To confirm this possibility, semiquantitative RT-PCR was performed with the original samples of RNA, in situ and suspended, from three different experiments. Semiquantitative RT-PCR analysis has previously been used to confirm differences in gene expression (15, 24, 26). Specific primers were designed to analyze the levels of expression of the genes presented in Table 2. During the amplification of the genes, different numbers of cycles were used to avoid PCR saturation. Samples from three independent experiments were analyzed. Figure 4 shows an example of results obtained from these experiments, and Table 3 shows results for the relative differential expression of the genes analyzed. These results come from at least three different RT-PCRs and from three different samples.

Two out of the five genes analyzed did not show differences in gene expression with RT-PCR even when a low number of PCR cycles was used. This result is not surprising, as one of the problems that RAP-PCR has, in addition to differential display, is the high proportion of false-positive results among clones obtained from differentially expressed bands (25). A major concern is the fact that one band may actually be com-

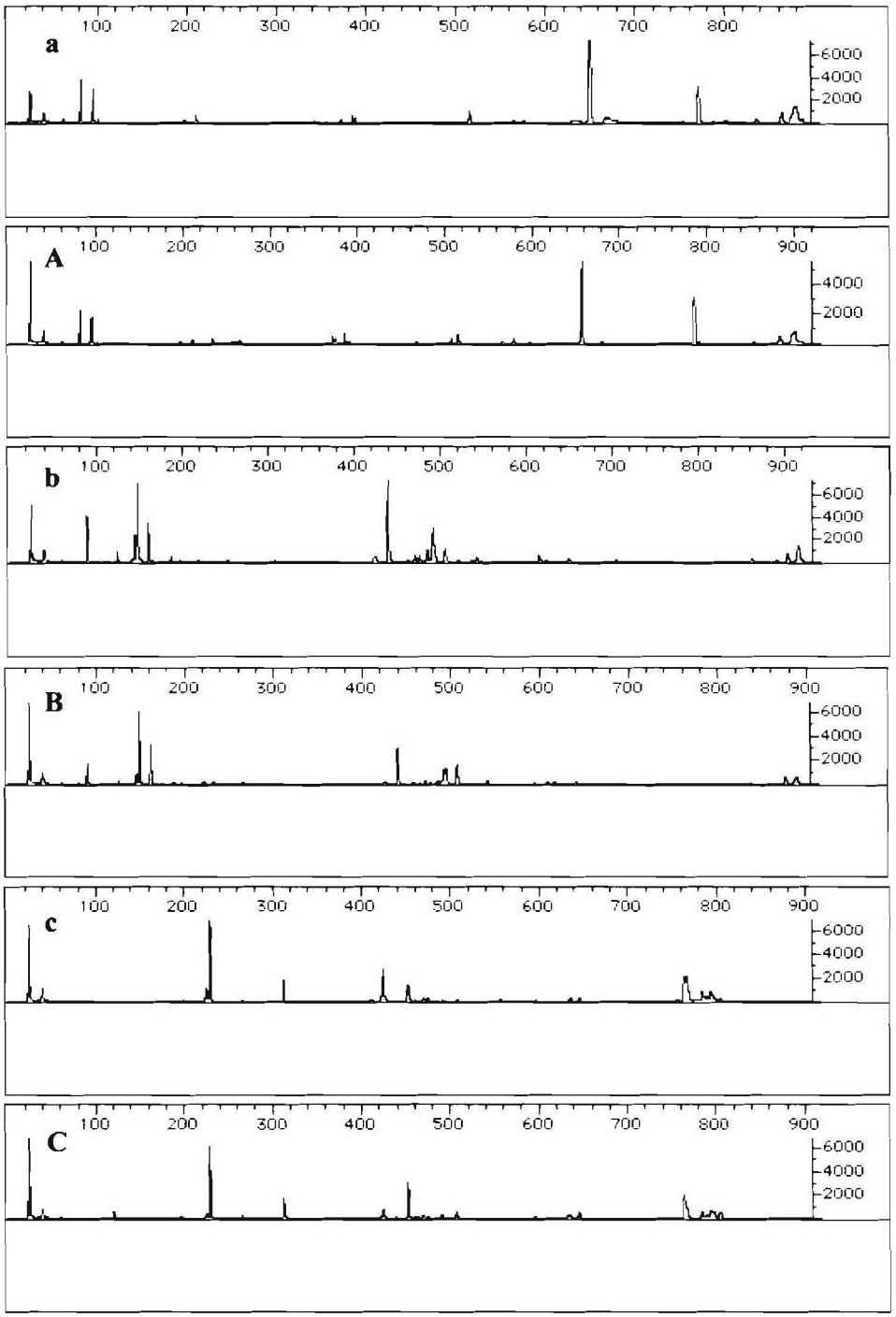

FIG. 1. T-RFLP profiles of the BBD mat bacterial communities. (a and A) HhaI-digested PCR products from BBD mat samples taken from coral and BBD mat samples suspended in seawater, respectively. (b and B) MspI-digested PCR products from BBD mat samples taken from coral and BBD mat samples suspended in seawater, respectively. (c and C) RsaI-digested PCR products from BBD mat samples taken from coral and BBD mat samples suspended in seawater, respectively.

posed of cDNAs derived from multiple genes (8, 25). Some of these genes may be differentially expressed, but others may be constitutively expressed. This was the case for clones DD 95-1 and DD 99-8. However, three of the clones analyzed did have differences in their levels of expression depending on whether they came from BBD mats infecting coral in situ or from BBD mats suspended in seawater. In all cases, these genes were up-regulated when the bacterial mat was infecting the coral.

Clone DD 95-4 had 51% homology with amino acid ABC transporter systems in bacteria and was up-regulated between

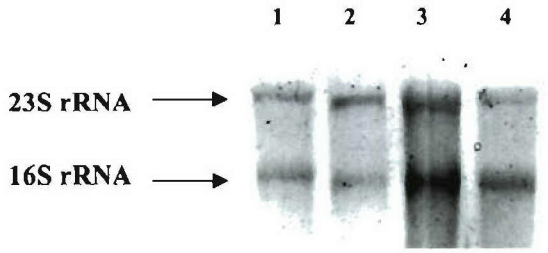

FIG. 2. Formaldehyde agarose gel showing RNA extractions of BBD microbial mats growing in situ on coral surfaces (lanes 1 and 2) and suspended in seawater (lanes 3 and 4).

31 and 40% (Table 3) during infection. In one sample, we found almost 100% up-regulation. Clone DD 99-9 was up-regulated between 9 and 34% (Table 3) during infection. As with DD 95-4, in one case there was almost complete transcriptional inhibition of gene DD 99-9 when the bacterial mat was living in seawater. This sequence presented high homology (93% identity) with photosystem I P700 chlorophyll A apoprotein A1 (PsaA) in cyanobacteria. Finally, the last gene that showed up-regulation during infection, clone DD 95-2, had

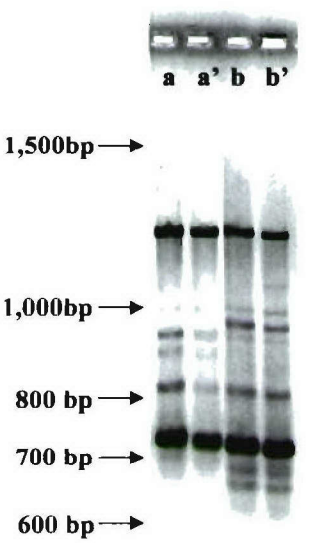

FIG. 3. Example of RAP-PCR results obtained by using a high-resolution agarose gel and the Lnr95 primer. Samples a and a' are duplicates from the same sample of RNA extracted from an in situ BBD mat growing on the coral surface. Samples b and b' are duplicates from the same sample of RNA extracted from a BBD mat suspended in seawater. Arrows indicate the positions of molecular weight standards not visible in the photo.

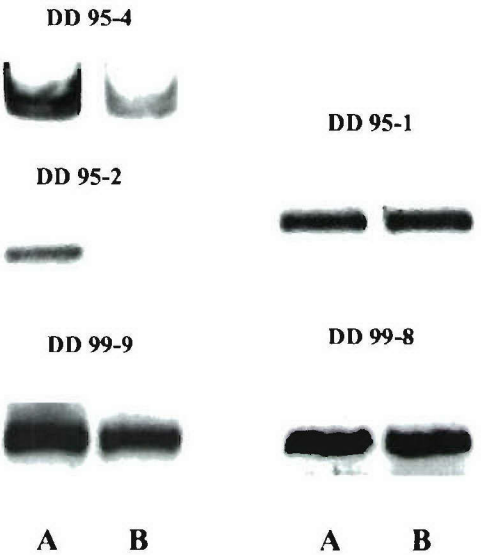

FIG. 4. RT-PCR analysis to assess relative differences in gene expression. Clone designations are given above the pictures. (A) BBD mat growing in situ on coral; (B) BBD mat in seawater.

25% homology with AraC-type DNA binding domain-containing proteins. All samples analyzed were completely inhibited for RNA synthesis of the DD 95-2 gene when the bacterial mat was removed from the infection site (Table 3). PCR analysis of the DNA obtained from these samples showed that the gene was present in the bacterial community. Therefore, the complete repression of DD 95-2 expression was not due to the absence of bacteria harboring this gene in the samples suspended in seawater.

DISCUSSION

Due to the difficulties in studying differences in gene expression in prokaryotes, most studies using RAP-PCR have been done only in recent years and have been restricted to laboratory conditions (5, 9, 16, 43). With the present study, we demonstrated that RAP-PCR may be used successfully to analyze differential gene expression in environmental samples. The differences in the gene expression of infectious BBD bacterial mats, which cause the death of a large number of coral worldwide (31), have been analyzed. The final goal of analyzing differences in gene expression is to determine the mechanism or mechanisms of pathogenesis and to look for clues about the environmental factors that lead to disease.

Significant differences between transcription levels of a set of different genes in the in situ and in the suspended BBD mat samples were observed. When removed from the coral tissue for 3 days, the BBD mat genes that were up-regulated during infection should be turned off or at least show a decreased level of activity. The short distances maintained between the infected bacterial mat and the samples suspended in seawater guaranteed identical environmental conditions (salinity, turbidity, light intensity, etc.) during the experiments. One of the major problems of analyzing differences in gene expression in bacteria comes from the fact that mRNA in prokaryotes does not have a poly(A) tail and that random primers therefore

TABLE 2. Best BLASTX hits for the sequences obtained from RAP-PCR profiles

Clone	Accession no.	Fragment size (bp)	BLASTX results		
			Accession no.	Protein encoded by gene	Organism
DD 95-1	AY494600	670	gi|28898568|	Conserved hypothetical protein	*V. parahaemolyticus*
DD 95-4	AY494601	568	gi|24372841|	Hypothetical amino acid ABC transporter	*S. oneidensis*
DD 99-8	AY494602	482	gi|21228041|	Glutamine-binding protein	*M. mazei*
DD 95-2	AY494603	410	gi|23137865|	AraC-type DNA binding domain-containing proteins	*C. hutchinsonii*
DD 99-9	AY494604	417	gi|97659|	Photosystem I P700 PsaA	*Synechocystis* sp. (strain PCC 6803)

have to be used in order to synthesize cDNA. Those primers are likely to anneal to rRNA, which constitutes the largest fraction of RNA in the samples, thus preventing efficient conversion of the small portion of mRNA into cDNA. It has been reported that when prokaryotic RNA was used, up to 40% of differentially expressed bands identified using differential display analysis were of ribosomal origin (30, 31). However, the results obtained by using RAP-PCR analysis show that this method successfully overcomes that problem. None of the cloned differentially expressed genes was a 16S rRNA gene, probably because bands that appear in all samples and at a high concentration are most likely to be the ones that come from rRNA.

A possible mechanism of pathogenesis for BBD in which an anoxic environment and the production of sulfide are toxic for the coral tissue and result in coral death has been proposed (37). However, there is no definitive proof that this is the real mechanism for tissue destruction (36), and nothing is known about what conditions lead to disease. The photosynthetic filamentous cyanobacterium *P. corallyticum* is the most conspicuous bacterium in BBD, and it is not known what its role during infection is. It is not yet understood why a photosynthetic organism is infecting a coral; perhaps this species requires something from the coral to survive or to obtain a growth advantage through the infectious process.

One of the sequences was up-regulated during infection; clone DD 95-4 had homology with amino acid ABC transporter systems in bacteria. Amino acids are important in both carbon and nitrogen metabolism of bacteria; for this reason, the ABC transport systems of bacteria have been widely studied (22). Nevertheless, there is no clear connection between the up-regulation of this ABC transporter and pathogenesis. In the case of BBD, the observed up-regulation of this gene could be due to the presence of amino acids available for consumption as a consequence of coral tissue destruction.

TABLE 3. Results for semiquantitative RT-PCR products analyzed by densitometry

Clone	RT-PCR result for[a]:		Differential expression range of up- or down-regulation (%)
	BBD mat growing on coral	BBD mat in seawater	
DD 95-1	++	++	0
DD 95-4	++	+	31–40
DD 99-8	++	++	0
DD 95-2	++	−	100
DD 99-9	++	+	9–34

[a] −, no expression detected; +, low levels of transcript expression; ++, high levels of transcript expression.

Of equal importance are the results obtained for the other two cDNAs analyzed. Clone DD 99-9 was up-regulated during infection and presented 100% homology with photosystem I P700 PsaA in cyanobacteria. Photosystem I is a membrane complex of 12 different proteins that produces the reduced NADPH needed to reduce CO_2 in the reactions of the Calvin cycle (48). PsaA along with PsaB coordinates the two chlorophylls forming the dimer in P700 (42, 48). Studies of differential expression in *Synechocystis* spp. under different environmental conditions have previously been reported (4, 28, 46). The level of expression of *psaA* is controlled by several environmental factors, such as day-night light cycles (13, 29). Singh and Sherman, using a customized amplification library, have shown that the expression of *psaA* increases when iron is available and decreases with iron depletion (44). Iron is an essential trace element for most bacteria and a limiting factor for primary production in seawater (12, 27, 47). During BBD infection, with the destruction of coral tissue and the death of the symbiotic dinoflagellates (*Symbiodinium* spp.) living inside the coral, the availability of iron increases at levels that allow the staggering growth of *P. corallyticum*. The low levels of available iron in seawater could explain, at least in part, why *P. corallyticum* is so difficult to detect in samples other than that of the BBD infectious mat (18, 36). Finally, the last gene that showed up-regulation during infection, clone DD 95-2, had 25% identity with AraC-type DNA binding domain-containing proteins. All samples analyzed showed complete inhibition of RNA synthesis for the DD 95-2 gene when the bacterial mat was removed from the infection site on the coral tissue surface. In animal pathogens, AraC-like transcriptional activators coordinate the expression of type III secretion genes (17), which are essential for the virulence of a large number of gram-negative pathogens. Moreover, some plant pathogens also utilize this kind of signal regulator (17). Most type III secretion systems have been found in *Proteobacteria*. However, DD 95-2 had homology to a gene present in *Cytophaga hutchinsonii*. Previous works have shown that members of the *Cytophaga-Flexibacter-Bacteroides* group are present in large numbers in the BBD bacterial mat (14, 19). Therefore, it is reasonable to hypothesize that these bacteria play an important role in the disease. Moreover, this group of bacteria includes microorganisms that are well-known pathogens in a variety of organisms that inhabit a wide variety of environments (3, 11, 32, 45).

Conclusions. RAP-PCR has been successfully used to detect genes that are differentially expressed under different environmental conditions in complex bacterial communities. This

work has identified genes that are involved in the pathogenesis of BBD, one of the most important infectious coral diseases. Three genes that are up-regulated when a BBD bacterial mat is infecting coral have been identified. One of the cDNAs, DD 95-4, had homology with amino acid ABC transporter systems in bacteria but no clear link with the mechanism of pathogenesis of the disease.

Conversely, the other two cDNAs analyzed may have a more direct link to the pathogenesis of BBD. DD 99-9 was up-regulated during infection and presented homology with photosystem I P700 PsaA in cyanobacteria. It has been shown that the expression of *psaA* increases when iron is available and decreases with iron depletion (44). The up-regulation of this gene could be linked to the increased levels of iron available due to coral tissue destruction. Finally, DD 95-2 was completely repressed when the bacterial mat was not in contact with the coral tissue. Furthermore, DD 95-2 has homology with AraC-type DNA binding domain-containing proteins, which are important regulators for expression of genes involved in virulence in gram-negative bacteria.

ACKNOWLEDGMENTS

We thank the Office of Naval Research (ONR-N00014-00-1-0609) for support of this research.

We also thank J. Klaus for his thorough review of the manuscript.

The conclusions of this study are those of the authors and do not necessarily reflect those of the funding agencies.

REFERENCES

1. **Ahmed, N., A. A. Siddiqui, and A. Ahmed.** 2000. DDRT-PCR: use of agarose gels for detection of amplified products. Mol. Vis. **6**:144–147.
2. **Antonius, A.** 1981. The "band" diseases in coral reefs. p. 7–14. *In* Fourth International Coral Reef Symposium, vol. 2. E. D. Gomez et al. (ed.). Proceedings of the University of the Philippines Marine Center, Manila, Philippines.
3. **Bader, J. A., C. A. Shoemaker, and P. H. Klesius.** 2003. Rapid detection of columnaris disease in channel catfish (*Ictalurus punctatus*) with a new species-specific 16-S rRNA gene-based PCR primer for *Flavobacterium columnare*. J. Microbiol. Methods **52**:209–220.
4. **Bhaya, D., D. Vaulot, P. Amin, A. W. Takahashi, and A. R. Grossman.** 2000. Isolation of regulated genes of the cyanobacterium *Synechocystis* sp. strain PCC 6803 by differential display. J. Bacteriol. **182**:5692–5699.
5. **Bidle, K. A., and D. H. Bartlett.** 2001. RNA arbitrarily primed PCR survey of genes regulated by ToxR in the deep-sea bacterium *Photobacterium profundum* strain SS9. J. Bacteriol. **183**:1688–1693.
6. **Bockelmann, R., B. Bonnekoh, and H. Gollnick.** 1999. Optimized visualization and PCR reamplification of differentially displayed cDNA bands detected by silver staining in polyacrylamide gels as established in the model of dithranol-treated keratinocytes. Skin Pharmacol. Appl. Skin Physiol. **12**:54–63.
7. **Bosch, I., H. Melichar, and A. B. Pardee.** 2000. Identification of differentially expressed genes from limited amounts of RNA. Nucleic Acids Res. **28**:E27.
8. **Callard, D., B. Lescure, and L. Mazzolini.** 1994. A method for the elimination of false positives generated by the mRNA differential display technique. BioTechniques **16**:1096–1907.
9. **Chakrabortty, A., S. Das, S. Majumdar, K. Mukhopadhyay, S. Roychoudhury, and K. Chaudhuri.** 2000. Use of RNA arbitrarily primed-PCR fingerprinting to identify *Vibrio cholerae* genes differentially expressed in the host following infection. Infect. Immun. **68**:3878–3887.
10. **Chen, J. J., and K. Peck.** 1996. Non-radioisotopic differential display method to directly visualize and amplify differential bands on nylon membrane. Nucleic Acids Res. **24**:793–794.
11. **Cipriano, R. C., L. A. Ford, and J. D. Teska.** 1995. Association of *Cytophaga psychrophila* with mortality among eyed eggs of Atlantic salmon (*Salmo salar*). J. Wildl. Dis. **31**:166–171.
12. **Coale, K. H., K. S. Johnson, S. E. Fitzwater, R. M. Gordon, S. Tanner, F. P. Chavez, L. Ferioli, C. Sakamoto, P. Rogers, F. Millero, P. Steinberg, P. Nightingale, D. Cooper, W. P. Cochlan, and R. Kudela.** 1996. A massive phytoplankton bloom induced by an ecosystem-scale iron fertilization experiment in the equatorial Pacific Ocean. Nature **383**:495–501.
13. **Colon-Lopez, M. S., and L. A. Sherman.** 1998. Transcriptional and translational regulation of photosystem I and II genes in light-dark- and continuous-light-grown cultures of the unicellular cyanobacterium *Cyanothece* sp. strain ATCC 51142. J. Bacteriol. **180**:519–526.
14. **Cooney, R. P., O. Pantos, M. D. Le Tissier, M. R. Barer, A. G. O'Donnell, and J. C. Bythell.** 2002. Characterization of the bacterial consortium associated with black band disease in coral using molecular microbiological techniques. Environ. Microbiol. **4**:401–413.
15. **Deora, R.** 2002. Differential regulation of the *Bordetella bipA* gene: distinct roles for different BvgA binding sites. J. Bacteriol. **184**:6942–6951.
16. **Du, L. D., and P. E. Kolenbrander.** 2000. Identification of saliva-regulated genes of *Streptococcus gordonii* DL1 by differential display using random arbitrarily primed PCR. Infect. Immun. **68**:4834–4837.
17. **Francis, M. S., H. Wolf-Watz, and A. Forsberg.** 2002. Regulation of type III secretion systems. Curr. Opin. Microbiol. **5**:166–172.
18. **Frias-Lopez, J., G. T. Bonheyo, Q. Jin, and B. W. Fouke.** 2003. Cyanobacteria associated with coral black band disease in Caribbean and Indo-Pacific reefs. Appl. Environ. Microbiol. **69**:2409–2413.
19. **Frias-Lopez, J., A. L. Zerkle, G. T. Bonheyo, and B. W. Fouke.** 2002. Partitioning of bacterial communities between seawater and healthy, black band diseased, and dead coral surfaces. Appl. Environ. Microbiol. **68**:2214–2228.
20. **Froussard, P.** 1992. A random-PCR method (rPCR) to construct whole cDNA library from low amounts of RNA. Nucleic Acids Res. **20**:2900.
21. **Harvell, C. D., K. Kim, J. M. Burkholder, R. R. Colwell, P. R. Epstein, D. J. Grimes, E. E. Hofmann, E. K. Lipp, A. D. Osterhaus, R. M. Overstreet, J. W. Porter, G. W. Smith, and G. R. Vasta.** 1999. Emerging marine diseases—climate links and anthropogenic factors. Science **285**:1505–1510.
22. **Hosie, A. H., and P. S. Poole.** 2001. Bacterial ABC transporters of amino acids. Res. Microbiol. **152**:259–270.
23. **Hughes, T. P., A. H. Baird, D. R. Bellwood, M. Card, S. R. Connolly, C. Folke, R. Grosberg, O. Hoegh-Guldberg, J. B. Jackson, J. Kleypas, J. M. Lough, P. Marshall, M. Nystrom, S. R. Palumbi, J. M. Pandolfi, B. Rosen, and J. Roughgarden.** 2003. Climate change, human impacts, and the resilience of coral reefs. Science **301**:929–933.
24. **Johnson, B. J., I. Estrada, Z. Shen, S. Ress, P. Willcox, M. J. Colston, and G. Kaplan.** 1998. Differential gene expression in response to adjunctive recombinant human interleukin-2 immunotherapy in multidrug-resistant tuberculosis patients. Infect. Immun. **66**:2426–2433.
25. **Li, F., E. S. Barnathan, and K. Kariko.** 1994. Rapid method for screening and cloning cDNAs generated in differential mRNA display: application of Northern blot for affinity capturing of cDNAs. Nucleic Acids Res. **22**:1764–1765.
26. **Macaluso, K. R., A. Mulenga, J. A. Simser, and A. F. Azad.** 2003. Differential expression of genes in uninfected and *Rickettsia*-infected *Dermacentor variabilis* ticks as assessed by differential-display PCR. Infect. Immun. **71**:6165–6170.
27. **Martin, J. H., K. H. Coale, K. S. Johnson, S. E. Fitzwater, R. M. Gordon, S. J. Tanner, C. N. Hunter, V. A. Elrod, J. L. Nowicki, T. L. Coley, R. T. Barber, S. Lindley, A. J. Watson, K. Van Scoy, C. S. Law, M. I. Liddicoat, R. Ling, T. Stanton, J. Stockel, C. Collins, A. Anderson, R. Bidigare, M. Ondrusek, M. Latasa, F. J. Millero, K. Lee, W. Yao, J. Z. Zhang, D. Friederich, C. Sakamoto, F. Chavez, K. Buck, Z. Kolber, R. Greene, P. Falkowski, S. W. Chisholm, F. Hoge, R. Swift, J. Yungel, S. Turner, P. Nightingale, A. Hatton, P. Liss, and N. W. Tindale.** 1994. Testing the iron hypothesis in ecosystems of the equatorial Pacific Ocean. Nature **371**:123–129.
28. **Mate, Z., L. Sass, M. Szekeres, I. Vass, and F. Nagy.** 1998. UV-B-induced differential transcription of psbA genes encoding the D1 protein of photosystem II in the cyanobacterium *Synechocystis* 6803. J. Biol. Chem. **273**:17439–17444.
29. **Muramatsu, M., and Y. Hihara.** 2003. Transcriptional regulation of genes encoding subunits of photosystem I during acclimation to high-light conditions in *Synechocystis* sp. PCC 6803. Planta **216**:446–453.
30. **Nagel, A., J. T. Fleming, and G. S. Sayler.** 1999. Reduction of false positives in prokaryotic mRNA differential display. BioTechniques **26**:641–643.
31. **Nagel, A. C., J. T. Fleming, G. S. Sayler, and K. L. Beattie.** 2001. Screening for ribosomal-based false positives following prokaryotic mRNA differential display. BioTechniques **30**:988–990.
32. **Nomura, S.** 1997. Recent knowledge on fish pathogenic bacteria *Aeromonas salmonicida*, *Listonella anguillara* and *Cytophaga columnaris*, and their virulence factors. Nippon Saikingaku Zasshi **52**:393–416.
33. **Pandolfi, J. M., R. H. Bradbury, E. Sala, T. P. Hughes, K. A. Bjorndal, R. G. Cooke, D. McArdle, L. McClenachan, M. J. Newman, G. Paredes, R. R. Warner, and J. B. Jackson.** 2003. Global trajectories of the long-term decline of coral reef ecosystems. Science **301**:955–958.
34. **Richardson, L. L.** 1998. Coral disease: what is really known? Trends Ecol. Evol. **13**:438–443.
35. **Richardson, L. L.** 1996. Horizontal and vertical migration patterns of *Phormidium corallyticum* and *Beggiatoa* spp. associated with black-band disease of corals. Microb. Ecol. **32**:323–335.
36. **Richardson, L. L.** 1997. Occurrence of the black band disease cyanobacterium on healthy corals of the Florida Keys. Bull. Mar. Sci. **61**:485–490.
37. **Richardson, L. L., K. G. Kuta, S. Schnell, and R. G. Carlton.** 1997. Ecology of the black band disease microbial consortium. p. 597–600. *In* H. A. Lessios and I. G. Macintyre (ed.). Eighth International Coral Reef Symposium, vol. 1. Smithsonian Tropical Research Institute, Balboa, Panama.

38. **Rompf, R., and G. Kahl.** 1997. mRNA differential display in agarose gels. BioTechniques **23:**28, 30, 32.
39. **Rosenberg, E., and Y. Ben-Haim.** 2002. Microbial diseases of corals and global warming. Environ. Microbiol. **4:**318–326.
40. **Rützler, K., and D. L. Santavy.** 1983. The black band disease of Atlantic reef corals. I. Description of the cyanophyte pathogen. Mar. Ecol. **4:**301–319.
41. **Sambrook, J., and D. W. Russell.** 2001. Molecular cloning: a laboratory manual, 3rd ed. Cold Spring Harbor Laboratory Press, Cold Spring Harbor, N.Y.
42. **Schubert, W. D., O. Klukas, N. Krauss, W. Saenger, P. Fromme, and H. T. Witt.** 1997. Photosystem I of *Synechococcus elongatus* at 4 A resolution: comprehensive structure analysis. J. Mol. Biol. **272:**741–769.
43. **Shepard, B. D., and M. S. Gilmore.** 1999. Identification of aerobically and anaerobically induced genes in *Enterococcus faecalis* by random arbitrarily primed PCR. Appl. Environ. Microbiol. **65:**1470–1476.
44. **Singh, A. K., and L. A. Sherman.** 2000. Identification of iron-responsive, differential gene expression in the cyanobacterium *Synechocystis* sp. strain PCC 6803 with a customized amplification library. J. Bacteriol. **182:**3536–3543.
45. **Toncheva-Panova, T., and J. Ivanova.** 2000. Influence of physiological factors on the lysis effect of *Cytophaga* on the red microalga *Rhodella reticulata*. J. Appl. Microbiol. **88:**358–363.
46. **Vinnemeier, J., and M. Hagemann.** 1999. Identification of salt-regulated genes in the genome of the cyanobacterium *Synechocystis* sp. strain PCC 6803 by subtractive RNA hybridization. Arch. Microbiol. **172:**377–386.
47. **Webb, E., J. Moffett, and J. Waterbury.** 2001. Iron stress in open-ocean cyanobacteria (*Synechococcus*, *Trichodesmium*, and *Crocosphaera* spp.): identification of the IdiA protein. Appl. Environ. Microbiol. **67:**5444–5452.
48. **Webber, A. N., and W. Lubitz.** 2001. P700: the primary electron donor of photosystem I. Biochim. Biophys. Acta **1507:**61–79.

APPLIED AND ENVIRONMENTAL MICROBIOLOGY, Oct. 2004, p. 5955–5962 Vol. 70, No. 10
0099-2240/04/$08.00+0 DOI: 10.1128/AEM.70.10.5955–5962.2004
Copyright © 2004, American Society for Microbiology. All Rights Reserved.

Bacterial Community Associated with Black Band Disease in Corals

Jorge Frias-Lopez,* James S. Klaus, George T. Bonheyo, and Bruce W. Fouke

Department of Geology, University of Illinois, Urbana, Illinois

Received 16 April 2004/Accepted 2 June 2004

Black band disease (BBD) is a virulent polymicrobial disease primarily affecting massive-framework-building species of scleractinian corals. While it has been well established that the BBD bacterial mat is dominated by a cyanobacterium, the quantitative composition of the BBD bacterial mat community has not described previously. Terminal-restriction fragment length polymorphism (T-RFLP) analysis was used to characterize the infectious bacterial community of the bacterial mat causing BBD. These analyses revealed that the bacterial composition of the BBD mat does not vary between different coral species but does vary when different species of cyanobacteria are dominant within the mat. On the basis of the results of a new method developed to identify organisms detected by T-RFLP analysis, our data show that besides the cyanobacterium, five species of the division *Firmicutes*, two species of the *Cytophaga-Flexibacter-Bacteroides* (CFB) group, and one species of δ-proteobacteria are also consistently abundant within the infectious mat. Of these dominant taxa, six were consistently detected in healthy corals. However, four of the six were found in much higher numbers in BBD mats than in healthy corals. One species of the CFB group and one species of *Firmicutes* were not always associated with the bacterial communities present in healthy corals. Of the eight dominant bacteria identified, two species were previously found in clone libraries obtained from BBD samples; however, these were not previously recognized as important. Furthermore, despite having been described as an important component of the pathogenetic mat, a *Beggiatoa* species was not detected in any of the samples analyzed. These results will permit the dominant BBD bacteria to be targeted for isolation and culturing experiments aimed at deciphering the disease etiology.

Coral reefs are among the most biologically diverse ecosystems on earth and harbor a large number of unique marine taxa. However, over the last few decades, 27% of coral reefs have been destroyed worldwide, and in places such as Belize, up to 75% of the coral reef habitat has been lost (38). The destruction of coral reef ecosystems is a complex phenomenon and can be attributed to a combination of factors (16, 19, 30). One of the leading causes of reef degradation has been a dramatic increase in reef coral mortality due to disease (30). While historically the study of coral diseases and their role in the ecology of reef ecosystems has been minimal, with increases in both the number and severity of coral diseases, this topic has rapidly gained scientific attention (26, 30). However, while the number of newly described coral diseases has steadily increased, in most cases their etiology has remained unknown (26).

Black band disease (BBD) is one of the most widespread and destructive coral diseases. This is largely due to its preferential infection of the massive-framework-building corals that serve as ecological cornerstones of the reef ecosystem (11). Antonius first described BBD in the 1970s as a black bacterial mat that migrates in a top-down manner across the surface of the coral, destroying the tissue and leaving behind bare skeleton (5, 15). After the tissue has been stripped from the coral surface, algae rapidly colonize the naked skeleton, preventing any subsequent recovery from the infection. Black band disease has been extremely devastating to certain massive corals, suggesting that certain species of coral are more immune to BBD infection than others (3).

BBD is a polymicrobial disease presumably caused by a consortium of microorganisms rather than a single pathogen (26, 28). Early descriptions of the disease, based solely on optical or electron microscopy, reported that the BBD mat consortium was dominated by a filamentous, nonheterocystous, cyanobacterium first classified as *Phormidium corallyticum* (31, 35). Further optical microscopy studies revealed that there were other organisms accompanying *P. corallyticum* in the BBD mat: the motile sulfide-oxidizing bacterium *Beggiatoa*, the sulfate-reducing bacterium *Desulfovibrio*, numerous heterotrophic bacteria, and marine fungi (10, 15, 25).

Molecular techniques have now shown that the composition of the bacterial community living in the infectious mat is significantly more complex than was initially recognized. As many as 64 different species of bacteria have been identified living in the BBD mat (9, 14). These methods have confirmed the presence of *Desulfovibrio* and related species in the infectious community but have not been able to verify the presence of *Beggiatoa*, one of the organisms previously described as a major component of the BBD bacterial mat (9, 14). On the basis of the known 16S rRNA gene sequences, the primers used in these studies should not have had any problem amplifying sequences from *Beggiatoa* spp. (9).

Molecular analysis of BBD has given new insights into the nature of the cyanobacteria present in the BBD mat. Results using specific primers revealed that the dominant cyanobacteria within BBD mat samples belong to at least three different taxa, despite producing similar patterns and symptoms of disease (13). However, since these species of cyanobacteria have not been formally classified, the name *P. corallyticum* refers to

* Corresponding author. Mailing address: Department of Geology, University of Illinois, 1301 W. Green St., Urbana, IL 61801. Phone: (217) 333-0672. Fax: (217) 244-4996. E-mail: friaslop@uiuc.edu.

any of the different filamentous cyanobacteria present in the BBD mat. While there exists a general consensus as to the importance of *P. corallyticum* during disease development, the reasons to consider it the primary pathogen remain largely circumstantial (9, 28).

To understand the process of infection and to elucidate the possible environmental factors involved in its development, it is first necessary to identify those organisms that play a crucial role in the disease. The aim of the present study is to characterize the composition of the dominant and potentially important bacteria present in the BBD bacterial mat. Terminal-restriction fragment length polymorphism (T-RFLP) analysis was used to identify the most abundant bacteria present in BBD mats. Once identified, the most-probable-number PCR (MPN-PCR) technique was used to quantify the abundance of those species.

Results show that the species of coral being infected does not affect the composition of the infectious bacterial mat. Instead, differences in the mat composition appear to be linked to the species of cyanobacteria dominant in the infection. Quantification of the most abundant organisms present in the infectious mat shows that there are three major groups of bacteria that accompany the cyanobacterium: (i) members of the division *Firmicutes* (five species), (ii) *Cytophaga-Flexibacter-Bacteroides* (CFB) group (two species), and (iii) δ-proteobacteria (one species). Of the eight species identified using specific primers, two were not consistently detected in healthy corals, making them ideal candidates for future studies on the etiology of the disease. Other species, while consistently detected, were present at much lower numbers than those found during infection. The combined results of T-RFLP and quantification suggest that the presence of the filamentous cyanobacterium is the driving force that controls the final composition of the BBD mat.

MATERIALS AND METHODS

Fieldwork and sample collection. BBD mat samples were collected from infected corals at three different locations along the southwestern coast of Curaçao, Netherlands Antilles, in the Caribbean Sea, and at two different locations on the northern coast of New Britain, Papua New Guinea, in the Indo-Pacific Sea. The three sites on Curaçao included a sea aquarium, a water plant, and Playa Kalki (13). At each of these three locations, both healthy and BBD-infected colonies of *Montastrea annularis* and *Diploria strigosa* were collected. On New Britain, Papua New Guinea, BBD mat samples of infected colonies of *Porites lutea* were collected off the northern coast at Father's Reef (13). All samples were collected from a water depth between 4 and 5 m. Small 4-cm^2 sections of mat and coral skeleton were individually collected using a small chisel and placed in a sterile disposable 50-ml polypropylene centrifuge tube while using standard scuba techniques to access the reefs. Portions of BBD mats that could be physically peeled off the coral surface using forceps were placed in their own sterile disposable 15-ml polypropylene centrifuge tube. Immediately upon return to shore, the seawater within each tube was decanted, and coral samples were immersed in 80% ethanol for molecular analyses. Live *D. strigosa* specimens were also collected in Curaçao, transported to the lab in Illinois, and kept alive in an aquarium. One of these colonies developed BBD and was processed as described above.

DNA extraction. DNA extraction was performed as described previously (14). Bead beating and freeze-thaw cycling protocols were used to extract community genomic DNA from the cells collected from the crushed coral slurries. The same procedure was performed in parallel using ultrapure water as a negative control and 50 μl of an *Escherichia coli* culture that had been allowed to grow overnight as a positive control.

PCR and T-RFLP analyses. Specific primers to amplify 16S rRNA genes from cyanobacteria were used (24) to characterize the cyanobacterium infecting the specimen of *D. strigosa* that developed BBD spontaneously in the aquarium. The amplified products were cloned and sequenced as described below. The cyanobacteria infecting corals sampled from the environment had been characterized previously (13).

T-RFLP analysis was performed by the method of Liu et al. (20). Universal bacterial oligonucleotide primers used in the PCR amplifications were obtained from Integrated DNA Technologies (Coralville, Iowa): forward primer Univ9F (5'-GAGTTTGATYMTGGCTC) with a 5' carboxyfluorescine (FAM) label and reverse primer Univ1509R (5'-GYTACCTTGTTACGACTT). Reaction mixtures included the following: 10 μl of TaqMaster buffer (an agent which improves thermostability and processivity of the polymerase), 5 μl of *Taq* reaction buffer containing 15 mM $MgCl_2$ (Eppendorf, Westbury, N.Y.), 4 μl of a mixture of deoxynucleoside triphosphates (2.5 mM concentration of each deoxynucleoside triphosphate) (Gibco/BRL, Rockville, Md.), 1 μl each of forward and reverse primers (200 ng each), 5 to 30 μl of the sample preparation, and water to bring the total volume to 49.5 μl. An initial denaturation or hot start of 5 min at 95°C was followed by the addition of 0.5 μl (2 U) of MasterTaq polymerase (Eppendorf). The hot start was followed by 30 or 35 cycles of the following incubation pattern: 94°C for 1 min, 55°C for 1 min, and 72°C for 2 min. A final extension step of 5 min at 72°C concluded the reaction.

PCR products were combined to a final volume of 300 μl, purified using the Wizard PCR prep kit (Promega, Madison, Wis.), and eluted with 30 μl of water. Clean DNA (10 μl) was aliquoted into each of three tubes, and restriction digestions were performed with RsaI, HhaI, and MspI. The final volume of each digest was 20 μl. At least 300 ng of total DNA per digestion was used. Tubes were first incubated overnight at 37°C, covered with aluminum foil to prevent photobleaching of the FAM label, and kept at −20°C.

Prior to loading on a gel, 1 μl of sample was added to a loading buffer consisting of 1.25 μl of deionized formamide, 0.25 μl of blue loading dye, and 0.3 μl of size standard (tetrachloro-6-carboxyfluorescine [TAMRA] 2500). The samples were then mixed and denatured at 95°C for 3 min prior to loading onto a 5% Long Ranger (proprietary acrylamide formula from BioWhittaker) and 7 M urea gel. Analyses were run on a 377-XL sequencer (Applied Biosystems, Foster City, Calif.) with a run time of 5 h. The data were analyzed using the ABI GeneScan software. T-RFLP profiles were analyzed using the TAP T-RFLP program at the Ribosomal Database Project II website (http://rdp.cme.msu.edu/html/analyses.html).

Cloning and sequencing. To identify the most abundant peaks from the T-RFLP analysis, digested products were purified by electrophoresis in a 6% polyacrylamide gel under native conditions in a SE 600 series vertical slab gel unit from Hoefer Scientific Instruments (San Francisco, Calif.). One lane in each gel contained the 100-bp DNA size standard ladder available from Invitrogen (Carlsbad, Calif.). The DNA bands that were selected had sizes that corresponded approximately to the results obtained from the T-RFLP analysis (error margin, 50 bp).

To elute the DNA from the acrylamide, 200 μl of crush and soak solution (0.5 M ammonium acetate, 0.1% sodium dodecyl sulfate, 0.1 mM EDTA) was added to the excised band, and the acrylamide was crushed and incubated overnight at 37°C. On the following day, the solid acrylamide was concentrated via centrifugation for 10 min at 16,000 × *g*. The supernatant was transferred to a clean tube, and another 200 μl of crush and soak solution was added to the solid acrylamide pellet. Following centrifugation, the recovered supernatant was pooled with the initial fraction. DNA was then precipitated and recovered. The DNA fragments obtained from HhaI and MspI digestions were blunted using T4 DNA polymerase (Invitrogen) or the large Klenow polymerase subunit (Invitrogen), following the manufacturer's instructions.

In order to clone the product into pGEM-T vector (Promega), the DNA was incubated for 10 min at 72°C in the presence of *Taq* polymerase and dATP (2.5 mM). The gel-purified PCR product was then cloned into pGEM-T and transformed into competent DH5αMCR *E. coli* cells using the manufacturer's instructions and standard techniques (32). Clones were checked for the presence of the insert by PCR using the primers M13 (−21) and T7 (−26). A RFLP analysis of the products was performed to select for clones that presented identical patterns. PCR products were digested with MspI and HinP1 enzymes and analyzed in a 1.6% Metaphor agarose gel. Only clones with the correct sizes and present in more than one RFLP analysis were selected for sequence analysis. These clones were transferred to petri dishes containing Luria broth agar supplemented with 100 μg of ampicillin (Roche Molecular Biochemicals, Indianapolis, Ind.) per ml and incubated overnight at 37°C.

Inoculation, culturing, template preparation, and sequencing were performed by the High Throughput Laboratory of the University of Illinois W. M. Keck Center for Comparative and Functional Genomics. The petri cultures were used to inoculate 2-ml 96-well culture blocks containing Circle Grow medium (Bio 101

TABLE 1. Primers used to amplify the specific 16s rRNA sequences for MNP-PCR analysis

Clone	Direction[a]	Primer sequence
CD22E1	Fwd	5′-CCCGTAGGAGTCTGGTCCGT-3′
	Rev	5′-AGAGGAAGGTCCCCCACACT-3′
CD22B1	Fwd	5′-TTGGAAGCGCAACCCTTG-3′
	Rev	5′-GAGTGCCCAGCATTACCTGC-3′
CD22E6	Fwd	5′-ACTGGGACTGGCTTTTTGGG-3′
	Rev	5′-ACGGGCGGCTAAGGAGTAAT-3′
R3-M4	Fwd	5′-GGAGGATCCGAGCGTTATCC-3′
	Rev	5′-CGCCTACGCACCCTTTAAAC-3′
CD22B8	Fwd	5′-GGATTCGCTAGTAATCGCGC-3′
	Rev	5′-CCGGGAACGTATTCACCG-3′
CD22E5	Fwd	5′-GGGTGAGTAACGCGTGGGTA-3′
	Rev	5′-TCGATGTGTTATCCCCCTGC-3′
CD22D4	Fwd	5′-TCTGACCGTTTCTGTAATGGAAAC-3′
	Rev	5′-CACCTGTCACTTCTGCTCCG-3′
CD22D5	Fwd	5′-CTAACTCCGTGCCAGCAGC-3′
	Rev	5′-CGATTAACGCTCGCACCCT-3′
CD1C11	Fwd	5′-CTGTAGGTGGCCAGCT-3′
	Rev	5′-TTCCCTTCGCAGGTTCGCTGC-3′

[a] Fwd, forward; Rev, reverse.

Inc., Vista, Calif.) supplemented with ampicillin. Plasmid template DNA was purified from the cultures using an automated system and the QIAwell 96 Turbo prep BioRobot kit (QIAGEN, Valencia, Calif.). The first round of sequencing was completed using the T7 (−26) primer and Big Dye Terminator chemistry (version 2.0) from Applied Biosystems. Sequencing was performed on an ABI 3700 capillary sequencer and then processed in the Bioinformatics Unit of the W. M. Keck Center.

MPN-PCR and dot blot analyses. MPN-PCR quantification was performed as follows. First, eight primer sets specific for the different bacterial species identified were created (Table 1). Additionally, a primer pair specific for the 16S rRNA gene of cyanobacterium CD1C11 (GenBank accession number AY038527) (13) was also used for the MPN-PCR experiments. Primer sequence specificity was tested using Probe Match at the Ribosomal Database Project II website (http://rdp.cme.msu.edu/html/index.html). The primer pairs were tested for the ability to amplify the 16S rRNA gene from the different clones isolated during this project. No cross-reactivity was detected. To assess the sensitivity of PCR amplification, we performed experiments using different concentrations of *E. coli* and universal primers for the 16S rRNA gene. Successful amplification occurred with as little as 10 to 50 cells. *E. coli* has seven copies of the 16S rRNA gene in its genome (17); therefore, the sensitivity for the number of DNA molecules of 16S rRNA ranges from 70 to 350 copies of DNA. For the MPN-PCR analysis, the sensitivity was determined to be 350 copies of 16S rRNA DNA.

Dot blot analysis was used as a sensitive and rapid means to process a large number of samples. Serial dilutions ($1\times$ to $10^{-4}\times$ concentration) of chromosomal DNA from BBD mat samples containing cyanobacterium CD1C11 and three healthy coral samples were prepared in triplicate. The nine specific primers for the different species and cyanobacteria (Table 1) were used to amplify DNA (target DNA) from the dilution series. These PCR products were applied to a nylon membrane (GeneScreen; NEN Life Sciences Products, Boston, Mass.) using a Minifold I sample filtration manifold (Schleicher & Schuell, Keene, N.H.) and bound using a Spectrolinker XL-1500 UV-cross-linker (Spectronics Corp., Westbury, N.Y.).

The probes were synthesized by PCR amplifying 16S rRNA genes from BBD mat samples with the universal bacterial oligonucleotide primers. The probes used for the dot blot analyses were always obtained from a different BBD mat sample than that used to create the target DNA. Probes were labeled and detected using the Renaissance random primer fluorescein labeling kit (Perkin-Elmer Life Sciences, Boston, Mass.) following the manufacturer's instructions. MPN-PCR data were converted to number of 16S rRNA genes using standard MPN tables (37). Concentrations of bacteria present in healthy and BBD coral samples (Table 1) were compared using the Mann-Whitney U test statistic and the SPSS 10.0 statistical package (SPSS Inc., Chicago, Ill.).

Sequence and phylogenetic analyses. The sequences obtained were compared with the GenBank database using the Basic Local Alignment Search Tool (BLAST) network service (2). Consensus sequences were analyzed using CHIMERA_CHECK version 2.7 at the Ribosomal Database Project II website (http://rdp.cme.msu.edu/html/index.html) (21).

Sequences were aligned using the Clustal X program, and phylogenetic analysis and trees were obtained using the program PAUP* version 4.0b10 (34). Trees were constructed by parsimony and by bootstrapping 10,000 trees from resampled data.

Nucleotide sequence accession numbers. The sequences of the partial gene fragments identified in this work are deposited in GenBank under accession numbers AY497293 through AY497300.

RESULTS

Characterization of the bacterial communities in different samples of BBD mats. T-RFLP was used to identify the most abundant organisms present in the BBD bacterial mat. A total of 12 BBD mat samples were analyzed: 2 samples were from infected *P. lutea* (New Britain), 1 was from *M. annularis* (Curaçao), and the other 9 were from *D. strigosa* (Curaçao). An additional sample from *D. strigosa* living in an aquarium at the University of Illinois was also analyzed.

In order to check the reliability of T-RFLP in our samples, one sample from *D. strigosa* was analyzed five times, and another three samples from *D. strigosa* were analyzed in duplicate. Additionally, the sample from *M. annularis* and one of the samples from *P. lutea* were also analyzed in duplicate. All repetitions for a given sample provided an identical pattern.

T-RFLP profiles for all BBD samples were the same except for two cases (Fig. 1). The distinct profiles corresponded to a sample of *P. lutea* taken in New Britain, Papua New Guinea, and the sample of *D. strigosa* that spontaneously developed BBD in the aquarium. In both cases, the BBD mat was inhabited by a unique species of cyanobacteria. The sample of *P. lutea* was infected with a species of cyanobacteria previously identified as cyanobacterium PNG-50 (13). The sample in the aquarium that developed BBD was infected by the cyanobacterium BBT. Although different species of cyanobacteria are associated with BBD, all of them are phylogenetically related to marine nonheterocystous filamentous cyanobacteria but not to marine *Phormidium* species (Fig. 2).

When cyanobacterial sequence CD1C11 was detected in the BBD mat, the resulting T-RFLP profile was identical regardless of the species of coral infected. Furthermore, comparison of T-RFLP profiles generated from healthy coral samples shows that only one peak is shared between BBD samples and healthy corals (18).

Identification of the predominant bacteria in the BBD mat. To identify the microorganisms corresponding to the T-RFLP profiles, the patterns were analyzed using the TAP T-RFLP program (21). Unfortunately, no exact matches were found for any of the profiles derived from BBD samples. To overcome this problem, a polyacrylamide gel was used to separate and identify DNA fragments corresponding in size to the peaks obtained from the T-RFLP analysis (Fig. 3). Bands with sizes closely matching those of the peaks identified by T-RFLP were excised, cloned, and sequenced. In all cases, at least four clones from the same band were sequenced. On several occasions, a

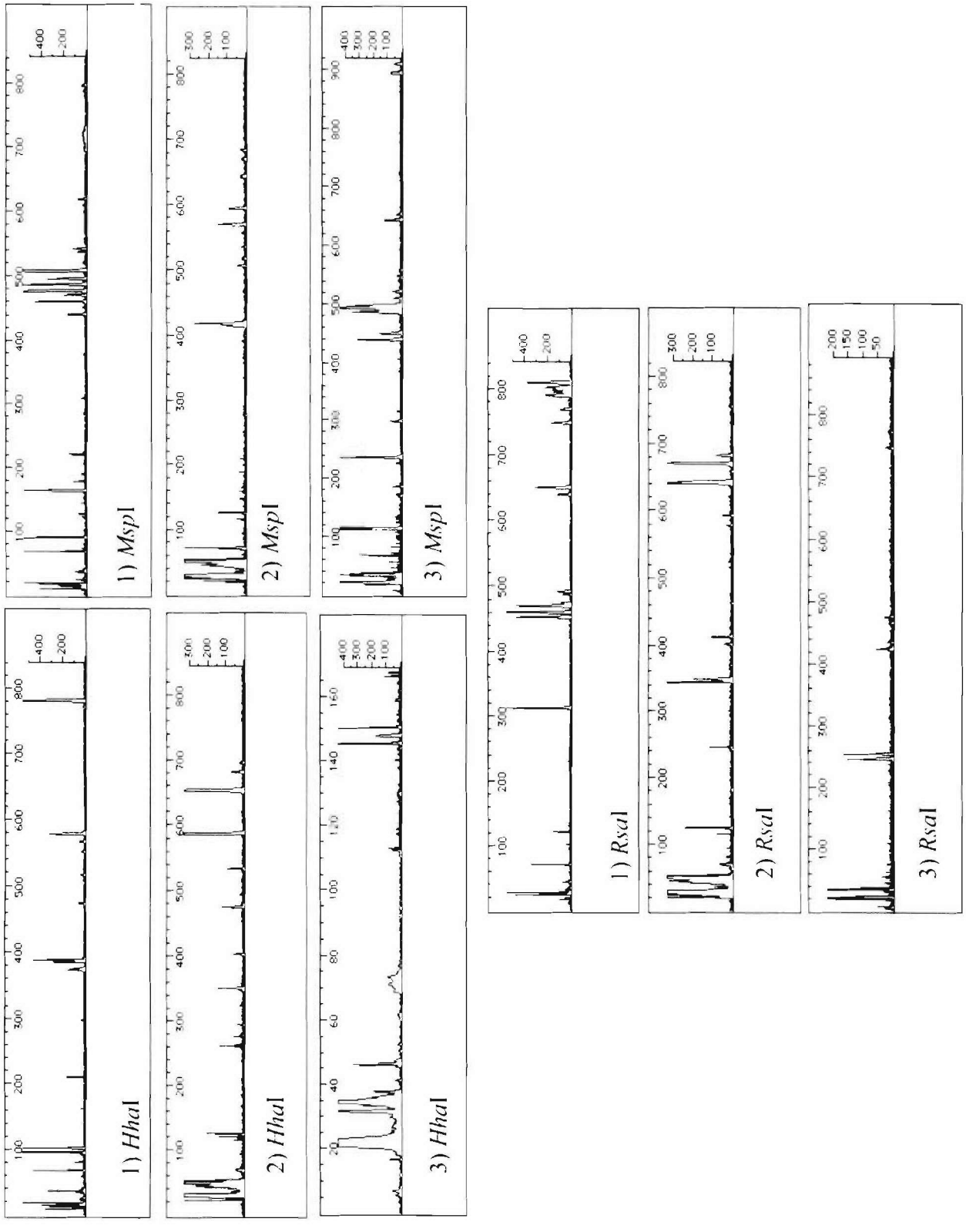

FIG. 1. T-RFLP analysis of the bacterial communities (see text for details). Profiles: 1) Representative result of 12 samples that contained cyanobacterium CD1C11; 2) representative result of 2 samples that contained cyanobacterium PNG-50; 3) representative result of 2 samples that contained cyanobacterium BBT.

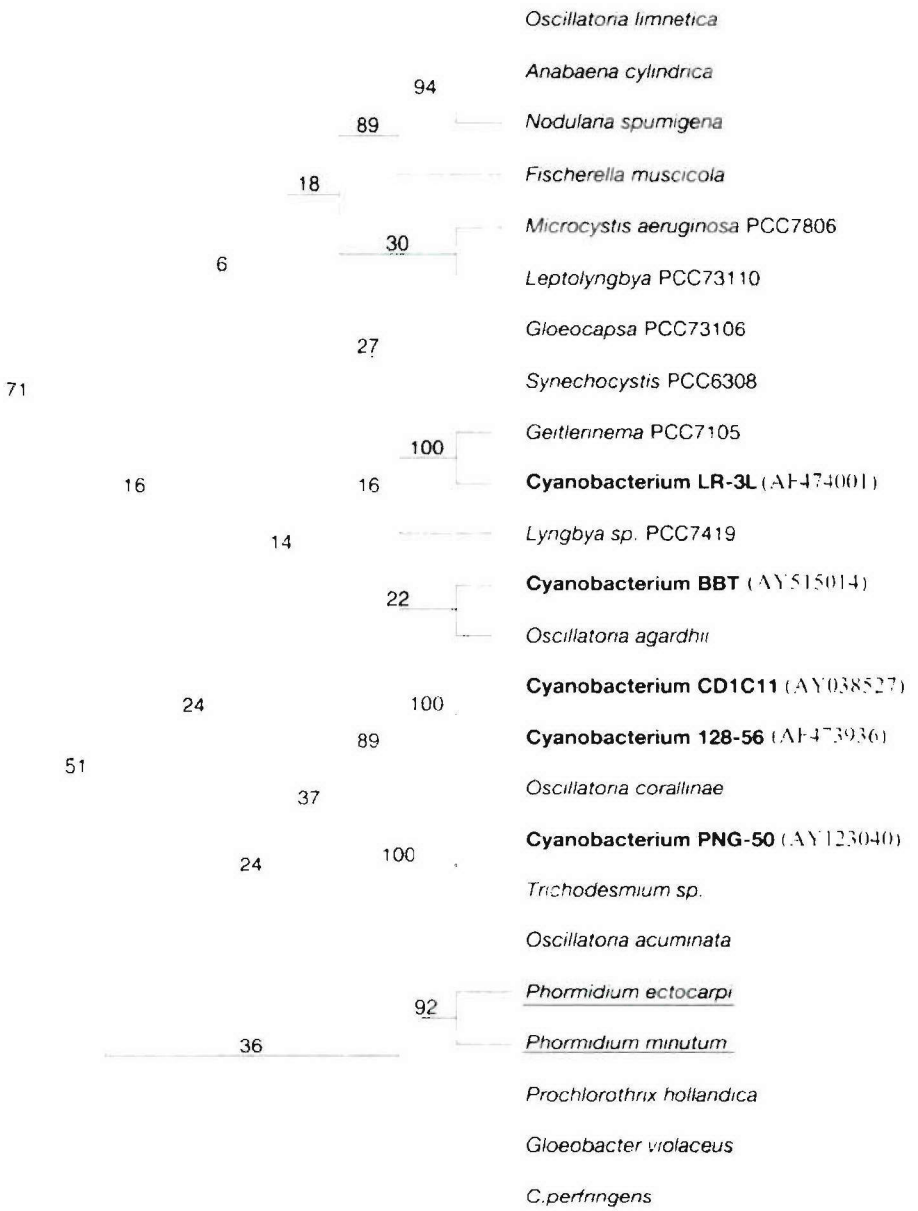

FIG. 2. Phylogenetic consensus tree based on parsimony analysis of 16S rRNA gene sequences of BBD cyanobacteria (bold type) and other representative cyanobacteria. Clone CD1C11 and cyanobacteria PNG-50, LR-L3, and 128-56 were previously analyzed (13). The numbers at the nodes are the bootstrap values based on a total of 10,000 replicate resamplings. GenBank accession numbers are shown in parentheses. Marine *Phormidium* spp. are underlined. *C. perfringens*, *Clostridium perfringens*.

band derived from one restriction enzyme digest was identical to sequences derived from one or both of the other enzymes. The recurrence of a sequence is a further indication that the bands selected correspond to the most abundant bacteria present in our samples. Eight different sequences were identified (Table 2). No chimeric sequences were detected, and E-values and scores in all cases were lower than E^{-103}.

Quantitative analysis of the bacteria present in the BBD mat. To confirm which of the eight species represented a numerically large fraction of the bacterial mat, the MPN-PCR method was used to quantify the abundance of the species presented in Table 3. This method has been successfully used to quantify microorganisms in different environmental samples (1, 12, 22). To process a larger number of samples simultaneously, the presence of PCR product was checked by DNA dot blot analysis (Table 3). The eight different sequences were detected in all of the samples analyzed. Of these, clones CD22E1, CD22E6, CD22B8, CD22E5, CD22D4, and CD22D5 were also detected in all healthy coral tissue samples; however, clones CD22E1, CD22B1, R3-M4, and CD22B8 were detected at significantly lower concentrations. Furthermore, CD22B1 and R3-M4 were not always detected in the healthy coral tissue

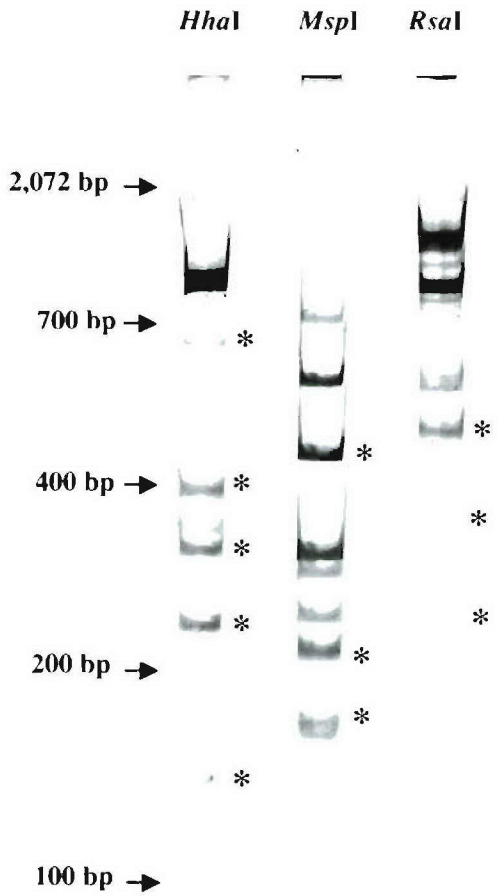

FIG. 3. Polyacrylamide gel showing the patterns obtained after digestion with the three different restriction enzymes used for T-RFLP analysis. Bands with sizes observed in all T-RFLP profiles for a given restriction enzyme (*) were excised, cloned, and sequenced. The locations of DNA size standards (not visible) are indicated by arrows to the left of the gel.

(Table 3). Although clones CD22E5 and CD22E6 appeared to be present at higher concentrations in BBD mat samples than in healthy coral samples, due to the large variation in the BBD mat samples, the differences did not prove statistically significant. Clones CD22D4 and CD22D5 were consistently detected at the same level in BBD mat and healthy tissue samples (Table 3).

TABLE 3. Frequencies of the different bacteria identified as present in high numbers in BBD mats[a]

Primer or clone	Division	No. of bacteria[b]		No. of positive results in healthy coral samples (n = 3)
		BBD mat (n = 4)	Healthy coral samples (n = 3)	
Universal primers		100	100	3
Clones				
CD1C11		44.40 ± 41.92[c]	<0.0001 ± 0	0
CD22E1	CFB	22.126 ± 20.56[c]	0.75 ± 0.36	3
CD22B1	*Firmicutes*	6.51 ± 6.27[c]	0.26 ± 0.22	2
CD22E6	*Firmicutes*	16.84 ± 28.72	0.75 ± 0.36	3
R3-M4	CFB	14.21 ± 8.69[c]	0.64 ± 0.55	2
CD22B8	*Firmicutes*	17.89 ± 2.21[c]	0.75 ± 0.36	3
CD22E5	*Firmicutes*	14.42 ± 11.96	2.22 ± 1.51	3
CD22D4	*Firmicutes*	8.35 ± 7.67	8.32 ± 9.45	3
CD22D5	δ-Proteobacteria	9.05 ± 4.54	9.70 ± 8.40	3

[a] Results were obtained by MPN-PCR and refer to the total number of bacteria obtained using universal primers.
[b] Average (percent respect to the total DNA) ± standard deviation.
[c] Significantly different ($P < 0.05$) from the value for healthy coral sample as determined by the Mann-Whitney U test.

Microscopy suggests that filamentous cyanobacteria constitute the majority of the BBD biomass (13, 14). However, the use of cyanobacterium-specific primers suggests that the DNA from this group represents less than half of the total DNA present in the samples (Table 3). Three major groups of bacteria besides cyanobacteria are present at high numbers in the infecting BBD mat: CFB, *Firmicutes*, and δ-proteobacteria. Clone CD22E1, one of the CFB division sequences that was detected in low numbers in healthy coral tissues, was the next most abundant bacterium after the cyanobacteria in the BBD mat. The δ-proteobacterium *Desulfovibrio* sp. is consistently present in important numbers during infection (9.05%). Nevertheless, it is also present at the same level (9.7%) in the healthy coral samples analyzed (Table 3). This species was previously identified as a part of the BBD mat (7, 28). Three additional species were present in high numbers in BBD mats and at low numbers in healthy corals. CD22B1, a member of the division *Firmicutes*, was present at relatively low numbers (6.5%) compared with the other species analyzed, and it was detected in only two of three samples. Clone R3-M4 represented 14.21% of the population in the BBD-infected corals

TABLE 2. Best matches of the different sequences obtained from the clone libraries based on the T-RFLP results

Clone	Length of the band (bp)	GenBank accession no.	Best match (BLASTN)	% Identity/ E-value	Division
CD22E1	449	AY497293	Uncultured CFB group bacterium partial 16S rRNA gene, clone P. palm C/A 42	87/E^{-103}	CFB
CD22B1	469	AY497294	Uncultured *Firmicutes* clone CD4B11	98/E^{-138}	*Firmicutes*
CD22E6	481	AY497295	Uncultured *Firmicutes* clone CD5D10	99/0.0	*Firmicutes*
R3-M4	527	AY497296	*Cytophaga fermentans*	91/0.0	CFB
CD22B8	402	AY497297	Uncultured *Firmicutes* 128-3-6	99/E^{-170}	*Firmicutes*
CD22E5	559	AY497298	Uncultured *Firmicutes* clone CD5C11	98/0.0	*Firmicutes*
CD22D4	607	AY497299	Uncultured bacterium p-1921-s962-3	90/0.0	*Firmicutes*
CD22D5	245	AY497300	Uncultured δ-proteobacterium 128-9-6	99/E^{-130}	δ-Proteobacteria

but only 0.64% in the healthy corals. Moreover, it was completely absent in one of the healthy coral samples analyzed (Table 3).

DISCUSSION

A filamentous cyanobacterium classified as *P. corallyticum*, along with *Desulfovibrio* sp. and *Beggiatoa* sp., have been proposed as the primary pathogens for BBD (27, 31, 33, 35). However, the evidence supporting this hypothesis is purely circumstantial (9). In that regard, other bacteria have been proposed as possible initiators of the disease (28). This study has identified the most abundant and potentially most important organisms of BBD. These findings will advance future studies of the mechanisms of BBD pathogenesis and roles of the different bacteria in the disease.

Recent work has indicated that healthy corals have a distinct bacterial community associated with them. The composition of that community is dependent upon the species of coral and is not merely a reflection of the bacterial community present in the surrounding water (18, 29). Furthermore, clone libraries obtained from BBD mat samples show that there is a complex and specific bacterial community associated with the pathogenic mats that is distinct from the communities growing on healthy corals (9, 14). On the basis of these clone libraries, it seems that the composition of the bacterial community undergoes a switch from a healthy to diseased profile (9). The relative proportion of clones representing members of the *Firmicutes* and CFB groups increases in the BBD mat (9, 14). Other groups disappear when healthy corals become diseased (γ- and β-proteobacteria), and finally, there are groups not present in healthy corals that make their appearance in diseased corals (ε-proteobacteria) (9, 14). Due to the complexity of the BBD mat, it is difficult to assess which bacteria play an active role in the development of the disease.

After analyzing all of the bands selected from the T-RFLP results, eight different sequences belonging to three different divisions were determined to be important in the BBD mat. The results show that one species of δ-proteobacteria, two species of CFB group, and five species of *Firmicutes* were the most abundant bacteria present in the infectious mat. Cooney et al. (9) previously identified two of these species in BBD mats. However, an α-proteobacterium that had been described as an important part of the infectious mat (9) has not been detected in the present study.

The first descriptions of the bacterial composition of BBD mats referred to the presence of two major groups of bacteria besides the filamentous cyanobacterium: a sulfate-reducing bacterium presumed to be *Desulfovibrio* (15) and a sulfide-oxidizing bacterium interpreted to be *Beggiatoa* (10). There are reports proposing that these two microorganisms play an active role in the destruction of coral tissue (27, 28), including reported oscillations in sulfide and oxygen levels in the BBD mat due to the action of *Beggiatoa* (7, 28). However, the presence of *Beggiatoa* has been suggested only on the basis of microscopy (10, 15). In the present study, *Beggiatoa* was not detected as a member of the infectious bacterial mat. Previous results obtained by different groups also failed to identify *Beggiatoa* as a part of the BBD mat (9, 14), and as mentioned previously, the primers used in these studies should have recognized the 16S rRNA genes from *Beggiatoa* spp. (9). A lingering possibility is that *Beggiatoa* exists at cell counts below PCR detection limits. If *Beggiatoa* is not present, the oxidation of sulfide in the BBD mat would need to be explained by the activity of other organisms. Previous work consistently detected the presence of an ε-proteobacterium in the BBD samples, although it probably represents a small fraction of the total community (9, 14). These species of ε-proteobacterium were not present in healthy corals. Marine ε-proteobacteria are capable of oxidizing sulfide into sulfate (39), which could explain the observations made by other researchers regarding the sulfide/sulfate profiles observed in BBD and attributed to *Beggiatoa* (7, 28).

The sulfate-reducing bacterium *Desulfovibrio* was identified both optically and by using 16S rRNA-targeted oligonucleotide probes (4, 15, 33). The species of δ-proteobacteria we have identified as an important part of the BBD mat is nearly identical to δ-proteobacteria clone 128-9-6, which has high homology with *Desulfovibrio* species (9). Nonetheless, the same species of δ-proteobacteria was also present in all the healthy coral samples analyzed and at levels comparable to those observed during infection.

One member of the CFB group, clone R3-M4, was not consistently found in the healthy coral samples, although it represented a large fraction of DNA isolated from the BBD mat (14.2%). This species has homology with *Cytophaga fermentans,* and similar sequences were previously identified in BBD clone libraries (14). Cooney et al. have also found that there is a *Cytophaga* species present in BBD but not in healthy coral samples (9). The species identified by those researchers seems to be different from the species we have identified. The CFB group includes well-known pathogens that infect a variety of organisms inhabiting many different environments. For example, the CFB group includes species that are responsible for a number of diseases in freshwater and saltwater fish (6, 8, 23, 36). The other CFB group species identified as important in BBD (clone CD22E1) makes up an important fraction of the bacterial community, up to 22.12%. This clone was present only at low levels on healthy corals (0.75%), indicating that BBD disease is somehow advantageous for its growth.

Five species of the division *Firmicutes* were identified; each species constituted an important fraction of the infectious mat. Four of five species of *Firmicutes* present in healthy coral samples increased their relative number during infection. Clone CD22B1 has homology with clone CD4B11 (GenBank accession number AY038526), an uncultured firmicute previously identified in BBD samples, but not in healthy corals using clone libraries (16). This clone was present in only two of three healthy coral samples analyzed. However, it may not be important for the progression of the disease, since it is found in widely variable proportions (from 0.50 to 15.33%) during infection.

Clone CD22B8 has homology with clone 128-3-6 (GenBank accession number AF473927), an uncultured member of the *Firmicutes* that was previously identified in BBD samples by other researchers (10). Although present in all healthy coral samples, there was a 24-fold increase in its relative proportion from healthy to diseased communities.

Finally, the cyanobacteria present in the BBD-infected coral samples are completely absent in the healthy coral samples

analyzed. This further confirms the importance of the cyanobacteria in the development of the disease.

The complex community of microorganisms present in BBD mats has made it difficult to understand the onset and progression of the disease. The strategy of comparative T-RFLP analysis, cloning, and sequencing used in this study has identified a subset of bacterial species likely to play important roles in the etiology of BBD. Having identified these species, classical methods of culture may be employed to determine how each may contribute to the disease. This same strategy could be applied in the study of other diseases or to analyze microbial activity in complex systems.

ACKNOWLEDGMENT

We thank the Office of Navel Research (ONR-N00014-00-1-0609) for support of this research.

The conclusions of this study are those of the authors and do not necessarily reflect those of the funding agency.

REFERENCES

1. **Alam, M. J., K. I. Tomochika, S. I. Miyoshi, and S. Shinoda.** 2002. Environmental investigation of potentially pathogenic *Vibrio parahaemolyticus* in the Seto-Inland Sea, Japan. FEMS Microbiol. Lett. **208:**83–87.
2. **Altschul, S. F., W. Gish, W. Miller, E. W. Myers, and D. J. Lipman.** 1990. Basic local alignment search tool. J. Mol. Biol. **215:**403–410.
3. **Antonius, A.** 1981. The "band" diseases in coral reefs, p. 7–14. *In* E. D. Gomez et al. (ed.), The reef and man. Proceedings of the Fourth International Coral Reef Symposium, vol. 2. Marine Sciences Center, University of the Philippines, Quezon City.
4. **Antonius, A.** 1977. Coral mortality in reefs: a problem for science and management. *In* D. L. Taylor (ed.), Geology. Proceedings of the Third International Coral Reef Symposium, vol. 2. Rosenstiel School of Marine and Atmospheric Science, Miami, Fla.
5. **Antonius, A.** 1973. New observations on coral destruction in reefs, p. 3. Proceedings of the 10th Meeting of the Association of Island Marine Laboratories, vol. 10. Caribbean University of Puerto Rico, Mayaguez.
6. **Bader, J. A., C. A. Shoemaker, and P. H. Klesius.** 2003. Rapid detection of columnaris disease in channel catfish (*Ictalurus punctatus*) with a new species-specific 16-S rRNA gene-based PCR primer for *Flavobacterium columnare*. J. Microbiol. Methods **52:**209–220.
7. **Carlton, R. G., and L. L. Richardson.** 1995. Oxygen and sulfide dynamics in a horizontally migrating cyanobacterial mat: black band disease of corals. FEMS Microbiol. Ecol. **18:**155–162.
8. **Cipriano, R. C., L. A. Ford, and J. D. Teska.** 1995. Association of *Cytophaga psychrophila* with mortality among eyed eggs of Atlantic salmon (*Salmo salar*). J. Wildlife Dis. **31:**166–171.
9. **Cooney, R. P., O. Pantos, M. D. Le Tissier, M. R. Barer, A. G. O'Donnell, and J. C. Bythell.** 2002. Characterization of the bacterial consortium associated with black band disease in coral using molecular microbiological techniques. Environ. Microbiol. **4:**401–413.
10. **Ducklow, H. W., and R. Mitchell.** 1979. Observations on naturally and artificially diseased tropical corals: a scanning electron microscopy study. Microb. Ecol. **5:**215–223.
11. **Edmunds, P. J.** 1991. Extent and effect of black band disease on a Caribbean reef. Coral Reefs **10:**161–165.
12. **Fredslund, L., F. Ekelund, C. S. Jacobsen, and K. Johnsen.** 2001. Development and application of a most-probable-number-PCR assay to quantify flagellate populations in soil samples. Appl. Environ. Microbiol. **67:**1613–1618.
13. **Frias-Lopez, J., G. T. Bonheyo, Q. Jin, and B. W. Fouke.** 2003. Cyanobacteria associated with coral black band disease in Caribbean and Indo-Pacific reefs. Appl. Environ. Microbiol. **69:**2409–2413.
14. **Frias-Lopez, J., A. L. Zerkle, G. T. Bonheyo, and B. W. Fouke.** 2002. Partitioning of bacterial communities between seawater and healthy, black band diseased, and dead coral surfaces. Appl. Environ. Microbiol. **68:**2214–2228.
15. **Garrett, P., and H. Ducklow.** 1975. Coral diseases in Bermuda. Nature **253:**349–350.
16. **Hughes, T. P., A. H. Baird, D. R. Bellwood, M. Card, S. R. Connolly, C. Folke, R. Grosberg, O. Hoegh-Guldberg, J. B. Jackson, J. Kleypas, J. M. Lough, P. Marshall, M. Nystrom, S. R. Palumbi, J. M. Pandolfi, B. Rosen, and J. Roughgarden.** 2003. Climate change, human impacts, and the resilience of coral reefs. Science **301:**929–933.
17. **Keener, J., and M. Nomura.** 1996. Regulation of ribosome synthesis, p. 1417–1431. *In* F. C. Neidhardt, R. Curtiss III, J. L. Ingraham, E. C. C. Lin, K. B. Low, B. Magasanik, W. S. Reznikoff, M. Riley, M. Schaechter, and H. E. Umbarger (ed.), *Escherichia coli* and *Salmonella*: cellular and molecular biology. ASM Press, Washington, D.C.
18. **Klaus, J. S., J. Frias-Lopez, G. T. Bonheyo, J. M. Heikoop, and B. W. Fouke.** Bacterial communities inhabiting the healthy tissues of two Caribbean reef corals: interspecific and spatial variation. Coral Reefs, in press.
19. **Knowlton, N.** 2001. The future of coral reefs. Proc. Natl. Acad. Sci. USA **98:**5419–5425.
20. **Liu, W. T., T. L. Marsh, H. Cheng, and L. J. Forney.** 1997. Characterization of microbial diversity by determining terminal restriction fragment length polymorphisms of genes encoding 16S rRNA. Appl. Environ. Microbiol. **63:**4516–4522.
21. **Maidak, B. L., J. R. Cole, T. G. Lilburn, C. T. Parker, Jr., P. R. Saxman, R. J. Farris, G. M. Garrity, G. J. Olsen, T. M. Schmidt, and J. M. Tiedje.** 2001. The RDP-II (Ribosomal Database Project). Nucleic Acids Res. **29:**173–174.
22. **Mantynen, V., S. Niemela, S. Kaijalainen, T. Pirhonen, and K. Lindstrom.** 1997. MPN-PCR-quantification method for staphylococcal enterotoxin c1 gene from fresh cheese. Int. J. Food Microbiol. **36:**135–143.
23. **Nomura, S.** 1997. Recent knowledge on fish pathogenic bacteria *Aeromonas salmonicida*, *Listonella anguillara* and *Cytophaga columnaris*, and their virulence factors. Nippon Saikingaku Zasshi **52:**393–416. (In Japanese.)
24. **Pichel, F., and G. Muyzer.** 1997. PCR primers to amplify 16S rRNA genes from cyanobacteria. Appl. Environ. Microbiol. **63:**3327–3332.
25. **Ramos-Flores, T.** 1983. Lower marine fungus associated with black line disease in star corals (*Montastrea annularis*). Biol. Bull. **165:**429–435.
26. **Richardson, L. L.** 1998. Coral disease: what is really known? Trends Ecol. Evol. **13:**438–443.
27. **Richardson, L. L.** 1996. Horizontal and vertical migration patterns of *Phormidium corallyticum* and *Beggiatoa* spp. associated with black-band disease of corals. Microb. Ecol. **32:**323–335.
28. **Richardson, L. L., K. G. Kuta, S. Schnell, and R. G. Carlton.** 1997. Ecology of the black band disease microbial consortium, p. 597–600. Proceedings of the Eighth International Coral Reef Symposium, vol. 1. Smithsonian Tropical Research Institute, Balboa, Panama.
29. **Rohwer, F., V. Segritan, F. Azam, and N. Knowlton.** 2002. Diversity and distribution of coral-associated bacteria. Mar. Ecol. Prog. Ser. **243:**1–10.
30. **Rosenberg, E., and Y. Ben-Haim.** 2002. Microbial diseases of corals and global warming. Environ. Microbiol. **4:**318–326.
31. **Rützler, K., and D. L. Santavy.** 1983. The black band disease of Atlantic reef corals. I. Description of the cyanophyte pathogen. Mar. Ecol. **4:**301–319.
32. **Sambrook, J., and D. W. Russell.** 2001. Molecular cloning: a laboratory manual, 3rd ed. Cold Spring Harbor Laboratory Press, Cold Spring Harbor, N.Y.
33. **Schnell, S., B. Assmus, and L. L. Richardson.** 1996. Role of sulfate-reducing bacteria in the black band disease of corals. Abstr. Annual Meeting of the VAAM (Vereinigung fuer Allgemeine und Angewandte Mikrobiologie) and GBCH (Gesellschaft fuer Biologische Chemie), abstr.
34. **Swofford, D. L.** 2002. PAUP*: phylogenetic analysis using parsimony (and other methods), version 4. Sinauer Associates, Sunderland, Mass.
35. **Taylor, D.** 1983. The black band disease of Atlantic reef corals. II. Isolation, cultivation, and growth of *Phormidium corallyticum*. Pubblicazioni della stazione zoologica di Napoli I. Marine Ecol. **4:**320–328.
36. **Toncheva-Panova, T., and J. Ivanova.** 2000. Influence of physiological factors on the lysis effect of *Cytophaga* on the red microalga *Rhodella reticulata*. J. Appl. Microbiol. **88:**358–363.
37. **U.S. Department of Agriculture.** 2003. Microbiology laboratory guidebook. Most probable number tables. Appendix 2.02. Office of Public Health and Science, Food Safety and Inspection Service, U.S. Department of Agriculture, Atlanta, Ga.
38. **Wilkinson, E. B. C. (ed.).** 2003. Status of coral reefs of the world: 2002. Australian Institute of Marine Science, Cape Ferguson, Townsville,Queensland, Australia.
39. **Wirsen, C. O., S. M. Sievert, C. M. Cavanaugh, S. J. Molyneaux, A. Ahmad, L. T. Taylor, E. F. DeLong, and C. D. Taylor.** 2002. Characterization of an autotrophic sulfide-oxidizing marine *Arcobacter* sp. that produces filamentous sulfur. Appl. Environ. Microbiol. **68:**316–325.

Coral Reefs (2005) 24: 129–137
DOI 10.1007/s00338-004-0447-1

REPORT

James S. Klaus · Jorge Frias-Lopez
George T. Bonheyo · Jeffrey M. Heikoop
Bruce W. Fouke

Bacterial communities inhabiting the healthy tissues of two Caribbean reef corals: interspecific and spatial variation

Received: 28 January 2004 / Accepted: 21 September 2004 / Published online: 30 December 2004
© Springer-Verlag 2004

Abstract Bacterial communities inhabiting healthy tissues of the reef-building corals *Diploria strigosa* and *Montastraea annularis* were evaluated across a human-induced environmental gradient along the southern coast of Curaçao, Netherlands Antilles. Variations in bacterial communities inhabiting coral tissues were determined using terminal restriction fragment length polymorphisms (T-RFLP) of 16S rRNA genes, and the $\delta^{15}N$ value of coral tissue was used to assess the relative amount of human contaminants at each reef locality. Bacterial communities of *D. strigosa* were more variable than *M. annularis*, but there were no systematic differences in the populations of healthy *M. annularis* and *D. strigosa*. The $\delta^{15}N$ value of coral tissues showed as much as a 1.5‰ increase in the impacted versus the non-impacted localities. While *M. annularis* showed no significant variation in bacterial community structure due to local reef conditions, the bacterial communities of *D. strigosa* showed dramatic shifts in community structure. The most abundant bacterial taxa inhabiting *D. strigosa* display increased dominance at impacted localities. By linking variations in microbial communities with an understanding of variations in local environmental conditions, this study provides a means of assessing potential factors that may impact the microbial habitat of coral tissues as well as overall reef health.

Biological Editor H.R. Lasker

J. S. Klaus (✉) · J. Frias-Lopez · G. T. Bonheyo · B. W. Fouke
Department of Geology, University of Illinois,
1301, W. Green Street, Urbana, IL 61801, USA
E-mail: jklaus@uiuc.edu
Tel.: +1-217-3330672
Fax: +1-217-2444996

J. M. Heikoop
Earth and Environmental Sciences Division,
Los Alamos National Laboratory,
Los Alamos, NM 87545, USA

Keywords Bacteria · Coral disease · T-RFLP · Nitrogen isotopes · Pollution

Introduction

Bacterial communities inhabiting reef coral tissues are extremely diverse. Estimates based on 14 different 16S rRNA gene sequence libraries suggest as many as 6,000 different ribotypes are associated with corals (Rohwer et al. 2002). The ability to harbor these diverse communities is attributable to the trapping of bacteria at the coral-seawater interface as well as the physiologically favorable microenvironment for bacterial growth associated with coral tissues (Ducklow and Mitchell 1979). The composition of these communities is in part controlled by the coral itself and the physical and chemical marine environmental conditions of the reef tract (allogenic succession) (Savage 1977). In turn, bacteria control community composition by manipulating the physical and chemical microenvironment of the tissues they inhabit via their metabolic activities and physical presence (autogenic succession).

Coral-associated bacteria can be divided into four functional groups: (a) bacteria with possible roles in coral nutrition, (b) pathogenic bacteria, (c) bacteria which can act as a probiont, aiding the growth of beneficial bacteria but limiting the growth of pathogenic forms, and (d) purely commensal bacteria with no impact on the other three groups. Based on this understanding, Porter and Tougas (2001) proposed a coral disease model in which climate change as well as pollution alter the interactions between the coral host and healthy microbiota, thereby increasing the probability of disease outbreak. Pantos et al. (2003) elaborated on this idea outlining five different mechanisms through which ecosystem stress could affect bacterial communities inhabiting coral tissues: (1) direct affect on bacteria, (2) affect on coral physiology and the surface microenvironment, (3) compromised coral antibiotic function, (4)

loss of a potential bacterial symbiotic function, and (5) altered coral physiology due to damage response.

In support of the coral disease model, numerous authors have suggested a possible linkage between the increasing frequency of coral diseases in the Caribbean and human disturbance and reduced environmental quality (Antonius 1988; Bruckner et al. 1997; Goreau et al. 1998; Kim and Harvell 2002; Peters 1993; Taylor 1983). Furthermore, patterns of disease distribution obtained from the global coral disease database (Green and Bruckner 2000) have shown that 97% of all locations in the Caribbean affected by coral diseases correspond to areas where human activities are expected to have medium to high impacts. However, due to the low incidence of coral disease, fluctuations in local environmental conditions, and difficulty identifying and quantifying numerous potentially controlling factors, the relationship between coral disease and environmental quality remains a debated issue (Bruckner and Bruckner 1999; Kuta and Richardson 2002). To establish a better understanding of the relationship between coral disease and the environment, additional information is needed on how healthy bacterial populations change under varying environmental conditions.

The goal of the present study was to evaluate whether changes in the composition and structure of the microbial communities inhabiting coral tissue can be used as a sensitive indicator of environmental changes that impact coral reef ecosystems. Specifically, does the daily discharge of over 10,000 m^3 of sewage (Gast 1998a), in addition to other pollutants, associated with the large commercial and military seaport near Willemstad, Curaçao, Netherlands Antilles (Fig. 1) have an effect on bacterial communities inhabiting tissues of healthy colonies of *Montastraea annularis* or *Diploria strigosa*? In addition, do the bacterial communities collected from the healthy portions of disease infected colonies of *D. strigosa* deviate significantly from those of non-infected colonies?

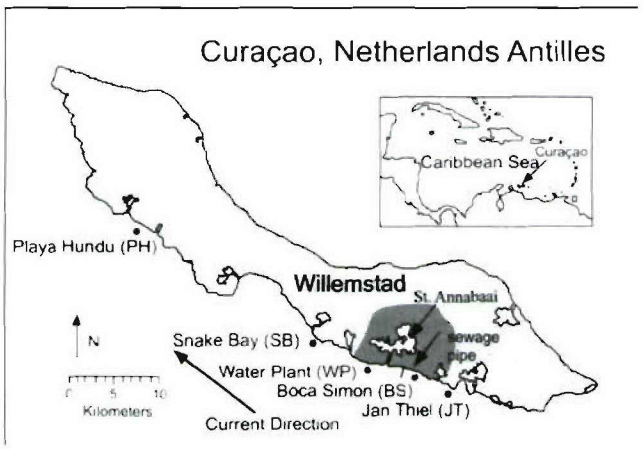

Fig. 1 Map of Curaçao, Netherlands Antilles, in the southern Caribbean Sea. The five sites chosen for this project are distributed along the leeward coast of the island as indicated. The major seaport of St. Annabaai and one of its major sewage outlet pipes are shown. Boca Simon and Water Plant, directly up and downcurrent from St. Annabaai, are the most environmentally impacted sites. Playa Hundu is the least impacted site

The present study concentrated on shallow fringing reefs at four localities along a 35-km stretch of the reef tract. The $\delta^{15}N$ and $\delta^{13}C$ values of coral tissues were used to assess the relative impact of human activities at each locality. Due to transformations of dissolved inorganic nitrogen (DIN) through ammonia volatilization, denitrification of nitrate, and nitrification of ammonia, wastewater derived from sewage treatment plants is generally enriched in the heavy isotope of nitrogen, ^{15}N (Heikoop et al. 1998, 2000a, b). Carbon isotopes are utilized to determine the relative proportions of autotrophic and heterotrophic modes of coral nutrition (Risk et al. 1994).

The numerically dominant representatives of the bacterial community of coral tissue were characterized through the use of terminal restriction fragment length polymorphisms (T-RFLP) of 16S rRNA genes. The variation in bacterial communities was analyzed quantitatively using a combination of statistical procedures, including multidimensional scaling (MDS), one-way analysis of similarity (ANOSIM), and similarity percentages (SIMPER) (Clarke and Warwick 2001).

Materials and Methods

Coral tissue $\delta^{15}N$ and $\delta^{13}C$

To assess human impacts on the reefs of Curaçao, Netherlands Antillies, tissue samples of *M. annularis* were collected from five different reef localities for nitrogen and carbon isotope analysis. These locations include: Jan Thiel (8 km upcurrent from the seaport and the large urban center of Willemstad), Boca Simon and Water Plant (immediately adjacent to the seaport and urban center), and Snake Bay and Playa Hundu (9 and 32 km downcurrent, respectively) (Fig. 1). Whole colonies of *M. annularis* were collected at a water depth of approximately 5 m with a hammer and chisel. An area of tissue approximately 25 cm^2 was removed from the upper growth surface of each colony using a small microdrill. Samples were decalcified using 1 N hydrochloric acid, then rinsed in distilled water and dried using a Vacufuge Concentrator 5301 (Eppendorf, Westbury, NY, USA). All samples contain a combination of host coral tissue and zooxanthellae. Samples (0.5–1.0 mg) were analyzed in continuous flow mode utilizing a Eurovector Elemental analyzer coupled to a Micromass Isoprime mass spectrometer located in the Department of Earth and Environmental Science at Los Alamos National Laboratory. Typical precision based on replicates of coral tissue samples and in house coral tissue standards is $< 0.2‰$ (1σ). Values were calibrated using in house standards comprised of deep-sea coral tissue (Heikoop et al. 2002) which were originally

analyzed in the laboratory of Zachary Sharp at the University of New Mexico and calibrated against IAEA-N3 and USGS RSIL N11 potassium nitrate standards.

Coral sample collection for molecular analysis

Healthy tissues from both non-infected and black band disease (BBD) infected coral samples were collected from shallow fringing reefs (~5 m water depth) approximately 75 m offshore at four localities along the reef tract: Boca Simon and Water Plant, (immediately adjacent to the seaport and large urban center of Willemstad), and Snake Bay and Playa Hundu, (9 and 32 km downcurrent, respectively). Four healthy colonies each of *M. annularis* and *D. strigosa* were collected and analyzed from each locality. Healthy coral tissue was also collected approximately 5 cm preceding the advancing BBD bacterial mat on three colonies of *D. strigosa* at the Water Plant locality. Samples were collected from the surface by removing a 2×2-cm portion of the uppermost 1 cm of the coral colony with a chisel and placing the sample in a sterile disposable 50 ml polypropylene centrifuge tube. Upon returning to the shore, the seawater within each tube was decanted, immersed in 80% ethanol, crushed, and homogenized, creating a slurry of coral tissue, zooxanthellae, mucus, microorganisms, and skeletal material. Previous studies have shown there to be very little overlap between the bacterial species detected from reef-water and coral tissues (Frias-Lopez et al. 2002; Rohwer et al. 2001). Based on these studies, we chose to focus solely on the bacterial communities of *D. strigosa* and *M. annularis*.

DNA extraction

A combined bead beating and freeze-thaw cycling protocol was used to extract genomic DNA from coral slurries. To begin, 2 ml of sample was concentrated via centrifugation and resuspended in 800 µl of sterile ultra pure water and 200 µl phenol TE 7–8, to which approximately 800 µl of 0.1 mm zirconia-silica beads were then added (BioSpec Products, Bartlesville, OK, USA). These samples were frozen at −80°C and rapidly thawed by plunging the tubes into a 65°C water bath. This freeze-thaw cycle was repeated three times, with the tubes vigorously agitated on a vortex apparatus after each thaw cycle. Samples were shaken on a reciprocating Mini-BeadBeater-8 (BioSpec Products) for 1 min at the "homogenize" speed setting. Standard phenol DNA extraction procedures were used (Sambrook et al. 1989), and ethanol-precipitated lysate was used in all subsequent procedures.

PCR amplification and T-RFLP

Optimization of PCR was performed for each sample by adjusting the amount of genomic DNA extract used to obtain a strong band on an agarose gel, without visible nonspecific product (Blackwood et al. 2003). The genes encoding for 16S rDNA were amplified with a Mastercycler gradient thermocycler (Eppendorf) by PCR using specific 16S rRNA primers for bacteria. Primers used in the PCR amplifications were Univ 9F (5′-GAGTTTGATYMTGGCTC) and Univ 1509R (5′-GYTACCTTGTTACGACTT) (Integrated DNA Technologies Coralville, IA, USA). Univ 9F was labeled at the 5′ end with phosphoramidite fluorochrome 6-carboxyfluorescein (6-FAM). PCR was performed using a reaction mixture of 0.2 mM of each deoxynucleoside triphosphate (Gibco/BRL, Rockville, MD, USA), 200 ng each of the forward and reverse primers, 0.5–10 µl of the sample preparation, 1X Taq Master, 1X Taq Buffer (50 mM KCl, 10 mM Tris-HCl pH 8.3, 1.5 mM $Mg(OAc)_2$) and water to bring the total volume to 50 µl.

To obtain an adequate mass of DNA for T-RFLP analysis, the previously described PCR reactions were performed in quadruplet. Pooled replicates were purified using the Wizard PCR prep kit (Promega, Madison, WI, USA). DNA was eluted with 30 µl of sterile water heated to 65°C. Restriction digests were performed independently using three tetrameric enzymes (*Hha*I, *Msp*I, and *Rsa*I). A volume of 8 µl of purified PCR product was added to 9 µl of sterile water and 3 µl of restriction enzyme master mix containing 10 U of restriction enzyme and 1X reaction buffer. Incubation was done at 37°C for 6 h followed by 15 min at 65°C to denature the restriction enzyme.

Prior to loading on a gel, 1 µl of sample was added to a "loading cocktail" (1.25 µl deionized formamide, 0.25 µl blue loading dye, and 0.3 µl TAMRA 2500 size standard), vortexed, spun down, and denatured at 95°C for 3 min. Samples were then run on a 5% Long Ranger acrylamide (BioWhittaker) and 7 M urea gel for approximately 5 h. T-RFLP profiles were obtained using an Applied Biosystems Inc. (ABI) 377-XL sequencer. The data was analyzed using the ABI GeneScan software.

To test the variability of sample T-RFLP profiles due to potential differences in DNA extraction, PCR amplification, or enzyme digestion efficiency, sample BS-DSTR-1 was processed and analyzed in triplicate (BS-DSTR-1 A, -B, -C). T-RFLP profiles obtained from these three replicate analyses showed minimal variation (Fig. 2). After pooling results from profiles of the three enzyme digests, a total of 31 different terminal restriction fragments (T-RFs) were identified. Twenty-three of the T-RFs were detected on all three samples and another seven T-RFs were found on two of the three samples. Relative peak heights were nearly identical for the three replicate samples. These results indicate that the T-RFLP methodology applied in this study is robust, and comparisons of profiles between different samples should reflect the relative similarity of the microbial communities present in each sample.

Data processing and statistical analyses

Sample versus T-RFLP peak data matrices were constructed using all peaks above a threshold of 50 U above background. To avoid detection of primers and uncertainties associated with fragment size determination, peaks smaller than 40 base pairs (bp) and larger than 550 bp were culled from the data set. To account for variation in fragment size determination between samples, peaks were manually aligned and placed into groups. Abundance data was obtained from the relative peak height following sample standardization (Blackwood et al. 2003). The similarity of T-RFLP peak profiles among all possible pairs of samples was calculated using the Bray–Curtis (BC) similarity coefficient (Bray and Curtis 1957).

Ordination by non-metric MDS (Kruskal 1964) was performed to examine differences in T-RFLP peak patterns among samples. This method was chosen because it makes no assumptions about the underlying distribution of data. Each ordination was run with 30 random starting configurations and proceeded through multiple iterations until the fit of a non-parametric regression of d (distances between samples on the MDS) against δ (similarities in the BC matrix) could not be improved. Sample points closest together on the resulting scatter plot represent the T-RFLP profiles that are most similar. To test the significance of T-RFLP peak differences due to the host species or reef site, the BC similarity matrix was subjected to the ANOSIM procedure (Clarke and Warwick 2001). This analysis is based on a non-parametric permutation procedure applied to the rank similarity matrix. If samples within a group are identical; Global $R=1$. SIMPER (Clarke and Warwick 2001) was used to determine peak contributions to the average dissimilarity of samples between different sample groups.

In cases where ANOSIM and MDS show no differences in T-RF composition among communities of different host species, a null model was used to determine whether the observed similarities were greater or less than expected from a species assemblage drawn randomly from a list of all T-RFs reported in the data set (Connor and Simberloff 1978). The expected number of shared T-RF is: $S_e = n_1 n_2 / N$, where n_1 and n_2 are the observed numbers of T-RFs and N is the size of the species pool. Expected and observed numbers of shared T-RFs were compared using a two-sample t-test.

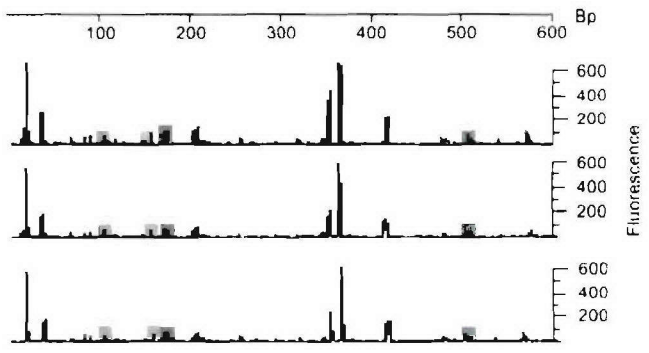

Fig. 2 T-RFLP profiles for enzyme digest *Hha*I collected in triplicate from sample BS-DSTR-1. Fragment sizes scaled in base pairs (*bp*)

Results

Coral tissue $\delta^{15}N$ and $\delta^{13}C$

Coral tissue $\delta^{15}N$ data from *M. annularis* was up to ~1.5‰ higher at sites adjacent to the urban center of Willemstad (Fig. 3). These results reflect higher proportions of sewage in reef seawater immediately adjacent to the seaport at Willemstad, with sewage levels becoming increasingly diluted downcurrent. Tissue $\delta^{13}C$ values ranged between −10.88 and −15.24‰ (mean = −13.62‰) with no significant correlation to $\delta^{15}N$ ($r=0.388$, $p=0.067$), or significant differences between localities.

T-RFLP analysis of bacterial communities

A combined total of 119 different T-RFs were identified from the 96 different T-RFLP profiles analyzed from healthy coral samples (32 *Hha*I, 32 *Msp*I, and 32 *Rsa*I). The rank abundance profile (Fig. 4) for all 119 unique T-RFs shows that while no single peak was identified from all 32 samples, 11 different T-RFs were found on at least 30% of the samples analyzed. A total of 90 different T-RFs were detected from colonies of *M. annularis*, and 77 from *D. strigosa*.

Species variability

No statistically significant differences in T-RF composition with respect to host species (*M. annularis* vs.

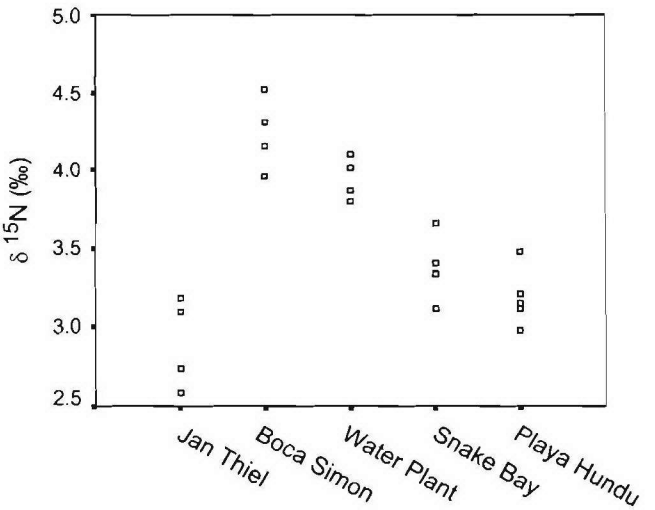

Fig. 3 Coral tissue $\delta^{15}N$ from *M. annularis* collected at five localities along the leeward coast of Curaçao

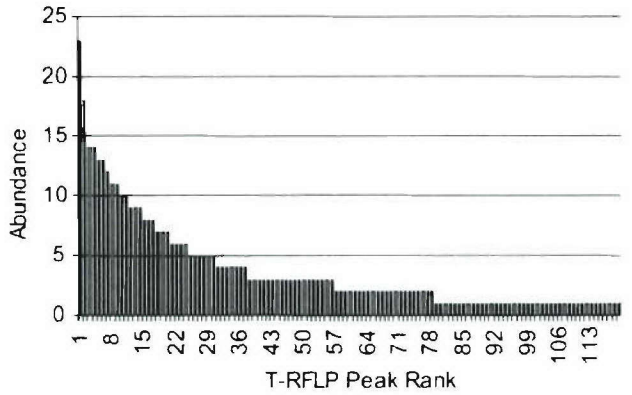

Fig. 4 Rank-abundance curve of T-RFLP peaks detected in 16 samples of healthy *M. annularis* and 16 samples of healthy *D. strigosa* ($n = 119$)

D. strigosa) were detected. The ANOSIM statistical test for differences in T-RF composition does not indicate a host species effect ($r = 0.065$, $p < 0.083$). MDS ordination of all samples from all environments shows almost complete overlap of samples from the two host species analyzed (Fig. 5). To investigate whether the similarity of the T-RF profiles between host species were any different than that expected by chance, the null model of Connor and Simberloff (1978) was applied. Results show that more T-RFs were shared than predicted by the null model (student's $t = 9.606$, $p < 0.0001$).

Reef locality variability

To test the effect of reef locality on the composition of the most abundant bacterial species, separate data matrices for *M. annularis* (16 samples) and *D. strigosa* (16 samples) were constructed and analyzed. For *M. annularis*, the ANOSIM statistical test for differences in T-RF composition between localities showed no significant locality affect ($r = 0.149$, $p < 0.073$). Ordination of samples by MDS shows very little clustering of samples by locality (Fig. 6a). Bacterial populations of *M. annularis* thus do not appear to be affected by reef locality and the proximity to the seaport at Willemstad.

The results of the ANOSIM test for samples collected from *D. strigosa* however suggest distinct variation in T-RF composition based on reef locality ($r = 0.678$, $p < 0.002$). In the MDS ordination of *D. strigosa* from all four localities, samples show distinct clustering by locality (Fig. 6b). Samples collected from Water Plant, the locality directly downcurrent from the seaport, are very tightly clustered. Samples from Boca Simon, directly upcurrent from the seaport and large sewage outflow pipe, also show distinct clustering of samples. The two downcurrent localities, Snake Bay and Playa Hundu, show considerable overlap and increased variation in their T-RF composition.

The reduced variability at Water Plant and Boca Simon observed in the MDS ordination is further supported by the average similarity of T-RFs within each locality. The average similarity in T-RF composition for *D. strigosa* samples collected at Water Plant (64.65%) and Boca Simon (57.07%), is considerably higher than

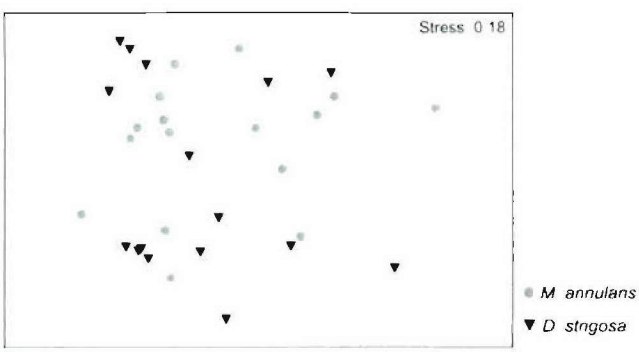

Fig. 5 Non-metric MDS ordination of bacterial assemblages inhabiting the coral tissues of healthy *M. annularis* (16 samples) and *D. strigosa* (16 samples). Overlap between bacterial assemblages found on *M. annularis* and *D. strigosa* suggest the dominant bacterial populations are not host specific

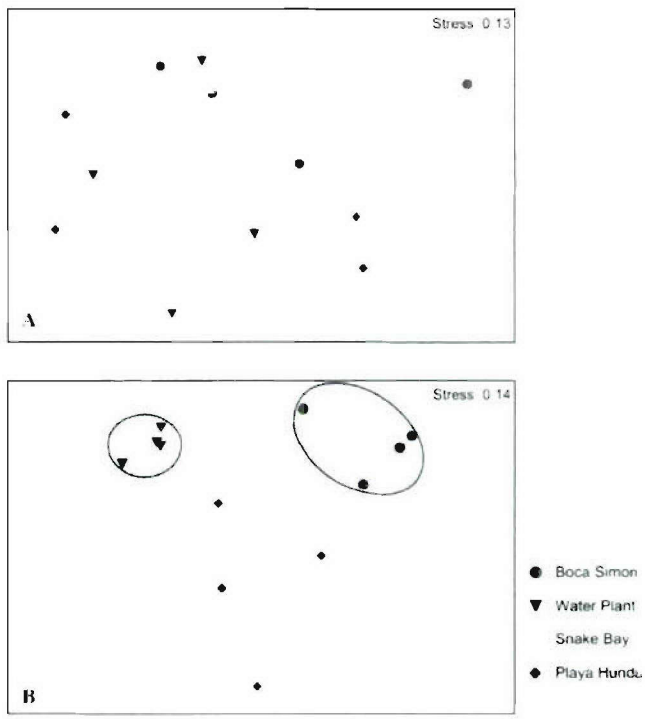

Fig. 6 a Non-metric MDS ordination of bacterial assemblages inhabiting the coral tissues of healthy *M. annularis* (16 samples) collected from four localities along the leeward reef tract of Curaçao. Overlap between bacterial assemblages found at different localities suggests the dominant bacterial populations inhabiting tissues of *M. annularis* are not controlled by differences in local water quality. **b** Non-metric MDS ordination of bacterial assemblages inhabiting tissues of *D. strigosa* (16 samples). Clustering of bacterial assemblages found at different localities suggests the dominant bacterial populations inhabiting tissues of *D. strigosa* are in part controlled by differences in local water quality. Localities immediately upcurrent (Boca Simon) and downcurrent (Water Plant) of the large seaport at St. Annabaai show the tightest clustering within their bacterial populations

those of Snake Bay (22.16%) and Playa Hundu (18.63%). Results from SIMPER analysis reveal the major peaks responsible for the differences among the four reef localities (Table 1). Water Plant is distinguished from Snake Bay and Playa Hundu by the greater relative abundance of *Msp*I-149, *Hha*I-342, *Rsa*I-106, and decreased abundance of *Msp*I-484 and *Hha*I-373. Boca Simon is distinguished from Snake Bay and Playa Hundu by the greater relative abundance of *Msp*I-136, *Hha*I-360, *Msp*I-79, *Rsa*I-117 and *Hha*I-203 as well as a lesser relative abundance of *Msp*I-484. A plot of the average *k*-dominance curves (Lambshead et al. 1983) (*x*-axis logged) of T-RF peaks for each locality shows a higher dominance of abundant T-RFs at polluted localities (BS and WP) in comparison to the two downcurrent localities (Fig. 7).

The three samples of seemingly healthy tissues from BBD infected colonies of *D. strigosa* collected at Water Plant also showed significant differences from both the downcurrent (Snake Bay and Playa Hundu) and near-harbor (Boca Simon and Water Plant) samples ($r = 0.267$, $p < 0.008$). The average similarity in T-RF composition for diseased samples was 32.23%, and all three samples plotted together in an MDS ordination with other healthy *D. strigosa* (Fig. 8). The diseased samples are most easily distinguished from near-harbor and downcurrent localities by the greater relative abundance of *Msp*I-82, *Msp*I-100, *Msp*I-125, *Msp*I-149, *Msp*I-507, *Rsa*I-84, *Rsa*I-91, *Hha*I-79, *Hha*I-87, as well as a lesser relative abundance of *Hha*I-365 and *Hha*I-342. A plot of the average *k*-dominance curves of T-RF peaks for diseased ($n = 3$), near-harbor ($n = 8$) and downcurrent ($n = 8$) samples show a higher dominance of abundant T-RFs in diseased and near-harbor samples in comparison to the downcurrent samples (Fig. 9).

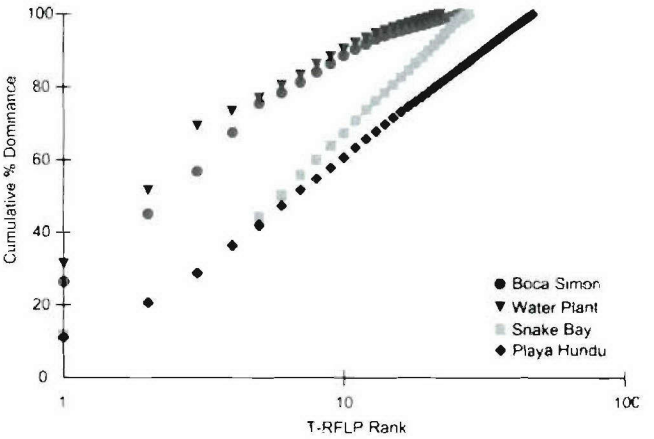

Fig. 7 Average *k*-dominance curves (*x*-axis logged) of T-RF peaks obtained from four colonies of healthy *D. strigosa* at each of four localities along the leeward coast of Curaçao

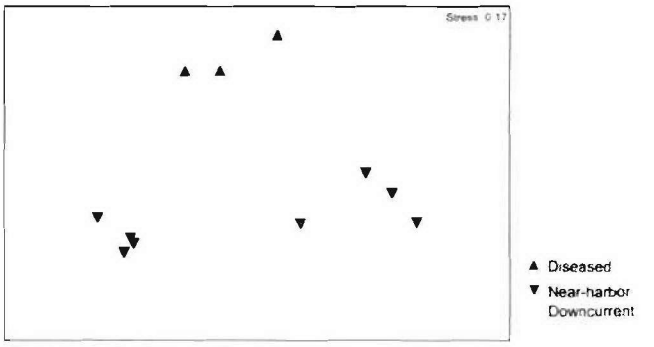

Fig. 8 Non-metric MDS ordination of bacterial assemblages associated with near-harbor (eight samples), downcurrent (eight samples), and seemingly healthy tissues of BBD infected (three samples) colonies of *D. strigosa*

Discussion

The island of Curaçao is 61 km long and 14 km wide at its widest point (Fig. 1). It is surrounded by fringing reefs up to 250 m from shore where the seafloor slopes down from 8–10 to 30–50 m water depth (Van Duyl 1985). The approximately 150,000 people living on Curaçao are concentrated in the capital city of Willemstad, which surrounds the large natural harbor of St. Anna-

Table 1 T-RFs distinguishing healthy bacterial communities of *D. strigosa* at four localities

	Boca Simon		Water Plant		Snake Bay		Playa Hundu	
	Avg. abu.[a]	Avg. sim.[b]	Avg. abu.	Avg. sim.	Avg. abu.	Avg. sim.	Avg. abu.	Avg. sim.
*Msp*I-136	26.46	12.87	0	0	2.28	0	2.14	0
*Hha*I-360	18.57	11.89	0	0	3.95	0	4.17	0
*Msp*I-79	11.76	9.87	0	0	0	0	0	0
*Hha*I-203	10.72	9.37	0	0	1.59	0	0	0
*Rsa*I-117	7.97	8.23	0	0	0	0	0	0
*Hha*I-373	1.49	0	0	0	6.12	4.68	3.31	5.19
*Msp*I-149	0.55	0	31.36	12.41	7.57	4.75	11.17	0
*Hha*I-342	0	0	20.14	10.88	11.73	1.94	8.74	0
*Rsa*I-106	0	0	17.92	10.73	2.22	0	0	0
*Msp*I-484	0	0	0	0	9.56	1.39	22.04	7.89

[a]Average (%) abundance per locality
[b]T-RF contribution to the mean BC (%) similarity at each locality

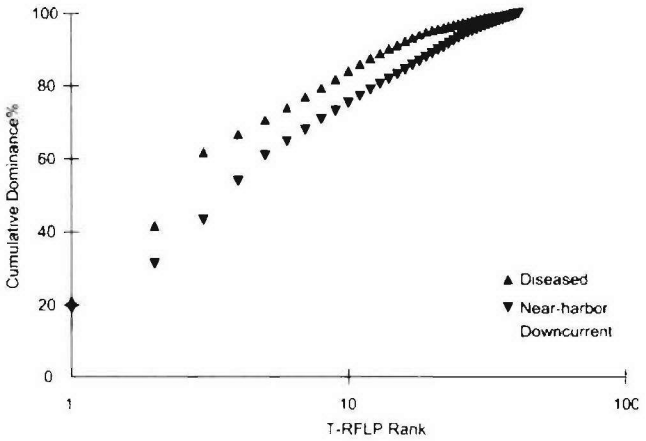

Fig. 9 Average *k*-dominance curves (*x*-axis logged) of T-RF peaks obtained from near-harbor (eight samples), downcurrent (eight samples), and seemingly healthy tissues of BBD infected (three samples) colonies of *D. strigosa*

baai. This large commercial, municipal, and military harbor, and the urban center of Willemstad are major sources of pollutants such as nutrients, metals, hydrocarbons, and other toxic chemicals (Gast 1998b). Gast (1998a) has shown that elevated ammonium, nitrite and nitrate associated with sewage discharge, and groundwater seepage onto the reef can be measured up to 4 km downcurrent of the harbor. In association with this eutrophication, bacterial production was increased from 100–500 to about 1,200 ngC l^{-1} h^{-1} (Gast 1998a). While direct linkages have yet to be established, it is believed that contaminants are having a detrimental effect on the shallow water reef ecosystems (Bak and Nieuwland 1995; Gast 1998b; Meesters et al. 2001). Gast (1998b) reports both coral cover and species diversity to be reduced up to 50% near Boca Simon in comparison to more pristine localities further upcurrent. Furthermore, changes in coral population structure near Boca Simon indicate a decline in new coral recruits (Meesters et al. 2001).

The values of coral tissue $\delta^{15}N$ from *M. annularis* presented here (Fig. 3) agree with the previously reported trends of eutrophication on Curaçao (Gast 1998a, b; Gast et al. 1998) and provide a very simple means of assessing the potential anthropogenic influence on individual reef localities. The ~1.5‰ increase in coral tissue $\delta^{15}N$ from *M. annularis* at sites adjacent to the urban center of Willemstad is consistent with Heikoop et al. (2000b), which demonstrated that on average the $\delta^{15}N$ of *Porites lobata* tissues in the Indo-Pacific is increased by 1.56‰ at polluted localities.

Microbial communities of healthy reef corals

It is well established that coral tissues harbor diverse bacterial communities (Frias-Lopez et al. 2002; Gast et al. 1998; Rohwer et al. 2001); and histological evidence suggests these communities are primarily associated with the coral surface microlayer or coelenteron (Bythell et al. 2002). The open question is: what influence do these bacterial communities have on the life processes of reef corals and the overall health of the ecosystem?

The consistent presence of a strain would imply that it might be specifically adapted to live in association with coral tissues, potentially having an important role maintaining coral nutrition or excluding potential pathogens. While no single isolate was detected on all 32 samples analyzed in the present study, 11 different T-RF peaks were shown to occur on at least 11 (30%) of the samples analyzed. These frequent occurrences, along with the fact that none of these peaks matched theoretical restriction enzyme digests of 16S rRNA gene sequence libraries of reef water samples (Frias-Lopez et al. 2002), supports the notion that these bacteria may be highly adapted to coral surfaces. In a previous study of coral-associated bacteria, Rohwer et al. (2001) showed that 25 samples of healthy tissues of *Montastraea franksi* collected from five different reefs near Bocas del Toro, Panama, all contained α-proteobacteria closely related to *Silicibacter lacuscaerulensis*, a potential nitrogen fixing bacteria. Additionally, Rohwer et al. (2002) confirmed the presence of a γ-proteobacteria, PA1, in over 50 healthy tissue samples of *Porites asteroides* and Pantos et al. (2003) identified a β-proteobacteria with high similarity to *Comamonas* present in three different samples analyzed. Further characterization of the role of these specific coral-associated strains will be very informative, and the T-RFLP data presented here suggests that there are potentially many more strains worthy of additional study.

Rohwer et al. (2002) also showed that the frequency of different bacterial groups detected in clone libraries varied substantially between *M. franksi*, *D. strigosa*, and *P. asteroides* collected from the same environmental setting. From the T-RFLP data presented here, we found the dominant bacterial species associated with *M. annularis* and *D. strigosa* to be very similar. In fact, over half of the T-RFs detected in this study were present in samples of both *M. annularis* and *D. strigosa*. This does not contradict the findings of Rhower et al. (2002). Clone library and T-RFLP data sets are fundamentally different. While T-RFLP is able to detect quantitative differences in the most abundant taxa, it does not detect lesser abundant organisms. It is altogether possible that despite seeing few distinct differences between the dominant bacterial species associated with *M. annularis* and *D. strigosa*, the relative abundance of less common species from more broadly defined bacterial groups (i.e., α-proteobacteria) would be characteristic of the host species. Rhower et al. (2002) detected several ribotypes common between the different host species analyzed. If these common ribotypes were in fact the most abundant organisms of the microbial community, recognizing unique communities from the different host corals using T-RFLP might be difficult. It is also possible that differences between these two studies

could be attributed to differences in the host species investigated (e.g., *M. annularis* vs. *M. franksi*) or the local reef conditions from which they were collected.

The reduced variation in bacterial communities inhabiting *D. strigosa* at Water Plant and Boca Simon observed in the MDS ordination (Fig. 6b), as well as their characteristic community structure in comparison to the downcurrent localities, suggests that certain bacterial species are being selected or enriched for. These shifts in the structure of bacterial communities inhabiting healthy tissues of *D. strigosa* could be due to either environmental factors acting directly on the bacterial communities, or indirectly via a physiological response of the coral (i.e., changes in the rate of photosynthesis or respiration) induced by these same environmental factors. Furthermore, there is currently very little known about reef-water microbial communities. While recent molecular screening studies have found very little overlap between the bacterial species detected from reef-water and coral tissues (Frias-Lopez et al. 2002; Rohwer et al. 2001), these two communities must interact at some level.

No consistent changes were detected in the bacterial communities of *M. annularis* among the four localities sampled in the present study. One explanation for this negative response is that the natural variation in the dominant bacterial communities of *M. annularis* may be too great to detect shifts in community structure using only the dominant bacterial species. However, if changes in bacterial community structure are primarily due to a host physiological response, the lack of change in the bacterial communities may reflect the absence of a response in host physiology to the local reef conditions. A variable host response is consistent with coral bleaching studies, which show the physiological response of both reef corals and zooxanthellae to various environmental factors differ between species (Brown 1997). It is interesting to note that on the reefs of Curaçao the impact of local reef conditions on the population structure of *D. strigosa* appears to be more pronounced than that of *M. annularis* (Meesters et al. 2001).

Increased dominance of specific bacterial strains is a common response observed in disturbed environments (Haack et al. 2004; Salyers and Whitt 1994; Torsvik et al. 2002). The bacterial communities inhabiting *D. strigosa* at impacted localities showed an increased dominance of the most prevalent T-RFs, as do communities associated with the apparently healthy tissues of diseased corals (Fig. 7). This increase in dominant T-RFs is also consistent with Pantos et al. (2003) who reported a greater number of DGGE bands in healthy coral tissues from *M. annularis* in than apparently healthy tissues of colonies infected with a plague-like disease. The similar response of bacterial communities inhabiting tissues of *D. strigosa* at impacted localities, and those inhabiting healthy tissues of diseased corals does not, however; necessarily reflect a common cause, or prove that the shifts in bacterial communities observed on *D. strigosa* collected from impacted localities make a coral any more susceptible to disease. However, the observed shifts in the bacterial communities inhabiting *D. strigosa* at impacted localities is consistent with the coral disease model presented by Porter and Tougas (2001).

The primary goal of this study was to determine if human-induced spatial heterogeneities in reef environments affect the patterning of bacterial communities inhabiting the tissues of healthy reef corals. By combining DNA fingerprinting techniques used to characterize the most abundant organisms with multivariate statistical methods, we have shown that local environmental conditions can influence the patterning of bacterial communities inhabiting coral tissues, however similar trends may not be expected for all coral species. A better understanding of how bacterial communities respond to environmental conditions will require highly controlled studies targeting specific environmental factors. However, the strength of these studies depend on further characterization of natural reef-water microbial communities, as well as a greater understanding of how coral physiology affects the microbial communities inhabiting their tissues.

Acknowledgements This work was supported by research grants from the Office of Naval Research (N00014-00-1-0609), the Geological Society of America, the American Association of Petroleum Geologists, and the UIUC Department of Geology. We acknowledge the support of CARMABI in our field efforts and Alison Rodden and Amanda Tribble for help with data collection.

References

Antonius A (1988) Distribution and dynamics of coral diseases in the eastern Red Sea. In: Proceedings of the 6th international coral reef symposium, vol 2, pp 293–298

Bak RPM, Nieuwland G (1995) Long-term change in coral communities along depth gradients over leeward reefs in the Netherlands Antilles. Bull Mar Sci 56:609–619

Blackwood CB, Marsh T, Sang-Hoon K, Paul EA (2003) Terminal restriction fragment length polymorphism data analysis for quantitative comparison of microbial communities. Appl Environ Microbiol 69:926–932

Bray JR, Curtis JT (1957) An ordination of the upland forest communities of southern Wisconsin. Ecol Monogr 34:77–87

Brown BE (1997) Coral bleaching: causes and consequences. Coral Reefs 16(suppl):S129–S138

Bruckner AW, Bruckner RJ (1999) Rapid assessment of coral reef condition and short-term changes to corals affected by disease in Curaçao, Netherlands Antilles. International conference on scientific aspects of coral reef assessment, monitoring, and restoration. Abstract 62

Bruckner AW, Bruckner RJ, Williams EH Jr (1997) Spread of black-band disease epizootic through the coral reef system in St Ann's Bay Jamaica. Bull Mar Sci 61:919–928

Bythell JC, Barer MR, Cooney RP, Guest JR, O'Donnell AG, Pantos O, Le Tissier MD (2002) Histopathological methods for the investigation of microbial communities associated with disease lesions in reef corals. Lett Appl Microbiol 34:359–364

Clarke KR, Warwick RM (2001) Change in marine communities: an approach to statistical analysis and interpretation. Primer-E, Plymouth, p 175

Connor EF, Simberloff DS (1978) Species number and compositional similarity of the Galapagos flora and avifauna. Ecol Monogr 48:219–248

Frias-Lopez J, Zerkle AL, Bonheyo GT, Fouke BW (2002) Partitioning of bacterial communities between seawater and healthy, black band diseased, and dead coral surfaces. Appl Environ Microbiol 68:2214–2228

Gast GJ (1998a) Microbial densities and dynamics in fringing coral reef waters. PhD thesis, University of Amsterdam

Gast GJ (1998b) Nutrient pollution in coral reef waters. Reef Care Curaçao Workshop Nutr Pollut 5:13

Gast GJ, Wiegman S, Wieringa E, Van Duyl FC, Bak RPM (1998) Bacteria in coral reef water types: removal of cells, stimulation of growth and mineralization. Mar Ecol Prog Ser 167:37–45

Goreau TJ, Cervino J, Goreau M, Hayes R, Hayes M, Richardson L, Smith G, DeMeyer K, Nagelkerken I, Garzon-Ferrera J, Gil D, Garrison G, Williams EH, Bunkley-Williams L, Quirolo C, Patterson K, Porter JW, Porter K, (1998) Rapid spread of diseases in Caribbean coral reefs. Rev Biol Trop 46:157–171

Green EP, Bruckner AW (2000) The significance of coral disease epizootiology for coral reef conservation. Biol Conserv 96:347–361

Haack CS, Fogarty LR, West TG, Alm EW, McGuire JT, Long DT, Hyndman DW, Forney LJ (2004) Spatial and temporal changes in microbial community structure associated with recharge-influenced chemical gradients in a contaminated aquifer. Environ Microbiol 6:438–448

Heikoop JM, Dunn JJ, Risk MJ, Sandeman IM, Schwarcz HP, Waltho N (1998) Relationship between light and the $\delta^{15}N$ of coal tissue: examples from Jamaica and Zanzibar. Limnol Oceanogr 43:909–920

Heikoop JM, Dunn JJ, Risk MJ, Tomascik T, Schwarcz HP, Sandeman IM, Sammarco PW (2000a) $\delta^{15}N$ and $\delta^{13}C$ of coral tissue show significant inter-reef variation. Coral Reefs 19:189–193

Heikoop JM, Risk MJ, Lazier AV, Edinger EN, Jompa J, Limmon GV, Dunn JJ, Brown DR, Schwarz HP (2000b) Nitrogen-15 signals of anthropogenic nutrient loading in reef corals. Mar Poll Bull 40:628–636

Heikoop JM, Risk MJ, Hickmott DD, Shearer CK, Beukens R, Atudorei V (2002) Potential climate signals from the deep-sea gorgonian coral *Primnoa resedaeformis*. Hydrobiologia 471:117–124

Kim K, Harvell C (2002) Aspergillosis of sea fan corals: dynamics in the Florida Keys. CRC Press, Boca Raton, pp 827–881

Kruskal JB (1964) Multidimensional scaling by optimizing goodness of fit to a nonmetric hypothesis. Psychometrika 29:1–27

Kuta K, Richardson L (2002) Ecological aspects of black band disease of corals: relationships between disease incidence and environmental factors. Coral Reefs 21:393–398

Lambshead PJD, Platt HM, Shaw KM (1983) The detection of differences among assemblages of marine species based on an assessment of dominance and diversity. J Nat Hist 17:859–874

Meesters EH, Hilterman M, Kardinaal E, Keetman M, de Vries M, Bak RPM (2001) Colony size-frequency distributions of scleractinian coral populations: spatial and interspecific variation. Mar Ecol Prog Ser 209:43–54

Pantos O, Cooney RP, Le Tissier MD, Barer MR, O'Donnell AG, Bythell JC (2003) The bacterial ecology of a plague-like disease affecting the Caribbean coral *Montastrea annularis*. Environ Microbiol 5:370–382

Peters EC (1993) Diseases of other invertebrate phyla: Porifera, cnidaria, ctenophora, annelida, echinodermata. CRC Press, Florida, pp 393–449

Porter JW, Tougas JI (eds) (2001) Reef ecosystems: threats to their biodiversity. Encyclopedia of biodiversity 5. Academic, New York, pp 73–95

Risk MJ, Sammarco PW, Schwarcz HP (1994) Cross-continental shelf trends in $\delta^{13}C$ in coral on the Great Barrier Reef. Mar Ecol Prog Ser 106:121–130

Rohwer F, Breitbart M, Jara J, Azam F, Knowlton N (2001) Diversity of bacteria associated with the Caribbean coral *Montastraea franksi*. Coral Reefs 20:85–91

Rohwer F, Segritan V, Azam F, Knowlton N (2002) Diversity and distribution of coral-associated bacteria. Mar Ecol Prog Ser 243:1–10

Salyers AA, Whitt DD (1994) Bacterial pathogenesis a molecular approach. ASM Press, Washington, p 418

Sambrook J, Fritsch EF, Maniatis T (1989) Molecular cloning: a laboratory manual. Cold Spring Harbor Laboratory Press, Cold Spring Harbor

Savage DC (1977) Microbial ecology of the gastrointestinal tract. Ann Rev Microbiol 31:107–133

Taylor DL (1983) The black band disease of Atlantic orals. II. Isolation, cultivation, and growth of *Phormidium corallyticum*. Mar Ecol 4:321–328

Torsvik V, Øverås L, Thingstad TF (2002) Prokaryotic diversity—magnitude, dynamics and controlling factors. Science 296:1064–1066

Van Duyl FC (1985) Atlas of the living reefs of Curaçao and Bonaire (Netherlands Antilles). Foundation for Scientific Research in Surinam and the Netherlands Antilles, Utrecht

Cytotoxic activity of Black Band Disease (BBD) extracts against the symbiotic dinoflagellate *Symbiodinium* sp.

Jorge FRIAS-LOPEZ*, James S. KLAUS & Bruce W. FOUKE

Department of Geology, University of Illinois, 1301 W. Green Street, Urbana, IL 61801, USA.

*Corresponding author. Jorge Frias-Lopez,

Present address: MIT, Department of Civil and Environmental Engineering, 15 Vassar St. 48-336b

e-mail:jfrias@mit.edu

Abstract. Black band disease (BBD) is an infectious bacterial disease caused by the migration of a black mat of microorganisms across the surface of coral colonies, consuming healthy coral tissue and leaving dead skeleton behind. Although a complex community of bacteria composes the infectious bacterial mat, the most abundant organism present in the mat is a large filamentous, non-heterocyst cyanobacterium, identified as *Phormidium corallyticum*. In spite of our knowledge on the composition of the BBD mat, the mechanisms by which this disease destroys coral tissue remains unclear.

The results presented in this paper show that an extract from the BBD mat has toxic effects on the growth and viability of the symbiotic dinoflagellate *Symbiodinium* sp. Nonetheless, neither the pellet recovered from the extraction nor extracts from other bacteria have such an effect, suggesting that neither LPS nor membrane proteins are involved in BBD toxicity. Moreover, this compound has a molecular weight lower than 10,000 Da and is heat stable. All these results indicate that there is a toxic compound possibly involved in the mechanism of pathogenesis of BBD in corals. Further studies will involve the isolation and characterization of such compound.

Keywords coral, black band disease, toxin, cyanobacteria.

Introduction

Coral diseases have recently been recognized as key elements in the health status of coral reefs. Reports describing new coral diseases and their incidence have been increasingly appearing in the literature. However, despite the new awareness of their importance, our knowledge on the etiology and origin of these diseases is still limited.

Black band disease (BBD) is one of the most widespread and well-studied coral diseases. It is well established that BBD is an infectious disease caused by the activity of a complex bacterial mat. This bacterial mat forms a ring-shaped black band that moves from top-to-bottom across coral colonies. BBD is able to infect a large number of different species of corals. In the Caribbean, BBD has frequently been detected infecting colonies of *Diploria strigosa*, *D. labyrinthoformis*, *Montastrea annularis*, and *M. cavernosa* (Antonius 1981; Edmunds 1991; Rützler and Santavy 1983). These are among the most ecologically important scleractinian corals in those reefs and therefore coral mortality caused by BBD is an important force in the restructuring of these coral reef communities (Edmunds 1991; Kuta and Richardson 1997). Moreover, once the coral is infected by BBD the bacterial mat migrates at a high rate, destroying the coral colony in a short period of time.

Although the bacterial mat causing BBD has been characterized, the cause, origin and mechanisms of infection of the disease remain unknown. By far, the most abundant organism in the BBD microbial mat is a large filamentous cyanobacterium, identified optically as *Phormidium corallyticum* (Richardson 1998; Rützler and Santavy 1983). Nonetheless, the BBD mat is composed of highly complex bacterial communities, with a number of different bacterial species that are not found on healthy coral or surrounding seawater (Cooney et al. 2002; Frias-Lopez et al. 2002). The role of specific BBD microorganisms in the progression of the disease remains unclear.

In this study, we present results indicating that the production of a small toxic compound that has cytotoxic activity against *Symbiodinium* sp., the symbiotic dinoflagellate living in corals. These results may explain in part the role of *Phormidium corallyticum* in the disease as well as the mechanism of tissue destruction.

Material and Methods

BBD Sample Collection

Sampling was conducted using standard SCUBA techniques on the coral reefs of Curaçao, Netherlands Antilles. Colonies of *Diploria strigosa* exhibiting the distinct BBD ring were sampled at water depths of approximately 3m near the Curaçao Water Plant. Portions of active BBD mats were physically peeled off the infected coral surfaces using forceps and placed in 15ml Falcon tubes filled with RNAlater (Ambion, Austin, TX) and samples were then immediately frozen at –20°C.

BBD Sample Fractionation

Bead beating was used to extract the soluble fraction from the cells. Sample was added to a 2 ml screw-capped microcentrifuge tube with O-ring and spun down for 5 minutes at 16,000 x *g*. Before bead beating, RNAlater (Ambion, Austin, TX) was decanted and samples were washed twice in 1ml of filtered seawater. The pellet was resuspended in 400µl of sterile ultra pure water and approximately 200µl of 0.1 mm zirconia/silica beads (BioSpec Products, Bartlesville, OK). The tubes were shaken on a reciprocating Mini-BeadBeater-8 (BioSpec Products, Bartlesville, OK) for 1 minute at the homogenize speed setting.

After bead beating samples were centrifuged for 5 minutes at 16,000 x *g*, both the pellet and supernatant were saved. To check heat stability of the possible toxic compound active supernatant was boiled for 10 minutes. A pellet obtained from a parallel sample of a 10 mL *E. coli* culture, also preserve in RNAlater (Ambion, Austin, TX), was treated using the same experimental procedure and the whole extract was used as a negative control.

Fractions of different molecular sizes were obtained by ultrafiltration. Centricon YM-10 (Millipore, Bedbofd, MA, USA) centrifugal filter devices were used to obtain fractions of different molecular weight: <10,000 Da and >10,000 Da. Filters were blocked overnight at 4^0C with a solution of 1mg/mL BSA in PBS. Supernatants were then fractionated following manufacturers instructions.

Symbiodinium Cultures

A collection strain of *Symbiodinium microadriaticum* was used in all experiments: *Symbiodinium microadriaticum* NEPCC 411 (Canadian Center for the Culture of Microorganisms (CCCM)). Total DNA was extracted using CTAB (hexadecyltrimethyl ammonium bromide) according to Coffroth et al. (Coffroth et al. 1992) .18S rRNA was amplified by PCR using primers ss5 (5'-GGTTGATCCTGCCAGTAGTCATATGCTTG-3') and ss3z (5'-AGCACTGCGTCAGTCCGAATAATTCACCGC-3') according to Rowan and Powers (Rowan, Powers 1991) *Symbiodinium* was cultured in 30ml of f/2 media (Guillard and Ryther 1962) in 150 ml flasks topped with foam stoppers and incubated at 25.5^0C in 12 h light/dark cycles.

f/2 medium was sterilized by filtration through 0.22µm filter (Guillard and Ryther 1962) and store at 4^0C in the dark. An antibiotic solution according to Polne-Fuller (Polne-Fuller 1991) was added to avoid contaminations. The solution should be prepared in 100 mL 0.22 µm filtered seawater and diluted 1:10 for use.

Cell Viability Assays

3mL of f/2 medium was inoculated with *Symbiodinium* to a final OD_{600} of 0.1 in 15mL Erlenmeyer flasks and incubated at 25.5^0C in 12 h light/dark cycles. The CellTiter 96® AQueous One Solution Cell Proliferation Assay (Promega, Madison Wi) is a colorimetric method for determining the number of viable cells in proliferation or cytotoxicity assays. Cell viability was tested using the CellTiter 96 Aqueous One Solution Cell Proliferation Assay (Promega, Madison, WI) following manufacturers instructions. Briefly, 20µl of CellTiter 96® AQueous One Solution Reagent were pipetted into each well of the 96-well assay plate containing 100µl of each samples. Plates were incubated for 2 hours at 25.C°C under light. Cell proliferation and viability is measured by the formation of a colored formazan product recording absorbance at 490nm.

Growth Inhibition Assays on Symbiodinium

For these assays *Symbiodinium* were cultured in 6 well tissue culture plates (Becton Dickinson, Franklin Lakes, NJ) containing 2.5mL of f/2 medium each well. All wells were inoculated with 100µl of a cell suspension of *Symbiodinium* at OD_{600} 0.3. The volume of the different fractions added to the wells varied depending of their protein content. The protein concentration was measured using the DC Protein Assay (BIORAD, Hercules, CA) according to manufactures instructions. The same amount of protein was added to the different wells, approximately 0.1mg of total protein.

Growth was checked daily by visual assessment of the increase in color due to the multiplication and attachment to the surface of the plate of *Symbiodinium* cells.

RESULTS

Cell Viability Assays

The 18S rRNA sequence from the culture showed that the *Symbiodinium* strain used for the experiments was actually not a *Symbiodinium microadriaticum* but a member of *Symbiodinium* clade B. This is also a clade frequently identified living in symbiosis in scleractinian corals. The supernatants and whole extracts inhibited completely the respiration and viability of the *Symbiodinium* cultures after 4 days of incubation (Fig. 1).

However, the *E. coli* extract did not have any effect on the *Symbiodinium* growth. Molecules associated with the membranes present in the pellet (LPS and proteins) did not have a toxic effect on *Symbiodinium*. After an initial inhibition, cells started to grow again and reached the same levels of activity as the negative controls.

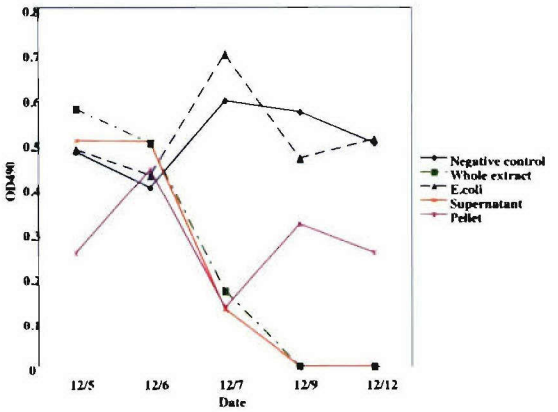

Fig.1- Assessment of the effect of different fractions on cell viability. OD490 shows indicates respiration that correlates with the number of cells. See text for details.

Growth Inhibition of Symbiodinium sp.

Due to the low number of cells of *Symbiodinium* added as inoculum, visible growth was not observed until at least 4 days of incubation. Figure 2 shows a representative example of growth and inhibition observed on the plates.

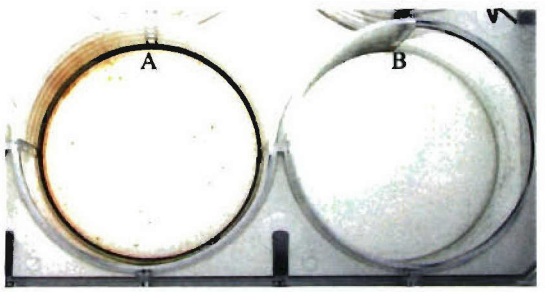

Fig.2- Example of growth inhibition by BBD supernatant (A) compared to a negative control (B).

Table 1 shows the results for the effect of the different fractions on *Symbiodinium* growth. Both whole extract and supernatant had inhibitory activity of *Symbiodinium* growth. When viability was checked, neither *E. coli* extract nor pellet from BBD exhibited cytotoxic effects on the *Symbiodinium* cultures assessed.

The fraction containing compounds of molecular weight smaller than 10,000 Da still maintained toxic activity. Finally, treatment at 100^0C for 10 minutes did not have any effect on the toxicity of the extract.

Table 1. Effect of the different fractions on the growth of *Symbiodinium* sp. (+) represents growth, (-) indicates inhibition of Symbiodinium growth.

	Negative control	*E.coli* whole extract	BBD whole extract	BBD supernatant	BBD pellet	Whole extract 95°C	<10,000 Da fraction
Extraction 1	+	+	-	-	+	-	-
Extraction 2	+	+	-	-	+	-	-
Extraction 3	+	+	-	-	+	-	-

Discussion

Although we have a fairly good knowledge about the composition of the bacterial communities causing BBD (Frias-Lopez, et al. 2002), its mechanism of pathogenesis is still poorly understood. Thus the role of the most abundant organisms in BBD during infection, the cyanobacterium *Phormidium corallyticum*, remains a mystery.

Among the microorganisms present in BBD, *Beggiatoa* spp. and *Desulfovibrio* spp. had previously been identified as potentially important bacteria in the development of the disease. The only mechanism of pathogenesis proposed to date involved the reduction of sulfate to sulfide by bacteria. *Beggiatoa* spp. and *Desulfovibrio* spp. would be the organisms responsible for the pathogenesis of BBD (Richardson 1996; Richardson et al. 1997). Sulfide would be the toxic compound responsible for coral tissue destruction. A similar process that involves members of these two groups has been described in marine sediments under anaerobic conditions. However, *Beggiatoa* has only been identified using optical microscopy. Molecular techniques have failed to detect the presence of *Beggiatoa* in BBD bacterial mats (Cooney et al. 2002; Frias-Lopez et al. 2002).

In the present study we wanted to assess the possibility of the production of a toxic compound that could be involved in coral tissue destruction. *Symbiodinium* sp., the symbiotic dinoflagellate living inside the coral, has proven a good and easy to use model to test toxicity of BBD.

Cyanobacteria such as *Microcystis*, *Anabaena*, *Nostoc* and *Oscillatoria* are well known for their ability to produce toxins (Carmichael 1994; Codd et al. 2001). While most of these toxins have a low molecular weight, they differ in their structure, modes of action, and toxicities. The best-studied cyanobacterial toxins are the microcystins and nodularins, both small cyclic peptides. While microcystins are primarily produced by freshwater cyanobacterial genera, nodularins have been detected

from members of the genus *Nodularia*, a marine cyanobacterium (Carmichael 1992; Gulledgea et al. 2002). Since the most abundant organism found in BBD is a filamentous cyanobacterium, it is reasonable to think that a toxic compound may be involved in BBD virulence.

Our results have shown that there is a compound, which has a molecular weight lower than 10,000 Da, which inhibits the growth of *Symbiodinium* and stops viability. Moreover, like other cyanotoxins, this compound has been shown to be heat-stable, (Sivonen and Jones 1999).

Although we have no direct evidence which microorganism is responsible for the production of the toxic compound, due to its overwhelming presence during infection *Phormidium corallyticum* is the most likely candidate.

In summary, we have shown that during BBD infection there is production of a toxic compound that could play an important role in coral tissue destruction during infection. Future studies are needed to purify and characterize this compound. Additionally, it should be determined which bacteria among those present in BBD are responsible for the production of this toxin.

References

Antonius A (1981) The "band" diseases in coral reefs. Fourth International Coral Reef Symposium, Manila, Philippines. 2: 7-14

Carmichael WW (1992) Cyanobacteria secondary metabolites--the cyanotoxins. J Appl Bacteriol 72: 445-459

Carmichael WW (1994) The toxins of cyanobacteria. Sci Am 270: 78-86

Codd GA, Metcalf JS, Ward CJ, Beattie KA, Bell SG, Kaya K, Poon GK (2001) Analysis of cyanobacterial toxins by physicochemical and biochemical methods. J AOAC Int 84: 1626-1635

Coffroth MA, Lasker HR, Diamond ME, Bruenn JA, Bermingham E (1992) DNA fingerprints of a gorgonian coral: a method for detecting clonal structure in a vegetative species. Marine Biology 114: 317-325

Cooney RP, Pantos O, Le Tissier MD, Barer MR, O'Donnell AG, Bythell JC (2002) Characterization of the bacterial consortium associated with black band disease in coral using molecular microbiological techniques. Environmental Microbiology 4: 401-413

Edmunds PJ (1991) Extent and effect of black band disease on a caribbean reef. Coral Reefs 10: 161-165

Frias-Lopez J, Zerkle AL, Bonheyo GT, Fouke BW (2002) Partitioning of bacterial communities between seawater and healthy, black band diseased, and dead coral surfaces. Applied & Environmental Microbiology 68: 2214-2228

Guillard RR, Ryther JH (1962) Studies of marine planktonic diatoms. I. *Cyclotella nana* Hustedt, and *Detonula confervacea* (cleve) Gran. Canadian Journal of Microbiology 8: 229-239

Gulledgea BM, Aggena JB, Huangb HB, Nairnc AC, Chamberlin AR (2002) The microcystins and nodularins: cyclic polypeptide inhibitors of PP1 and PP2A. Curr Med Chem 9: 1991-2003

Polne-Fuller M (1991) A novel technique for preparation of axenic cultures of *Symbiodinium* (Pyrrophyta) through selective digestion by amoebae. Journal of Phycology 27: 552-554

Richardson LL (1998) Coral disease: what is really known? Trends in Ecolology & Evolution 13: 438-443

Richardson LL (1996) Horizontal and vertical migration patterns of *Phormidium corallyticum* and *Beggiatoa* spp. associated with black-band disease of corals. Microbial Ecology 32: 323-335

Richardson LL, Kuta KG, Schnell S, Carlton RG (1997) Ecology of the black band disease microbial consortium. Eighth International Coral Reef Symposium, Balboa, Panama 1: 597-600

Rowan R, Powers DA (1991) A molecular genetic classification of zooxanthellae and the evolution of animal-algal symbioses. Science 251: 1348-1351

Rützler K, Santavy DL (1983) The black band disease of Atlantic reef corals. I. Description of the cyanophyte pathogen. Marine Ecology-PUBBLICAZIONI DELLA STAZIONE ZOOLOGICA DI NAPOLI I 4: 301-319.

Sivonen K, Jones G (1999) Toxic cyanobcteria in water. A guide to their public health consequences, monitoring and management. World Health Organization

The effect of temperature and aquaria conditions on bacterial communities inhabiting healthy tissues of *Diploria strigosa*

James S. KLAUS*, Jorge FRIAS-LOPEZ, and Bruce W. FOUKE

Department of Geology, University of Illinois, Urbana, Illinois 61801
*Corresponding author: J. KLAUS
FAX: 217-244-4996, e-mail: jklaus@uiuc.edu

Abstract The occurrence of coral diseases associated with bacterial infection increases dramatically with increasing sea surface temperatures. However, the mechanism by which elevated seawater temperature actually induces or causes coral disease is poorly understood. One possibility is that increasing seawater temperature causes a change in the community structure of bacteria inhabiting healthy coral tissues, To assess the effect of increasing seawater temperature on the bacterial communities inhabiting the brain coral *D. strigosa*, colonies were collected directly from the reef were compared to colonies maintained in both heated and control flow-through aquaria. Heated aquaria were maintained at 30.5° C (2.5° C above ambient) and coral colonies were left in the aquaria for up to two weeks prior to sampling. Bacterial assemblages were compared statistically through the use of Terminal-Restriction Fragment Length Polymorphisms (T-RFLP) of 16S rRNA genes. The bacterial communities inhabiting coral colonies maintained in the unheated flow-through aquaria were statistically different from colonies sampled directly from the reef. However, colonies maintained in the heated aquaria were statistically similar to those sampled from the unheated aquaria.

Keywords Bacteria, Coral disease, T-RFLP, Temperature

Introduction

Recent reports have highlighted the impact of coral diseases on reefs worldwide (Green and Bruckner 2000), and suggest that both the intensity and number of different diseases may be on the rise (Richardson 1998; Harvell et al. 1999). The correlation of disease occurrence to numerous environmental factors, including temperature (Gil-Agudelo and Garzon-Ferreira 2001;Kuta and Richardson 2002; Richardson et al. 1998; Rosenberg and Ben-Haim 2002), depth (Kuta and Richardson 2002), sedimentation (Bruckner et al. 1997; Taylor 1983) nutrients (Antonius 1988; Kim and Harvell 2000; Taylor 1983) and pollution, (Antonius 1988; Bruckner et al. 1997) hints at the complex interactions between disease and the environment. Of these factors, one of the most striking correlations to disease occurrence is temperature (Kuta and Richardson 2002, Rosenberg and Ben-Haim 2002). In the case of bleaching by *Vibrio shiloi* increased temperature triggers the expression of virulence factors (Rosenberg and Ben-Haim 2002). At high seawater temperatures, *V. shiloi* produces an adhesin that allows it to adhere to and then penetrate coral surfaces. Once inside the coral tissue *V. shiloi* toxins inhibit and lyse symbiotic zooxanthellae. In other coral diseases such as plague, dark spot disease and black band disease, the correlation to temperature is less absolute, and the mechanism by which elevated temperatures affect disease incidence is poorly understood. In these cases, the relationship between temperature and disease may not be entirely tied to the pathogen(s), but instead may involve the temperature response of a whole microbial community. One of the best defense mechanisms to the growth of pathogenic microbes is the maintenance of a healthy microbial community. These microorganisms can inhibit pathogens through interspecific competition and secretion of antibiotic substances (Klaus et al. *2005*; Rohwer et al. 2002, Pantos et al. 2003)

It is well established that coral tissues harbor diverse bacterial communities, primarily associated with the coral surface microlayer or coelenteron (Bythell et al. 2002; Frias-Lopez et al. 2002; Gast et al. 1998; Rohwer et al. 2001). However, the affect of seawater temperature on these communities remains poorly understood. To further understand the ecological process link between coral disease and temperature, additional information is needed on how the healthy bacterial community associated with coral tissue responds to varying temperature conditions.

The goal of the present study was to assess the effect of temperature on the bacterial communities of healthy colonies of *Diploria strigosa*. The bacterial community associated with naturally occurring colonies as well as those maintained in heated and unheated experimental aquaria were characterized through the use of terminal restriction fragment length polymorphisms (T-RFLP) of 16S rRNA genes. The variation in bacterial communities was analyzed quantitatively using a combination of statistical procedures, including multidimensional scaling (MDS), one-way analysis of similarity (ANOSIM), and

similarity percentages (SIMPER) (Clarke and Warwick 2001).

Materials and Methods

Sample Collection and Experimental Setup

Twenty healthy colonies of *D. strigosa* were collected from shallow fringing reefs (~5 m water depth) approximately 75 m offshore of the island of Curaçao Netherlands Antilles. Upon returning to shore, four colonies were rinsed with filtered seawater and immediately sampled for molecular microbial analysis. Samples were collected from the surface by removing a 2 cm by 2 cm portion of the uppermost 1 cm of the coral colony with a chisel and placing the sample in a sterile disposable 50 ml polypropylene centrifuge tube. The sample was immersed in 80% ethanol, crushed and homogenized, creating a slurry of coral tissue, zooxanthellae, mucus, microorganisms, and skeletal material. The remaining 16 colonies were put into heated and control aquaria housed at the Curaçao Sea Aquarium. The Curaçao Sea Aquarium maintains a large flow-through tank system in which seawater is pumped through from the adjacent reef (approximately 5 m water depth). The reef water was pumped directly from a small sedimentation reservoir to one of two experimental aquaria. One aquaria was maintained at ambient temperature (control = 28° C) while the other was heated 2.5° C above ambient temperature (heated = 30.5° C). Eight colonies were put in each tank and sampled as above; half after six days and half after fourteen days. Previous studies have shown very little overlap between the bacterial species detected from reef-water and coral tissues (Frias-Lopez et al. 2002; Rohwer et al. 2001). Based on these studies we chose to focus solely on the bacterial communities of *D. strigosa*.

T-RFLP Analysis

Total DNA was prepared from coral samples using the UltraClean Soil DNA Kit (Mo Bio Laboratories, Carlsbad, CA). This kit has proven to be one of the most efficient and consistent methods for obtaining DNA from coral tissues (Rohwer et al. 2001; Klaus unpublished data). Optimization of PCR was performed for each sample by adjusting the amount of genomic DNA extract used to obtain a strong band on an agarose gel, without visible nonspecific product (Blackwood et al. 2003). The genes encoding for 16S rDNA were amplified with a Mastercycler gradient thermocycler (Eppendorf) by PCR using specific 16S rRNA primers for bacteria. Primers used in the PCR amplifications were Univ 9F (5'-GAGTTTGATYMTGGCTC) and Univ 1509R (5'-GYTACCTTGTTACGACTT) (Integrated DNA Technologies, Coralville, IA). Univ 9F was labeled at the 5' end with phosphoramidite fluorochrome 6-carboxyfluorescein (6-FAM). PCR was performed using a reaction mixture of 0.2 mM of each deoxynucleoside triphosphate (Gibco/BRL, Rockville, Md), 200 ng each of the forward and reverse primers, 0.5 to 10 _l of the sample preparation, 1X Taq Master, 1X Taq Buffer (50mM KCl, 10mM Tris-HCl pH 8.3, 1.5 mM $Mg(OAc)_2$) and water to bring the total volume to 50 _l.

To obtain an adequate mass of DNA for T-RFLP analysis, the previously described PCR reactions were performed in quadruplet. Pooled replicates were purified using the Wizard PCR prep kit (Promega, Madison, WI). DNA was eluted with 30 _l of sterile water heated to 65° C. Restriction digests were performed independently using three tetrameric enzymes (*Hha* I, *Msp* I, and *Rsa* I). Eight microliters of purified PCR product was added to 9 _l of sterile water and 3 _l of restriction enzyme master mix containing 10 U of restriction enzyme and 1X reaction buffer. Incubation was done at 37° C for 6 h followed by 15 min at 65° C to denature the restriction enzyme.

Prior to loading on a gel, 1 µl of sample was added to a "loading cocktail" (1.25µl deionized formamide 0.25µl blue loading dye and 0.3µl size standard, TAMRA 2500), vortexed, spun down, and denatured at 95° C for three minutes. Samples were then run on a 5% Long Ranger acrylamide (BioWhittaker) and 7M urea gel for approximately 5 hours. T-RFLP profiles were obtained using an Applied Biosystems, Inc. (ABI) 377-XL sequencer. The data was analyzed using the ABI GeneScan software.

Previous studies (Klaus et al. 2005) have shown that T-RFLP profiles obtained from replicate samples have minimal variation due to potential differences in DNA extraction, PCR amplification, or enzyme digestion efficiency. These results indicate that the T-RFLP methodology applied in this study is robust, and comparisons of profiles between different samples should reflect the relative similarity of the microbial communities present in each sample.

Statistical Analyses

Sample versus T-RFLP peak data matrices were constructed using all peaks above a threshold of 50 units above background. To avoid detection of primers peaks smaller than 50 base pairs (bp) were culled from the data set. To account for variation in fragment size determination between samples, peaks were manually aligned and placed into groups. Abundance data was obtained from the relative peak height following sample standardization (Blackwood et al. 2003). The similarity of T-RFLP peak profiles among all possible pairs of samples was calculated using the Bray-Curtis (BC) similarity coefficient (Bray and Curtis 1957).

Ordination by non-metric multidimensional scaling (MDS) (Kruskal 1964) was performed to examine differences in T-RFLP peak patterns among samples. Each ordination was run with 30 random starting configurations and proceeded through multiple iterations until the fit of a non-parametric regression of d (distances between samples on the MDS) against _ (similarities in the Bray-Curtis matrix) could not be improved. To test the significance of T-RFLP peak differences due to ecologically distinct sample groups, the Bray-Curtis similarity matrix was subjected to the analysis of similarities procedure (ANOSIM) (Clarke and Warwick

2001). This analysis is based on a non-parametric permutation procedure applied to the rank similarity matrix. If samples within a group are identical; Global R = 1. Similarity percentages (SIMPER) (Clarke and Warwick 2001) were used to determine peak contributions to the average dissimilarity of samples between different sample groups.

Results

A combined total of 241 different T-RF's were identified from the sixty different T-RFLP profiles analyzed from healthy *D. strigosa* (20 *Hha* I, 20 *Msp* I, and 20 *Rsa* I). The rank abundance profile (Fig. 1) for all 241 unique T-RF's shows that only one peak was identified from all 20 samples. An additional 9 different T-RF's were found in at least 50 % of the samples analyzed. By comparing T-RFLP profiles with theoretical digest patterns generated from previously constructed coral tissue clone libraries, (Frias-Lopez et al. 2002) several of the dominant T-RF peaks can be tentatively identified. Based on these assessments T-RF's MspI-125, and RsaI-643 appear to be related to *Chromatium* sp. RW (AF384210) of the _-proteobacteria subdivision. Additionally, T-RF's HhaI-210 and MspI-496 appear related to the uncultured _-proteobacterium clone 26 (AF369718), and T-RF's HhaI-82 and MspI-453 to a magnetite-containing magnetic *Vibrio* sp. (Lo6455) of the _-proteobacteria subdivision.

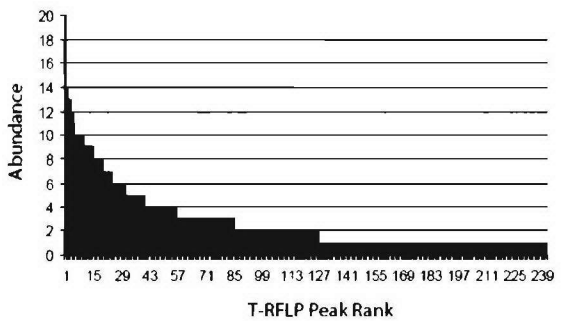

Fig. 1. Rank-abundance curve of T-RFLP peaks detected in all 20 samples of *D. strigosa* (n= 241).

Multivariate Analysis

To test the effect of the experimental aquaria on the composition of the most abundant bacterial species, colonies of *D. strigosa* sampled directly from the reef were compared to colonies sampled from control aquaria after 6 days and 14 days. The bacterial communities of reef samples were found to be distinct from all control samples analyzed. The ANOSIM statistical test for differences in T-RF composition show reef samples to be significantly different from control samples after 6 days ($R = 0.729$, $P < 0.029$) and 14 days ($R = 0.938$, $P < 0.029$). Furthermore, the control samples collected after 6 days were significantly different from those collected after 14 days ($R = 0.729$, $P < 0.029$). These results are further supported by the MDS ordination of samples (Fig. 2) in which the reef samples and two sets of control samples all form distinct clusters. Results from SIMPER analysis reveal the major peaks responsible for the differences among sample groups (Table 1).

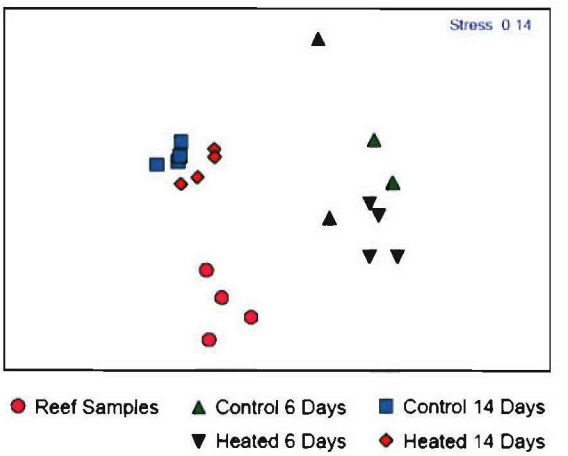

Fig. 2. Nonmetric multidimensional scaling (MDS) ordination of bacterial assemblages inhabiting the tissues of *D. strigosa* (n=20).

To assess the effects of temperature on bacterial communities associated with coral tissues, T-RFLP profiles from control and heat-treated colonies were compared. No statistically significant differences in T-RF composition with respect to heat treatment were detected. The ANOSIM statistical test for differences in T-RF composition did not detect any differences between control and heated samples after 6 days ($R = 0.135$, $P < 0.171$) or 14 days ($R = 0.198$, $P < 0.171$). While MDS ordination does suggest some clustering of heated and control samples, this is not outside the range of variation within sample groups (Fig. 2).

K-dominance Curves

While the T-RFLP method is capable of assessing phylotype richness in simple artificial communities with few members (Avaniss-Aghajani et al. 1994; Liu et al. 1997; Moeseneder et al. 1999) it has not proved successful at assessing complex natural communities (Dunbar et al. 2000; Moeseneder et al. 1999). Despite this shortcoming in assessing richness, examination of the cumulative dominance distribution generated from T-RFLP profiles can provide insight into the diversity and relative dominance of assemblages.

The average k-dominance curves (Lambshead et al. 1983) for the five sample groups analyzed exhibited distinct separation. A higher dominance of abundant T-RF's was observed in heat-treated colonies compared to both control and reef colonies (Fig. 3). The curve for the pooled reef samples had the most moderate slope of the sample groups, suggesting greater bacterial diversity.

Table 1. T-RF's distinguishing healthy bacterial communities of *D. strigosa*.

	Reef		Control 6 days		Heated 6 days		Control 14 days		Heated 14 days	
	Avg. abu.[a]	Avg. sim.[b]	Avg. abu.	Avg. sim.	Avg. abu.	Avg. sim.	Avg. abu.	Avg. sim.	Avg. abu.	Avg. sim.
*Rsa*I-643	0.84	0.55	14.60	3.94	15.81	9.23	0	0	0	0
*Msp*I-503	9.85	3.23	1.40	0	0.97	0	4.03	3.01	5.66	4.28
*Rsa*I-985	3.69	2.33	0	0	0	0	0	0	0	0
*Rsa*I-1002	0	0	8.14	1.32	0	0	0	0	0	0
*Hha*I-164	4.38	2.23	0.29	0	0	0	3.24	2.55	5.13	3.93
*Hha*I-89	2.95	2.01	0	0	1.39	0	0	0	0	0
*Msp*I-148	2.56	2.02	0	0	0	0	0.12	0	0.07	0
*Rsa*I-80	3.49	1.65	0	0	0	0	0	0	0	0
*Hha*I-913	0	0	5.33	0.58	0.53	0	0	0	0	0
*Msp*I-441	3.72	1.01	0.69	0	1.20	0.49	3.02	1.48	0.93	0
*Hha*I- 893	1.10	0	0.34	0	0	0	13.79	5.92	15.25	7.51
*Rsa*I-976	0.05	0	0	0	0	0	9.88	5.46	5.82	3.95

[a] Average % abundance per locality.

[b] T-RF contribution to the mean Bray-Curtis % similarity at each locality.

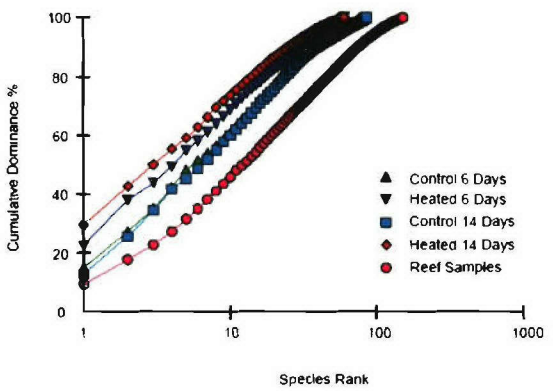

Fig. 3. Average k-dominance curves (x-axis logged) of T-RF peaks obtained from reef samples (n=4), control aquaria samples after 6 days (n=4) and 14 days (n=4), and heated aquaria samples after 6 days (n=4) and 14 days (n=4).

Discussion

In a recent review, Knowlton and Rohwer (2003) describe the coral host as a habitat. The physical and chemical conditions of this habitat are in part controlled by the coral itself and in part by the surrounding marine environment. In addition, microorganisms manipulate the physical and chemical conditions via their metabolic activities and physical presence. Thus habitat stability is maintained through a complex set of interactions. Within this habitat, the response of the coral-zooxanthellae symbiosis to thermal stress has been actively studied for decades (Brown 1997; Fitt et al. 2001; Baker et al. 2004; Rowan 2004). Here we provide a first attempt to understand the affect of thermal stress on bacterial communities.

Results of the ANOSIM statistical tests indicate that there was no significant change in bacterial communities due to the temperature treatment. This negative response suggests that, at least on short time scales, bacterial communities are stable in composition despite the physiologic responses known to occur in corals subjected to similar temperature treatments (Brown 1997). However, the current data set is characterized by a large shift in the bacterial communities found in control samples from those collected directly from the reef. It is possible that the factors responsible for the shift in control samples might also be obscuring the real signal of community change due to temperature.

There are several factors that could have affected the colonies maintained in the aquaria. While the reef samples were collected from approximately 5 m depth and exposed to normal diurnal light cycles, the control samples were maintained in shallow aquaria shaded in both the early morning and the late afternoon. The more intense yet shortened light cycles may have had an impact on the structure of bacterial communities. It is also possible that the water quality inside the aquaria was different from that found on the natural reef. Before being pumped into the aquaria, the seawater was channeled into sedimentation tanks and further passed through sedimentation filters. However, the elimination of suspended particulate matter (SPM) may have had an impact on the coral associated bacterial communities. Recent studies have shown that SPM can strongly alter the trophic environment of symbiotic corals (Anthony 2000; Anthony and Fabricius 2000). The colonies of *D. strigosa* used in this study were collected from shallow, high sediment, nearshore enviornments, and possibly acclimated to sustain a positive energy balance through heterotrophic suspension feeding. Therefore, removal of SPM from the flow-though aquaria may have forced a shift towards a more phototrophic energy balance. Lastly, to maintain the temperature of the heated aquaria, the flow rate had to be kept fairly low. It is therefore possible that the long residence time of seawater within the aquaria would result in a shift in available nutrient

concentrations. These factors were not adequately controlled for in the experimental setup, and the extent of their control on bacterial communities remains largely unknown. Future experiments should directly target these potentially important factors.

While the multivariate statistical techniques applied in the present study did not detect significant differences between the control and heated aquaria samples, a greater dominance of abundant T-RF's was observed in the heat-treated colonies compared to the control colonies. Furthermore, a greater dominance of abundant T-RF's was observed in the control aquaria colonies than on the reef colonies. An increased dominance of specific bacterial strains is a common response observed in disturbed environments (Haack et al. 2004; Salyers and Whitt 1994; Torsvik et al. 2002). Recent surveys of bacterial communities inhabiting *D. strigosa* showed an increased dominance of the most prevalent T-RF's at impacted localities versus control localities, as did communities associated with diseased corals versus healthy corals (Klaus et al. 2005).

Given the problems with the experimental setup, and the somewhat conflicting results found between the multivariate analyses and the dominance analyses, further studies are needed to confirm the community-level response of bacteria associated with coral tissues.

Acknowledgements
This work was supported by research grants from the Office of Naval Research (N00014-00-1-0609), the Geological Society of America, and the American Association of Petroleum Geologists. We acknowledge the support of CARMABI with field efforts and Heather Hentchel with sample preparation.

References

Anthony KRN (2000) Enhanced particle-feeding capacity of corals on turbid reefs (Great Barrier Reef, Australia). Coral Reefs 19: 59-67

Anthony KRN, Fabricius KE (2000) Shifting roles of heterotrophy and autotrophy in coral energetics under varying turbidity. J Exp Mar Biol Ecol 252: 221-253

Antonius A (1988) Distribution and Dynamics of Coral Diseases in the Eastern Red Sea. Proc 6th Int Coral Reef Symp 2: 293-298.

Avaniss-Aghajani E, Jones K, Champman D, Brunk C (1994) A molecular technique for identification of bacteria using small subunit ribosomal RNA sequences. BioTechniques 17: 1731-1737

Baker AC, Starger CJ, McClanahan TR, Glynn PW (2004) Corals' adaptive response to climate change. Nature 430: 471

Blackwood CB, Marsh T, Sang-Hoon K, Paul EA (2003) Terminal Restriction Fragment Length Polymorphism Data Analysis for Quantitative Comparison of Microbial Communities. Appl Environ Microbiol 69: 926-932

Bray JR, Curtis JT (1957) An ordination of the upland forest communities of southern Wisconsin. Ecol Monogr 34: 77-87

Brown BE (1997) Coral bleaching: causes and consequences. Coral Reefs 16, Suppl.: S129-S138

Bruckner AW, Bruckner RJ, Williams EH, Jr. (1997) Spread of black-band disease epizootic through the coral reef system in St. Ann's Bay, Jamaica. Bull Mar Sci 61: 919-928

Bythell JC, Barer MR, Cooney RP, Guest JR, O'Donnell AG, Pantos O, Le Tissier MD (2002) Histopathological methods for the investigation of microbial communities associated with disease lesions in reef corals. Lett Appl Microbiol 34: 359-364

Clarke KR, Warwick RM (2001) Change in marine communities: an approach to statistical analysis and interpretation. Primer-E Ltd, Plymouth (175)

Dunbar J, Ticknor LO, Kuske CR (2000) Assessment of microbial diversity in four southwestern United States soils by 16S rRNA terminal restriction fragment analysis. Appl Environ Microbiol 66: 2943-2950

Fitt WK, Brown BE, Warner ME, Dunne RP (2001) Coral bleaching: interpretation of thermal tolerance limites and thermal thresholds in tropical corals. Coral Reefs 20: 51-65

Frias-Lopez J, Zerkle AL, Bonheyo GT, Fouke BW (2002) Partitioning of bacterial communities between seawater and healthy, black band diseased, and dead coral surfaces. Appl Environ Microbiol 68: 2214-2228

Gast GJ, Wiegman S, Wieringa E, Van Duyl FC, Bak RPM (1998) Bacteria in coral reef water types: removal of cells, stimulation of growth and mineralization. Mar Ecol Prog Series 167: 37-45

Gil-Agudelo DL, Garzon-Ferreira J (2001) Spatial and seasonal variation of dark spots disease in coral communities of the Santa Marta area (Columbia Caribbean). Bull Mar Sci 69: 619-629

Green EP, Bruckner AW (2000) The significance of coral disease epizootiology for coral reef conservation. Biol Conserv 96: 347-361

Haack CS, Fogarty LR, West TG, Alm EW, McGuire JT, Long DT, Hyndman DW, Forney LJ (2004) Spatial and temporal changes in microbial community structure associated with recharge-influenced

chemical gradients in a contaminated aquifer. Environ Microbiol 6: 438-448

Harvell CD, Kim K, Burkholder JM, Colwell RR, Epstein PR, Grimes DJ, Hofmann EE, Lipp EK, Osterhaus AD, Overstreet RM, Porter JW, Smith GW, Vasta GR (1999) Emerging marine diseases-climate links and anthropogenic factors. Science 285: 1505-1510

Kim K, Harvell C (2002) Aspergillosis of sea fan corals: dynamics in the Florida Keys. CRCPress, Boca Raton (827-881)

Klaus JS, Frias-Lopez J, Bonheyo GT, Heikoop JM, Fouke BW (2005) Bacterial communities inhabiting the healthy tissues of two Caribbean reef corals: interspecific and spatial variation. Coral Reefs 24: 129-137

Knowlton N, Rohwer F (2003) Multispecies microbial mutualisms on coral reefs: the host as a habitat. The American Naturalist 162: 51-62

Kruskal JB (1964) Multidimensional scaling by optimizing goodness of fit to a nonmetric hypothesis. Psychometrika 29: 1-27

Kuta K, Richardson L (2002) Ecological aspects of black band disease of corals: relationships between disease incidence and environmental factors. Coral Reefs 21: 393-398

Lambshead PJD, Platt HM, Shaw KM (1983) The detection of differences among assemblages of marine species based on an assessment of dominance and diversity. J Nat Hist 17: 859-874

Liu W, Marsh TL, Cheng H, Forney LJ (1997) Characterization of microbial diversity by determining terminal restriction fragment length polymorphisms of genes encoding 16S rRNA. Appl Environ Microbiol 63: 4516-4522

Moeseneder M, Arrieta JM, Muyzer G, Winter C, Herndl GJ (1999) Optimization of terminal-restriction fragment length polymorphism analysis for complex marine bacterioplankton communities and comparison with denaturing gradient gel electrophoresis. Appl Environ Microbiol

Pantos O, Cooney RP, Le Tissier MD, Barer MR, O'Donnell AG, Bythell JC (2003) The bacterial ecology of a plague-like disease affecting the Caribbean coral Montastrea annularis. Environ Microbiol 5: 370-382

Peters EC (1993) Diseases of other invertebrate phyla: Porifera, cnidaria, ctenophora, annelida, echinodermata. CRC Press, Florida (393-449)

Richardson LL (1998) Coral diseases: what is really known? Trends in Ecology & Evolution 13: 438-443

Richardson LL, Goldberg, W.M., Carlton, R.G., Halas, J.C. (1998) Coral disease outbreak in the Florida Keys: Plague Type II. REVISTA DE BIOLOGIA TROPICAL 46: 187-198

Rohwer F, Breitbart M, Jara J, Azam F, Knowlton N (2001) Diversity of bacteria associated with the Caribbean coral *Montastraea franksi*. Coral Reefs 20: 85-91

Rohwer F, Segritan V, Azam F, Knowlton N (2002) Diversity and distribution of coral-associated bacteria. Mar Ecol Prog Series 243: 1-10

Rosenberg E, Ben-Haim Y (2002) Microbial diseases of corals and global warming. Environmental Microbiology 4: 318-326

Rowan R (2004) Coral bleaching: thermal adaptation in reef coral symbionts. Nature 430: 742

Salyers AA, Whitt DD (1994) Bacterial Pathogenesis A Molecular Approach. ASM Press, Washington D.C. (418)

Sambrook J, Fritsch EF, Maniatis T (1989) Molecular cloning: a laboratory manual. Cold Spring Harbor Laboratory Press, Cold Spring Harbor, N.Y.

Taylor DL (1983) The Black Band Disease of Atlantic Corals. II. Isolation, Cultivation, and Growth of *Phormidium corallyticum*. Mar Ecol 4: 321-328

Torsvik V, Øverås L, Thingstad TF (2002) Prokaryotic diversity - magnitude, dynamics and controlling factors. Science 296: 106

Coral microbial communities, zooxanthellae, and mucus along gradients of seawater depth and coastal pollution

James S. Klaus[1*], Ingmar Janse[1], Jeffrey M. Heikoop[2], Robert A. Sanford[1], and Bruce W. Fouke[1]

[1]Department of Geology, University of Illinois, Urbana, Illinois 61801

[2]Earth and Environmental Sciences Division, Los Alamos National Laboratory, Los Alamos, New Mexico, 87545

[*]Corresponding author. Mailing address.

James S. Klaus, Department of Geology, University of Illinois, 1301 W. Green Street, Urbana, IL 61801. Phone: (217) 333-0672. Fax: (217) 244-4996. E-mail: jklaus@uiuc.edu

Summary

The high incidence of coral disease in shallow coastal marine environments suggests seawater depth and coastal pollution have an impact on the microbial communities inhabiting healthy coral tissues. A study was undertaken to determine how bacterial communities inhabiting tissues of the coral *Montastraea annularis* change at 5 m, 10 m and 20 m water depth in varying proximity to the urban center and seaport of Willemstad, Curaçao, Netherlands Antilles. Analyses of terminal restriction fragment length polymorphisms (TRFLP) of 16S rRNA gene sequences show significant differences in bacterial communities of polluted and control localities only at the shallowest seawater depth. Furthermore, distinct differences in bacterial communities were found with increasing water depth. Comparisons of TRFLP peaks with sequenced clone libraries indicate the black band disease cyanobacterium clone CD1C11 is common and most abundant on healthy corals in less than 10 m water depth. Similarly, sequences belonging to a putative new division of phototrophic bacteria, herein named CAB-I, were also more common in shallow water.

To assess the influence of environmental and physiologic factors on bacterial community structure, canonical correspondence analysis was performed using explanatory variables associated with: (1) light availability; (2) seawater pollution; (3) coral mucus composition; (4) the community structure of symbiotic algae; and (5) the photosynthetic activity of symbiotic algae. 11% of the variation in bacterial communities was accounted for by covariation with these variables; the most important being photosynthetically active radiation (sunlight) and the coral uptake of sewage-derived compounds as recorded by the $\delta^{15}N$ of coral tissue.

Introduction

Although coral reefs can extend to water depths greater than 100 m (Goreau and Wells 1967), diseases of hermatypic scleractinian corals are most prevalent and ecologically destructive in warm, shallow (less than 10 m), near-shore reef environments. This is in part due to elevated seawater temperatures (Gil-Agudelo and Garzon-Ferreira, 2001; Kuta and Richardson, 2002; Cervino et al., 2004; Rosenberg and Falkovitz, 2004), increased concentrations of pollutants (Bruckner et al., 1997; Kim and Harvell, 2002; Patterson et al., 2002; Kaczmarsky et al., 2005), and high light intensity (Kuta and Richardson, 2002; Richardson and Kuta, 2003). The correlation of coral disease incidence with these conditions suggests that the fluctuating physical and chemical conditions of shallow water environments cause systematic differences in the microbial communities inhabiting corals. The resident microbiota is one of the primary defense mechanisms against pathogen invasion of host tissues (Salyers and Whitt, 1994). Under healthy conditions these communities contribute to pathogen inhibition through interspecific competition for space and nutrients and secretion of antibiotic substances (Salyers and Whitt, 1994; Koh, 1997; Riley and Gordon, 1999; Riley et al., 2003). Thus, differences in the microbial community of a healthy coral could influence susceptibility to invasion by transient pathogenic microbes. Furthermore, as with coral bleaching by *Vibrio shiloi* (Rosenberg and Falkovitz, 2004), environmental factors can affect microbes such that indigenous microorganisms change from being mutualistic to pathogenic.

Culture-independent surveys of microbial 16S rRNA gene sequences have shown coral bacterial communities to be extremely diverse (Rohwer et al., 2001; Cooney et al., 2002; Frias-Lopez et al., 2002; Rohwer et al., 2002; Bourne and Munn, 2005).

47 Furthermore, these communities appear to be distinct for different coral species (Rohwer
48 et al., 2002) and unique from the overlying water column (Rohwer et al., 2002; Frias-
49 Lopez et al., 2004). Coral microbes reside primarily within or upon a mucus layer
50 secreted onto the surface of exposed coral tissues (Ducklow, 1979a; Bythell et al., 2002);
51 Fig. 1). The high concentration of proteins, polysaccharides, and lipids that comprise
52 coral mucus make it a suitable environment for microbial growth (Ducklow, 1979a,
53 1979b; Ferrier-Pages, 2000; Wild et al., 2004). While data are sparse, it is widely
54 assumed that mucus composition must play an important role in shaping microbial
55 communities (Ritchie and Smith, 2004). This is supported by experiments showing
56 selective carbon source utilization by cultured bacteria differs among 11 coral species
57 (Ritchie and Smith, 1997). Mucus is the combined product of corals and their associated
58 symbiotic algae, zooxanthellae. In corals with active symbionts it has been calculated
59 that as much as 98% of the net carbon assimilated by zooxanthellae gets released as
60 exudates, including coral mucus (Ikeda and Miyachi, 1995). Furthermore, previous
61 studies have detected significant amounts (up to 47 molar %) of arabinose in coral mucus
62 (Ducklow and Mitchell, 1979, Meikle et al. 1988). Arabinose is not a common
63 constituent of animal cells, suggesting the possible involvement of zooxanthellae, as it is
64 a universal constituent of plant cells. Therefore, different species of zooxanthellae
65 (Baker, 2003) as well as variation in photosynthetic activity could likely influence the
66 composition of coral mucus and thus, the coral microbiota.
67 Despite the potential importance of environmental and physiologic factors in
68 shaping the healthy microbiota of coral tissues, there are limited data on the subject. This
69 study provides the first characterization of how bacterial communities inhabiting the

70 tissues of healthy colonies of *M. annularis* change along gradients of seawater depth and
71 coastal pollution. Based on a generalized model of coral-zooxanthellae-microbe
72 interactions (Fig. 1; (Dubinsky, 1990; Knowlton and Rohwer, 2003) we have identified
73 five categories of ecological parameters that potentially influence microbial communities
74 associated with coral tissues. These include: (1) light intensity of the seawater
75 environment; (2) concentration of seawater pollution; (3) coral mucus chemical
76 composition; (4) the structure of zooxanthelle communities; and (5) the relative
77 photosynthetic activity of zooxanthellae.
78 The leeward coast of the island of Curaçao, Netherlands Antilles, is an especially
79 conducive natural laboratory in which to study changes in coral microbes along gradients
80 of pollution and water depth (Fig. 2). The approximately 150,000 people living on
81 Curaçao are concentrated in the capital city of Willemstad, surrounding the natural harbor
82 of St. Annabaai. The large commercial and military harbor, and the urban center of
83 Willemstad are a major point source of pollutants such as nutrients, metals, hydrocarbons
84 and other toxic chemicals (Gast, 1998a, 1998b). Elevated nutrients associated with
85 sewage discharge, and groundwater seepage onto the reef could be measured up to 4 km
86 downcurrent from the harbor. In association with this eutrophication, bacterial
87 production was increased from 100-500 to about 1,200 ngC l^{-1} h^{-1} (Gast 1998a).
88 Furthermore, the island is surrounded by shallow fringing reefs up to 250 m from shore
89 where the seafloor slopes down from 8-10 m to 30-50 m water depth (Van Duyl, 1985).
90 This provides a consistent depth gradient to sample along the length of the island.
91 The current study advances our understanding of coral-associated microbial
92 communities by providing an evaluation of changes in coral tissue bacterial communities

across gradients in water depth and coastal pollution. Characterizing the variation in bacterial communities along these gradients has allowed us to determine the abundance and taxomomic significance of key phototrophic bacteria and provides evidence for disease-related microorganisms inhabiting healthy coral tissues. A statistical evaluation of the covariation between microbial communities and the basic ecological parameters of the coral microbial habitat provides insights into key factors controlling the coral microbiota.

Results

Variation in the local environment

Light intensity at the three reef sites (Jan Thiel, Water Plant, Playa Hundu; Fig. 2) varied between 33% and 36% surface PAR (photosynthetically active radiation) at 5 m, 18% and 22% at 10 m, and 9% and 11% at 20 m, with minimal differences between localities. Over the month of July, 2004 temperatures between 5 m and 20 m water depth were consistently 27.5 ± 0.5°C at all three localities.

Coral tissue $\delta^{15}N$ from 36 colonies of *M. annularis* ranged between 2.47‰ and 5.95‰, with average values approximately 1.75‰ higher at Jan Thiel and Water Plant compared to Playa Hundu (see Supplemental Information for values). This is supported by Kruskal-Wallis statistical tests indicating significant differences in $\delta^{15}N$ between reef localities (Chi-square = 21.743, d.f. = 2, p = 0.000). These trends in $\delta^{15}N$ suggest greater uptake of sewage-derived compounds by corals adjacent to the population center of Willemstad and are generally consistent with previous analyses on the island of Curaçao (Klaus et al., 2005) as well as in the Indo-Pacific (Heikoop et al., 2000b). No significant differences in coral tissue $\delta^{15}N$ were detected between different water depths (Chi-square = 0.379, d.f. = 2, p = 0.827).

Variation in zooxanthelle photosynthesis ($\delta^{13}C$)

Coral tissue $\delta^{13}C$ for the 36 samples ranged between -13.48‰ and -16.63‰, with average values becoming approximately 1.0‰ lighter from 5 m to 20 m water depth (see Supplemental Information for values). This trend is supported by Kruskal-Wallis statistical tests indicating significant differences in $\delta^{13}C$ between corals sampled at each

123 seawater depth (Chi-square = 6.615, d.f. = 2, p = 0.037), and is consistent with previous
124 reports of reduced photosynthetic activity of zooxanthellae under lower light conditions
125 (Heikoop et al., 2000b; Swart et al., 2005). Although less pronounced, significant
126 differences were also detected between localities (Chi-square = 7.552, d.f. = 2, p =
127 0.023). On average, values of $\delta^{13}C$ are 0.5‰ lighter at Jan Thiel compared to Water
128 Plant and Playa Hundu.
129
130 *Variation in coral mucus composition*
131 Analyses of coral mucus included amino acid composition and monosaccharide
132 composition for all 36 colonies of *M. annularis* collected. In general, the dominant
133 monosaccharides detected were fucose (34%), *N*-acetylglucosamine (31%), and
134 glucosamine (11%), while serine (18%), aspartic acid (11%), glutamic acid (11%), and
135 threonine (10%) were the dominant amino acids (see Supplemental Information for
136 values). ANOSIM statistical tests based on a sample similarity matrix of Euclidean
137 distances revealed no significant differences in amino acid or monosaccharide
138 composition due to water depth (Global R = -0.001, p = 0.49) or locality (Global R =
139 0.044, p = 0.094).
140
141 *Variation in zooxanthellae communities*
142 Current taxonomy of the symbiotic algal genus *Symbiodinium* is subdivided into
143 seven clades labeled A-G (Baker, 2003). Based on RFLP analyses of clones obtained
144 from 5 m (n = 74), 10 m (n = 75) and 20 m (n = 90), 10 unique ribotypes of
145 *Symbiodinium* were identified. Phylogentic analysis of multiple sequenced clones from

each ribotype revealed that all clones belonged to either clade B or C. Sequences from the colony sampled at 5 m were affiliated primarily with clade B, while sequences from 10 m and 20 m were affiliated with clade C. TRFLP profiles of the 28S rRNA gene of *Symbiodinium* digested with the *Cfo*I enzyme were used to characterize differences in *Symbiodinium* communities for all 36 *M. annularis* colonies. Ordination of these TRFLP profiles shows distinct differences in *Symbiodinium* communites from 5 m versus those at 10 m and 20 m (Fig. 3a). This is further supported by the ANOSIM statistical test for differences between depths (5 m vs. 10 m $r = 0.535$, $p = 0.001$; 5 m vs. 20 m $r = 0.784$, $p = 0.001$; 10 m vs. 20 m $r = 0.058$, $p = 0.074$). The TRF peaks most important in distinguishing the communities at different water depths include *Cfo*I-137, *Cfo*I-458, and *Cfo*I-510. The relative abundance of these peaks within the 36 colonies is illustrated in Figure 3b-d. By comparing TRF peak sizes to theoretical enzyme digests of sequenced clones from the current study as well as downloaded sequences from GenBank, it was determined that *Cfo*I-137 belongs to clade B and dominates in shallow water, while *Cfo*I-458 and *Cfo*I-510 belong to clade C and are more common at 10 m and 20 m. The TRF peak *Cfo*I-149 associated with *Symbiodinium* clade A was also detected and found to be more common in shallow water samples. No significant differences were detected between *Symbiodinium* communities sampled at the same depth from different localities.

Variation in bacterial communities

Bacterial 16S rRNA clone libraries derived from colonies of *M. annularis* sampled at 5 m (PH-5m), 10 m (PH-10m), and 20 m (PH-20m) are affiliated with different assemblages of bacteria (Fig. 4). The clone library constructed from colony PH-5m was dominated by sequences of a unique bacterium (54%) that appears to be a new bacterial

division; CAB-I. Phylogenetic analyses that include numerous reference bacteria suggest an association between CAB-I and Cyanobacteria (Fig. 5a). However, additional analyses including a representative collection of Cyanobacteria and plastid sequences show CAB-I to be distinct from and thus outside this division (Fig. 5b). In addition to CAB-I, the clone library of PH-5m also contained a large percentage of γ-proteobacteria (13%), bacteroidetes (13%), and α-proteobacteria (12%). The clone library from the 10 m colony (PH-10m) contained fewer sequences of CAB-I (28%) and a greater percentage of α-proteobacteria (26%) and bacteroidetes (28%). The colony sampled at 20 m (PH-20m) generated no sequences of CAB-I and contained a larger percentage of plastid sequences (18%). In general, sequences from the 20 m sample were more evenly distributed. Bacterial sequences were found in roughly equal percentages of γ-proteobacteria (18%), α-proteobacteria (17%), and planctomycetes (16%). Overall, clones of CAB-I exhibited decreasing abundance with increasing water depth, and clones of plastids, Cyanobacteria and Firmicutes increasing abundance with increasing water depth. Because sequencing was performed on only one colony from each depth, these trends were evaluated by comparing theoretical enzyme digests of sequenced clone libraries (see Supplemental Information) with TRFLP profiles from the 36 sampled colonies of *M. annularis*.

A combined total of 421 TRFs (169 *Cfo*I, 147 *Msp*I, 105 *Rsa*I) were identified from the 36 samples analyzed in the present study. On average 27 *Cfo*I, 23 *Msp*I and 13 *Rsa*I peaks were detected for each sample. Of the 421 peaks identified, 111 were detected in only a single sample.

The ANOSIM test for differences in samples collected at 5 m, 10 m, and 20 m suggests distinct variation in TRF composition based on the water depth from which the coral colony was collected (Global $R = 0.102$, $p < 0.011$). In the NMDS ordination of all 36 samples, a distinct gradation is observed from samples collected at 5 m to samples collected at 20 m (Fig. 6a). While no distinct differences were detected between 5 m and 10

196 m (r = 0.011, p = 0.316), or 10 m and 20 m (r = 0.066, p = 0.105), the samples from 5 m
197 and 20 m were significantly different (r = 0.248, p = 0.002). SIMPER analysis (Table 1)
198 reveals the major TRFs responsible for the differences in the microbial communities at 5 m
199 and 20 m. TRFs displayed increased abundances at either 5 m or 20 m water depth (Fig.
200 6b-d).

201 Two of the most abundant TRFs from the SIMPER analysis, *Msp*I-149 and *Rsa*I-
202 228, are affiliated with the black band disease (BBD) cyanobacterium clone CD1C11
203 (reported in (Frias-Lopez et al., 2003; Frias-Lopez et al., 2004). These TRFs make up as
204 much as 58% of the TRFLP fingerprint based on peak height. Furthermore, Mann-
205 Whitney U tests confirm that both *Msp*I-149 (Z = -2.320, p = 0.020) and *Rsa*I-228 (Z = -
206 1.987, p = 0.001) are more common in 5 m samples than 20 m samples. This is illustrated
207 by the relative abundance of TRF *Rsa*I-228 (Fig. 6c). The expected *Cfo*I TRF for CD1C11
208 of 670 bp was observed, however this cut site was also found to be common to other
209 sequences of Cyanobacteria.

210 Four additional TRFs were identified to test the seawater depth distribution of
211 Cyanobacteria (*Cfo*I-226, *Cfo*I-670, *Msp*I-158, and *Msp*I-491). Mann-Whitney U tests
212 show all four Cyanobacterial TRFs to be more common in samples from 5 m than 20 m
213 (*Cfo*I-226 Z = -2.321, p = 0.020; *Cfo*I-670 Z = -1.909, p = 0.056; *Msp*I-161, Z = -3.208, p
214 = 0.001; *Msp*I-491 Z = -3.126, p = 0.002). Two TRFs were also identified to test the depth
215 distribution of plastids, *Cfo*I-212 and *Msp*I-504. Neither TRF showed statistically
216 significant differences in their occurrences (*Cfo*I-212 Z = -0.751, p = 0.478; *Msp*I-504, Z =
217 -0.752 p = 0.478).

218 Three TRFs were identified to test the depth trend of CAB-I observed in the clone
219 libraries (*Cfo*I-167, *Msp*I-507, and *Rsa*I-606). Mann-Whitney U tests comparing
220 occurrences between 5 and 20 m show that TRFs *Cfo*I-167 (Z = -3.209, p = 0.001) and
221 *Msp*I-507 (Z = -3.868, p = 0.000) are more common at 5 m than 20 m, whereas no

222 difference in the depth distribution of *Rsa*I-606 (Z = -1.294, p = 0.196) was detected. Other
223 bacterial sequences likely share the *Rsa*I-606 terminal fragment.
224 The 16S rRNA gene clone libraries showed increased occurrences of sequences
225 affiliated with Firmicutes and Planctomycetes at greater seawater depths. Although only
226 one unique sequence of Firmicute was detected, TRF *Msp*I-153 was statistically more
227 abundant at 20 m (Z = -2.439, p = 0.015), while no significant differences were detected in
228 the distribution of the other two TRFs (*Cfo*I-236 Z = -0.482, p = 0.630; *Rsa*I-486 Z = 1.00,
229 p = 1.00). While several TRFs affiliated with the planctomycetacia were identified, the only
230 TRF present in enough samples to warrant statistical evaluation, *Rsa*I-131, showed no
231 significant difference in abundance between 5 m and 20 m water depth (Z = -0.839, p =
232 0.402).
233 The ANOSIM procedure was also used to test for significant differences in TRF
234 composition at the different reef localities. Significant differences between localities were
235 found for the 5 m samples (Global R = 0.324, p = 0.007) while no differences were
236 detected at 10 m (Global R = 0.125, p = 0.154) or 20 m (Global R = 0.125, p = 0.150).
237 While the 5 m replicate samples from Playa Hundu and Jan Thiel were fairly similar, the
238 samples from Water Plant had very low similarity among replicate samples and could not be
239 characterized by a specific microbial consortium.

240

241 *Canonical correspondence analysis*

242 Canonical correspondence analysis (CCA) was used to assess the relative
243 similarity of coral colonies as a function of both bacterial TRFLP data and environmental
244 and physiologic explanatory variables. These include: (1) light intensity (PAR), (2) coral
245 tissue $\delta^{15}N$, (3) coral tissue $\delta^{13}C$, (4-5) the relative abundance of zooxanthellae TRFs
246 (Zoox-1, Zoox-2; represented by the first two NMDS axes of Figure 3), and (6-7) the

247 combined amino acid and monosaccharide composition of coral mucus (muc-1, muc-2;
248 represented by the first two principle component axes (muc-1 = 26% of variance, muc-2
249 = 15% of variance). The cross-correlation between these seven explanatory variables is
250 shown in Table 2.

251 Axis 1 and 2 of the resulting CCA biplot (Fig. 7) account for 10.65% (6.17% on
252 axis 1 and 4.47% on axis 2) of the total variability in bacterial TRFLP profiles. Lines
253 pointing in the same direction depict positively correlated variables while lines at a 90°
254 angle depict uncorrelated variables. Distinct clustering of samples at each water depth
255 can be seen along axis 1. This axis is correlated to PAR, Zoox-1 and $\delta^{13}C$. Similarly, a
256 gradation can be seen along axis 2 separating samples from Playa Hundu from those of
257 Water Plant and Jan Thiel. Axis 2 is correlated to $\delta^{15}N$ and Zoox-2. Results of forward
258 selection and permutation tests indicate no additional variability in the bacterial TRFLP
259 data would be explained by variables in addition to PAR and $\delta^{15}N$. This does not mean
260 the other variables do not contribute to variation in bacterial communities, only that they
261 are less predictive. The variables PAR, $\delta^{13}C$, and Zoox-1 are partially correlated (Table
262 2), thus, their individual variations do not explain completely unique aspects of the data.

Discussion

Bacterial communities inhabiting M. annularis

One striking difference in the clone libraries from 5 m, 10 m, and 20 m was the relative abundance of 16S rRNA gene sequences affiliated with the candidate new division CAB-I (Fig. 4). While sequences affiliated with CAB-I have been reported in previous coral-associated clone libraries, (Frias-Lopez et al., 2002; Rohwer et al., 2002) they have not previously been reported at such high abundance, nor singled-out as an important part of the coral bacterial community. Furthermore, the greater abundance of CAB-I TRFs at shallow water depth, and the association with Cyanobacteria in phylogenetic analyses (Fig. 5a), suggests that these microorganisms are responsive to light and potentially phototrophic. Although further work is required, these lines of evidence imply that CAB-I is a deep-rooted sister division of the clade that now encompasses Cyanobacteria and plastids. While the relationship CAB-I and the coral is currently unknown, previous studies have shown endosymbiotic Cyanobacteria capable of fixing nitrogen to be symbiotic in the related coral, *Montastraea cavernosa* (Lesser et al. 2004).

The bacterial 16S rRNA clone libraries from 5 m, 10 m and 20 m exhibit striking qualitative differences in composition, and were utilized to evaluate the taxonomic identity of TRFs. The clone libraries suggest that Cyanobacteria and plastids increase in abundance at greater water depths. However, all TRFs from Cyanobacteria were more common in shallow water and none of the plastid TRFs showed any abundance trends with seawater depth. This discrepancy in the two techniques (clone libraries vs. TRFLP) is most likely due to the small number of clones sequenced from each clone library, or

286 the coral colonies chosen for sequencing not being characteristic of the more generalized
287 trends observed over the population. In addition to CAB-I and Cyanobacteria, the
288 abundance of several other TRFs varied with seawater depth (Table 1). TRFs affiliated
289 with α-proteobacteria, γ-proteobacteria and bacteroidetes exhibited either increasing or
290 decresing abundance. These variable distributions suggest that microbes within these
291 groups are ecologically partitioned along the seawater depth gradient. TRFs from these
292 phyla showed no consistent response to water depth, and are not typically thought to be
293 light-sensitive, thus, the trends in their distribution suggest either microhabitat changes
294 unaccounted for, or species-specific trophic interactions with other bacteria, viruses, or
295 protozoa (Torsvik et al., 2002).
296 Significant differences in the bacterial TRFLP data along the coastal pollution
297 gradient were found only at the shallowest water depth. This suggests that the shallow
298 near-shore reefs of Curaçao are being disproportionately impacted by anthropogenic
299 influences. Previous studies on Curaçao found significant differences in the bacterial
300 communities of *Diploria strigosa* at impacted sites, but no differences in the communities
301 of *M. annularis* (Klaus et al., 2005). These studies together suggest the influence of
302 anthropogenic pollutants will vary both temporally and between host coral species.
303 These patterns are similar to those observed in coral disease monitoring studies
304 (Bruckner, 2002). Patterns of disease occurrence vary seasonally, annually, over broad
305 geographic regions, and between coral species (Bruckner, 2002).
306
307 *Controls on bacterial community structure*

An additional aspect of the present study was assessment of the potential factors responsible for the observed variations in bacterial communities. Based on canonical correspondence analyses, 10.65% of the variation in TRFLP profiles was accounted for by changes in environmental and physiologic factors. Forward selection tests found that no additional information was gained by adding variables in addition to PAR and $\delta^{15}N$. Variation in PAR is primarily associated with changes in water depth, while variation in $\delta^{15}N$ is primarily associated with human pollution. While this suggests bacterial communities respond largely to the external environment versus factors more closely linked to coral physiology ($\delta^{13}C$, muc-1, muc-2, zoox-1, zoox-2), the correlation of zoox-1 and $\delta^{13}C$ to PAR makes it difficult to rule out independent effects from these variables.

Results of the CCA leave a large amount of the variation in bacterial TRFLP data unexplained (89%). While this is common for ecological communities, in particular microbes (Fahey et al., 2005), it suggests additional factors may be important in shaping bacterial community structure. A recent study of ascomycete fungal communities compared variation within versus between four different land systems. A correlation of fungal communities to landsystems was either not present, or extremely weak (Green et al. 2004). The authors concluded these communities respond at a much finer spatial scale than that used to define land systems. Similarly, it is possible that the explanatory variables used in the present study could be improved to provide a greater amount of ecologically meaningful information. For example, microsensors (O_2, pH, NO_x^-, H_2S) could be used to evaluate variation in the microenvironment of the coral surface microlayer. Furthermore, in the current study we used monosaccharide and amino acid composition as proxy variables to describe the variation in coral mucus. Overall, we

found little variation in the mucus composition of *M. annularis* at different depths and localities. These variables could be insufficient in capturing important variation in the nutritional or rheological properties of mucus associated with the actual carbohydrate, protein and lipid composition (Murty et al., 1987; Meikle et al., 1988). Lastly, assessment of the physiologic state of the coral and zooxanthellae could be improved by including protein or gene expression data in addition to $\delta^{13}C$ or other more direct measurements of photosynthetic activity.

Given that coral-associated bacterial communities are estimated to have as many as 6,000 unique ribotypes, (Rohwer et al., 2002) the weak correlation to explanatory variables is not that surprising. It is likely that much of the observed variation in these communities can be attributed to high spatial and temporal heterogeneity associated with the complex interactions of such a diverse community (Torsvik et al., 2002). It is also likely that a component of the variation in these communities is associated with inactive bacteria. By incubating corals with tracer amounts of Br-dUPT and comparing bacterial clone libraries generated with immunoprecipitated DNA and the total DNA, Rohwer and Kelley (2004) report that little overlap was found between growers and nongrowers (PTPtest; $P<0.0001$). Therefore, the explanatory power of variables used in the current study could likely have been improved by focusing solely on the actively growing community.

The current study focuses on intraspecies variation in bacterial communities and its correlation to environmental and physiologic factors. However, it should be noted that ecological factors with little utility in explaining intraspecies variation may be important in explaining the variation in microbial communities found between different coral

354 species. For example, the monosaccharide and amino acid composition of different coral
355 species can be markedly different (Ducklow, 1979b; Meikle et al., 1988). It is likely that
356 these more pronounced differences could be important in explaining the interspecies
357 variation in coral-associated bacterial communities documented by Rohwer et al. (2002).
358
359 *Implications for coral health*
360 Scleractinian corals maintain themselves through dynamic yet delicate
361 interactions with the surrounding seawater environment and multiple unique associations
362 with microorganisms (Knowlton and Rohwer, 2003). Temperature changes of ~2°C have
363 been shown to trigger bleaching events that span entire ocean basins (Berkelmans and
364 Oliver, 1999; Harvell et al., 2002). Furthermore, patterns of coral disease distribution
365 obtained from the global coral disease database indicate that 97% of all locations in the
366 Caribbean affected by coral diseases correspond to areas where human activities are
367 expected to have medium to high impacts (Green and Bruckner, 2000).
368 The variation we observed in bacterial communities associated with healthy
369 colonies of *M. annularis* highlights the sensitivity of the coral microbiota to
370 environmental change. As a result of this sensitivity, corals living under certain
371 environmental conditions may be preferentially at risk of disease. This is best
372 demonstrated by the abundance patterns obtained from TRFs of the BBD cyanobacterium
373 clone CD1C11. While BBD Cyanobacteria had been optically identified from dark
374 aggregates found on healthy coral tissues (Richardson, 1997), prior to the current study it
375 was not thought to be commonly associated with healthy coral tissues (Cooney et al.,
376 2002; Frias-Lopez et al., 2003; Frias-Lopez et al., 2004). We detected TRFs associated

377 with CD1C11 in 31 of the 36 samples analyzed, and found it to be most abundant at the
378 shallowest water depth. When present, CD1C11 comprised between 1% and 58% of the
379 coral microbiota based on TRF peak height. While the increased abundance of CD1C11
380 in shallow water is consistent with the increased incidence of BBD in shallow water
381 (Kuta and Richardson, 2002), it is not consistent with previous physiologic studies of
382 purported BBD Cyanobacteria (Richardson and Kuta, 2003). The threshold for
383 maximum photosynthetic rate (Pmax) in culture was obtained at very low light intensities
384 (27.9 $\mu E\ m^{-2}\ s^{-1}$; (Richardson and Kuta, 2003) leading the authors to conclude the
385 occurrence of BBD in shallow water was due to self-shading, a behavioral strategy by
386 which filamentous Cyanobacteria form clumps to minimize light exposure (Castenholz,
387 1982). However, given that subsequent phylogenetic studies have shown the strain used
388 in these studies to differ from the common BBD cyanobacterium CD1C11 (Frias-Lopez
389 et al., 2003; Frias-Lopez et al., 2004), we find it just as likely that the high incidence of
390 BBD in shallow water is directly related to the increased abundance of CD1C11 on
391 healthy coral colonies living in high light environments. Future culturing studies using
392 confirmed strains of CD1C11 are necessary to assess the ecological physiology of the
393 BBD Cyanobacteria. Regardless of the relationship between BBD Cyanobacteria and the
394 environment, TRFLP profiling is a powerful assay of the potential vulnerability of local
395 reefs to BBD outbreak.
396

Conclusions

The variation in microbial assemblages along environmental gradients provides valuable insights into the dynamic nature of microbial communities and the ecological factors that control their structure. This study shows how bacterial communities inhabiting coral tissues change in response to seawater depth and coastal pollution. Differences in bacterial communities sampled across a pollution gradient are found only at the shallowest water depth. This suggests the shallow near-shore reefs of Curaçao are disproportionately impacted by anthropogenic factors. Additionally, the analyses completed in this study indicate that bacterial communities associated with *M. annularis* vary systematically along a seawater depth gradient of 5 m, 10 m, and 20 m. The taxonomic identity of bacterial TRFs exhibiting variation with increasing seawater depth was determined by comparison with 16S rRNA clone libraries for bacteria.

Canonical correspondence analysis (CCA) including seven environmental and physiologic explanatory variables related to light intensity (PAR), seawater pollution ($\delta^{15}N$), coral mucus (Muc-1, Muc-2), and the diversity (Zoox-1, Zoox-2) and activity ($\delta^{13}C$) of zooxanthellae accounted for 11% of the variation in bacterial communities along the gradients of water depth and pollution. Forward selection tests indicated no additional variation was accounted for by adding variables in addition to PAR and $\delta^{15}N$.

Prior to the current study, the BBD Cyanobacterium CD1C11 was not thought to be commonly associated with healthy coral tissues. Here we report that 31 of the 36 sampled corals were positive for the BBD Cyanobacterium. Furthermore, we found CD1C11 to comprise as much as 58% of the healthy microbial community and to be more common in shallow water (5 m) compared to deeper water (20 m).

Finally, and unexpectedly, we report findings of a unique coral-associated bacterium, CAB-I. Preliminary studies indicate CAB-I to be phototrophic and a deep-rooted sister division to the clade that now encompasses Cyanobacteria and plastids. Additional studies of CAB-I are required to confirm its phototrophic nature, refine its taxonomic status, and assess its diversity and distribution.

Experimental procedures

Coral sampling

The current study is based on analyses of the Caribbean reef coral *Montastraea annularis*. We selected *M. annularis* because it is ecologically dominant, has a relatively large depth distribution (0-25 m), and is known to be susceptible to numerous coral diseases. In July 2004 tissue samples, coral mucus samples, and small colony fragments of *M. annularis* were collected from 36 colonies. Four replicate samples were collected at 5 m, 10 m, and 20 m, at three localities along the leeward coast of Curaçao (Fig. 2). Based on previous studies (Gast, 1998a, 1998b; Klaus et al., 2004) Water Plant, immediately adjacent to the seaport and urban center of Willemstad, was thought to be the most heavily polluted locality, and Playa Hundu, a remote locality approximately 32 kilometers downcurrent, was thought to be the most pristine.

Tissue samples for molecular analyses of bacteria and zooxanthellae were collected from the upper surface of the colony by removing a 2 cm by 2 cm portion of the uppermost 1 cm of the coral colony with a chisel and placing the sample in a sterile 50 ml polypropylene tube. Upon returning to shore the seawater within each tube was decanted and coral samples were then immersed in 80% ethanol and crushed, creating a slurry of coral tissue, zooxanthellae, mucus, microorganisms, and skeletal material.

Coral mucus samples were collected from small fragments of the same colonies sampled for molecular analyses. These fragments were placed in clean plastic bags and brought to shore where mucus was drawn from the coral surface into 50 ml polypropylene tubes and frozen at -40°C. After sampling coral mucus, the remaining

446 fragments were dried for three days at 35°C to preserve them for subsequent analyses of
447 coral tissue $\delta^{15}N$ and $\delta^{13}C$.
448
449 *Characteriztion of the reef environment*
450 Three variables were used to characterize environmental variation both along the
451 depth gradient and between the three reef localities sampled: (1) temperature; (2)
452 photosynthetically active radiation (PAR); and (3) the $\delta^{15}N$ of coral tissue. Measurements
453 of temperature and PAR were taken at each depth at each reef locality at noon on a
454 normal sunny day. Temperature was measured on a Genesis ReactPro dive computer
455 (Genesis Scuba, Clarence Center, NY) to an accuracy of ± 0.5°C. Measurements of PAR
456 were obtained using a LI-192 light sensor connected to the LI-1000 data logger (LI-COR
457 Biosciences, Lincoln, NE). PAR measurements typically have ± 5% uncertainty. Values
458 of PAR used in the present study represent averages of ten measurements.
459 The $\delta^{15}N$ of coral tissue (Heikoop et al., 1998; Heikoop et al., 2000a; Heikoop et
460 al., 2000b; Klaus et al., 2005) was used to determine the relative amount of sewage-
461 derived compounds being taken up by corals at each sampling site. To do this an area of
462 tissue approximately 25 cm^2 was removed from the upper growth surface of each colony
463 using a small microdrill. Samples were then decalcified using 1 N hydrochloric acid,
464 rinsed in distilled water, and dried using a Vacufuge Concentrator 5301 (Eppendorf,
465 Westbury, N.Y.). Thus, each sample is composed of a combination of host coral tissue
466 and zooxanthellae. Each sample (0.5 to 1.0 mg) was then analyzed in continuous flow
467 mode utilizing a Eurovector Elemental analyzer coupled to a Micromass Isoprime mass
468 spectrometer located in the Department of Earth and Environmental Science at Los

469 Alamos National Laboratory. Typical precision for $\delta^{15}N$ based on replicates of coral
470 tissue samples and in-house coral tissue standards was <0.21‰ (1σ). Values were
471 calibrated using in-house standards including deep-sea coral tissue (Heikoop et al., 2002)
472 that was originally analyzed in the laboratory of Zachary Sharp at the University of New
473 Mexico and calibrated against IAEA-N3 and USGS RSIL N11 potassium nitrate
474 standards.
475
476 *Characterization of zooxanthellae primary production*
477 The relative photosynthetic activity of zooxanthellae within each coral sample
478 was assessed using the $\delta^{13}C$ value of coral tissue. Values of $\delta^{13}C$ are useful for
479 determining the relative photosynthetic activity of corals sampled from different depths
480 and localities (Heikoop et al., 2000b; Swart et al., 2005). More negative values are
481 typically characteristic of reduced photosynthesis. Coral tissue $\delta^{13}C$ was analyzed in
482 tandem with coral tissue $\delta^{15}N$ (see above). Typical precision of $\delta^{13}C$ based on replicates
483 of coral tissue samples and in-house coral tissue standards is <0.2‰ (1σ).
484
485 *Characterization of coral mucus*
486 The monosaccharide and amino acid composition of healthy coral mucus in all 36
487 colonies of *M. annularis* was determined to assess the potential role of coral mucus
488 composition in structuring bacterial communities. Mucus samples were centrifuged at
489 15,000 g and the supernatant was dialyzed using Spectra Por6 1000 kDa dialysis
490 membranes (Fischer Scientific, Pittsburgh, PA) with 4 changes of 20 volumes cold (4°C)
491 demineralized water during 48 hours. The dialyzed mucus was concentrated by freeze-

492 drying. The lyophilized mucus was then transferred to 2ml screw-cap tubes, weighed and
493 then solubilized to a concentration of 3 – 15 mg/ml.
494 Monosaccharides were quantified after a two-step sulfuric acid hydrolysis
495 (Hoebler et al., 1989) using the Dionex DX500 HPLC system consisting of an AS3500
496 autosampler, GP 50 gradient pump, and ED 40 pulsed electrochemical detector equipped
497 with a gold working electrode, utilizing a CarboPac PA-1 column and guard, and a 50 µl
498 injection volume. The degassed mobile phase consisted of water, at 1 ml/min, with
499 postcolumn addition of 300 mM NaOH (0.5 ml/min) (Bourquin et al., 1990).
500 To quantify amino acids, 1-4 mg dialyzed mucus concentrate was transferred to 2
501 ml screw-thread glass vials with phenolic caps and PTFE/ silicone septa (National
502 Scientific Company, Duluth, GA). The samples were then freeze-dried and hydrolyzed in
503 0.5 ml of anoxic 6N HCl (Spitz, 1973). The samples were analyzed on a Model 126AA
504 amino acid analyzer with a 12 cm System 6300 Sodium Ion exchange column (Beckman
505 Coulter, Fullerton, CA). The amino acids were eluted from the column using sodium
506 citrate buffers (Beckman Coulter). After post-column derivatization with ninhydrin, the
507 absorbance was measured at 570 nm. The instrument was calibrated with a Beckman
508 Hydrolysate standard.
509
510 *Characterization of zooxanthellae and bacterial communities*
511 Communities of zooxanthellae (belonging to group *Symbiodinium)* and bacteria
512 associated with *M. annularis* were characterized using a combined approach of terminal
513 restriction fragment length polymorphism (TRFLP) and sequencing of clone libraries to
514 taxonomically identify terminal restriction fragments (TRFs). The UltraClean Soil DNA

515 Kit (Mo Bio, Solana Beach, CA) was used to extract genomic DNA from coral slurries.
516 To perform the extraction, 2 ml of sample was concentrated via centrifugation,
517 resuspended in 300 µl of MicroBead solution, and prepared as recommended by the
518 manufacturer.

519 Genes encoding for 16S rDNA in bacteria and 28S rDNA in *Symbiodinium* were
520 amplified by PCR using a Mastercycler gradient thermocycler (Eppendorf). Primers used
521 in the PCR amplifications of bacteria were U9F (5'-GAGTTTGATYMTGGCTC) and
522 U1509R (5'-GYTACCTTGTTACGACTT) (Integrated DNA Technologies, Coralville,
523 IA). Primers used in the PCR amplifications of the *Symbiodinium* were lsu-UFP1 (5'-
524 CCCGCTAATTTAAGCATATAAGTA), and lsu-URP1 (5'-
525 GTTAGACTCCTTGGTCGTGTTTCA) (Zardoya et al., 1995; van Oppen et al., 2001).
526 PCR was performed using a reaction mixture of 0.2 mM of each deoxynucleoside
527 triphosphate (Promega, Madison, WI), 200 ng each of the forward and reverse primers,
528 0.5 to 10 µl of the sample preparation, 1X Taq Master, 1X Taq Buffer (50mM KCl,
529 10mM Tris-HCl pH 8.3, 1.5 mM $Mg(OAc)_2$) and water to bring the total volume to 50 µl.
530 The PCR profile was: one cycle of 4 min at 94°C, 35 cycles of 30 sec at 94°C, 30 sec at
531 55°C (60°C for lsu-UFP1 and lsu-URP1) and 90 sec at 72°C, followed by 5 min at 72°C.
532 Optimization of PCR was performed for each sample by adjusting the amount of genomic
533 DNA extract used to obtain a strong band on an agarose gel, without visible nonspecific
534 product (Blackwood et al., 2003).

535 Bacterial and *Symbiodinium* clone libraries were constructed for one coral colony
536 at 5 m, 10 m, and 20 m from Playa Hundu. Gel-purified PCR product was cloned into
537 pGEM-T (Promega) and transformed into calcium chloride competent DH5αMCR *E. coli*

538 (Sambrook et al., 1989). Clones were screened for the presence of the insert and forward
539 orientation by PCR using plasmid primer T7 and U1509R or lsu-URP1. *Symbiodinium*
540 clone libraries were additionally screened by RFLP using *Cfo*I and *Msp*I to maximize the
541 number of unique clones for sequencing. Complete, forward oriented clones were
542 patched into 2 ml 96-well plates filled with Luria broth and 100 μg/ml ampicillin (Roche
543 Molecular Biochemicals, Indianapolis, IN) and incubated overnight at 37°C.
544 Sequencing was performed in the High Throughput Laboratory of the University
545 of Illinois W. M. Keck Center for Comparative and Functional Genomics. The 96-well
546 culture plates were used to inoculate 2 ml 96-well culture plates containing Circle Grow
547 media (Bio100) supplemented with ampicillin. Plasmid template DNA was purified from
548 the cultures using an automated system and the QIAwell 96 Turbo prep BioRobot Kit
549 (Qiagen, Valencia, CA). Sequencing was performed using the T7 plasmid primer.
550 Plasmid templates were prepped on a Qiagen Bio Robot 9600, and Big Dye Terminator
551 chemistry (v.2.0) (Applied Biosystems, Foster City, CA) was used for sequencing
552 reactions. Sequencing was performed on a 3730XL capillary sequencer (Applied
553 Biosystems).
554 For TRFLP analysis primers Univ 9F and lsu-UFP1 were both labeled at the 5'
555 end with phosphoramidite fluorochrome 6-carboxyfluorescein (6-FAM). Pooled PCR
556 replicates were purified using the Wizard PCR prep kit (Promega, Madison, WI).
557 Restriction digests were then performed independently using three tetrameric enzymes
558 (*Cfo*I, *Msp*I, and *Rsa*I). For each digest eight microliters of purified PCR product was
559 digested with 10 U of restriction enzyme in a total volume of 20 μl. Incubation was done
560 at 37°C for 9 hr followed by 15 min at 65°C to denature the restriction enzyme.

561 The precise lengths of TRFLP fragments were determined by multicapillary
562 electrophoresis with a model 3730xl capillary sequencer (Applied Biosystems). 1 µl of
563 the digested DNA was mixed with 10 µl of Hi-Di formamide solution (Applied
564 Biosystems), and 0.15 µl MapMarker1000 ROX-labeled sizing standard (Bioventures,
565 Muffreesboro, TN). The mixture was separated in fragment analysis mode with the
566 following run parameters: prerun voltage, 15.0 kV; prerun time, 180 sec; injection
567 voltage, 1.5kV; injection time, 15 sec; run voltage, 15.0 kV; run temperature, 63°C; run
568 time, 3000 sec. The linear polymer matrix consisted of the performance-optimized
569 polymer type 7 (Applied Biosystems). The lengths of the fragments were determined
570 using the Local Southern size-calling algorithm of the Genemapper Analysis Software
571 Version 3.7 (Applied Biosystems). To assure accuracy within one base pair a correction
572 factor based on a 6-Fam labeled sizing ladder was subsequently applied.
573 Sample versus TRFLP peak data matrices were constructed using peaks above a
574 threshold of 50 units above background. To avoid detection of primers and uncertainties
575 associated with fragment size determination, peaks smaller than 50 base pairs (bp) and
576 larger than 1050 bp were culled from the data set. Aligned peaks were placed into bins
577 typically less than two base pairs. Abundance data were obtained from the relative peak
578 height following sample standardization (Blackwood et al., 2003). The taxonomic
579 identity of TRFs were assessed by comparison with theoretical digests of 16S rRNA gene
580 sequences from the present study as well as over 900 coral-associated bacterial sequences
581 obtained from previous studies (Frias-Lopez et al., 2002; Frias-Lopez et al., 2003; Frias-
582 Lopez et al., 2004).
583

584 *Sequence and phylogentic analyses*

585 Sequences were classified through an iterative process of: (1) comparison with the
586 GenBank database using the Basic Local Allignment Search Tool (BLAST) (Altschul et
587 al., 1990); (2) comparison using the sequence match tool of the Ribosomal Database
588 Project II website, (Cole et al., 2005); and (3) phylogenetic analyses with numerous
589 reference sequences. Sequences were aligned using the Clustal X program, and
590 phylogentic analysis and trees were obtained using the program PAUP* version 4.0b10
591 (Swofford, 2002).

592

593 *Nucleotide sequence accession numbers*

594 The sequences of the partial gene fragments were deposited in GenBank under
595 accession numbers DQ200400 through DQ200711.

596

597 *Ordinations of TRFLP data*

598 To assess the variation in zooxanthellae and bacterial communities, sample
599 similarity matrices were independently constructed based on: (1) *Symbiodinium* TRFLP
600 profiles; and (2) bacterial TRFLP profiles. Similarity values were obtained using the
601 Bray-Curtis dissimilarity coefficient (Bray and Curtis, 1957) following a square-root
602 transformation.

603 Ordination by non-metric multidimensional scaling (NMDS) (Kruskal, 1964) was
604 used to visually examine differences among samples. Each ordination was run with 60
605 random starting configurations and proceeded through multiple iterations until the fit of a
606 non-parametric regression of d (distances between samples on the NMDS plot) against δ

(Bray-Curtis dissimilarities or Euclidean distances) could not be improved. To test the significance of differences due to seawater depth or reef site, similarity matrices were subjected to the analysis of similarities procedure (ANOSIM) (Clarke and Warwick, 2001). This analysis is based on a non-parametric permutation procedure applied to the rank similarity matrix. If samples within a group are identical, then Global R = 1. Similarity percentages (SIMPER) (Clarke and Warwick, 2001) were used to determine TRF peak contributions to the average dissimilarity of samples between different sample groups. NMDS ordinations and statistical tests were performed using PRIMER 5 v. 5.2.9 (PRIMER-E, Plymouth, UK) and SPSS 10.0 (SPSS Inc., Chicago, IL).

Covariation in bacteria, the environment, and coral physiology

Cannonical correspondence analysis (CCA) was used to determine which environmental and physiologic factors were most important in explaining the observed variation in the coral microbiota. In CCA analyses each canonical ordination axis corresponds to a direction in the multivariate scatter of TRFLP data which is maximally related to a weighted linear combination of the explanatory variables (Legendre and Legendre, 1998). Analyses were performed using Brodgar v.2 (Highland Statistics LTD, Aberdeenshire, UK).

Acknowledgements - This work was supported by a research grant from the Office of naval Research (N00014-00-1-0609), and a UIUC Department of Geology Wanless Fellowship awarded to JSK. We acknowledge the support of CARMABI in our field

629 efforts. We also thank Al Piggot for assistance in the lab, Toti Larson and Marcey Hess
630 for running isotopic analyses, and Laura Bauer for running monosaccharide analyses.
631

631 **References**

632 Altschul, S.F., Gish, W., Miller, W., Meyers, E.W., and Lipman, D.J. (1990) Basic local
633 alignment search tool. *J Mol Biol* **59**: 143-169.

634 Baker, A.C. (2003) Flexibility and specificity in coral-algal symbiosis: diversity, ecology,
635 and biogeography of *Symbiodinium*. *Annu Rev Ecol Syst* **34**: 661-689.

636 Berkelmans, R., and Oliver, J.K. (1999) Large-scale bleaching of corals on the Great
637 Barrier Reef. *Coral Reefs* **18**: 55-60.

638 Blackwood, C.B., Marsh, T., Sang-Hoon, K., and Paul, E.A. (2003) Terminal restriction
639 fragment length polymorphism data analysis for quantitative comparison of
640 microbial communities. *Appl Environ Microbiol* **69**: 926-932.

641 Bourne, D., and Munn, C. (2005) Diversity of bacteria associated with the coral
642 *Pocillopora damicornis* from the Great Barrier Reef. *Environ Micriobiol* **7**: 1162-
643 1174.

644 Bourquin, L.D., Garleb, K.A., Merchen, N.R., and Fahey, G.C.J. (1990) Effects of intake
645 and forage level on site and extent of digestion of plant cell wall monomeric
646 components by sheep. *J Anim Sci* **68**: 2479-2495.

647 Bray, J.R., and Curtis, J.T. (1957) An ordination of the upland forest communities of
648 southern Wisconsin. *Ecol Monogr* **34**: 77-87.

649 Bruckner, A.W. (2002) Priorities for effective management of coral diseases. In *NOAA*
650 *Technical Memorandum NMFS-OPR-22*: U.S. Department of Commerce, p. 54.

651 Bruckner, A.W., Bruckner, R.J., and Williams, E.H., Jr. (1997) Spread of black-band
652 disease epizootic through the coral reef system in St. Ann's Bay, Jamaica. *B Mar*
653 *Sci* **61**: 919-928.

654 Bythell, J.C., Barer, M.R., Cooney, R.P., Guest, J.R., O'Donnell, A.G., Pantos, O., and Le
655 Tissier, M.D. (2002) Histopathological methods for the investigation of microbial
656 communities associated with disease lesions in reef corals. *Lett Appl Microbiol*
657 **34**: 359-364.
658 Castenholz, R.W. (1982) Motility and taxes. In *The Biology of Cyanobacteria*. Carr, N.G.
659 (ed). Berkeley: University of California Press, pp. 413-440.
660 Cervino, J.M., Hayes, R.L., Polson, S.W., Polson, S.C., Goreau, T.J., Martinez, R.J., and
661 Smith, G.W. (2004) Relationship of *Vibrio* species infection and elevated
662 temperatures to yellow blotch/band disease in Caribbean corals. *Appl Environ*
663 *Microbiol* **70**: 6855-6864.
664 Clarke, K.R., and Warwick, R.M. (2001) *Change In Marine Communities: An Approach*
665 *To Statistical Analysis And Interpretation*. Plymouth: Primer-E Ltd.
666 Cole, J.R., Chai, B., Farris, R.J., Wang, Q., Kulam, S.A., McGarrell, D.M. et al. (2005)
667 The Ribosomal Database Project (RDP-II): sequences and tools for high-
668 throughput rRNA analysis. *Nucleic Acids Res* **33**: D294-D296.
669 Cooney, R.P., Pantos, O., Le Tissier, M.D., Barer, M.R., O'Donnell, A.G., and Bythell,
670 J.C. (2002) Characterization of the bacterial consortium associated with black
671 band disease in coral using molecular microbiological techniques. *Environ*
672 *Micriobiol* **4**: 401-413.
673 Dubinsky, Z. (ed) (1990) *Coral Reefs*. Amsterdam, The Netherlands: Elsevier Science
674 B.V.
675 Ducklow, H.W., Mitchell, R. (1979a) Bacterial populations and adaptations in the mucus
676 layers on living corals. *Limnol Oceanogr* **24**: 715-725.

677 Ducklow, H.W., Mitchell, R. (1979b) Composition of mucus released by coral reef
678 coelenterates. *Limnol Oceanogr* **24**: 706-714.
679 Fahey, A., Lethbridge, G., Earle, R., Ball, A.S., Timmis, K.N., and Mcgenity, T.J. (2005)
680 Effects of long-term benzene pollution on bacterial diversity and community
681 structure in ground water. *Environ Micriobiol* **7**: 1192-1199.
682 Ferrier-Pages, C., Leclercq, N., Jaubert, J., Pelegri, S.P. (2000) Enhancement of pico- and
683 nanoplankton growth by coral exudates. *Aquat Microb Ecol* **21**: 203-209.
684 Frias-Lopez, J., Zerkle, A.L., Bonheyo, G.T., and Fouke, B.W. (2002) Partitioning of
685 bacterial communities between seawater and healthy, black band diseased, and
686 dead coral surfaces. *Appl Environ Microbiol* **68**: 2214-2228.
687 Frias-Lopez, J., Bonheyo, G.T., Jin, Q., and Fouke, B.W. (2003) Cyanobacteria
688 associated with coral black band disease in Caribbean and Indo-Pacific reefs. *Appl*
689 *Environ Microbiol* **69**: 2409-2413.
690 Frias-Lopez, J., Klaus, J.S., Bonheyo, G.T., and Fouke, B.W. (2004) Bacterial
691 community that causes black band disease in corals. *Appl Environ Microbiol* **70**:
692 5955-5962.
693 Gast, G.J. (1998a) Microbial densities and dynamics in fringing coral reef waters. PhD
694 Thesis, University of Amsterdam.
695 Gast, G.J. (1998b) Nutrient Pollution in Coral Reef Waters. In *Reef Care Curacao*
696 *Workshop on Nutrient Pollution.* Curacao, Netherlands Antilles, p. 13.
697 Gil-Agudelo, D.L., and Garzon-Ferreira, J. (2001) Spatial and seasonal variation of dark
698 spots disease in coral communities of the Santa Marta area (Columbia Caribbean).
699 *B Mar Sci* **69**: 619-629.

700 Green, E.P., and Bruckner, A.W. (2000) The significance of coral disease epizootiology
701 for coral reef conservation. *Biol Conserv* **96**: 347-361.
702 Harvell, C.D., Mitchell, C.E., War, J.R., Altizer, S., Dobson, A.P., Ostfeld, R.S., and
703 Samuel, M.D. (2002) Climate warming and disease risks for terrestrial and marine
704 biota. *Science* **296**: 2158-2162.
705 Heikoop, J.M., Dunn, J.J., Risk, M.J., Sandeman, I.M., Schwarcz, H.P., and Waltho, N.
706 (1998) Relationship between light and the $\delta^{15}N$ of coal tissue: Examples from
707 Jamaica and Zanzibar. *Limnol Oceanogr* **43**: 909-920.
708 Heikoop, J.M., Risk, M.J., Hickmott, D.D., Shearer, C.K., Beukens, R., and Atudorei, V.
709 (2002) Potential climate signals from the deep-sea gorgonian coral *Primnoa*
710 *resedaeformis*. *Hydrobiologia* **471**: 117-124.
711 Heikoop, J.M., Dunn, J.J., Risk, M.J., Tomascik, T., Schwarcz, H.P., Sandeman, I.M.,
712 and Sammarco, P.W. (2000a) $\delta^{15}N$ and $\delta^{13}C$ of coral tissue show significant inter-
713 reef variation. *Coral Reefs* **19**: 189-193.
714 Heikoop, J.M., Risk, M.J., Lazier, A.V., Edinger, E.N., Jompa, J., Limmon, G.V. et al.
715 (2000b) Nitrogen-15 signals of anthropogenic Nutrient loading in reef corals. *Mar*
716 *Pollut Bull* **40**: 628-636.
717 Hoebler, C., Barry, J.L., David, A., and Delort-Laval, J. (1989) Rapid acid hydrolysis of
718 plant cell wall polysaccharides and simplified quantitative determination of their
719 neutral monosaccharides by gas-liquid chromatography. *J Agr Food Chem* **37**:
720 360-367.
721 Ikeda, Y., and Miyachi, S. (1995) Carbon dioxide fixation by photosynthesis and
722 calcification for a solitary coral, *Fungia sp*. *Bull Inst Oceanogr* **14**: 61-67.

723 Kaczmarsky, L.T., Draud, M., and Williams, E.H. (2005) Is there a relationship between
724 proximity to sewage effluent and the prevalence of coral disease? *Caribbean*
725 *Journal of Science* **41**: 124-137.
726 Kim, K., and Harvell, C. (2002) *Aspergillosis Of Sea Fan Corals: Dynamics In The*
727 *Florida Keys*. Boca Raton: CRCPress.
728 Klaus, J.S., Frias-Lopez, J., Bonheyo, G.T., Heikoop, J.M., and Fouke, B.W. (2005)
729 Bacterial communities inhabiting the healthy tissues of two Caribbean reef corals:
730 interspecific and spatial variation. *Coral Reefs* **24**: 129-137.
731 Knowlton, N., and Rohwer, F. (2003) Multispecies microbial mutualisms on coral reefs:
732 the host as a habitat. *Am Nat* **162**: 51-62.
733 Koh, E.G.L. (1997) Do scleractinian corals engage in chemical warfare against microbes?
734 *J Chem Ecol* **22**: 379-398.
735 Kruskal, J.B. (1964) Multidimensional scaling by optimizing goodness of fit to a
736 nonmetric hypothesis. *Psychometrika* **29**: 1-27.
737 Kuta, K., and Richardson, L. (2002) Ecological aspects of black band disease of corals:
738 relationships between disease incidence and environmental factors. *Coral Reefs*
739 **21**: 393-398.
740 Legendre, P., and Legendre, L. (1998) *Numerical Ecology*. Amsterdam, The Netherlands:
741 Elsevier.
742 Lesser MP, Mazel CH, Gorbunov MY, Falkowski PG (2004) Discovery of symbiotic
743 nitrogen-fixing cyanobacteria in corals. Science 305: 997-1000
744 Meikle, P., Richards, G.N., and Yellowlees, D. (1988) Structural investigation on the
745 mucus from six species of coral. *Mar Biol* **99**: 187-193.

746 Murty, V.L.N., Sarosiek, J., Slomiany, A., and Slomiany, B.L. (1987) Effect of lipids and
747 proteins on the viscosity of gastric mucus glycoprotein. *Biochem Bioph Res Co*
748 **121**: 521-529.
749 Patterson, K.L., Porter, J.W., Ritchie, K.B., Polson, S.W., Mueller, E., Peters, E.C. et al.
750 (2002) The etiology of white pox, a lethal disease of the Caribbean elkhorn coral,
751 *Acropora palmata*. *P Natl Acad Sci U S A* **99**: 8725-8730.
752 Richardson, L.L. (1997) Occurence of the black band disease cyanobacterium on healthy
753 corals of the Florida Keys. *B Mar Sci* **61**: 485-490.
754 Richardson, L.L., and Kuta, K.G. (2003) Ecological physiology of the black band disease
755 cyanobacterium *Phormidium corallyticum*. *FEMS Microbiol Eco* **43**: 287-298.
756 Riley, M., and Gordon, D. (1999) The ecological role ob bacteriocins in bacterial
757 competition. *Trends Microbiol* **7**: 129-133.
758 Riley, M., Goldstone, C., Wertz, J., and Gordon, D. (2003) A phylogenetic approach to
759 assessing the targets of microbial warfare. *J Evolution Biol* **16**: 690-697.
760 Ritchie, K.B., and Smith, G.W. (1997) Physiological comparisons of bacterial
761 communities from various species of scleractinian corals. *Proc 8th Int Coral Reef*
762 *Symp* **1**: 521-526.
763 Ritchie, K.B., and Smith, G.W. (2004) Microbial communities of coral surface
764 mucopolysaccharide layers. In *Coral Health and Disease*. Rosenberg, E., and
765 Loya, Y. (eds). Berlin: Springer-Verlag, pp. 259-264.
766 Rohwer, F., and Kelley, S. (2004) Culture-independent analyses of coral-associated
767 microbes. In *Coral Health and Disease*. Rosenberg, E., and Loya, Y. (eds).
768 Berlin: Springer-Verlag, pp. 265-277.

769 Rohwer, F., Segritan, V., Azam, F., and Knowlton, N. (2002) Diversity and distribution
770 of coral-associated bacteria. *Mar Ecol-Prog Ser* **243**: 1-10.
771 Rohwer, F., Breitbart, M., Jara, J., Azam, F., and Knowlton, N. (2001) Diversity of
772 bacteria associated with the Caribbean coral *Montastraea franksi*. *Coral Reefs* **20**:
773 85-91.
774 Rosenberg, E., and Falkovitz, L. (2004) The *Vibrio shiloi/Oculina patagonica* model
775 system of coral bleaching. *Annu Rev Microbiol* **58**: 143-159.
776 Salyers, A.A., and Whitt, D.D. (1994) *Bacterial Pathogenesis A Molecular Approach*.
777 Washington D.C.: ASM Press.
778 Sambrook, J., Fritsch, E.F., and Maniatis, T. (1989) *Molecular Cloning: A Laboratory*
779 *Manual*. Cold Spring Harbor, N.Y.: Cold Spring Harbor Laboratory Press.
780 Spitz, H.D. (1973) A new approach for sample preparation of protein hydrolyzates for
781 amino acid analysis. *Anal Biochem* **56**: 66-73.
782 Swart, P., Saied, A., and Lamb, K. (2005) Temporal and spatial variation in the $\delta^{15}N$ and
783 $\delta^{13}C$ of coral tissue and zooxanthellae in *Montastraea faveolata* collected from the
784 Florida reef tract. *Limnol Oceanogr* **50**: 1049-1058.
785 Swofford, D.L. (2002) *PAUP*: Phylogenetic Analysis Using Parsimony (And Other*
786 *Methods), version 4*. Sunderland, Mass: Sinauer Associates.
787 Torsvik, V., Ovreas, L., and Thingstad, T.F. (2002) Prokaryotic diversity-magnitude,
788 dynamics, and controlling factors. *Science* **296**: 1064-1066.
789 Van Duyl, F.C. (1985) Atlas of the living reefs of Curacao and Bonaire (Netherlands
790 Antilles). In: Foundation for Scientific Research in Surinam and the Netherlands
791 Antilles, Utrecht.

van Oppen, M.J.H., Palstra, F.P., Piquet, A.M.-T., and Miller, D.J. (2001) Patterns of coral-dinoflagellate associations in *Acropora*: significance of local availability and physiology of *Symbiodinium* strains and host-symbiont selectivity. *P Roy Soc Lond B Bio* **268**: 1759-1767.

Wild, C., Rasheed, M., Werner, U., Franke, U., Johnstone, R., and Huettel, M. (2004) Degradation and mineralization of coral mucus in reef environments. *Mar Ecol-Prog Ser* **267**: 159-171.

Zardoya, R., Costas, E., Lopez-Rodas, V., Garrido-Pertierra, A., and Bautista, J.M. (1995) Revised dinoflagellate phylogeny inferred from molecular analysis of large-subunitrobosomal RNA gene sequences. *J Mol Evol* **41**: 637-645.

803

804 **Table 1.** Comparison between 5 m and 20 m reef depths in TRF abundance, averaged
805 over the 12 replicates for each depth.

TRF	Mean Abundance[a]		Mean δ_i[b]	$\sum\delta_i$%[c]	Probable Division-level ID
	5 m	20 m			
*Rsa*I-90	28.97	31.26	2.21	2.21	Bacteroidetes
*Msp*I-438	8.02	22.42	2.17	4.38	α-proteobacteria
*Cfo*I-60	5	14.8	2	6.38	α-proteobacteria
*Msp*I-149	18.71	7.15	1.92	8.3	Cyanobacteria
*Rsa*I-228	14.68	8.24	1.87	10.17	Cyanobacteria
*Cfo*I-670	13.72	3.3	1.68	11.85	Cyanobacteria
*Rsa*I-58	7.65	10.23	1.6	13.45	plastid/Plancto
*Rsa*I-421	3.97	10.86	1.55	15	α-proteo/Cyanobacteria
*Msp*I-450	10.83	6.68	1.45	16.45	α-proteobacteria
*Msp*I-504	6.9	11.51	1.28	17.73	plastid/Cyanobacteria
*Cfo*I-712	5.17	5.61	1.19	18.92	α-proteobacteria
*Msp*I-91	7.92	4.85	1.19	20.11	Bacteroidetes
*Cfo*I-96	7.26	4.74	1.18	21.28	Bacteroidetes
*Cfo*I-212	11.85	15.17	1.17	22.46	plastid
*Msp*I-495	7.56	6.94	1.16	23.62	γ-proteobacteria/plastid
*Msp*I-213	0	8.4	1.15	24.76	CAB-II
*Rsa*I-131	4.05	4.58	1.11	25.87	Planctomycetacia
*Cfo*I-167	3.7	0.05	1.04	26.91	CAB-I
*Rsa*I-87	8.55	0	1.02	27.93	Bacteroidetes
*Cfo*I-514	1.7	4.03	1	28.93	α-proteobacteria
*Cfo*I-980	3.86	1.1	0.99	29.92	N.I.
*Rsa*I-754	4.02	1.73	0.97	30.89	γ-proteobacteria
*Msp*I-507	2.66	0	0.96	31.84	CAB-I
*Cfo*I-164	3.9	1.76	0.92	32.76	N.I.
*Rsa*I-312	3.24	1.42	0.9	33.66	Bacteroidetes
*Cfo*I-512	0.3	3.63	0.88	34.55	α-proteobacteria
*Cfo*I-908	0.79	2.97	0.85	35.39	N.I.
*Cfo*I-1042	5.93	7.11	0.83	36.23	N.I.
*Msp*I-146	0	7.39	0.79	37.02	γ-proteobacteria
*Cfo*I-1050	1.72	2.2	0.78	37.79	Plastid
*Cfo*I-340	0.02	6.27	0.77	38.57	α-proteobacteria
*Rsa*I-836	2.3	0.8	0.72	39.29	α-proteobacteria
*Msp*I-491	1.5	0.13	0.69	39.98	Cyanobacteria

806 [a]: Mean abundance of standardized peak height for each enzyme.
807 [b]: Contribution of the *i*th species to mean Bray-Curtis dissimilarity between the two environments.
808 [c]: Cumulative percentage of δ_i.
809 [d]: TRFs not identified from 936 theoretical digests of coral associated sequences.
810

810

811 **Table 2.** Correlation matrix of environmental and coral physiologic variables used in
812 CCA.

	PAR	$\delta^{15}N$	$\delta^{13}C$	Zoox-1	Zoox-2	Muc-1
$\delta^{15}N$	-0.12	*****	*****	*****	*****	*****
$\delta^{13}C$	0.47	-0.15	*****	*****	*****	*****
Zoox-1*	0.78	-0.30	0.35	*****	*****	*****
Zoox-2§	0.06	-0.35	0.18	0.06	*****	*****
Muc-1†	0.27	0.26	0.05	0.17	-0.03	*****
Muc-2¥	-0.31	0.22	-0.42	-0.06	0.14	0.02

813 *First NMDS axis describing variation in zooxanthellae communities.
814 §Second NMDS axis describing variation in zooxanthellae communities.
815 †First PCA axis (26%) describing variation in mucus composition.
816 ¥Second PCA axis (15%) describing variation in mucus compostition.

FIGURES

Figure 1 - Schematic cross-section of the coral holobiont showing the potential mechanisms by which the coral, symbiotic algae, bacteria and seawater environment interact.

Figure 2 - Map of Curaçao, Netherlands Antilles, in the southern Caribbean Sea. The three sites chosen for this project are distributed along the leeward coast of the island as indicated. The major seaport of St. Annabaai and the urban center of Willemstad are shown. Water Plant directly down-current from St. Annabaai is the most environmentally impacted site. Playa Hundu is the least impacted site.

Figure 3 - NMDS ordination of *Symbiodinium* communities inhabiting the tissues of *M. annularis* (n = 36). Ordination based on the Bray-Curtis similarity coefficient between TRFLP profiles of the 28S rRNA gene of *Symbiodinium* digested with the *Cfo*I enzyme. (A) Plot showing the relative similarity of *Symbiodinium* communites from 5 m, 10 m and 20 m. (B) Plot showing the relative abundance of clade B TRF *Cfo*I-137 mapped on the ordination of (A). (C) Plot showing the relative abundance of clade C TRF *Cfo*I-458 mapped on the ordination of (A). (D) Plot showing the relative abundance of clade C TRF *Cfo*I-510 mapped on the ordination of (A).

Figure 4 - Pie diagrams illustrating the diversity of the partial 16S rRNA bacterial sequences comprising clone libraries associated with *M. annularis* from 5 m, 10 m and 20 m at Playa Hundu.

Figure 5 – Phylogenetic consensus trees based on parsimony analysis of nearly complete16S rRNA gene sequences. (A) Tree showing the phylogentic grouping of CAB-I and Cyanobacteria compared to other well know bacterial reference sequences. (B) Tree showing phylogentic relationship of CAB-I to representative sequences of all Cyanobacteria and plastids. The labeled nodes represent bootstrap values based on 10,000 replicate resamplings. GenBank accession numbers are shown in parentheses.

Figure 6 - NMDS ordination of bacterial communities inhabiting the tissues of *M. annularis* (n = 36). Ordination based on the Bray-Curtis similarity coefficient between TRFLP profiles of the 16S rRNA gene of bacteria digested with the enzymes *Cfo*I, *Msp*I and *Rsa*I. (A) Plot showing the relative similarity of bacterial communities from 5 m, 10 m and 20 m. (B) Plot showing the relative abundance of CAB-I TRF *Cfo*I-166 mapped on the ordination of (A). (C) Plot showing the relative abundance of BBD cyanobacterium CD1C11 TRF *Rsa*I-228 mapped on the ordination of (A). (D) Plot showing the relative abundance of α-proteobacteria TRF *Msp*I-436 mapped on the ordination of (A).

Figure 7 - Ordination biplot of 36 coral samples of *M. annularis* and seven environmental and physiologic explanatory variables. The ordination is obtained by canonical correspondence analysis (CCA) of the bacterial community TRFLP profiles combined with the explanatory variables. Together, axis 1 and axis 2 account for 10.56 % of the variation in TRFLP profiles. Explanatory variables are described within the text.

Figure 1

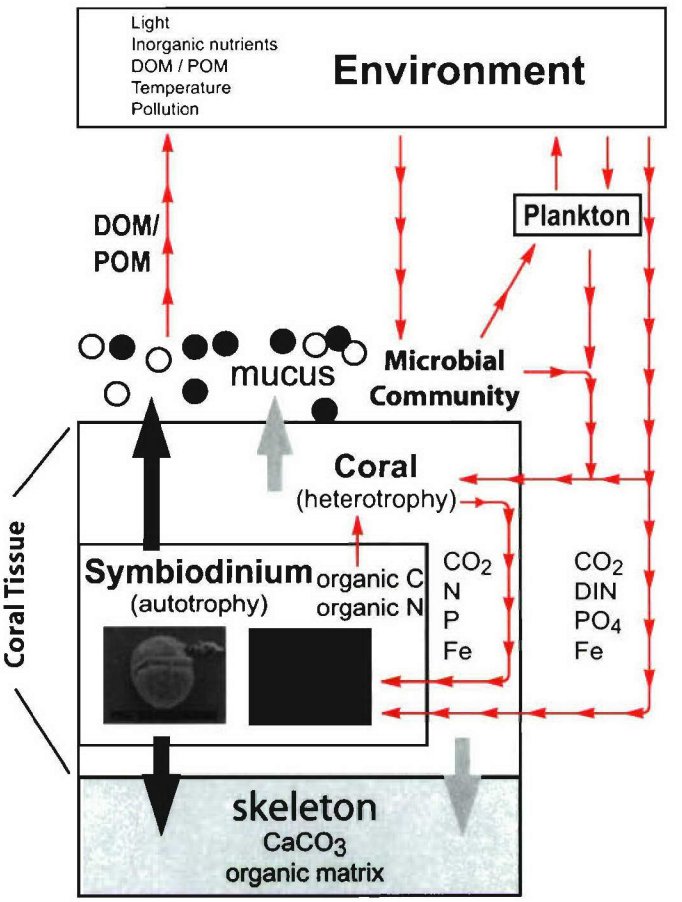
Light
Inorganic nutrients
DOM / POM
Temperature
Pollution
Environment
DOM/
POM
Plankton
mucus
Microbial
Community
Coral
(heterotrophy)
Coral Tissue
Symbiodinium
(autotrophy)
organic C
organic N
CO2
N
P
Fe
CO2
DIN
PO4
Fe
skeleton
CaCO3
organic matrix

Figure 2

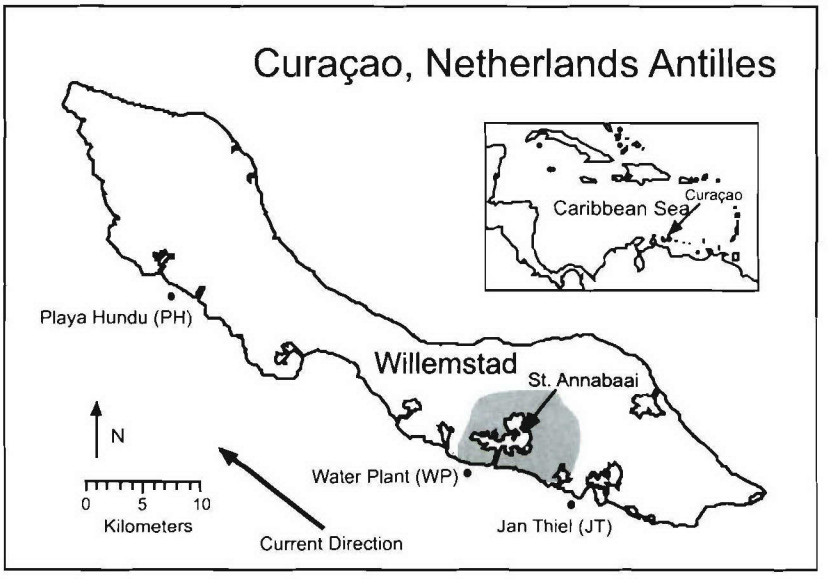
Curaçao, Netherlands Antilles
Caribbean Sea
Curaçao
Playa Hundu (PH)
Willemstad
St. Annabaai
N
0 5 10
Kilometers
Water Plant (WP)
Jan Thiel (JT)
Current Direction

Figure 3

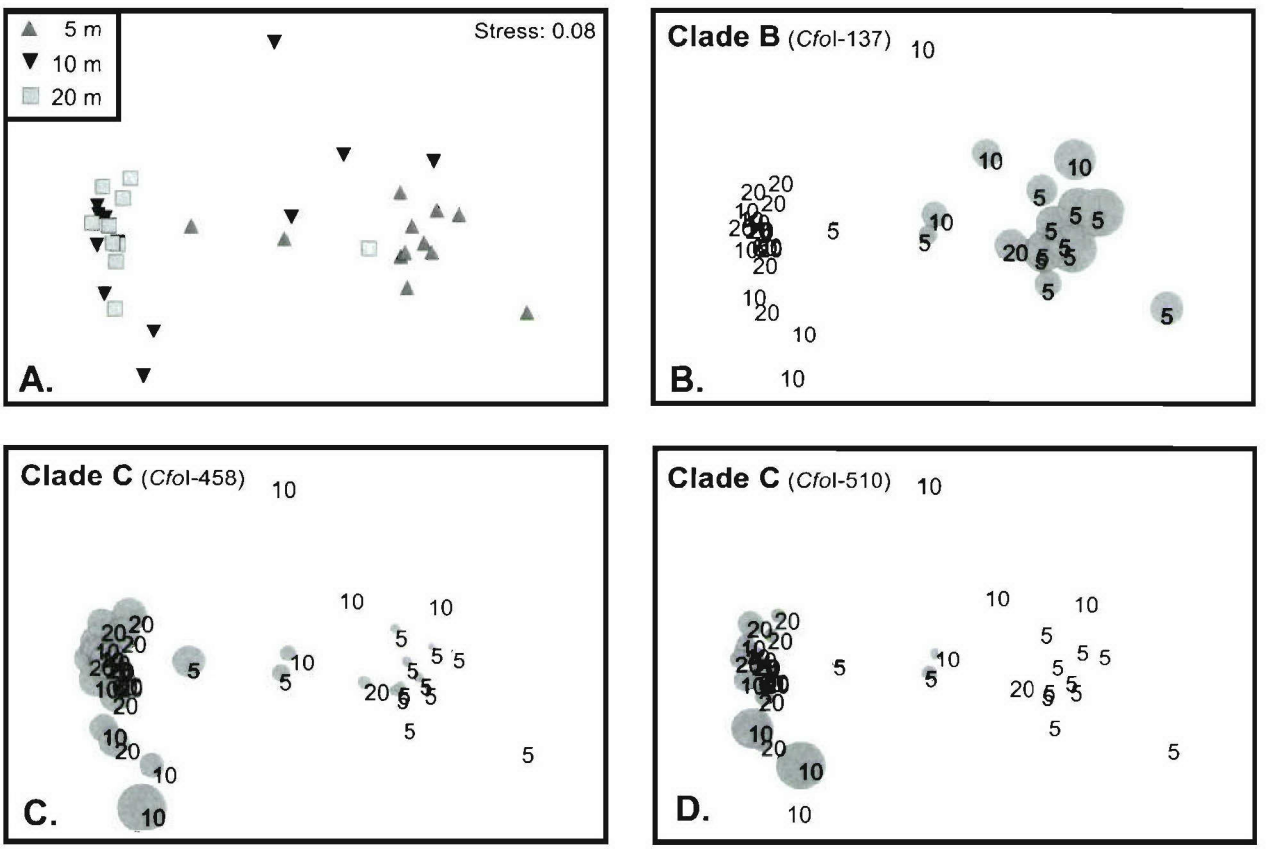
5 m
10 m
20 m
Stress: 0.08
A.
Clade B (Cfol-137)
B.
Clade C (Cfol-458)
C.
Clade C (Cfol-510)
D.

Figure 4

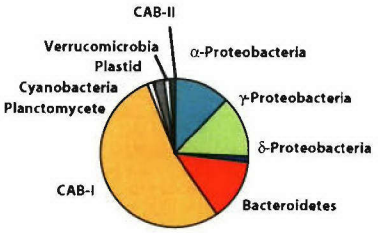

5 m (n=82)

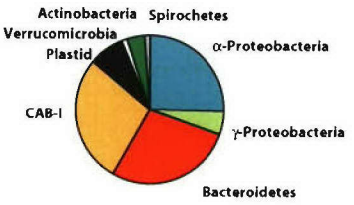

10 m(n=79)

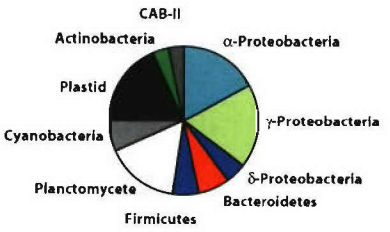

20 m (n=88)

Figure 5

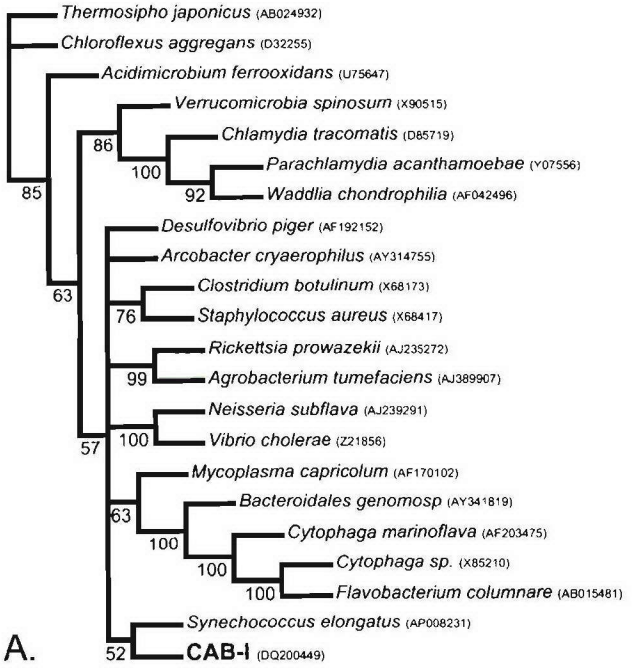
Thermosipho japonicus (AB024932)
Chloroflexus aggregans (D32255)
Acidimicrobium ferrooxidans (U75647)
Verrucomicrobia spinosum (X90515)
Chlamydia tracomatis (D85719)
Parachlamydia acanthamoebae (Y07556)
Waddlia chondrophilia (AF042496)
Desulfovibrio piger (AF192152)
Arcobacter cryaerophilus (AY314755)
Clostridium botulinum (X68173)
Staphylococcus aureus (X68417)
Rickettsia prowazekii (AJ235272)
Agrobacterium tumefaciens (AJ389907)
Neisseria subflava (AJ239291)
Vibrio cholerae (Z21856)
Mycoplasma capricolum (AF170102)
Bacteroidales genomosp (AY341819)
Cytophaga marinoflava (AF203475)
Cytophaga sp. (X85210)
Flavobacterium columnare (AB015481)
Synechococcus elongatus (AP008231)
CAB-I (DQ200449)
85
86
100
92
63
57
76
99
100
63
100
100
100
52
A.

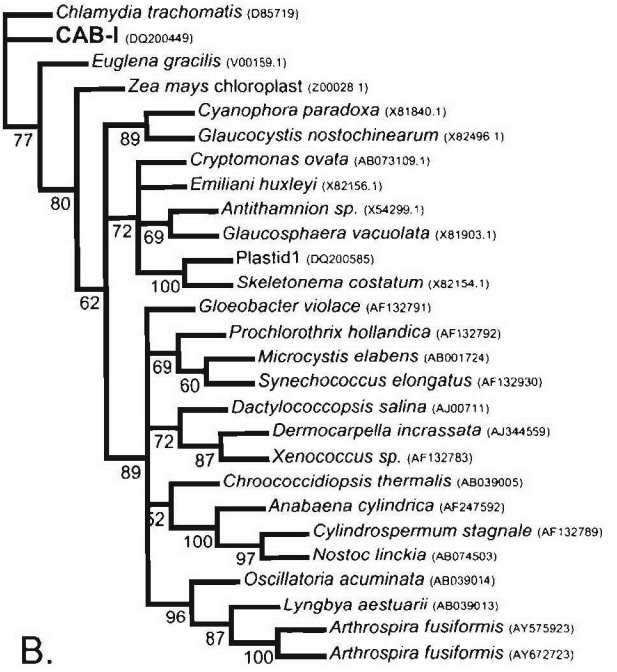
Chlamydia trachomatis (D85719)
CAB-I (DQ200449)
Euglena gracilis (V00159.1)
Zea mays chloroplast (Z00028.1)
Cyanophora paradoxa (X81840.1)
Glaucocystis nostochinearum (X82496.1)
Cryptomonas ovata (AB073109.1)
Emiliani huxleyi (X82156.1)
Antithamnion sp. (X54299.1)
Glaucosphaera vacuolata (X81903.1)
Plastid1 (DQ200585)
Skeletonema costatum (X82154.1)
Gloeobacter violace (AF132791)
Prochlorothrix hollandica (AF132792)
Microcystis elabens (AB001724)
Synechococcus elongatus (AF132930)
Dactylococcopsis salina (AJ00711)
Dermocarpella incrassata (AJ344559)
Xenococcus sp. (AF132783)
Chroococcidiopsis thermalis (AB039005)
Anabaena cylindrica (AF247592)
Cylindrospermum stagnale (AF132789)
Nostoc linckia (AB074503)
Oscillatoria acuminata (AB039014)
Lyngbya aestuarii (AB039013)
Arthrospira fusiformis (AY575923)
Arthrospira fusiformis (AY672723)
77
89
80
72
69
100
62
69
60
72
87
89
52
100
97
96
87
100
B.

Figure 6

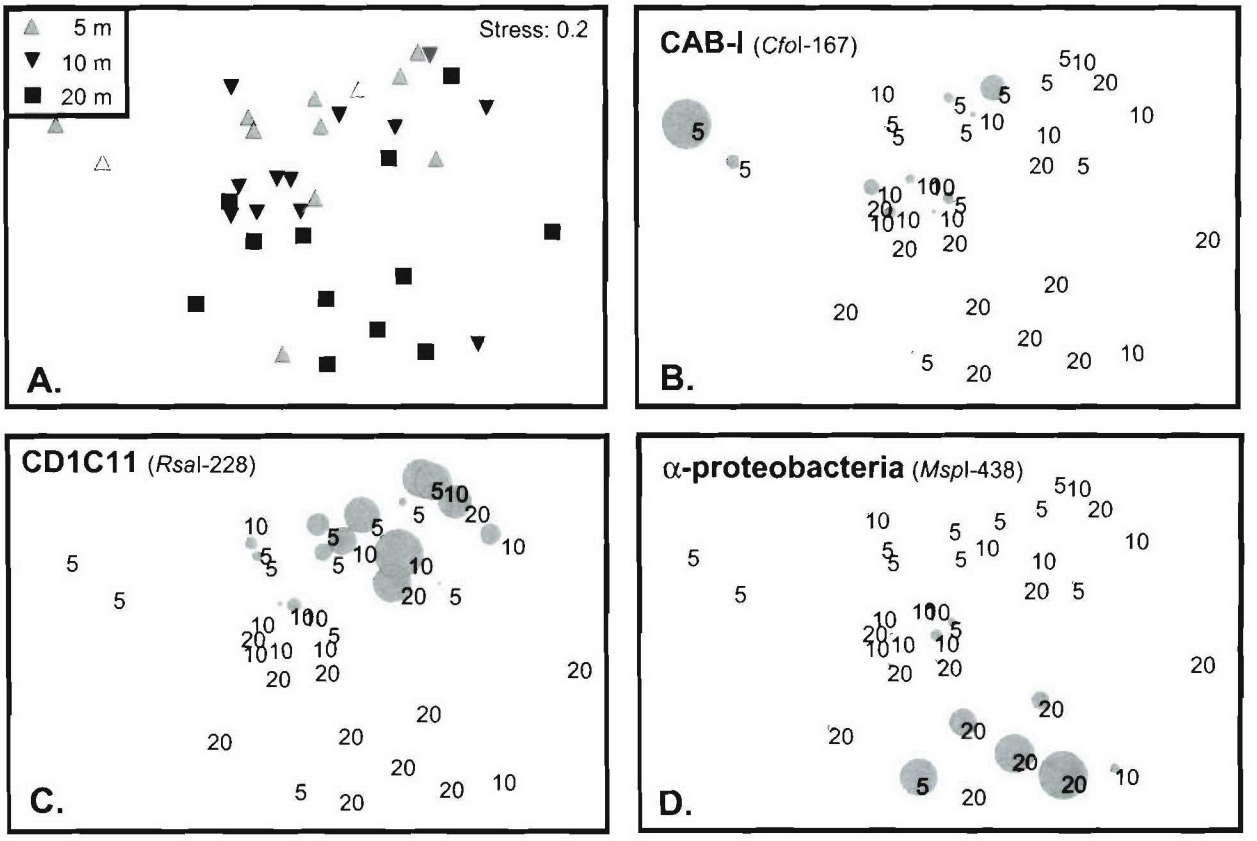
5 m
10 m
20 m
Stress: 0.2
A.
CAB-I (Cfol-167)
B.
CD1C11 (Rsal-228)
C.
α-proteobacteria (Mspl-438)
D.

Figure 7

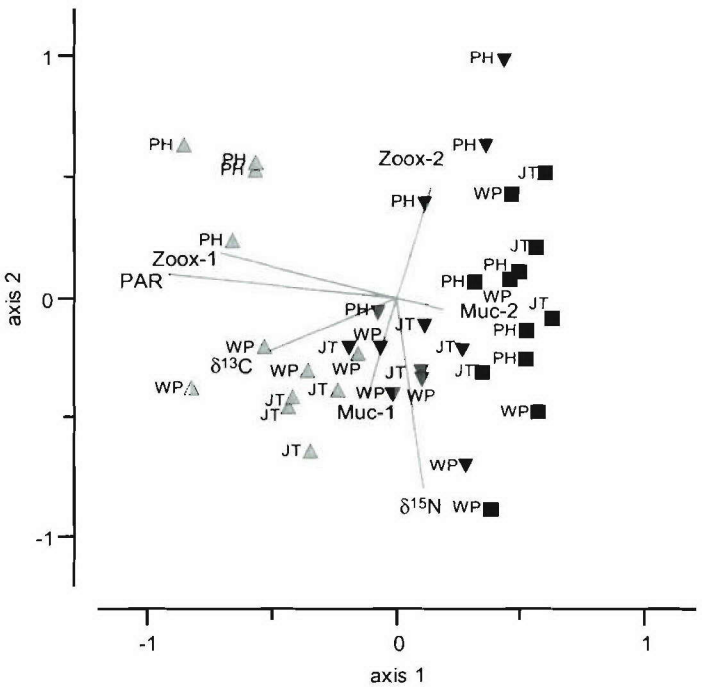
1
0
-1
axis 2
-1
0
1
axis 1
Zoox-2
Zoox-1
PAR
Muc-2
Muc-1
δ13C
δ15N
PH
JT
WP

Supplemental Material. Mean and standard deviations of environmental and coral physiologic variables (monosaccharides and amino acids as molar %).

	Jan Thiel						Water Plant						Playa Hundu					
	5 m		10 m		20 m		5 m		10 m		20 m		5 m		10 m		20 m	
	mean	std	mean	std	mean	std	mean	std	mean	std	mean	std	mean	std	mean	std	mean	std
% surface PAR	33.32	5.43	18.31	3.95	9.08	1.23	34.05	4.37	21.08	1.91	9.92	0.59	36.34	5.98	22.25	2.86	10.72	0.85
$\delta^{15}N$ (‰)	4.97	1.02	4.65	0.33	4.78	0.81	5.26	0.40	5.17	0.26	4.43	0.56	3.25	0.33	3.30	0.46	3.17	0.59
$\delta^{13}C$ (‰)	-14.78	0.41	-15.28	0.55	-16.02	0.61	-14.15	0.46	-14.47	0.49	-15.80	1.26	-14.47	0.44	-14.72	0.46	-14.61	0.12
Inositol	3.53	2.40	1.65	1.04	1.63	0.38	3.30	1.68	4.44	3.24	7.07	2.72	6.38	3.11	7.30	7.30	4.89	2.10
Fucose	32.40	5.56	25.70	12.56	39.83	3.01	33.90	4.61	34.94	4.30	35.58	6.73	37.15	4.86	34.09	9.68	34.53	6.06
Arabinose	0.23	0.46	0.43	0.45	0.23	0.13	0.23	0.46	0.01	0.03	0.23	0.27	0.00	0.00	0.05	0.10	0.00	0.00
Rhamnose	0.00	0.00	0.00	0.00	0.07	0.09	0.00	0.00	0.00	0.00	0.00	0.00	0.00	0.00	0.00	0.00	0.00	0.00
Galactose	6.01	1.30	7.84	1.86	5.27	0.23	5.57	1.06	4.75	0.22	2.42	0.52	0.00	0.00	3.62	2.51	2.51	2.91
Glucosamine	6.26	6.19	6.78	4.61	15.63	2.63	12.58	2.85	15.24	1.48	0.51	1.02	15.75	5.80	7.66	9.23	19.00	4.26
Glucose	12.03	5.97	16.48	3.71	1.67	1.19	5.06	4.20	3.70	1.97	13.94	2.80	3.69	4.03	10.94	8.70	3.27	3.74
Xylose	1.79	1.17	2.01	0.39	0.21	0.05	0.32	0.18	0.23	0.26	0.26	0.35	0.25	0.18	0.62	0.78	0.99	0.48
N-acetylglucosamine	31.53	3.67	32.73	6.56	34.50	1.43	32.77	4.30	32.73	1.68	25.31	3.96	28.10	5.51	29.28	11.43	29.51	4.87
Mannose	0.00	0.00	0.00	0.00	0.02	0.04	0.00	0.00	0.27	0.50	0.00	0.00	0.00	0.00	0.00	0.00	0.00	0.00
Fructose	0.00	0.00	0.00	0.00	0.00	0.00	1.28	1.96	0.56	1.11	3.21	2.84	1.83	2.72	0.00	0.00	0.00	0.00
Glucuronic acid	6.23	4.34	6.38	3.66	0.94	0.74	4.99	4.31	3.14	2.53	11.47	12.54	6.85	5.66	6.45	10.30	5.31	3.38
Aspartic acid	11.29	0.55	11.46	1.03	9.51	1.11	11.31	1.40	10.92	0.75	10.65	0.82	10.74	0.85	10.50	0.95	10.01	1.78
Threonine	8.95	0.62	9.44	0.96	10.80	1.59	9.70	0.85	9.60	0.94	9.91	0.96	9.42	0.87	10.35	0.84	10.61	1.62
Serine	15.25	2.04	15.53	3.87	21.96	4.84	17.39	3.38	17.29	2.71	19.45	4.71	16.77	2.07	20.16	2.47	20.37	5.97
Glutamic acid	12.14	1.31	11.21	0.94	9.80	0.85	11.02	1.27	10.31	1.86	11.06	0.69	11.80	1.76	11.60	2.27	10.14	2.14
Proline	5.36	0.53	4.89	1.04	5.58	1.34	5.17	0.64	4.99	0.60	4.77	0.46	5.41	0.43	4.79	0.69	4.32	1.72
Glycine	9.62	0.84	9.71	3.31	6.98	1.00	8.81	1.00	8.42	1.03	8.33	1.10	8.55	0.48	8.01	0.89	7.93	1.23
Alanine	6.43	0.34	6.67	0.68	5.22	0.63	6.19	0.61	6.13	0.42	6.24	0.26	6.20	0.54	5.58	0.19	5.79	0.95
Cysteine	0.00	0.00	0.00	0.00	1.02	1.24	0.00	0.00	0.56	1.12	0.00	0.00	0.32	0.63	0.00	0.00	0.20	0.39
Valine	6.12	0.50	6.54	0.45	6.84	0.69	6.92	0.51	6.72	0.18	6.40	1.05	6.42	0.18	6.41	0.48	6.66	0.77
Methionine	0.66	0.21	0.57	0.43	0.52	0.41	0.43	0.31	0.72	0.08	0.76	0.05	0.70	0.27	0.28	0.30	0.56	0.26
Isoleucine	3.66	0.33	3.71	0.19	3.44	0.06	3.64	0.24	3.73	0.18	3.48	0.32	3.54	0.17	3.38	0.46	3.71	0.29
Leucine	5.83	0.38	5.80	0.34	5.18	0.51	5.70	0.27	5.99	0.30	5.70	0.67	5.72	0.68	5.15	0.46	5.47	0.60
Tyrosine	2.58	0.41	2.41	0.48	2.62	0.53	2.34	0.73	2.94	0.53	2.45	1.00	2.82	0.58	2.33	0.75	2.39	0.40
Phenylalnine	2.89	0.26	3.02	0.16	2.73	0.35	3.04	0.29	3.20	0.17	2.84	0.39	2.99	0.33	2.94	0.37	3.11	0.41
Histidine	1.36	0.09	1.31	0.25	1.30	0.27	1.35	0.22	1.38	0.27	1.24	0.26	1.35	0.13	1.37	0.11	1.33	0.28
Lysine	4.89	0.51	4.40	0.93	4.16	0.39	4.26	0.76	4.45	0.53	4.14	0.37	4.51	0.19	4.35	0.24	4.52	0.85
Arginine	2.95	0.42	3.35	0.62	2.34	0.27	2.73	0.27	2.66	0.40	2.57	0.33	2.74	0.52	2.80	0.65	2.88	0.61

Supplemental Material. Depth distribution and theoretical enzyme digests of 58 unique bacterial sequences (97% similarity) identified from tissues of *M. annularis*.

Species	Accession number	Depth (m)			Enzyme		
		5	10	20	*Cfo*I	*Msp*I	*Rsa*I
Actinobacteria		**0**	**3**	**3**			
Actinobacteria-1	DQ200498	0	1	0	670	164	794
Actinobacteria-2	DQ200515	0	2	1	372	79	37
Actinobacteria-3	DQ200570	0	0	2	192	79	453
Alphaproteobacteria		**10**	**20**	**15**			
Alphaproteobacteria-1	DQ200416	1	0	0	60	438	825
Alphaproteobacteria-2	DQ200435	1	0	0	91	448	127
Alphaproteobacteria-3	DQ200464	1	0	0	341	159	835
Alphaproteobacteria-4	DQ200478	1	0	0	60	129	117
Alphaproteobacteria-5	DQ200502	0	1	0	91	86	
Alphaproteobacteria-6	DQ200503	0	1	0	338	127	115
Alphaproteobacteria-7	DQ200525	1	12	4	60	436	420
Alphaproteobacteria-8	DQ200566	0	0	4	510	436	115
Alphaproteobacteria-9	DQ200545	4	5	0	709	449	57
Alphaproteobacteria-10	DQ200606	1	0	4	60	436	419
Alphaproteobacteria-11	DQ200634	0	0	2	340	162	825
Alphaproteobacteria-12	DQ200541	0	1	1	81	149	421
Bacteroidetes		**11**	**22**	**6**			
Bacteroidetes-1	DQ200441	1	0	0	92	87	169
Bacteroidetes-2	DQ200466	1	0	0		87	307
Bacteroidetes-3	DQ200554	0	1	0	97	490	85
Bacteroidetes-4	DQ200581	0	0	1	99	94	315
Bacteroidetes-5	DQ200421	7	17	3	95	90	129
Bacteroidetes-6	DQ200521	0	4	0	95	90	311
Bacteroidetes-7	DQ200630	0	0	2	371	90	129
Bacteroidetes-8	DQ200448	2	0	0	98	93	316
Cyanobacteria		**2**	**0**	**6**			
Cyanobacteria-1	DQ200436	1	0	0	668	490	421
Cyanobacteria-2	DQ200576	0	0	4	669	158	422
Cyanobacteria-3	DQ200614	1	0	2	226	490	412
Deltaproteobacteria		**1**	**0**	**4**			
Deltaproteobacteria-1	DQ200431	1	0	0	93	508	466
Deltaproteobacteria-2	DQ200595	0	0	2	94	509	244
Deltaproteobacteria-3	DQ200572	0	0	2	60	292	488
Firmicutes		**0**	**0**	**5**			
Firmicutes-1	DQ200641	0	0	5	238	155	486
Gammaproteobacteria		**11**	**4**	**16**			
Gammaproteobacteria-1	DQ200442	1	0	0	570	494	882
Gammaproteobacteria-2	DQ200447	1	0	0	89	505	
Gammaproteobacteria-3	DQ200514	0	1	0	565	79	474
Gammaproteobacteria-4	DQ200520	0	1	0	210	144	881
Gammaproteobacteria-5	DQ200552	0	1	0	354	486	81
Gammaproteobacteria-6	DQ200612	0	0	1	60	452	640
Gammaproteobacteria-7	DQ200646	1	0	0	89	282	
Gammaproteobacteria-8	DQ200562	0	0	6		144	24
Gammaproteobacteria-9	DQ200474	8	1	3	210	493	752
Gammaproteobacteria-10	DQ200618	0	0	5	60	486	24
Gammaproteobacteria-11	DQ200557	0	0	1		Reverse	
CAB-I		**44**	**22**	**0**			
CAB-I-1	DQ200483	0	1	0	81	149	594
CAB-I-2	DQ200449	44	21	0	166	506	608
Planctomycetacia		**1**	**0**	**14**			
Planctomycetacia-1	DQ200461	1	0	0	361	138	
Planctomycetacia-2	DQ200594	0	0	1	355	152	119
Planctomycetacia-3	DQ200633	0	0	1		252	131
Planctomycetacia-4	DQ200643	0	0	1	614	271	24
Planctomycetacia-5	DQ200571	0	0	4	109	147	57
Planctomycetacia-6	DQ200626	0	0	3	614	159	122
Planctomycetacia-7	DQ200559	0	0	2		159	113
Planctomycetacia-8	DQ200603	0	0	2		307	131
Plastid		**0**	**6**	**16**			
Plastid-1	DQ200585	0	0	13	1055	496	58
Plastid-2	DQ200522	0	6	3	212	505	
Spirochaetes		**0**	**1**	**0**			
Spirochaetes-1	DQ200505	0	1	0		Reverse	
CAB-II		**1**	**0**	**3**			
CAB-II-1	DQ200426	1	0	0	377	65	493
CAB-II-2	DQ200587	0	0	3	551	213	866
Verrucomicrobiae		**1**	**1**	**0**			
Verrucomicrobiae-1	DQ200415	1	0	0	575	842	877
Verrucomicrobiae-2	DQ200501	0	1	0		603	883

ENVIRONMENTAL CONTROLS ON CORALLITE MORPHOLOGY IN THE REEF CORAL *MONTASTRAEA ANNULARIS*

James S. Klaus, *Ann F. Budd*, and *Bruce W. Fouke*

KEY WORDS: corals, species complexes, plasticity, morphometrics

ABSTRACT

Scleractinian reef-coral species display high phenotypic plasticity in skeletal morphology. Understanding environmental and physiologic controls on this variation in morphology is essential in explaining the distribution and abundance of coral species as well as understanding the susceptibility of coral species to pollution and global climate change. Furthermore, phenotypic plasticity provides a basis for delineating species boundaries and interpreting the adaptive significance of observed morphologic differences in closely related taxa. Here we assess phenotypic plasticity in the corallite morphology of genetically determined colonies of *Montastraea annularis* (Ellis and Solander, 1786), analyzing the three-dimensional morphology of calical surfaces and the two-dimensional corallite morphology represented in transverse thin sections. Samples were collected along gradients of seawater depth and coastal influence on the island of Curaçao, Netherlands Antilles and additionally compared to *M. annularis* and two closely related species, *M. franksi* (Gregory, 1895), and *M. faveolata* (Ellis and Solander, 1786), collected from Panama. Significant phenotypic plasticity was found between seawater depths and localities of Curaçao, as well as between the two geographic regions. Morphologic characters associated with calical surfaces were significantly more plastic than characters preserved in transverse thin sections. While characters preserved in thin section were more successful at classifying the three closely related species, characters associated with calical surfaces provide a basis for interpreting the adaptive significance of the observed differences between these three species.

High variability in skeletal morphology is a well know characteristic of scleractinian coral species. This includes variations in overall colony growth form (Goreau, 1963; Roos, 1967; Dustan, 1975; Veron and Pichon, 1976; Jaubert, 1977; Graus and Macintyre, 1982; Muko et al., 2000; Kaandorp et al., 2005), as well as corallite architecture observed both within and between coral colonies (Foster, 1979a, 1980, 1983, 1985; Budd, 1993; Budd et al., 1994). These changes in skeletal morphology allow corals to survive in a variety of environmental conditions (Porter, 1976; Lasker, 1981; Lesser et al., 1994; Kaandorp et al., 2005), and can influence the distribution, abundance, and evolutionary success of a species (Foster, 1979b; Jackson, 1979; Johnson and Budd, 1995; Klaus and Budd, 2003). Morphologic variation is due to the combined effects of genetic polymorphism and phenotypic plasticity. However, separating the individual effects of these two components can be difficult without genetic data distinguishing species and populations within species (Knowlton and Budd, 2001; Budd and Pandolfi, 2004; Fukami et al., 2004). Moreover, taxonomic classifications have historically underestimated the number of species within many common coral genera (Knowlton and Budd, 2001). Given the tendency for closely related taxa to partition themselves along environmental gradients, failure to recognize true species boundaries has led authors to invoke a large degree of phenotypic plasticity to explain observed morphologic variations along ecologically meaningful gradients (e.g. seawater depth). As ongoing molecular and nontraditional systematic studies continue to reveal cryptic species (Weil and Knowlton, 1994; Carlon and Budd, 2002), the extent of plasticity interpreted within coral species will likely decline (but see Miller and Benzie, (1997)).

44 The highly plastic nature of reef-corals is in part a byproduct of the coral skeletogenic
45 process. Corals calcify a hundred times faster than inorganic calcification on the reef, yet
46 exert little control over the specific shape and organization of their skeletal crystals
47 (Cohen and McConnaughey, 2003). Calcification occurs outside of the coral tissue in the
48 space adjacent to cells of the calicoblastic ectoderm (Barnes and Chalker, 1990). In this
49 space corals build their skeletons primarily from sclerodermites, three-dimensional fans
50 of aragonite similar to inorganically precipitated spherulitic crystal fibers (Given and
51 Wilkinson, 1985; Cohen and McConnaughey, 2003). These sclerodermites combine to
52 form trabeculae which themselves combine to form septa and the other skeletal structures
53 which comprise the individual corallites of a colony.
54 The accretionary growth of corals has been subdivided into two major components,
55 upward linear extension and skeletal thickening (Graus and Macintyre, 1982; Barnes and
56 Lough, 1993; Cohen et al., 2004). Upward growth has been shown to occur primarily at
57 night through the accretion of randomly-oriented fusiform-shaped crystals (Barnes and
58 Crossland, 1980; Gladfelter, 1982, 1983; Vago et al., 1997), while skeletal thickening
59 occurs during the daytime when corals exhibit calcification rates three to five times faster
60 in the presence of light and actively photosynthsizing symbiotic algae (zooxanthellae)
61 (Barnes and Crossland, 1980; Gladfelter, 1983; Le Tissier, 1988). Variations in skeletal
62 growth have been correlated with light-mediated photosynthesis (Goreau, 1959;
63 Vandermuelen et al., 1972; Chalker and Taylor, 1975; Graus and Macintyre, 1982;
64 Marubini and Thake, 1999; Muko et al., 2000; Marubini et al., 2002; Kaandorp et al.,
65 2005), turbidity and sediment load (Foster, 1979b; Carricart-Ganivet and Merino, 2001),
66 seawater nutrients (Edinger et al., 2000; Cook et al., 2002), hydrodynamics (Jokiel, 1978;

67 Bruno and Edmunds, 1998; Kaandorp et al., 2005), and temperature (Dodge and Vaisnys,
68 1975; Lough and Barnes, 2000); with varying degrees of influence on either vertical
69 extension or skeletal thickening.

70 In the present study we explore the magnitude and nature of phenotypic plasticity in
71 the common reef building coral *M. annularis* along gradients of seawater depth and
72 coastal influence on the island of Curaçao, Netherlands Antilles. Curaçao is an especially
73 conducive natural laboratory for this study (Fig. 1). The approximately 150,000 people
74 living on Curaçao are concentrated in the capital city of Willemstad, surrounding the
75 natural harbor of St. Annabaai. The large commercial and military harbor of St.
76 Annabaai, and the urban center of Willemstad are a major point source of pollutants such
77 as nutrients, metals, hydrocarbons and other toxic chemicals (Gast, 1998). Furthermore,
78 the island is surrounded by shallow fringing reefs up to 250 m from shore where a
79 stepped shelf break occurs from 8-10 m to 30-50 m water depth (Van Duyl, 1985). These
80 factors provide a consistent depth and environmental impact gradient to sample along the
81 length of the island.

82 We selected *M. annularis* because it is one of the most well studied reef-coral species,
83 and it clearly demonstrates the problem of distinguishing genotypic versus phenotypic
84 variation. Historically, *M. annularis* sensu lato was considered the model ecologic
85 generalist, exhibiting a high degree of phenotypic plasticity. It could be found from
86 intertidal to over 80 m water depth (Goreau and Wells, 1967), with colony morphologies
87 varying dramatically from hemispherical heads to vertical columns and horizontal plates.
88 Recent taxonomic studies based on molecular genetics, aggressive behavior, ecology,
89 growth rate, corallite morphometrics, and stable isotopes (Tomascik, 1990; Knowlton et

al., 1992; van Veghel and Bak, 1993), showed that *M. "annularis"* is actually a complex of at least three species: (1) *M. annularis* sensu strictu (Ellis and Solander, 1786), which forms smooth columns; (2) *M. faveolata* (Ellis and Solander, 1786), which forms bumby or keeled heads and sheets; and (3) *M. franksi* (Gregory, 1895), which forms bumpy mounds and plates. On the reefs of Curaçao *M. annularis* and *M. faveolata* are most common between 1 m and 20 m while *M. franksi* is typically found at depths greater than 10 m (Van Veghel, 1994a). Previous studies of the three species on Curaçao have characterized significant differences in genetics, as well as reproductive, behavioral, and morphologic aspects (van Veghel and Bak, 1993, 1994; van Veghel, 1994b; van Veghel and Kahmann, 1994; van Veghel and Bosscher, 1995).

Here we focus on the corallite morphology of genetically determined colonies of *M. annularis* s.s., analyzing the three-dimensional morphology of calical surfaces (Budd and Klaus, 2001; Knowlton and Budd, 2001; Fukami et al., 2004) and the two-dimensional corallite morphology as represented in transverse thin sections (Budd and Klaus, 2001; Pandolfi et al., 2002; Klaus and Budd, 2003; Budd and Pandolfi, 2004). We assess four different environmental and physiologic factors as possible causes of the observed phenotypic plasticity: (1) light intensity of the seawater environment; (2) seawater pollution; (3) relative photosynthetic activity of zooxanthellae; and (4) the diversity of zooxanthellae communities.

The $\delta^{15}N$ of coral tissue was used to determine the relative coral uptake of sewage at each sampling site. Due to transformations of dissolved inorganic nitrogen (DIN) through ammonia volatilization, denitrification of nitrate, and nitrification of ammonia, wastewater derived from sewage treatment plants is generally enriched in the heavy

isotope of nitrogen, ^{15}N (Heikoop et al., 1998, 2000a, 2000b). Values of coral tissue $\delta^{15}N$ reflect these differences, and thus, provide a means for relating the effect of pollution on skeletal morphology. Previous studies of *Montastraea sp.* have shown growth rates to be reduced in polluted reef environments (Tomascik, 1990).

The influence of photosynthetic activity on skeletal morphology was assessed using the $\delta^{13}C$ composition of coral tissue. Previous studies have shown values of $\delta^{13}C$ to reflect the relative ratios of autotrophic versus heterotrophic modes of coral feeding (Heikoop et al., 2000b; Swart et al., 2005). Under optimal conditions (e.g. high light intensitiy) coral tissue $\delta^{13}C$ is high (-10‰ to -14‰), and similar to those of zooxanthellae. In environments where zoxanthellae photosynthesis is reduced, coral tissue $\delta^{13}C$ approaches that of zooplankton (-20‰), the coral heterotrophic food source. A similar approach, utilizing the metabolic fractionations of $\delta^{13}C$ and $\delta^{18}O$ recorded in the coral skeleton, was recently used to show the influence of light-mediated photosynthesis on growth forms and skeletal chemistry of the branching coral *Madracis mirabilis* (Maier et al., 2003; Kaandorp et al., 2005).

In addition to photosynthetic activity, we assess the potential influence of different communities of the dinoflagellate genus *Symbiodinium* (zooxanthellae) on coral skeletal morphology. The current taxonomy of *Symbiodinium* is divided into seven clades labeled A-G (Baker, 2003). These clades have been shown to vary with environmental conditions (Rowan and Knowlton, 1995; Rowan et al., 1997; Baker, 2001) and possess unique physiologic characteristics (Chang, 1983; Iglesias-Prieto and Trench, 1997; Banaszak et al., 2000; Little et al., 2004). While it is well established that coral skeletogensis is enhanced in the presence of zooxanthellae; the influence of different

symbiont taxa on skeletogenesis is currently unknown. Communities of zooxanthellae were characterized by analyzing terminal restriction fragment length polymorphisms (T-RFLP) of 28S rRNA genes for *Symbiodinium*.

Lastly, we assess the extent to which phenotypic plasticity observed along the sampled environmental gradients obscures species boundaries within the *M. "annularis"* species complex. Species of *M. annularis*-like corals have been common in the Caribbean for the past 22 million years (Budd, 2000; Knowlton and Budd, 2001) and preliminary studies indicate a diverse and complex evolutionary history during this time (Budd, 1991; Budd and Klaus, 2001; Klaus and Budd, 2003; Budd and Pandolfi, 2004). Understanding how environmental factors affect species boundaries is essential to accurately interpret the complex evolutionary history of this group. To determine the extent to which phenotypic plasticity obscures taxonomic identification, corals collected from Curaçao were compared to colonies of *M. annularis*, *M. faveolata*, and *M. franksi*, collected from the San Blas and Bocas del Toro regions of Panama, which were identified based on genetic analyses.

MATERIALS AND METHODS

CORAL SAMPLING

To assess the effect of seawater depth and local environmental variation on the corallite morphology of *M. annularis*, small colony fragments were collected at 5 m, 10 m, and 20 m, at five localites along the leeward coast of Curaçao, Netherlands Antilles; (1) Jan Thiel approximately 8 km upcurrent of the seaport, (2,3) Boca Simon and Water Plant, immediately adjacent to the seaport and large urban center of Willemstad, and (3,4) Snake Bay and Playa Hundu, approximately 9 and 32 km downcurrent respectively (Fig.1). Four healthy colonies of *M. annularis* were sampled from each depth at each locality. Colony fragments were dried for three days at 35°C to preserve tissues for subsequent isotopic analyses.

At Jan Thiel, Water Plant, and Playa Hundu, tissue samples for molecular analyses were collected from the upper surface of each colony by removing a 2 cm by 2 cm portion of the uppermost 1 cm of the coral colony with a clean chisel and placing the sample in a sterile 50 ml centrifuge tube. Upon returning to the shore, the seawater within each tube was decanted, coral samples were immersed in 80% ethanol, and crushed and homogenized, creating a slurry of coral tissue, zooxanthellae, mucus, microorganisms, and skeletal material.

EXPLANATORY VARIABLES OF SKELETAL MORPHOLOGY

Measurements of temperature and photosynthetically active radiation (PAR) were taken at each depth of each reef locality at noon on a normal sunny day. Measurements of PAR were obtained using a LI-192 light sensor connected to the LI-1000 data logger

(LI-COR Biosciences, Lincoln, NE). PAR measurements typically have ± 5% uncertainty. Ten measurements were collected at each depth at each locality and are presented as the percentage of the mean surface PAR.

CORAL TISSUE $\delta^{15}N$ AND $\delta^{13}C$

The $\delta^{15}N$ and $\delta^{13}C$ of 36 coral tissue samples were determined by removing an area of tissue approximately 25 cm^2 from the upper growth surface of each colony using a small clean microdrill. Samples were then decalcified using 1 N hydrochloric acid, rinsed in distilled water, and dried using a Vacufuge Concentrator 5301 (Eppendorf, Westbury, N.Y.). Thus all samples contain a combination of host coral tissue and zooxanthellae. Samples (0.5 to 1.0 mg) were analyzed in continuous flow mode utilizing a Eurovector Elemental analyzer coupled to a Micromass Isoprime mass spectrometer located in the Department of Earth and Environmental Science at Los Alamos National Laboratory. Typical precision for $\delta^{15}N$ based on replicates of coral tissue samples and in house coral tissue standards was <0.21‰ (1σ). Values were calibrated using in-house standards including deep-sea coral tissues (Heikoop et al., 2002) that were originally analyzed in the laboratory of Zachary Sharp at the University of New Mexico and calibrated against IAEA-N3 and USGS RSIL N11 potassium nitrate standards. To eliminate any systematic changes in $\delta^{15}N$ due to light-mediated fractionation, the $\delta^{15}N$ values used in statistical analyses were transformed into the deviation from the mean $\delta^{15}N$ at each of the three depths sampled.

197 CHARACTERIZATION OF ZOOXANATHELLAE COMMUNITIES

198 Communities of *Symbiodinium* associated with *M. annularis* were characterized using
199 a combined approach of T-RFLP and sequencing of clone libraries to taxonomically
200 identify terminal restriction fragments (T-RFs). The UltraClean Soil DNA Kit (Mo Bio,
201 Solana Beach, CA) was used to extract genomic DNA from coral slurries. To perform
202 the extraction, 2 ml of sample was concentrated via centrifugation, resuspended in 300 µl
203 of MicroBead solution, and prepared as recommended by the manufacturer. Genes
204 encoding for 28S rDNA were amplified with a Mastercycler gradient thermocycler
205 (Eppendorf) by PCR using primers specific for *Symbiodinium*. Primers used in the PCR
206 amplifications of *Symbiodinium* were lsu-UFP1 (5'-
207 CCCGCTAATTTAAGCATATAAGTA), and lsu-URP1 (5'-
208 GTTAGACTCCTTGGTCGTGTTTCA) (Integrated DNA Technologies, Coralville, IA)
209 (Zardoya et al., 1995; van Oppen et al., 2001). For T-RFLP analysis primer lsu-UFP1
210 was labeled at the 5' end with phosphoramidite fluorochrome 6-carboxyfluorescein (6-
211 FAM). The PCR profile was: one cycle of 4 min at 94°C, 35 cycles of 30 sec at 94°C, 30
212 sec at 60°C and 90 sec at 72°C, followed by 5 min at 72°C.

213 *Symbiodinium* clone libraries were constructed for one colony at 5 m, 10 m, and 20 m
214 from Playa Hundu. Clones were screened for the presence of the insert and forward
215 orientation by PCR using plasmid primer T7 and lsu-URP1. Clone libraries were
216 additionally screened by RFLP using *Cfo*I and *Msp*I to maximize the number of unique
217 clones for sequencing. Inoculating, culturing, prepping and sequencing were performed
218 in the High Throughput Laboratory of the University of Illinois W. M. Keck Center for

Comparative and Functional Genomics. Sequencing was performed on a 3730XL capillary sequencer (Applied Biosystems).

For T-RFLP, restriction digests were performed using the enzyme *Cfo*I. For each digest eight microliters of purified PCR product was digested with 10 U of restriction enzyme in a total volume of 20 µl. Incubation was done at 37°C for 9 h followed by 15 min at 65°C to denature the restriction enzyme. The precise length of T-RFLP fragments was determined by multicapillary electrophoresis with a model 3730XL capillary sequencer (Applied Biosystems). See Klaus et al. (*submitted*) for specific run parameters. Sample versus T-RFLP peak data matrices were constructed using peaks above a threshold of 50 units above background. Peaks smaller than 50 base pairs (bp) and larger than 1050 bp were culled from the data set. Aligned peaks were placed into bins typically less than two base pairs. Abundance data was obtained from the relative peak height following sample standardization (Blackwood et al., 2003). Variation in *Symbiodinium* communities was assessed by nonmetric multidimensional scaling of the Bray-Curtis similarity index, and statistical tests using the ANOSIM procedure of the Primer 5 v. 5.2.9 statistiscal package (Primer-E, Plymouth, UK).

AMPLIFIED FRAGMENT LENGTH POLYMORPHISMS (AFLP)

Coral colonies sampled from Jan Thiel, Water Plant and Playa Hundu were genotyped for three loci previously shown to distinguish species of the *M. "annularis"* species complex (Fukami et al. 2004). The 920/880 locus (Lopez et al., 1999) was amplified by PCR using primers (880f) CCC TGA TCA GTA TTT TGGG, and (880r) GGA GGG CTC TGT TAT TCT ATC (Integrated DNA Technologies). The 500/null locus (Fukami

et al. 2004) was amplified with primers (500f) GCC TTG GTT GAT TCT GAA ATT CG and (500r) AGA TCG AAT TAT ACA CCC ACC CA. The 410/430/450 locus was amplified with primers (410f) GAT TCA TCC CGC TGT CAA AGA, and (410r) GCC AAC CAC AGA CAG AGC GGA. PCR was performed using a reaction mixture of 0.2 mM of each deoxynucleoside triphosphate (Promega, Madison, WI), 200 ng each of the forward and reverse primers, 0.5 to 10 µl of the sample preparation, 1X Taq Master, 1X Taq Buffer (50mM KCl, 10mM Tris-HCl pH 8.3, 1.5 mM $Mg(OAc)_2$) and water to bring the total volume to 50 µl. The PCR profile was 30 sec at 94°C, 45 sec at 65°C, and 60 sec at 72°C for 30 cycles. Band patterns of the PCR products were observed using 6% acrlyamide gels.

Morphologic Analyses

To analyze differences in corallite morphology among colonies, we digitized three-dimensional Cartesian coordinates (x-y-z) of 25 landmarks on calical surfaces (Fig. 2a) using a reflex microscope. The landmarks consisted of spatially homologous points designed to reflect the shape of the septal margin (the uppermost growing edge) and costal extensions between corallites. Three adjacent costosepta were digitized on six mature calices on the top of each colony. Size and shape coordinates (Bookstein 1991) were calculated from the data using the computer program GRF-ND (Generalized rotational fitting of n-dimensional landmark data, 1994, written by Dennis E. Slice, available at http:// life.bio.sunysb.edu/morph/). Centroid size was calculated by summing the squared distances from each of the 25 landmarks to a common centroid. Shape coordinates were calculated using 23 triangles formed by triplets of the 25 points, in

265 which the same pair of landmarks (#25, #10) served as a fixed x-y baseline positioned at
266 coordinates (0, 0) and (1, 0) within a plane oriented relative to the highest point (#12) in
267 the z dimension (i.e., the z-coordinate of #12 = 0). The 23 triangles were translated,
268 rotated, and rescaled relative to the baseline. Calculation of shape coordinates in three
269 dimensions involves translation of the triangle so that one vertex lies on the origin, rigid
270 rotation and scaling about the y and z axes so that a second point is coincident with (1, 0,
271 0), and rotation about the x axis to place the third point in the first quadrant of the x-y
272 plane. The x-y-z coordinates of the 23 unfixed third points (three coordinates x 23 points
273 = 69; 69 minus the z dimension for #12 = 68 total), termed ''shape coordinates,'' served
274 as variables in subsequent statistical analyses.
275 To characterize differences in the corallite wall architecture and thickening of skeletal
276 structures two-dimensional morphologic features were similarly measured in transverse
277 thin sections. We began by digitizing 27 landmarks on mature corallites as shown in
278 Figure 2b. Data were collected on six corallites from the upper portion of the same 60
279 colonies used in the three-dimensional analyses. Size and shape coordinates were
280 calculated for the two-dimensional data using the baselines formed by points (#1, #10)
281 and (#1, #12) using the Integrated Morphometrics Package (IMP)
282 (http://www2.canisius.edu/~sheets/morphsoft.html).
283 The three-dimensional and two-dimensional datasets were analyzed independently by
284 canonical discriminant analyses using SPSS 10.0 (SPSS Inc., Chicago, IL), and
285 redundancy analysis using Brodgar v. 2 (Highland Statistics Ltd, Aberdeenshire, UK).
286

286 RESULTS

287 ENVIRONMENTAL AND PHYSIOLOGIC VARIABLES

288 During the month of July, 2004 seawater temperatures between 5 m and 20 m water
289 depth were consistently 27.5 ± 0.5°C at Jan Thiel, Water Plant and Playa Hundu. Light
290 levels at these sites varied between 33% and 36% surface PAR at 5 m, 18% and 22% at
291 10 m, and 9% and 11% at 20 m (Fig. 3a). While depth profiles of PAR appear similar at
292 each locality, Kruskal-Wallis statistical tests indicate significant differences in PAR
293 between localities at both 10 m and 20 m water depth (5 m Chi-square = 3.361, d.f. = 2, p
294 = 0.186; 10 m Chi-square = 11.735, d.f. = 2, p = 0.003; 20 m Chi-square = 20.534, d.f. =
295 2, p = 0.000).

296 Coral tissue $\delta^{15}N$ was approximately 1.5‰ higher at Jan Thiel and Water Plant, the
297 two eastern and more urban localities compared to Playa Hundu (Fig. 3b). This is
298 supported by Kruskal-Wallis statistical tests indicating significant differences in $\delta^{15}N$
299 between reef sites compared across water depth (5 m Chi-square = 6.5, d.f. = 2, p =
300 0.039; 10 m Chi-square = 9.269, d.f. = 2, p = 0.010; 20 m Chi-square = 6.00, d.f. = 2, p =
301 0.050). These results suggest higher portions of sewage in reef seawater adjacent to the
302 population center of Willemstad. No significant differences in coral tissue $\delta^{15}N$ were
303 detected between the different depths sampled at each locality (JT Chi-square = 1.43, d.f.
304 = 2, p = 0.491; WP Chi-square = 1.654, d.f. = 2, p = 0.437; PH Chi-square = 1.283, d.f. =
305 2, p = 0.526).

306 With the exception of the 20 m samples from Playa Hundu, mean values of coral
307 tissue $\delta^{13}C$ show a decreasing trend with increasing water depth (Fig. 3c). At Jan Thiel
308 and Water Plant values of $\delta^{13}C$ shift as much as 1.5 ‰ more negative. This trend suggests

309 reduced photosynthetic activity of zooxanthellae under the lower light conditions found
310 at deeper seawater depths (Heikoop et al., 2000b; Swart et al., 2005). Despite this
311 general trend, a significant difference in coral tissue $\delta^{13}C$ between water depths was
312 found only at Jan Thiel (JT Chi-square = 6.282, d.f. = 2, p = 0.043; WP Chi-square =
313 2.094, d.f. = 2, p = 0.351; PH Chi-square = 0.589, d.f. = 2, p = 0.745). Similarly, while
314 values of $\delta^{13}C$ appear to vary between localities, no significant differences in $\delta^{13}C$ were
315 found between reef localities (JT, WP, PH) compared at each water depth (5 m Chi-
316 square = 3.310, d.f. = 2, p = 0.191; 10 m Chi-square = 2.337, d.f. = 2, p = 0.126; 20 m
317 Chi-square = 6.00, d.f. = 2, p = 0.174).
318 Analysis of RFLP banding patterns in clones obtained from *Symbiodinium* sampled at
319 5 m (n = 74), 10 m (n = 75) and 20 m (n = 90) yielded 10 unique ribotypes. Phylogentic
320 analysis of multiple sequenced clones from each ribotype revealed that all sequenced
321 clones belonged to either clade B or C of the seven clades reviewed in Baker (20030.
322 Sequences from the colony sampled at 5 m belonged primarily to clade B, while
323 sequences from 10 m and 20 m were all clade C. T-RFLP profiles of the 28S rRNA gene
324 of *Symbiodinium* digested with the *Cfo*l enzyme were used to characterize differences in
325 *Symbiodinium* communities for the 36 colonies sampled. Ordination based on these T-
326 RFLP profiles shows significant relative differences in *Symbiodinium* communites from 5
327 m versus those from 10 m and 20 m (Fig. 4a). This is further supported by the ANOSIM
328 statistical test for differences between depths (5 m vs. 10 m r = 0. 535, p = 0.001; 5 m vs.
329 20 m r = 0.784, p = 0.001; 10 m vs. 20 m r = 0.058, p = 0.074). The T-RFLP peaks most
330 important in distinguishing the communities of different depths included *cfo*I-137, *cfo*I-
331 458, and *cfo*I-510. The relative abundance of these peaks within the 36 colonies is

illustrated in Figure 4b-d. By comparing the peak sizes to theoretical enzyme digests of the sequenced clones, it was determined that *cfo*I-137 is affiliated with clade B, and dominates in shallow water, while *cfo*I-458, and *cfo*I-510 are affiliated with clade C, and are more common at 10 m and 20 m. Through comparison with sequences downloaded from the NCBI database, T-RF peak *cfo*I-149 was found to be affiliated with *Symbiodinium* clade A, and more common in shallow water samples.

AFLP Markers

Genotyping of visually identified colonies of *M. annularis* from Curaçao revealed a similar genetic pattern to those obtained from previous studies in Panama and the Bahamas (Fukami et al., 2004) (Fig. 5). Based on the 920/880, 500/null, and 410/430/450 AFLP markers over 75% of the sampled colonies displayed the common AAA (920/500/410) geonotype of *M. annularis*. While the AFLP genotypes for the remaining 25% do not reflect fixed allele differences between species, they are not inconsistent with these colonies being identified as *M. annularis*. Furthermore, these genotypes do not appear to show any patterns of occurrence with either depth or locality. Unlike previous studies in Panama and the Bahamas, two colonies did display the most common F1 genotype for hybrids between *M. annularis* and *M. faveolata* ((A/B)(A/B)A).

3-D Morphometric Analyses

Canonical discriminant analysis (CDA) was performed to test for morphologic plasticity in the three-dimensional corallite architecture of *M. annularis* associated with differences in seawater depth and location along the Curaçao reef tract. To reduce the

355 number of redundant variables, statistical analyses were performed using 14 3-
356 dimensional shape variables (of the 69 that were calculated) previously used to
357 distinguish the three modern species within the complex in Panama (Budd and Klaus,
358 2001). These size and shape coordinates consist of measures of the heights, and lengths,
359 of individual septa or costae (Fig. 2).

360 To test for morphologic differences due to seawater depth, CDA was performed with a
361 priori groups defined by the three sampling depths (5 m, 10 m, 20m). Significant
362 differences (Wilks' Lambda 0.239, Chi-square 72.214, df 28, $P < 0.000$) were detected
363 along the first discriminant axis comparing the 20 samples from each depth (Fig. 6a;
364 Appendix 1). Along this axis a gradation emerged from samples collected at 5 m to
365 samples collected at 20 m. Discrimnant axis 1 describes 92% of the variation between
366 the 60 colonies of *M. annularis* and shows a strong positive correlation to variables
367 associated with septum height (Y3, Y4, Y18, Y19), costa length (X4), septum length
368 (X15, X23), and wall thickness (X14). The overall morphologic change associated with
369 decreasing water depth can be visualized in the consensus configurations of the primary
370 septum for each depth (Fig. 7).

371 To test for morphologic differences between localities, CDA was performed with a
372 priori groups defined by localities (Fig. 1). Significant differences were detected along
373 the first two discriminant axes comparing the 12 colonies sampled at each locality (Fig.
374 6b; Appendix 2). Axis 1, describing 41% of the variance, distinguishes colonies sampled
375 at Boca Simon and Playa Hundu, from those sampled at Water Plant and Snake Bay.
376 This axis is correlated with septum height (Y19), and septum length (X23, X7). Axis 2
377 describes 38% of the variance and distinguishes colonies sampled at Jan Thiel from those

sampled at the other four localities. This axis is most strongly correlated with C-size and the relative development of major versus minor costae (X16). Given that colonies sampled from Boca Simon (immediately adjacent to the seaport) and Playa Hundu (32 km downcurrent) plot virtually on top of each other, the morphologic differences between localities do not appear to be related to the seaport or urban center of Willemstad.

Redundancy analysis (RDA) was used to assess four environmental and physiologic factors thought to be important in explaining the morphologic plasticity observed along the coastal and seawater depth gradients of Curaçao. In RDA each canonical ordination axis corresponds to a direction in the multivariate scatter of morphologic variables that is maximally related to a linear combination of the explanatory variables. Five explanatory variables are included in our analyses: (1) the % noon-time surface PAR (light); (2) coral tissue $\delta^{15}N$ (sewage indicator); (3) coral tissue $\delta^{13}C$ (autotrophy:heterotrophy); (4) Zoox-1 (the first MDS axis of *Symbiodinium* communities (Fig. 4)), and 5) Zoox-2 (the second MDS axis of *Symbiodinium* communities). The cross-correlations between explanatory variables are shown in Table 2. Significant correlations were detected between PAR and Zoox-1 as well as PAR and $\delta^{13}C$.

Minimal differences were found between RDA analyses performed using colonies of *M. annularis* from all AFLP genotypes versus those limited to the AAA genotype. We present our results based on the complete dataset. Combined, the five explanatory variables explain 41.1% of the variation observed in the 14 morphological variables (Fig. 8a, see Table 3 for numerical output). Of this, 93 % could be explained by the first two axes of the resulting RDA biplot (axis 1 = 35%, axis 2 = 6%). Furthermore, Monte Carlo significance tests of all canonical axes reveal a highly significant effect due to the

401 combined environmental and physiologic variables (F = 4.772, P = 0.001). Forward
402 selection tests for explanatory variables show that no significant amount of variance is
403 explained by adding variables in addition to PAR, and the $\delta^{13}C$ of coral tissue (Table 4).
404 PAR is by far the strongest explanatory variable, independently accounting for 77% of
405 the variation explained in the RDA analysis. The strong correlation of the three-
406 dimensional morphologic variables with PAR is demonstrated by the clustering of
407 samples from each depth along axis 1. Furthermore, a biplot of the 14 morphologic
408 variables against the six explanatory variables (Fig.8b) shows that nearly all three-
409 dimensional morphologic variables are positively correlated with PAR. Zoox-1,
410 generated from *Symbiodinium* community data, was also strongly correlated to axis 1 and
411 explained a large percentage of the variation (48%). Given the strong correlation
412 between PAR and Zoox-1, it is difficult to determine how much each factor contributes to
413 the observed morphologic variations. The variance explained by coral tissue $\delta^{13}C$ does
414 not appear to be strongly related in either seawater depth or locality. Based on partial
415 correlations between $\delta^{13}C$ and all 14 morphologic variables while controlling for PAR,
416 four variables were identified as being significantly correlated to values of coral tissue
417 $\delta^{13}C$. These included: Y4 ($r = -0.3908$, $p = 0.020$) and Y19 ($r = -0.5356$, $p = 0.001$), the
418 heights of the primary and secondary septa; X11 ($r = 0.4197$, $p = 0.012$), the development
419 of the minor costae, and X16 ($r = -0.3729$, $p = 0.027$), the relative development of major
420 versus minor costae. The negative correlation of $\delta^{13}C$ with Y4 and Y19 was somewhat
421 surprising. This suggests a greater height of the primary and secondary septa under
422 conditions of reduced photosynthetic activity.
423 To determine the extent to which the observed variations in calice topography obscure

taxonomic boundaries, colonies of *M. annularis* from Curaçao were compared to genetically determined colonies of *M. franksi*, *M. faveolata*, and *M. annularis* collected at approximately 10 m water depth in Panama (Budd and Klaus, 2001; Knowlton and Budd, 2001; Fukami et al., 2004). CDA comparisons were first made using the same 14 3-dimensional morphologic variables and six a priori groups; the three genetically determined species from Panama, and the three sampling depths on Curaçao. Results show distinct separation of the three species of Panama, and distinct separation of the two geographic regions; Curaçao and Panama (Fig. 9a; Appendix 3). While three significant discriminant axes were found, the first two axes explain 85.5 % of the total variation. Discriminant axis 1 (49%) separates the Curaçao samples from the three species of Panama, and is strongly correlated to variables associated with vertical septal extension (Y4, Y3, Y19, Y18). Samples from Curaçao, in general have greater septal heights than colonies collected from Panama regardless of species. Differences between the three species from Panama are primarily separated along discriminant axis 2 (36.3%), and are most strongly correlated to Csize and variables associated with wall thickness (X14), septum length (X7, X15), relative development of major versus minor costae (X1, X16), and costae length (X19). If the discriminant analysis is limited to just these seven characters unrelated to septal extension, we see that while the three Panama species are still distinguished, the Curaçao samples form a gradient that overlaps and bridges the gap between *M. annularis* and *M. franksi* (Fig. 9b; Appendix 4). Axis 1 (70.4%) is strongly correlated to wall thickness (X14) and Csize while axis 2 (20.1%) is strongly correlated to costae length (X19) and septum length (X15).

Samples not designated to an a priori group in CDA are automatically classifed into

447 the designated group they most closely resemble. If the a priori groups used in CDA are
448 limited to the three species from Panama (Fig. 9c; Appendix 5), using all 14 characters,
449 33% of the Curaçao colonies are classified as *M. annularis*, 57% are classified as *M.*
450 *faveolata*, and 10% are classified as *M. franksi*. If the CDA is limited to the seven
451 characters that most strongly discriminate the three species from Panama (Fig. 9d;
452 Appendix 6), then 52% of the Curaçao colonies are classified as *M. annularis*, 3% are
453 classified as *M. faveolata*, and 45% are classified as *M. franksi*.
454
455 2-D MORPHOLOGIC ANALYSES
456 To test the extent of morphologic plasticity in skeletal characters preserved in
457 transverse thin sections, discriminant analyses were performed using a total of 18
458 variables, which include five linear measurements, Csize, and 12 two-dimensional shape
459 variables (of the 39 that were calculated) previously used to distinguish species within the
460 complex (Budd and Klaus, 2001). While 100% of the cumulative variance was captured
461 on the first two discriminant axes comparing samples from 5 m, 10 m, and 20 m, no
462 significant differences between the sample groups were detected (Wilks' Lambda 0.377,
463 Chi-square 47.289, df 36, P = 0.099). Similarly, no significant differences were detected
464 between localities (Wilks' Lambda 0.199, Chi-square 76.763, df 72, P = 0.329).
465 Redundancy analysis (RDA) based on the same five environmental and physiologic
466 variables as before suggests low plasticity within the 2-dimensional variables. Monte
467 Carlo significance tests of all canonical axes revealed no significant effect due to the
468 explanatory variables (F = 0.9399, P = 0.5737).

To determine the extent to which regional differences in corallite wall architecture and thickening of skeletal structures obscure taxonomic boundaries, colonies of *M. annularis* from Curaçao were again compared to genetically determined colonies of *M. franksi*, *M. faveolata*, and *M. annularis* from Panama (Budd and Klaus, 2001; Knowlton and Budd, 2001; Fukami et al., 2004). Canonical discriminat analysis based on the six a priori groups defined by species and depth (Fig. 10a; Appendix 7) shows a clear separation between the three species of Panama and a slight offset along axis 1 between *M. annularis* of Curaçao and *M. annularis* of Panama. Two significant axes were identified. Axis 1 (65%) is strongly correlated to the extension of the costae beyond the corallite wall (X2 (1-10), X8 (1-10), X14 (1-10)), wall thickness (X12 (1-10), X17 (1-10)), the outer width of the tertiary wall costoseptum, and Csize. Axis 2 (24.2%) is most strongly correlated to the width of the secondary septa (M5) and the extension of the costae beyond the corallite wall (X8 (1-10). When left unclassified, over 92 % of the Curaçao *M. annularis* are correctly classified with the *M. annularis* of Panama (Fig. 10b).

Discussion and Conclusions

Controls on Skeletal Morphology

We detected significant phenotypic plasticity in the three-dimensional calice morphology of *M. annularis* sampled between 5 m and 20 m water depth along the leeward coast of Curaçao. Significant differences in skeletal morphology were detected between water depths (Fig. 6a), localities (Fig. 6b), and geographic regions (Fig. 9a). Approximately 41% of the observed morphologic variance was explained by environmental and physiologic variables.

When analyzed independently by RDA, PAR explained 32% of the total variance whereas the $\delta^{13}C$ values of coral tissues only explained 10% of the variance. The weak explanatory power of coral tissue $\delta^{13}C$ compared to PAR suggests that either $\delta^{13}C$ values do not accurately reflect relative differences in the amount of autotrophic feeding, or much of the morphologic variation we observed in the three-dimensional corallite morphology is unrelated to differences in primary production. Without isotopic measurements of seawater DIC we cannot rule out the possibility that values of coral tissue $\delta^{13}C$ may be, to at least some extent, directly related to local variations in the isotopic composition of seawater DIC (Goericke et al., 1994; Swart et al., 1996). Previous studies on Curaçao have shown $\delta^{13}C$ values of DIC to be similar over a depth range of 5 m to 40 m (Kaandorp et al., 2005), well beyond the depth range of the current study.

Assuming values of $\delta^{13}C$ reflect primarily the relative amounts of autotrophic versus heterotrophic feeding, the fact that morphologic variables associated with septal height are positively correlated to light and negatively correlated to coral tissue $\delta^{13}C$ is somewhat surprising. This negative correlation may reflect varying degrees of nutrient

507 limitation between coral colonies. Previous reports have shown that under nutrient-
508 limiting conditions corals can calcify more despite photosynthesizing less (Marubini and
509 Thake, 1999; Marubini et al., 2002). These trends have been used to support the
510 hypothesis that calcification is a means by which corals can stimulate symbiont
511 photosynthesis (McConnaughey et al., 2000; Cohen and McConnaughey, 2003). Protons
512 generated through calcification are thought to be pumped into the coelenteron where they
513 react with HCO_3^- to replenish CO_2 used in symbiont photosynthesis (McConnaughey and
514 Whelan, 1997; McConnaughey et al., 2000). Calcification is also thought to stimulate the
515 uptake of symbiont-limiting nutrients by altering the surface charge of coral tissues
516 (McConnaughey et al., 2000).
517 Variation in *Symbiodinium* community structure was highly correlated to PAR (Fig.
518 4), and when analyzed independently accounted for twice as much morphologic variation
519 (21%) as coral tissue $\delta^{13}C$ (10%). While it is well established that coral growth and
520 calcification are generally enhanced in the presence of algal symbionts (Pearse and
521 Muscatine, 1971; Barnes and Chalker, 1990; Muscatine, 1990), there is currently no data
522 as to how different clades or species of *Symbiodinium* influence skeletogenesis. The
523 symbiont genus *Symbiodinium* is extremely diverse, with complex patterns of host-
524 symbiont pairings and strong correlations to different light, and temperature regimes
525 (Baker, 2003; Coffroth and Santos, 2005). Preliminary studies suggest variations in
526 symbiont taxa can have a considerable influence on host physiology. For example,
527 growth rates of juvenile corals experimentally inoculated with *Symbiodinium* clade C
528 have been shown to grow two to three times faster than those inoculated with clade D
529 (Little et al., 2004). Furthermore *Symbiodinium* clade A has a high tendency for the

synthesis of mycosporine-like amino acids (UV-absorbing substances thought to provide photo-protective function against UVR) while clades B and C do not (Banaszak et al., 2000). These studies suggest that in addition to being genetically diverse, the genus *Symbiodinium* is also physiologically diverse. While the current study does not provide conclusive evidence that different symbiont taxa influence skeletal morphology, this is suggested by the strong correlation of *Symbiodinium* communities with skeletal morphology. Given that *Symbiodinium* community composition is highly correlated to other potential forcing factors (e.g. light and temperature), future studies assessing how different symbiont taxa influence skeletogenesis will require a more direct experimental approach, rather than the correlative analysis of the relationships that occur in nature.

Over half of the quantified variance in the three-dimensional dataset was unexplained by the environmental and physiologic variables (Table 2). While much of this variation is likely to be random, it could also be attributed to genetic differences or environmental factors not accounted for in the current study. For example, Jan Thiel is located at the eastern end of the island where seawater currents are often the strongest. Furthermore, it is immediately adjacent to a man-made beach. Results of canonical discriminant analysis showed corallites from Jan Thiel to be smaller with poorly developed costae. Therefore, although unproven, these morphologic differences could be related to the stronger currents and presumably higher sedimentation rates at Jan Thiel.

Contrary to the three-dimensional dataset, no significant variation in the morphologic characters expressed in transverse thin sections could be accounted for by the explanatory variables identified in this study. This was somewhat surprising given that previous coral colony transplant studies of *M. annularis* on Jamaica have shown similar skeletal

553 characters to be morphologically plastic (Foster, 1979a). Aside from using different
554 techniques to quantify morphologic variation, (shape coordinates versus linear
555 measurements), the primary difference between the two studies is the range of
556 environments investigated. In the previous study, colonies were transplanted between a
557 patch reef (3 m water depth), a lagoon (16 m), a sand channel (20 m), and a framework
558 reef (20 m). These environments were shown to vary greatly not only in available light,
559 but also in water energy, sedimentation rate, and the amount of available food (Foster,
560 1979a). Comparatively, the fringing reefs sampled along the leeward coast of Curaçao
561 are all fairly similar in these regards. Foster (1979a) did not attempt to discriminate
562 between the affects of the different environmental factors. However, results from the
563 present study, sampled over a similar depth gradient (5 m to 20 m), suggest that a
564 considerable amount of the variation observed in the Jamaican corals might be due to
565 factors other than the amount of available light.
566
567 IMPLICATIONS FOR TAXONOMIC STUDIES
568 Species of *M. annularis*-like corals (similar calice diameters and numbers of septa)
569 have been ecologically dominant on Caribbean reefs since at least the early Miocene (22
570 Ma) (Budd, 1991; Knowlton and Budd, 2001). Preliminary evidence from the fossil
571 record suggests a complex evolutionary history of this group with high rates of
572 origination and extinction within diverse species complexes (Budd, 1990, 1991; Budd et
573 al., 1994; Budd and Johnson, 1997; Budd and Klaus, 2001; Pandolfi et al., 2002; Klaus
574 and Budd, 2003; Budd and Pandolfi, 2004). Species of *M. annularis*-like corals
575 additionally show a trend of increasing dominance within the Caribbean over this time

period, with the most striking shift associated with late Pliocene to early Pleistocene faunal turnover (Knowlton and Budd, 2001; Klaus and Budd, 2003). Given the dominance of *M. annularis*-like corals over the past 22 m.y., the evolutionary history of this group is likely to have played an important role in shaping the modern Caribbean reef coral fauna. Understanding the evolutionary history of *M. annularis*-like corals is dependent upon the ability to track morphologic characters and recognize species boundaries within the loose environmental constraints of coral reef facies (i.e. backreef, reef crest, forereef). The current study suggests morphologic characters preserved in transverse thin sections record genotypic information adequate for comparing species boundaries over wide geographic regions and a considerable range of seawater depths. Given that no significant differences in morphology were detected effectively over the entire depth distribution of *M. annularis* (0-20 m) provides validation to several previous and ongoing studies using the morphologic variation preserved in transverse thin sections to study the evolutionary history of the species complex in the fossil record. Patterns of origination, extinction and character evolution mapped onto a high resolution chronostratigraphic framework should provide a basis for interpreting the complex history of this group and its influence on the changing nature of Cenozoic coral reefs within the Caribbean.

The strong correlation observed in the present study between the three-dimensional topography of calice surfaces and local and regional environmental conditions, highlights the need to use these characters somewhat cautiously in taxonomic studies. That said, plastic characters are useful in taxonomic studies (Foster, 1979b). Previous studies of the *M. annularis* complex have shown that three-dimensional characters are very good at

599 distinguishing species, and typically do a better job of preserving genetic relationships
600 between the members of the complex (Budd and Klaus, 2001; Knowlton and Budd,
601 2001). Furthermore, because morphologic characters associated with phenotypic
602 plasticity can become genetically fixed (Partridge et al., 1994; Brakefield et al., 1996;
603 Brakefield et al., 1998), understanding how skeletal morphology changes in relation to
604 environmental factors can provide evidence for ecologically-driven morphologic
605 divergence. For example, we detected an overall decrease in calice height with increasing
606 water depth (Fig. 6a), which mirrors the ecological zonation of the three species within
607 the complex. *Montastraea faveolata* and *M. annularis*, most common in shallow water,
608 have greater calice heights than *M. franksi*, which is more common at deeper depths. The
609 correlation of these characters to observed phenotypic plasticity in *M. annularis* along a
610 similar depth gradient suggests these characters may be adaptive. Variation in calice
611 relief are most likely an adaptation to the amount of available light. At shallow water
612 depths high calical relief would allow the coral to self shade its tissues from harmful UV
613 radiation (Jokiel, 1980; Falkowski et al., 1990), and possibly limit excessive symbiont
614 photosynthesis. At deeper depths, reduced calical relief would allow the individual polyp
615 to expose a greater percentage of tissue to the incoming light field.
616 Much remains to be learned about the nature and implications of phenotypic plasticity
617 in corals. While mechanisms of coral skeletogenesis and the ecological and evolutionary
618 significance of observed morphologic variations are undoubtedly related, the current
619 study represents one of the first attempts to treat these variables simultaneously. Recent
620 advances in the molecular genetics of corals and associated symbionts are radically
621 changing our view of the reef ecosystem. What used to be one coral species and one

symbiont species is now three coral species and a diverse and dynamic assemblage of multiple symbionts. These findings will begin to answer previously unexplained aspects of fundamental ecosystem processes including skeletal calcification and ecological zonation.

ACKNOWLEDGMENTS

This work was supported by a research grant from the Office of Naval Research (N00014-00-0609), and UIUC Department of Geology Wanless Fellowship awarded to J. Klaus. We acknowledge the support of CARMABI in our field efforts. We also thank Al Piggot for assistance with PCR analyses, J. Heikoop, T. Larson and M. Hess for running isotopic analyses, K. Seville for preparing thin sections, and T. Fadigan for measuring the 2-dimensional landmarks.

635 LITERATURE CITED

636 Baker, A.C. 2001. Reef corals bleach to survive. Nature 411: 765-766.

637 Baker, A.C. 2003. Flexibility and specificity in coral-algal symbiosis: diversity, ecology,
638 and biogeography of *Symbiodinium*. Annu. Rev. Ecol. Evol. S. 34: 661-689.

639 Banaszak, A.T., T.C. LaJeunesse, and R.K. Trench. 2000. The synthesis of mycosporine-
640 like amino acids (MAAs) by cultured, symbiotic dinoflagellates. J. Exp. Mar. Biol.
641 Ecol. 249: 219-233.

642 Barnes, D.J. and B. E. Chalker 1990. Calcification and photosynthesis in reef-building
643 corals and algae. Pages 109-131 *in* Z. Dubinsky, ed. Coral reefs. Ecosystems of the
644 world vol. 25. Elsevier Science, Amsterdam.

645 Barnes, D.J. and C.J. Crossland. 1980. Diurnal and seasonal variations in the growth of a
646 staghorn coral measured by time-lapse photography. Limnol. Oceanogr. 25: 1113-
647 1117.

648 Barnes, D.J. and J.M. Lough. 1993. On the nature and causes of density banding in
649 massive coral skeletons. J. Exp. Mar. Biol. Ecol. 167: 91-108.

650 Blackwood, C.B., T. Marsh, K. Sang-Hoon, and E.A. Paul. 2003. Terminal restriction
651 fragment length polymorphism data analysis for quantitative comparison of microbial
652 communities. Appl. Environ. Microbiol. 69: 926-932.

653 Bookstein, F.L. 1991. Morphometric tools for landmark data. Cambridge University
654 Press, Cambridge. 435 p.

655 Brakefield, P.M., F. Kesbeke, and P.B. Koch. 1998. The regulation of phenotypic
656 plasticity of eyespots in the butterfly *Bicyclus anynana*. Am. Nat. 152: 853-860.

657

658 _____, J. Gates, D. Keys, F. Kesbeke, P.J. Wijngaarden, A. Monteiro, V.
659 French, and S.B. Carroll. 1996. Development, plasticity and evolution of butterfly
660 eyespot patterns. Nature 384: 236-242.
661 Bruno, J.F. and P.J. Edmunds. 1998. Metabolic consequences of phenotypic plasticity in
662 the coral *Madracis mirabilis* (Duchassaing and Michelotti): the effect of morphology
663 and water flow on aggregate respiration. J. Exp. Mar. Biol. Ecol. 229: 187-195.
664 Budd, A.F. 1990. Longterm patterns of morphological variation witin and among species
665 of reef-corals and their relationship to sexual reproduction. Syst. Bot. 15: 150-165.
666 _____. 1991. Neogene Paleontology in the Northern Dominican Republic. 11. The
667 Family Faviidae (Anthozoa: Scleractinia). 5-83.
668 _____. 1993. Variation within and among morphospecies of *Montastraea*. Cour.
669 Forsch-inst. Senckenb. 164: 541-254.
670 _____. 2000. Diversity and extinction in the Cenozoic history of Caribbean reefs.
671 Coral Reefs 19: 25-35.
672 _____. and K.G. Johnson. 1997. Coral reef community dynamics of 8 myr of
673 evolutionary time: Stasis and turnover. Proc. 8th Intl. Coral Reef Symp. 1: 423-428.
674 _____. and J.S. Klaus. 2001. The origin and early evolution of the *Montastraea*
675 *annularis* species complex (Anthozoa: Scleractinia). J. Paleontol. 75: 527-545.
676 _____. and J.M. Pandolfi. 2004. Overlapping species boundaries and hybridization
677 within the *Montastraea "annularis"* reef coral complex in the Pleistocene of the
678 Bahamas Islands. Paleobiology 30: 396-425.
679 _____, K.G. Johnson, and D.C. Potts. 1994. Recognizing morphospecies in colonial
680 reef corals. I. Paleobiology 20: 484-505.

681 Carlon, D.B. and A.F. Budd. 2002. Incipient speciation across a depth gradient in a
682 scleractinian coral. Evolution 56: 2227-2242.
683 Carricart-Ganivet, J.P. and M. Merino. 2001. Growth responses of the reef-building coral
684 *Montastraea annularis* along a gradient of continental influence in the southern Gulf
685 of Mexico. B. Mar. Sci. 68: 133-146.
686 Chalker, B.E. and D.L. Taylor. 1975. Light-enhanced calcification and the role of
687 oxidative phosphorylation in calcification of the coral *Acropora cervicornis*. P. Roy.
688 Soc. B-Biol. Sci. 190: 179-189.
689 Chang, F.H. 1983. Winter phytoplankton and microzooplankton populations off the coast
690 of Westland, New Zealand, 1979. NZ. J. Mar. Freshw. Res. 17: 279-304.
691 Coffroth, M.A. and S.R. Santos. 2005. Genetic diversity of symbiotic dinoflagellates in
692 the genus *Symbiodinium*. Protist 156: 19-34.
693 Cohen, A.L., and T.A. McConnaughey. 2003. Geochemical perspectives on coral
694 mineralization. Pages 151-187 *in* P.M. Dove, J.J. De Yoreo, and S. Weiner, eds.
695 Biomineralization. Reviews in mineralogy and geochemistry vol. 54. The
696 Mineralogical Society of America, Washington, D.C.
697 Cohen, A.L., S.R. Smith, M.S. McCartney, and J. van Etten. 2004. How brain corals
698 record climate: an integration of skeletal structure, growth and chemisty of *Diploria*
699 *labyrinthiformis* from Bermuda. Mar. Ecol-Prog. Ser. 271: 147-158.
700 Cook, C.B., E.M. Mueller, M.D. Ferrier, and E. Annis. 2002. The influence of nearshore
701 waters on corals of the Florida reef track. Pages 771-778 *in* J.W. Porter and K.G.
702 Porter, eds. The Everglades, Florida Bay, and coral reefs of the Florida Keys: an
703 ecosystem sourcebook. CRC, Boca Raton.

704 Dodge, R.E. and J.R. Vaisnys. 1975. Hermatypic coral growth banding as environmental
705 recorder. Nature 258: 706-708.
706 Dustan, P. 1975. Growth and form in the reef building coral *Montastrea annularis*. Mar.
707 Biol. 33: 101-107.
708 Edinger, E.N., G.V. Limmon, J. Jompa, W. Widjatmoko, J.M. Heikoop, and M.J. Risk.
709 2000. Normal coral growth rates on dying reefs: are coral growth rates good
710 indicators of reef health? Mar. Pollut. Bull. 40: 404-425.
711 Ellis, J. and D. Solander. 1786. The natural history of many curious and common
712 zoophytes. London. 208 p.
713 Falkowski, P.G., P.L. Jokiel, and R.A. Kinzie III. 1990. Irradiance and corals. Pages 89-
714 108 *in* Z. Dubinsky, ed. Coral Reefs. Ecosystems of the world vol. 25. Elsevier
715 Science, Amsterdam.
716 Foster, A.B. 1979a. Phenotypic plasticity in the reef corals *Montastraea annularis* (Ellis
717 and Solander) and *Siderastrea siderea* (Ellis and Solander). J. Exp. Mar. Biol. Ecol.
718 39: 25-54.
719 _____. 1979b. Environmental variation in a fossil scleractinian coral. Lethaia 12:
720 245-262.
721 _____. 1980. Environmental variation in skeletal morphology within the Caribbean
722 reef corals *Montastraea annularis* and *Siderastrea siderea*. B. Mar. Sci. 30: 678-709.
723 _____. 1983. The relationship between corallite morphology and colony shape in
724 some massive reef-corals. Coral Reefs 2: 19-25.
725 _____. 1985. Variation within coral colonies and its importance for interpreting
726 fossil species. J. Paleontol. 59: 1359-1383.

727 Fukami, H., A.F. Budd, D.R. Levitan, J. Jara, R. Kersanach, and N. Knowlton. 2004.
728 Geographic differences in species boundaries among members of the *Montastraea*
729 *annularis* complex based on molecular and morphological markers. Evolution 58:
730 324-337.
731 Gast, G.J. 1998. Nutrient pollution in coral reef waters. Reef care Curaçao workshop on
732 nutrient pollution 5: 13.
733 Given, R.K. and B.H. Wilkinson. 1985. Kinetic control of morphology, composition and
734 mineralogy of abiotic sedimentary carbonates. J. Sediment. Petrol. 55: 109-119.
735 Gladfelter, E.H. 1982 Skeletal development in *Acropora cervicornis*. 1. Patterns of
736 calcium carbonate accretion in the axial corallite. Coral Reefs 1: 45-51.
737 _____. 1983. Skeletal development in *Acropora cervicornis*. Diel patterns of
738 calcium carbonate accretion. Coral Reefs 2: 91-100.
739 Goericke, R., J.P. Montoya, and B. Fry. 1994. Physiology of isotopic fractionation in
740 algae and cyanobacteria. Pages 187-221 *in* K. Lajtha, and R.H. Michener, eds. Stable
741 isotopes in ecology and environmental science. Blackwell, London.
742 Goreau, T.F. 1959. The physiology of skeletal formation in corals I. A method for
743 measuring the rate of calcium deposition by corals under different conditions. Biol.
744 Bull. 116: 59-75.
745 _____. 1963. Calcium carbonate deposition by coralline algae and corals in relation
746 to their roles as reef-builders. Ann. NY. Acad. Sci. 107: 127-167.
747 _____. and J.W. Wells. 1967. The shallow-water Scleractinia of Jamaica: revised list
748 of species and their vertical distribution range. B. Mar. Sci. 17: 442-453.

749 Graus, R.R. and I.G. Macintyre. 1982. Variation in growth forms of the reef coral
750 *Montastrea annularis* (Ellis and Solander): a quantitative evaluation of growth
751 response to light distribution using computer simulation. Pages 441-464 *in* K. Rutzler
752 and I.G. Macintyre eds. The Atlantic Barrier Reef Ecosystem at carrie Bow Cay,
753 Belize, I Structure and Communities. Smithsonian contributions to marine science.
754 Smithsonian Institution Press, Washington D.C.
755 Gregory, J.W. 1895. Contributions to the paleontology and physical geology of the West
756 Indies. Quat. J. Geol. Soc. Lon. 51: 255-312.
757 Heikoop, J.M., J.J. Dunn, M.J. Risk, I.M. Sandeman, H.P. Schwarcz, and N. Waltho.
758 1998. Relationship between light and the $\delta^{15}N$ of coal tissue: Examples from Jamaica
759 and Zanzibar. Limnol. Oceanogr. 43: 909-920.
760 _____, J.J. Dunn, M.J. Risk, T. Tomascik, H.P. Schwarcz, I.M. Sandeman, and,
761 P.W. Sammarco. 2000a. $\delta^{15}N$ and $\delta^{13}C$ of coral tissue show significant inter-reef
762 variation. Coral Reefs 19: 189-193.
763 _____, M.J. Risk, D.D. Hickmott, C.K. Shearer, R. Beukens, and V. Atudorei.
764 2002. Potential climate signals from the deep-sea gorgonian coral *Primnoa*
765 *resedaeformis*. Hydrobiologia 471: 117-124.
766 _____, M.J. Risk, A.V. Lazier, E.N. Edinger, J. Jompa, G.V. Limmon, J.J. Dunn,
767 D.R. Brown, and H.P. Schwarz. 2000b. Nitrogen-15 signals of anthropogenic nutrient
768 loading in reef corals. Mar. Pollut. Bull. 40: 628-636.
769 Iglesias-Prieto, R. and R.K. Trench. 1997. Acclimation and adaptation to irradiance in
770 symbiotic dinoflagellates. II. Response of chlorophyll-protein complexes to different
771 photon-flux densities. Mar. Biol. 130: 23-33.

772 Jackson, J.B.C. 1979. Morphological strategies of sessile animals. Pages 499-555 *in* G.
773 Larwood and B.R. Rosen eds. Biology and systematics of colonial organisms.
774 Academic Press, New York.
775 Jaubert, J. 1977. Light, metabolism and growth forms of the hermatypic coral *Synaraea*
776 *convexa* Verrill in the lagoon of Moorea (French Polynesia). Proc. 3rd Intl. Coral
777 Reef Symp. 1. 483-488.
778 Johnson, K.G. and A.F. Budd. 1995. Extinction selectivity and ecology of Neogene
779 Caribbean reef corals. Paleobiology 21: 52-73.
780 Jokiel, P.L. 1978. Effect of water motion on reef-corals. J. Exp. Mar. Biol. Ecol. 35: 87-
781 97.
782 _____. 1980. Solar ultaviolet radiation and coral reef epifauna. Science 207: 1069-
783 1071.
784 Kaandorp, J.A., P.M.A. Sloot, R.M. Merks, R.P.M. Bak, M.J.A. Vermeij, and C. Maier.
785 2005. Morphogenesis of the branching reef coral *Madracis mirabilis*. P. Roy. Soc. B-
786 Biol. Sci. 272: 127-133.
787 Klaus, J.S. and A.F. Budd. 2003. Comparison of Caribbean coral reef communities
788 before and after the Plio-Pleistocene faunal turnover: analyses of two Dominican
789 Republic reef sequences. Palaios 18: 3-21.
790 _____, J. Frias-Lopez, G.T. Bonheyo, J.M. Heikoop, and B.W. Fouke. 2005.
791 Bacterial communities inhabiting the healthy tissues of two Caribbean reef corals:
792 interspecific and spatial variation. Coral Reefs 24: 129-137.

793 Knowlton, N. and A.F. Budd. 2001. Recognizing coral species past and present. Pages
794 97-119 *in* J.B.C. Jackson, S. Lidgard, and F.K. Mckinney, eds. Evolutionary patterns:
795 growth, form and tempo in the fosil record. University of Chicago Press, Chicago.
796 _____, E. Weil, L.A. Weigt, and H.M. Guzman. 1992. Sibling species in
797 *Montastraea annularis*, coral bleacing, and the coral climate record. Science 255:
798 330-333.
799 Lasker, H.R. 1981. Phenotypic variation in the coral *Montastraea cavernosa* and its
800 effects on colony energetics. Biol. Bull. 160: 292-302.
801 Le Tissier, M. 1988. Diurnal patterns of skeletal formation in *Pocillopra damicornis*
802 (Linneaus). Coral Reefs 7: 81-88.
803 Lesser, M.P., V.M. Weis, M.R. Patterson, P.L. Jokiel. 1994. Effects of morphology and
804 water motion on carbon delivery and productivity in the reef coral, *Pocillopora*
805 *damicornis* (Linnaeus): diffusion barriers, inorganic carbon limitation, and
806 biochemical plasticity. J. Exp. Mar. Biol. Ecol. 178: 153-179.
807 Little, A.F., M.J.H. van Oppen, and B.L. Willis. 2004. Flexibility in algal endosymbioses
808 shapes growth in reef corals. Science 304: 1492-1494.
809 Lopez, J.V., R. Kersanach, S.A. Rehner, and N. Knowlton. 1999. Molecular
810 determinzation of species boundaries in corals: genetic analysis of the *Montastraea*
811 *annularis* complex using amplified fragment lengh polymorphism and a
812 microsatellite marker. Biol. Bull. 196: 80-89.
813 Lough, J.M. and D.J. Barnes. 2000. Environmental controls on growth of the massive
814 coral *Porites*. J. Exp. Mar. Biol. Ecol. 245: 225-243.

815 Maier, C., J. Patzold, and R.P.M. Bak. 2003. The skeletal isotopic composition as an
816 indicator of ecological and physiological plasticity in the coral genus *Madracis*. Coral
817 Reefs 22: 370-380.
818 Marubini ,F., and B. Thake. 1999. Bicarbonate addition promotes coral growth. Limnol.
819 Oceanogr. 44: 716-720.
820 _____, C. Ferrier-Pages, and J. Cuif. 2002. Suppression of skeletal growth in
821 scleractinian corals by decreasing ambient carbonate-ion concentration: a cross-
822 family comparison. P. Roy. Soc. B-Biol. Sci. 270: 179-184.
823 McConnaughey, T.A. and J.F. Whelan. 1997. Calcification generates protons for nutrient
824 and bicarbonate uptake. Earth-Sci. Rev. 42: 95-117.
825 _____, W.H. Adey, and A.M. Small. 2000. Community and
826 environmental influences on reef coral calcification. Limnol. Oceanogr. 45: 1667-
827 1671.
828 Miller, K.J. and A.H. Benzie. 1997. No clear genetic distinction between morphological
829 species within the coral genus *Platygyra*. B. Mar. Sci. 61: 907-917.
830 Muko, S., K. Kawasaki, K. Sakai, F. Takasu, and N. Shigesada. 2000. Morphological
831 plasticity in the coral *Porites sillimaniani* and its adaptive significance. B. Mar. Sci.
832 66: 225-239.
833 Muscatine, L. 1990. The role of symbiotic algae in carbon and energy flux in reef corals.
834 Pages 75-87 *in* Z. Dubinsky, ed. Coral Reefs. Ecosystems of the World, vol
835 25.Elsevier Science, Amsterdam.
836 Pandolfi, J.M., C.E. Lovelock, and A.F. Budd. 2002. Character release following
837 extinction in a Caribbean reef coral species complex. Evolution 56: 479-501.

838 Partridge, L., B. Barrie, K. Fowler, and V. French. 1994. Evolution and development of
839 body size and cell size in *Drosophila melanogaster* in response to temperature.
840 Evolution 48: 1269-1276.
841 Pearse, V.B. and L. Muscatine. 1971. Role of symbiotic algae (zooxanthellae) in coral
842 calcification. Biol Bull 14: 350-363.
843 Porter, J.W. 1976. Autotrophy, heterotrophy, and resource partitioning in Caribbean reef-
844 building corals. Am. Nat. 110: 731-742.
845 Roos, P.J. 1967. Growth and occurence of the reef coral *Porites asteroides* Lamarck in
846 relation to submarine irradiance distribution. Ph.D. Diss., Drukkerij Elinkwijk,
847 Utrecht 72 p.
848 Rowan, R. and N. Knowlton. 1995. Intraspecific diversity and ecological zonation in
849 coral algal symbiosis. P. Natl. Acad. Sci. USA 92: 2850-2853.
850 _____, N. Knowlton, A. Baker, and J. Jara. 1997. Landscape ecology of algal
851 symbionts creates variation in episodes of coral bleaching. Nature 388: 265-269.
852 Swart, P., A. Saied, and K. Lamb. 2005. Temporal and spatial variation in the $\delta^{15}N$ and
853 $\delta^{13}C$ of coral tissue and zooxanthellae in *Montastraea faveolata* collected from the
854 Florida reef tract. Limnol. Oceanogr. 50: 1049-1058.
855 _____, J.J. Leder, A.M. Szmant, and R.E. Dodge. 1996. The origin of variations in the
856 isotopic record of scleractinian corals: II. Carbon. Geochim. Cosmochim. Ac. 60:
857 2871-2885.
858 Tomascik, T. 1990. Growth rates of two morphotypes of *Montastrea annularis* along a
859 eutrophication gradient, Barbados, W.I. Mar. Pollut. Bull. 21: 376-381.

Vago, R., E. Gill, and J.C. Collingwood. 1997. Laser measurements of coral growth. Nature 386: 30-31.

Van Duyl, F.C. 1985. Atlas of the living reefs of Curaçao and Bonaire (Netherlands Antilles). Foundation for Scientific Research in Surinam and the Netherlands Antilles, Utrecht.

van Oppen, M.J.H., F.P. Palstra, A.M-T. Piquet, and D.J. Miller. 2001. Patterns of coral-dinoflagellate associations in *Acropora*: significance of local availability and physiology of *Symbiodinium* strains and host-symbiont selectivity. P. Roy. Soc. Lond. B. Bio. 268: 1759-1767.

van Veghel, M.L.J. 1994a. Polymorphism in the Caribbean reef building coral *Montastraea annularis*. Ph.D. Diss., University of Amsterdam, Amsterdam 128 p.

_____. 1994b. Reproductive characteristics of the polymorphic Caribbean reef building coral *Montastrea annularis*. I. Gametogenesis and spawning behavior. Mar. Ecol-Prog. Ser. 109: 209-219.

_____. and R.P.M. Bak. 1993. Intraspecific variation of a dominant Caribbean reef building coral, *Montastraea annularis*: genetic, behavioral and morphometric aspects. Mar. Ecol-Prog. Ser. 92: 255-265.

_____. and _____. 1994. Reproductive characteristics of the polymorphic Caribbean reef building coral *Montastrea annularis*. III. Reproduction in damaged and regenerating colonies. Mar. Ecol-Prog Ser. 109: 229-233.

_____. and H. Bosscher. 1995. Variation in linear growth and skeletal density within the polymorphic reef building coral *Montastrea annularis*. B. Mar. Sci. 56: 902-908.

883 _____ and M.E.H. Kahmann. 1994. Reproductive characteristics of the
884 polymorphic Caribbean reef building coral *Montastrea annularis*. II. Fecundity and
885 colony structure. Mar. Ecol-Prog. Ser. 109: 221-227.
886 Vandermuelen, J.H., J.H. Davies, and L. Muscatine. 1972. The effects of inhibitors of
887 photosynthesis on zooxanthellae from corals and other invertebrates. Mar. Biol. 16:
888 185-191.
889 Veron, J.E.N. and M. Pichon. 1976. Scleractinia of eastern Australia. Part I. Australian
890 Institute of Marine Sciences Mongraph. Series: 1-84.
891 Weil, E. and N. Knowlton. 1994. A multi-character analysis of the Caribbean coral
892 *Montastraea annularis* (Ellis and Solander, 1786), and its two sibling species, *M.*
893 *faveolata* (Ellis and Solander, 1786) and *M. franksi* (Gregory, 1895). B. Mar. Sci. 55:
894 151-175.
895 Zardoya, R., E. Costas, V. Lopez-Rodas, A. Garrido-Pertierra, and J.M. Bautista. 1995.
896 Revised dinoflagellate phylogeny inferred from molecular analysis of large-subunit
897 ribosomal RNA gene sequences. J. Mol. Evol. 41: 637-645.
898
899 ADDRESSES: (J.S.K.) Marine Geology and Geophysics, Rosenstiel School of Marine and
900 Atmospheric Science, University of Miami, Miami, Florida 33149. (A.F.B.) Department
901 of Geoscience, University of Iowa, Iowa City, Iowa 52242. (B.W.F.) Department of
902 Geology, University of Illinois, Urbana, Illinois 61801. CORRESPONDING AUTHOR:
903 (J.S.K.) E-mail: <jklaus@rsmas.miami.edu>.

904

905 Table 1. Cross-correlations between explanatory variables used in RDA (asterisks
906 indicate significant correlations $P < 0.05$).

	PAR	$\delta^{15}N$	$\delta^{13}C$	Zoox 1
$\delta^{15}N$	-0.04			
$\delta^{13}C$	0.45*	-0.08		
Zoox 1	0.75*	-0.26	0.31	
Zoox 2	0.04	-0.32	0.16	0.05

907

908

909 Table 2. Numerical output of Redundancy analyses performed on 3-D morphologic
910 variables.

	% morphologic Variance	% sum of canonical eigenvalues	Monte Carlo F-ratio	Monte Carlo P-value
3-D Axis 1	35.9	79.5		
3-D Axis 2	6.5	14.4		
Total	42.4	93.9	3.979	0.0001

911

912

913

914

915 Table 3. Numerical output of Redundancy analyses performed on three-dimensional
916 shape variables.

	Correlation with axis 1	Correlation with axis 2	% sum of all canonical eigenvalues	Forward selection tests	
				F statistic	P-value
PAR	0.99	0.04	77.40	17.741	0.001
$\delta^{13}C$	0.44	0.35	24.69	2.942	0.016
$\delta^{15}N$	0.52	-0.80	24.35	1.259	0.268
Zoox-1	0.77	-0.11	47.88	0.656	0.682
Zoox-2	-0.05	-0.06	2.28	0.619	0.714

917

FIGURES

Figure 1. Map of Curaçao, Netherlands Antilles, in the southern Caribbean Sea. The five sites chosen for this project are distributed along the leeward coast of the island as indicated. The major seaport of St. Annabaai and the urban area of Willemstad are shown. Boca Simon and Water Plant are the most environmentally impacted sites, while Playa Hundu is the least impacted site.

Figure 2. Schematic diagrams showing landmarks used in morphometric analyses. (A) Scanning electron micrograph of corallite and schematic diagrams (left, vertical profiles of costosepta; right, calical surface) showing landmark positions used in three-dimensional analyses. Points 10, 25 and 12 were used as a baseline. Scale bar is 1.5 mm. (B) Thin section photo and schematic diagram showing 27 two-dimensional landmarks collected on transverse thin sections of corallites. Only selected landmarks are indicated in thin section on left. Points 1 and 12, and points 1 and 14 were used as baselines. Scale bar is 1.5 mm.

Figure 3. Environmental and physiological variables used to explain morphologic variance collected at three depths at three localities along the leeward coast of Curaçao. (A) The percent noon-time surface PAR. Each point represents the mean and standard deviation of ten replicate measurements. (B) Coral tissue $\delta^{15}N$ from *Montastraea annularis*. Each point represents the mean and

standard deviation of four samples. (C) Coral tissue $\delta^{15}N$ from *Montastraea annularis*. Each point represents the mean and standard deviation of four samples.

Figure 4. NMDS ordination of *Symbiodinium* communities inhabiting the tissues of *Montastraea annularis* (n = 36). Ordination based on the Bray-Curtis similarity coefficient between T-RFLP profiles of the 28S rRNA gene of *Symbiodinium* digested with the *Cfo*I enzyme. (A) Plot showing the relative similarity of *Symbiodinium* communites from 5 m, 10 m and 20 m. (B) Plot showing the relative abundance of clade B T-RF *Cfo*I-137 mapped on the ordination of (A). (C) Plot showing the relative abundance of clade C T-RF *Cfo*I-458 mapped on the ordination of (A). (D) Plot showing the relative abundance of clade C T-RF *Cfo*I-510 mapped on the ordination of (A).

Figure 5. Frequency distribution of three-locus AFLP genotypes in Curaçao, Panama, and the Bahamas. Order of alleles is 920/880, 500/null, 450/430/410

Figure 6. Plots of the first two canonical functions in discriminant analyses distinguishing *Montastraea annularis* colonies collected from different water depths and localities on the leeward coast of Curaçao. (A) A priori groups defined by seawater depth. Function 1 (92% of variation) is positively correlated to septum height, costa length, septum length, and wall thickness. (B) A priori groups defined by locality. Function 1 (41%) is correlated with

963 septum height, and septum length. Function 2 (38%) is correlated with C-
964 size and the relative development of major versus minor costae.
965
966 Figure 7. Consensus configurations of the primary septocostae from 5 m, 10 m, and 20
967 m. The background mesh represents the morphologic deformation relative to
968 the 5 m consensus configuration.
969
970 Figure 8. Redundancy analysis (RDA) biplot of 36 coral samples of *Montastraea*
971 *annularis* based on 14 three-dimensional morphologic variables and seven
972 environmental and physiologic explanatory variables. Together, axis 1 and
973 axis 2 account for 41.1% of the variation observed in the morphologic
974 variables. Explanatory variables are described within the text. See tables 2
975 and 3 for numerical output.
976
977
978 Figure 9. Plots of the first two canonical functions in discriminant analyses comparing
979 the tree-dimensional morphology of *Montastraea annularis* colonies
980 collected from Curaçao to colonies of *Montastraea faveolata*, *Montastraea*
981 *annularis*, and *Montastraea franksi* collected in Panama. (A) CDA based on
982 14 three-dimensional variables with a priori groups defined the three species
983 from Panama, and the three seawater depths sampled in Curaçao. Function 1
984 (49%) is correlated to variables associated with septal height. Function 2
985 (36%) is strongly correlated to csize, wall thickness, septum length, the

relative development of major versus minor costate, and costae length. (B) CDA based on seven three-dimensional variables with a priori groups defined the three species from Panama, and the three seawater depths sampled in Curaçao. Function 1 (70%) is correlated to wall thickness and Csize. Function 2 (20%) is strongly correlated to costae length and septum length. (C) CDA based on 14 three-dimensional variables with a priori groups defined by the three species from Panama, with Curaçao samples left unclassified. 33% of the Curaçao samples are classifed as *Montastraea annularis*, 57% as *Montastraea faveolata*, 10% as *Montastraea franksi*. (D) CDA based on seven three-dimensional variables with a priori groups defined by the three species from Panama, with Curaçao samples left unclassified. 52% of the Curaçao samples are classifed as *Montastraea annularis*, 3% as *Montastraea faveolata*, 45% as *Montastraea franksi*.

Figure 10. Plots of the first two canonical functions in discriminant analyses comparing the two-dimensional morphology of *Montastraea annularis* colonies collected from Curaçao to colonies of *Montastraea faveolata*, *Montastraea annularis*, and *Montastraea franksi* collected in Panama. (A) CDA based on 18 two-dimensional variables with a priori groups defined the three species from Panama, and the three seawater depths sampled in Curaçao. Function 1 (65%) is correlated to the extension of the costae beyond the corallite wall, wall thickness, the outer width of the tertiary wall costoseptum and Csize. Function 2 (24%) is strongly correlated to the width of the secondary septa

and the extension of the costae beyond the corallite wall. (D) CDA based on 18 three-dimensional variables with a priori groups defined by the three species from Panama, with Curaçao samples left unclassified. 92% of the Curaçao samples are classifed as *Montastraea annularis*, 2% as *Montastraea faveolata*, 6% as *Montastraea franksi*.

1014 Appendix 1 - Structure matrix figure 6a

	Function 1
CSIZE	-0.089
X1	0.024
X4	-0.780
X7	-0.261
X11	-0.332
X14	0.512
X15	-0.074
X16	-0.464
X19	0.982
X23	0.656
Y18	0.206
Y19	-0.495
Y3	-0.024
Y4	1.235

1015

1016 Appendix 2 - Structure matrix figure 6b

	Function 1	Function 2
Y19	-0.312	-0.281
X7	0.275	-0.132
Y3	-0.202	-0.090
Y18	-0.169	-0.105
CSIZE	-0.101	0.509
X16	0.008	-0.345
X4	0.132	0.189
X19	0.126	0.141
X11	0.038	0.341
X23	0.311	0.105
X15	0.214	0.039
X14	0.003	0.004
Y4	-0.087	-0.114
X1	0.030	0.120

1017

1018 Appendix 3 - Structure matrix figure 9a

	Function 1	Function 2	Function 3
Y4	0.726	-0.063	0.309
Y3	0.670	-0.063	0.130
Y19	0.612	-0.143	0.443
Y18	0.542	-0.182	-0.032
X14	0.316	-0.592	-0.273
CSIZE	-0.011	0.483	0.199
X11	0.200	0.050	-0.543
X19	0.315	-0.174	-0.537
X23	0.283	-0.144	-0.470
X4	0.331	-0.130	-0.454
X1	0.055	-0.197	0.109
X7	0.214	-0.310	0.124
X16	0.046	-0.150	0.057
X15	0.315	-0.296	-0.315

1019 Appendix 4 - Structure matrix figure 9b

	Function 1	Function 2	Function 3
Y4	-0.681	0.626	0.291
CSIZE	0.512	-0.075	0.407
X19	-0.239	0.919	0.115
X15	-0.370	0.719	0.367
X7	-0.370	0.219	0.696
X1	-0.222	-0.016	0.278
X16	-0.163	0.016	0.132

1020

1021

1022 Appendix 5 - Structure matrix figure 9c

	Function 1	Function 2
Y19	0.618	-0.046
Y3	0.502	0.086
Y4	0.487	0.006
Y18	0.403	0.291
X7	0.390	0.263
X1	0.237	0.167
X16	0.132	-0.011
X19	0.143	0.663
X4	0.146	0.641
X23	0.121	0.582
X11	-0.086	0.574
X14	0.450	0.536
X15	0.250	0.481
CSIZE	-0.270	-0.359

1023

1024

1025

1026 Appendix 6 - Structure matrix figure 9d

	Function 1	Function 2
X14	-0.796	-0.330
X7	-0.632	-0.024
X15	-0.495	-0.420
CSIZE	0.488	0.247
X1	-0.387	-0.024
X16	-0.185	0.121
X19	-0.393	-0.742

1027

1028

1029 Appendix 7 - Structure matrix figure 10a

	Function 1	Function 2
X2_10	0.565	0.033
X8_10	0.538	-0.309
X12_10	0.522	0.267
X17_10	0.503	0.285
X14_10	0.502	0.069
Y18Y17	0.397	0.025
X13_12	0.172	-0.079
X7_12	-0.165	-0.047
M5	-0.227	0.390
M3	0.046	-0.152
Y17_12	0.041	0.189
CSIZE	-0.335	-0.194
M1	-0.036	0.022
M2	-0.233	0.152
X11_12	0.141	-0.008
Y9_10	-0.413	-0.132
Y15_10	0.180	0.108

1030

1031

1032 Appendix 8 - Structure matrix figure 10b.

	Function 1
X12_10	0.321
X17_10	0.319
X14_10	0.281
Y18Y17	0.186
X7_12	-0.105
X11_12	0.062
X8_10	0.070
Y9_10	-0.240
CSIZE	-0.215
X2_10	0.287
M2	-0.013
Y15_10	0.140
M3	-0.063
M5	0.120
M10	-0.093
Y17_12	0.110
M1	0.000
X13_12	0.036

1033

Figure 1

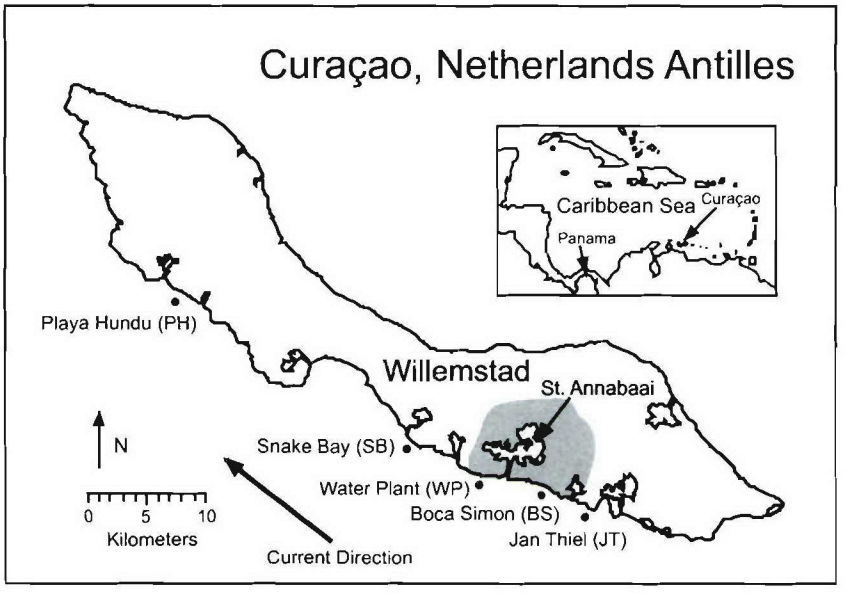
Curaçao, Netherlands Antilles
Caribbean Sea
Curaçao
Panama
Playa Hundu (PH)
Willemstad
St. Annabaai
N
Snake Bay (SB)
Water Plant (WP)
Boca Simon (BS)
Jan Thiel (JT)
0 5 10
Kilometers
Current Direction

Figure 2

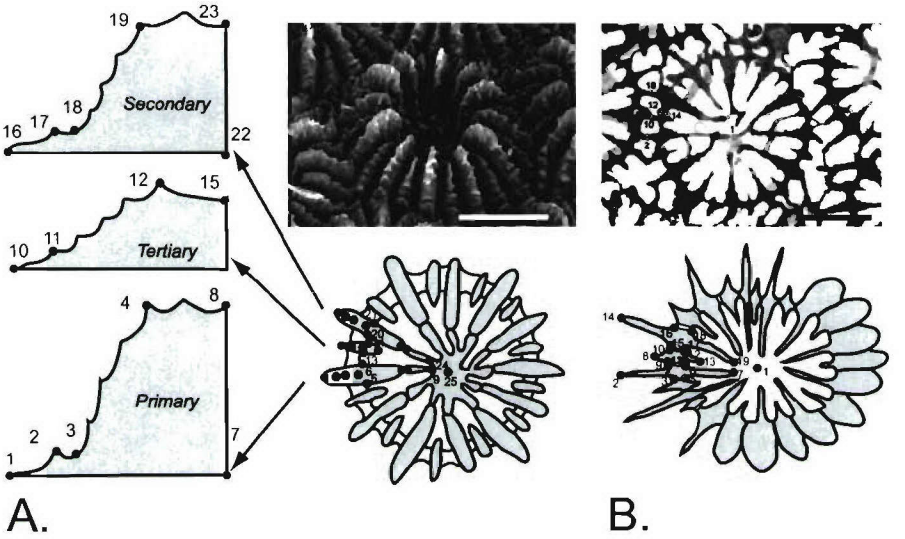
19
23
Secondary
16
17
18
22
12
15
Tertiary
10
11
4
8
Primary
1
2
3
7
A.
B.

Figure 3

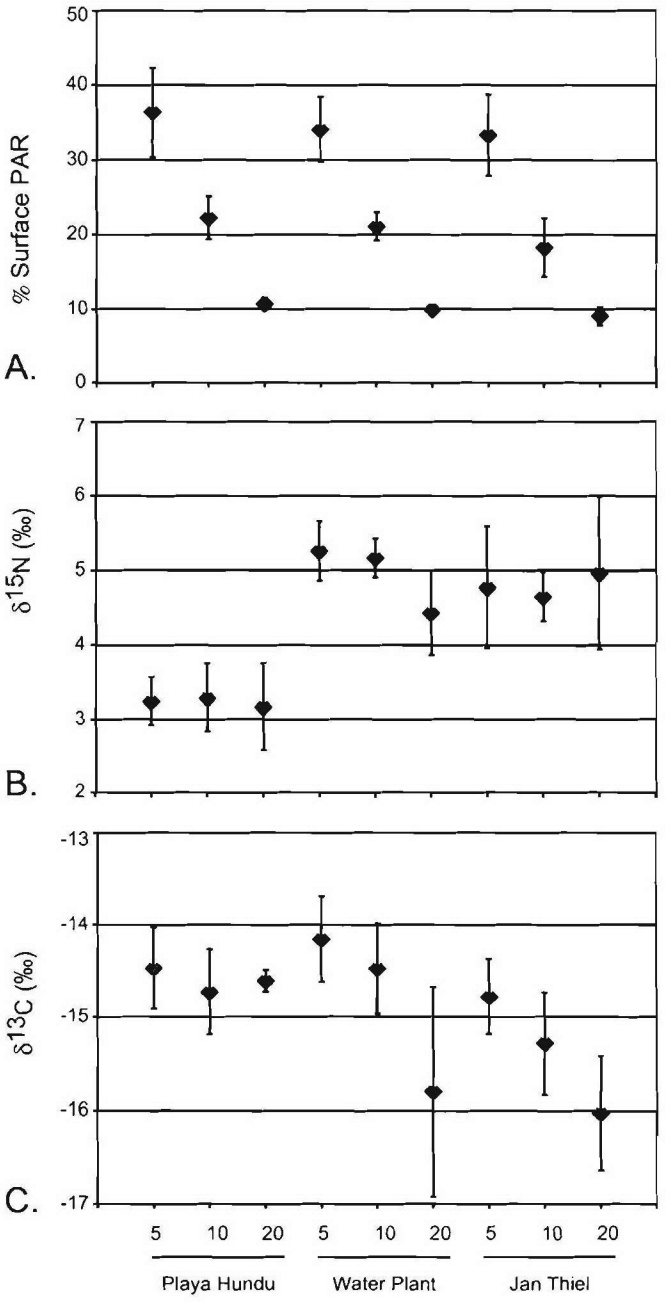
A.
% Surface PAR
50
40
30
20
10
0
B.
δ15N (‰)
7
6
5
4
3
2
C.
δ13C (‰)
-13
-14
-15
-16
-17
5
10
20
5
10
20
5
10
20
Playa Hundu
Water Plant
Jan Thiel

Figure 4

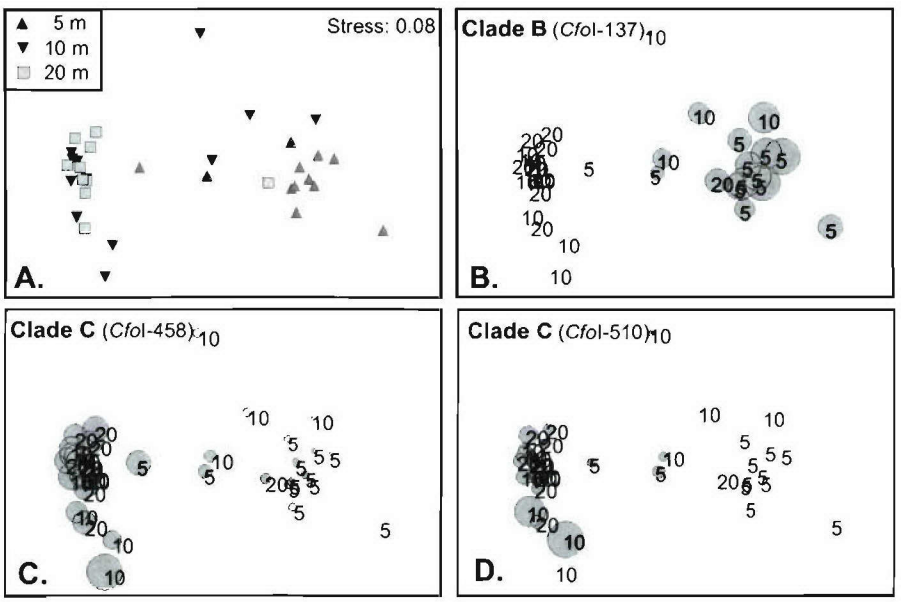
5 m
10 m
20 m
Stress: 0.08
A.
Clade B (Cfol-137)
B.
Clade C (Cfol-458)
C.
Clade C (Cfol-510)
D.

Figure 5

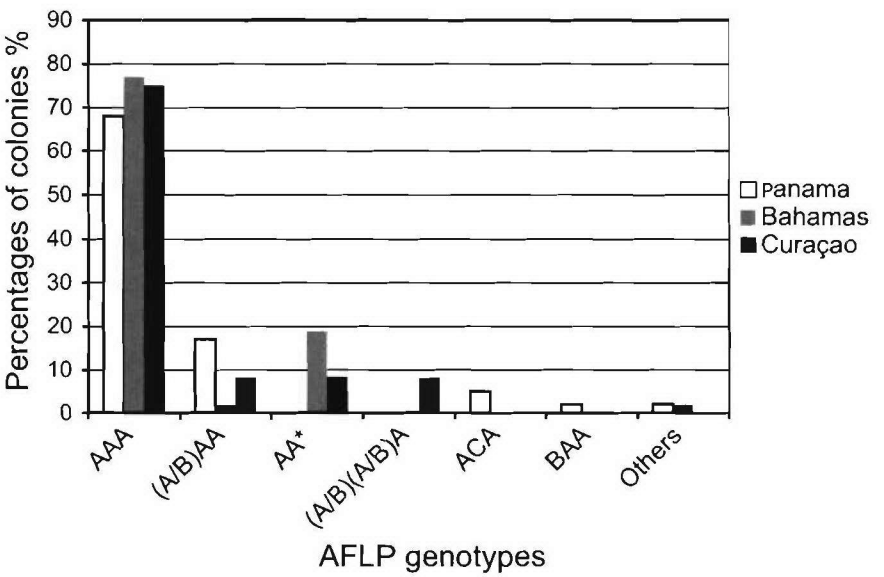
Percentages of colonies %
90
80
70
60
50
40
30
20
10
0
AAA
(A/B)AA
AA*
(A/B)(A/B)A
ACA
BAA
Others
AFLP genotypes
Panama
Bahamas
Curaçao

Figure 6

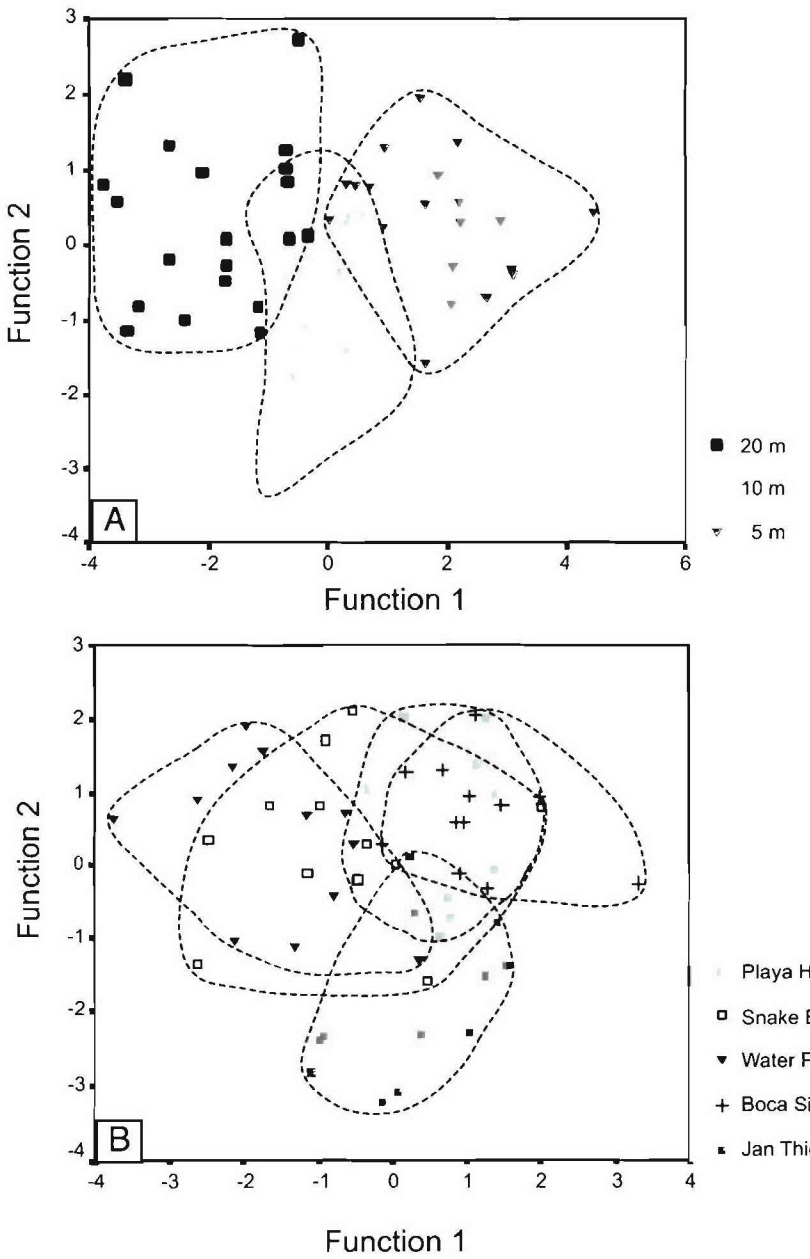
Function 2
Function 1
A
20 m
10 m
5 m
Function 2
Function 1
B
Playa Hundu
Snake Bay
Water Plant
Boca Simon
Jan Thiel

Figure 7

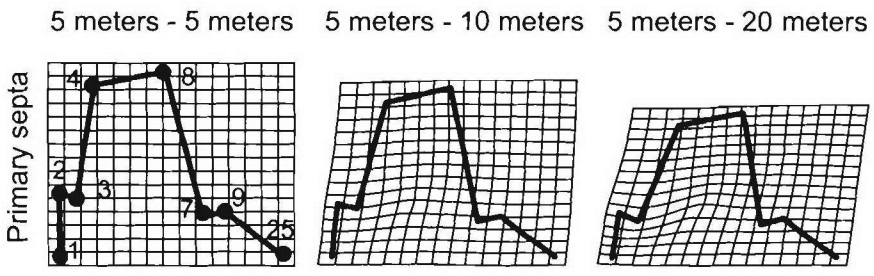
5 meters - 5 meters
5 meters - 10 meters
5 meters - 20 meters
Primary septa
4
8
2
3
7
9
25
1

Figure 8

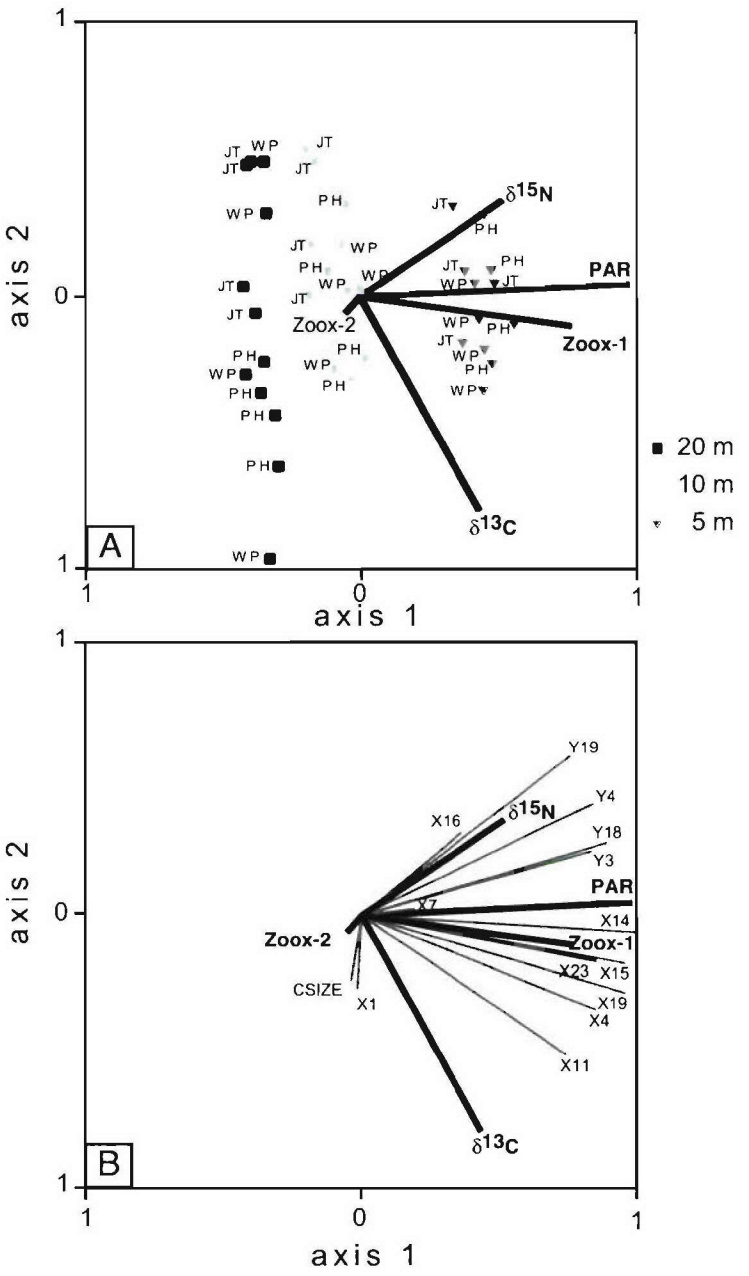
A
B
axis 1
axis 2
δ15N
δ13C
PAR
Zoox-1
Zoox-2
CSIZE
20 m
10 m
5 m
JT
WP
PH
X1
X4
X7
X11
X14
X15
X16
X19
X23
Y3
Y4
Y18
Y19

Figure 9

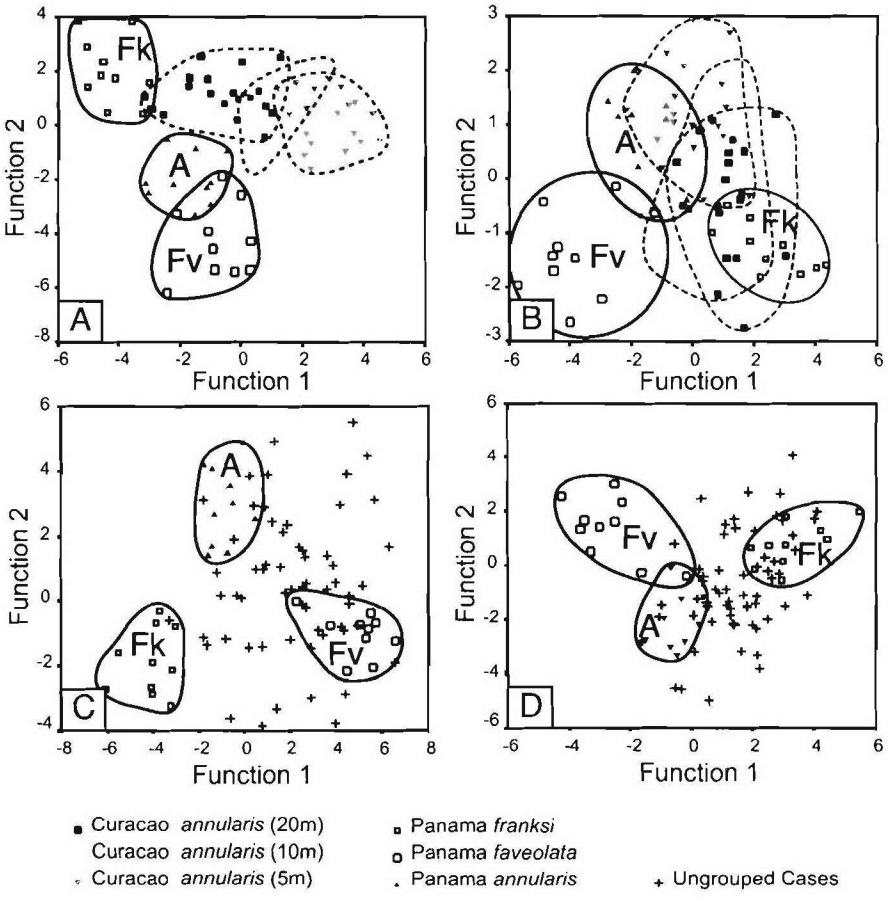
Fk
A
Fv
A
Function 2
Function 1
Curacao annularis (20m)
Curacao annularis (10m)
Curacao annularis (5m)
Panama franksi
Panama faveolata
Panama annularis
Ungrouped Cases

Figure 10

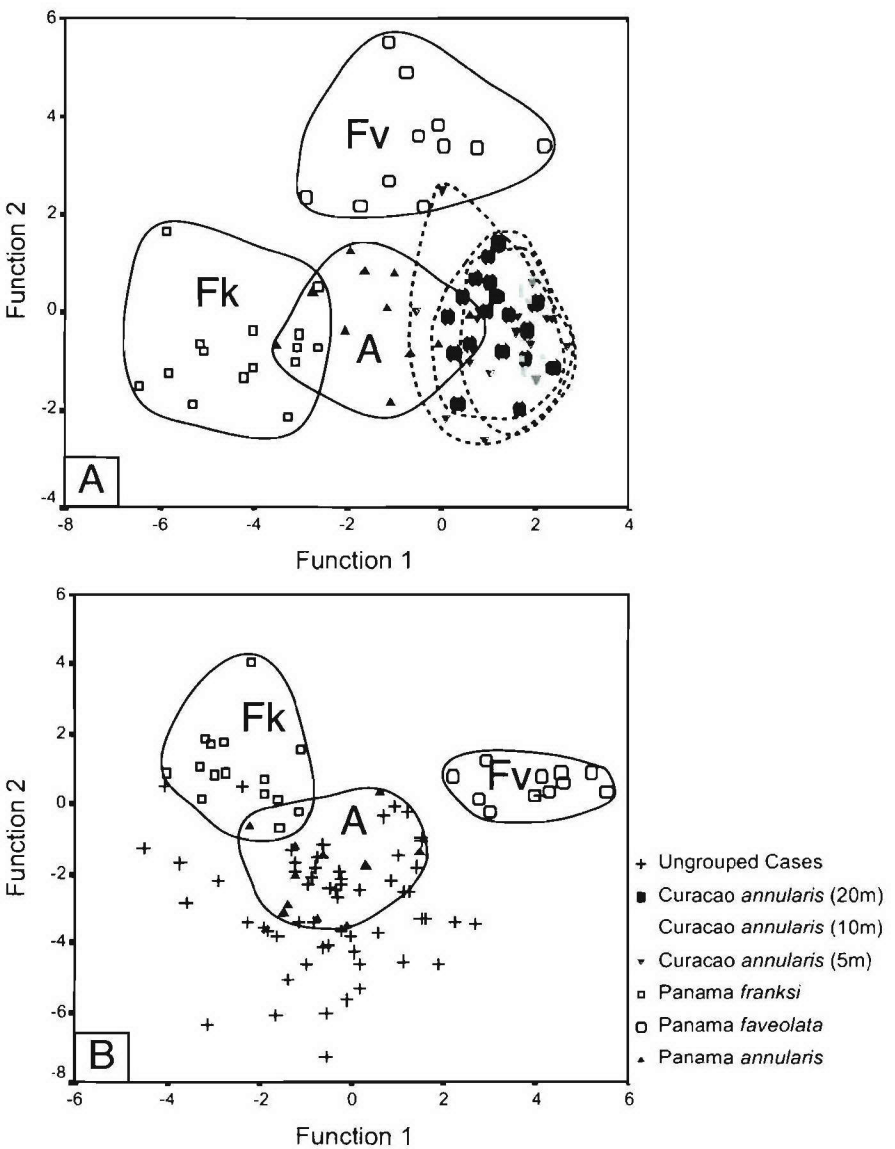
Fv
Fk
A
A
Function 2
Function 1
Fk
A
Fv
B
Function 2
Function 1
Ungrouped Cases
Curacao annularis (20m)
Curacao annularis (10m)
Curacao annularis (5m)
Panama franksi
Panama faveolata
Panama annularis

Characterization and Host Specificity of the Microbial Communities Associated with Healthy and Black Band Disease Infected Corals

Ingmar Janse[1*], James S. Klaus[2], Bruce W. Fouke

Department of Geology, University of Illinois, 1301 W. Green St., Urbana, Illinois. 61801, USA

[1]Current address: National Institute for Public Health and the Environment, Centre for Infectious Disease Control (RIVM-MGB), Anthonie van Leeuwenhoeklaan 9, 3721 MA Bilthoven, the Netherlands. Phone: +31 30 274 3666. Email: Ingmar.Janse@rivm.nl

[2]Current address: Rosenstiel School for Marine Sciences, 4600 Rickenbacker Causeway, Miami, FL, USA. Email: jklaus@rsmas.miami.edu

*Corresponding author

ABSTRACT

Over recent decades reef coral health has become increasingly challenged by diseases. Many massive framework building coral species are particularly susceptible to black band disease (BBD), a disease characterized by a microbial mat dominated by cyanobacteria that kills coral tissue while migrating over the colony surface. Black band disease mats infecting seven different coral species of five genera were studied to reveal host-specific interactions and to identify important microbes involved in the disease. *In situ* infection experiments showed that the BBD mats were infectious across coral species, and that exposure to mat samples without damaging the coral surface was sufficient for infection initiation. Genotypic variability of the dominant BBD cyanobacteria was analyzed at high resolution using cyanobacteria-specific terminal restriction fragment polymorphism (T-RFLP) analysis in combination with sequencing of the genes for rRNA internal transcribed spacer (rRNA-ITS). The dominant cyanobacteria on most coral species were nearly identical, yet two genotypes could be distinguished based on subtle variation in rRNA-ITS sequences. By selecting a restriction enzyme for discrimination of this genotypic variation in T-RFLP profiles, the distribution of these genotypes in BBD mats was revealed. The BBD infecting the Seafan *Gorgonia ventalina* was dominated by very different cyanobacterial taxa, suggesting host specificity at higher taxonomic levels. Clone library sequencing and T-RFLP analyses of rRNA genes and reverse-transcribed rRNA were performed to reveal the identity and activity of abundant members of the microbial communities of BBD mats. A potential role of these microbes in infection and immunity was studied by comparing the microbial communities of BBD mats to those associated with the healthy tissues of infected and non-infected corals. The dominant cyanobacterial genotype was detected on healthy tissues of several diseased coral species. In addition, the dominant cyanobacterial genotype was also detected on several species with no outward signs of disease. The variable abundances of the dominant cyanobacterial genotype in BBD mats and healthy coral tissues suggested an

opportunistic role for this organism in BBD disease. Besides *Cyanobacteria*, *Rhodobacteraceae*, *Vibrionaceae* and *Bacteroidetes* were identified as important constituents of BBD mats. Several genotypes were highly similar to genotypes identified previously in coral diseases. A higher relative abundance of several of these organisms in BBD mats compared to healthy coral tissue in multiple coral species, suggested a potential role for these organisms in infection. The high resolution analysis of BBD mat-coral host specificity supported the view that the BBD mat creates a microenvironment for particular bacterial groups. The creation and persistence of the BBD mat does not appear to be controlled by the coral host, but it can be affected by (unknown) factors that vary between corals at higher taxonomic levels.

Keywords: Coral Reefs, Black band disease, host specificity, *Cyanobacteria*, microbial community composition, T-RFLP, 16S rRNA, rRNA-ITS, reverse-transcribed rRNA,

INTRODUCTION

Coral reefs are the most biologically diverse and productive of aquatic ecosystems. They are also in severe decline, particularly in the Caribbean. The destruction of coral reef ecosystems can be attributed to a combination of factors, but one of the main threats to reefs is increasing coral mortality due to diseases (17, 30, 40). The increasing prevalence of these diseases is concerning in that many diseases infect multiple coral species, spread rapidly, and are most often fatal. In the Caribbean, diseases have already decimated reef building corals of the genus *Acropora* (2). Human activities near coral reefs, including habitat degradation, over-fishing, and pollution are known to have large effects on reef health (40). In addition, worldwide changes in climate and sea surface temperatures are blamed for increasing physiological stress and decreasing coral disease resistance (20), potentially facilitating pathogen transmission (37).

Many of the causal agents of coral diseases have yet to be identified, though microbial pathogens are being increasingly identified in association with coral diseases (31, 38, 40). Black band disease (BBD) is a coral disease characterized by a black to red bacterial mat that migrates across infected corals, killing healthy tissue and leaving behind dead skeleton. The disease occurs on both Caribbean and Indo-Pacific reefs. Most often fewer than 1% of coral colonies are affected, with 5–6% of susceptible species infected at peak times of disease (11, 26). Nevertheless, the menace of BBD to reefs is considerable due to the preferential susceptibility of major framework-building coral species. Mortality of such dominant reef elements is a potent force in restructuring coral reef ecosystems (11, 26).

The black band of infected corals is a pathogenic microbial mat dominated by a filamentous, nonheterocystous cyanobacterium microscopically identified as *P. corallyticum*. While the pathogenic mat is polymicrobial, a consensus exists as to the importance of the dominant

cyanobacterium during disease development (31, 40). Notably, BBD progression can be stopped by light deprivation of the cyanobacteria (18), (unpublished results IJ and JK). Nevertheless, the reasons to consider it the primary pathogen remain circumstantial and Koch's postulates have not yet been fulfilled (7, 10, 31, 40). A consortium rather than a single pathogen may be required for disease initiation (7). The cyanobacteria creates a ropy network that structurally supports the BBD mat and houses a complex, phylogenetically diverse community (10, 15). Based on 16S rRNA gene analysis, the dominant BBD cyanobacteria derived from infected corals from 4 different species and from different regions in the Caribbean (10, 14, 15), were found to be of one ribotype. This ribotype was classified as a member of the genus *Oscillatoria*. Besides cyanobacteria, up to 64 bacterial species have been identified in the BBD mat (10, 15), with species of the divisions *Firmicutes*, *Cytophaga-Flexibacter-Bacteroides* (CFB) group and *δ-Proteobacteria* being consistently abundant (14). Differences in the microbial communities of BBD mats and those associated with non-infected coral tissues could identify organisms involved in disease initiation or progression. Besides the dominant cyanobacterial genotype, several such potential pathogens were identified based on clone library frequencies and DGGE profiles (10, 14, 15). Since it is to be expected that infectious mat components are relatively active, and metabolically active cells usually contain higher numbers of ribosomes than quiescent cells (28), a reflection on the diversity of the active components in the microbial mats may be obtained from reverse-transcribed rRNA rather than rRNA genes.

BBD has been reported on 45 (of approximately 400) scleractinian species from the Indo-Pacific and 19 (of 66) scleractinian and 6 gorgonian species from the Caribbean (40). The preference of BBD for certain massive corals and the co-occurrence of infected and uninfected corals suggest that certain species of coral are less susceptible to BBD infection than others. This variation could be due to properties of BBD pathogens which determine their host-specificity, e.g. possession of specific receptors or pathogenicity plasmids, or their distribution, e.g. ability to thrive in the host

microenvironment as determined by a particular mucus type or light regime. The variation in coral susceptibility to disease could also be due to differences in coral defense against infection. To address the role of host-specificity –the association of microorganisms with only a few (specialism) or many (generalism) host species- in explaining differential susceptibility of coral species to infection, a detailed population analysis is required. Important biological differences such as those involved in host-specificity may not be reflected in significant levels of 16S rRNA sequence variation of the symbiont (3, 33). Several studies have used the highly variable ITS region of cyanobacterial rRNA gene operons to study strains whose 16S rRNA gene sequences are nearly identical (12, 21). The subtle genetic divergence patterns thus revealed were indicative of ecotypes, genetically closely related but physiologically distinct, sometimes within established 16S rRNA clusters (12, 34). Such multiple coexisting ecotypes may vary in relative abundance with changing environmental conditions.

Corals harbor diverse bacterial communities that are different from the overlying seawater and seem to exhibit some specificity within coral species (15, 25, 35, 36). The combined stresses of temperature increase and human impacts may lead to changes in these microbial-coral associations which may affect coral health and susceptibility to disease (23, 36). Such changes observed before signs of visible stress, may be used as bio-indicators of both environmental changes and disease. Differences in the microbial communities associated with healthy tissues of infected and non-infected colonies could reveal a role of these microbes in disease. Microbial community shifts could be the cause of an increased susceptibility to infection, or it could be the result of a whole colony response to infection. When comparing microbial community DGGE profiles from *M. annularis* coral tissue infected with white band disease (WBD) to that of non-infected remote colonies, Pantos et al (29) claimed to have found differences between these.

Here, we report on the characterization of BBD microbial communities infecting 7 different coral species covering 5 genera to reveal host-specificity –the association of microorganisms with only a few (specialism) or many (generalism) host coral species- and to identify microbes with potential roles in coral disease and immunity. *In situ* infection experiments between coral species were conducted. The dominant BBD mat cyanobacteria were analyzed at high resolution by using cyanobacteria-specific rRNA-ITS gene T-RFLP. Clone library sequencing and TRFLP from rRNA genes and reverse-transcribed rRNA genes were performed to reveal the identity, activity and relative abundances of BBD mat microbes. Potentially important bacteria in black band disease were identified based on their relative abundances in BBD mats and healthy tissues of infected and non-infected coral colonies.

MATERIALS AND METHODS

Sample collection. Coral colonies were collected along the leeward (Southwestern) coast of Curacao, Netherlands Antilles by making transects using standard SCUBA techniques. We encountered most infected coral specimens at the localities Water Plant and Boca Simon, immediately adjacent to the seaport and large urban center of Willemstad, and Jan Thiel which is approximately 8 km upcurrent from the seaport. Infected corals were either sampled directly or labeled for later synchronized sample collection (infection experiments). All sampling and experimentation was carried out in July 2004. Samples were collected from BBD mats (BBD), healthy tissue of infected colonies (HT), dead skeleton of infected colonies (DS), and healthy colonies distant from infected colonies (HC). BBD mat samples that could be physically peeled off were collected by using forceps, coral tissue samples were collected by removing a 2 x 2 cm portion of the uppermost 1 cm of the coral colony with a small chisel. Samples were placed in sterile disposable 15 or 50 ml tubes (depending on the sample size) and upon return to shore, within 1 hour, seawater was decanted and replaced by 80% ethanol to preserve DNA. BBD samples to be used for RNA analysis were collected in 15 ml tubes, immediately transported to the water surface where the seawater was decanted and replaced by RNAlater (Ambion). This procedure was completed within 3 minutes after sample collection. Samples were transported to the laboratory at approximately 10°C and then stored at -20°C until further processing.

***In situ* infection experiments.** The Water Plant was chosen as the site to perform *in situ* infection experiments because this location was found to harbor a high incidence of corals infected with BBD (as well as other diseases). Thereby we prevented the transport of BBD to a locality where it was before absent or at a very low incidence. Experiments were carried out at 3-6 m depth. BBD mat samples from infected colonies of *Diploria strigosa*, *Montastraea* cavernosa, *Colpophyllia natans* and *Meandrina meandrites* were collected at the Water Plant location and

from *Montastraea faveolata* at Jan Tiel. The mat samples were peeled from the BBD mat using tweezers and brought to the surface in sterile 50 ml polypropylene tubes. At the surface, the BBD samples were divided into 10 portions of similar size which were then transported to a site at the Water Plant locality where uninfected colonies of the species *D. strigosa*, *C. natans*, *M. cavernosa*, *M. faveolata*, and *Porites porites* were present in a range of 5 meters. These uninfected corals were exposed to the BBD flakes originating from different coral species by puncturing sterile disposable needles through the BBD flakes and into the coral surface. All 6 coral species were exposed to BBD mats collected from *D. strigosa*, *M. cavernosa*, *M. faveolata* and *C. natans*, but from *M. meandrites* there was just sufficient material to expose *D. strigosa*. The needles were placed approximately 10 cm apart and had a small transparent plastic cap (Fig. 1E) to prevent the consumption of BBD flakes by reef fish. Control needles without BBD flakes were attached similarly. The sets of needles were attached in duplicate on each coral. After 8 days, the site was revisited and photographs were made to check for signs of BBD disease. Infected *P. porites* colonies were then removed.

The potential effect of damaging the coral surface on the susceptibility of corals to BBD infection was studied by varying the exposure of healthy *D. strigosa* colonies to flakes harvested from a BBD infected *D. strigosa* colony with a thick black band approximately 10 meters away. On the healthy *D. strigosa* colonies, two fish lines were attached such that they held 4 patches of 8 x 8 cm nylon transparent plankton net lightly pressed against the coral surface. Underneath two of these patches we placed BBD flakes of approximately 0.5 x 0.5 cm, and one of these was punctured with a sterile needle. The other two control patches were manipulated accordingly such that the covered coral surface was exposed to the same physical stress, but no BBD flakes were put underneath. In a separate setup, a BBD flake was first placed on the coral surface, immediately followed by the attachment of the plankton net patch using the fish lines. This was to ensure a BBD exposure without any physical stress resulting from touching the coral surface

during the lifting of the patch. The site was visited after 3 and 10 days to make photographs and check for signs of BBD disease. The experiment was performed in triplicate (i.e. on three separate colonies).

Nucleotide extraction and amplification. Coral samples preserved in ethanol were crushed in the collection tubes by using sterilized tools, creating a slurry of coral tissue, Zooxanthellae, mucus, microorganisms, and skeletal material. Coral slurries of BBD flakes were transferred to 2 ml screw-capped tubes, centrifuged for 10 minutes at 12,000 xg, and genomic DNA was extracted from the pellet using the UltraClean Soil DNA Kit (Mo Bio, Solana Beach, CA) following the manufacturers instructions.

For RNA extraction from BBD samples stored in RNAlater, the samples were transferred to 2 ml screw-capped tubes, centrifuged for 10 minutes at 12,000 xg and the pellet was used for total RNA extraction by using TRIZOL reagent (Invitrogen) following the manufacturers instructions. DNA was removed using DNAfree (Ambion) and the RNA was stored in RNAsecure (Ambion). First-strand cDNA was synthesized as follows. One to ten µl RNA extract was incubated with 1 ul 4µM primer 1406R (see below), 1µl 10 mMl dNTPs in a total volume of 13 µl at 65°C for 5 min and then immediately put on ice. Then 4 µl 5x first strand buffer, 1 µl 0.1 M DTT, 1 µl RNAse inhibitor and 1µl Superscript III (Invitrogen) was added, followed by incubation for 60 min. at 55°C and inactivation for 15 min. at 70°C. The resulting cDNA was used for PCR amplification and TRFLP as described below.

PCR amplification was performed using the Master cycler kit (Eppendorf) according to the manufacturers instructions with 1/25 volume of the sample preparation, 0.2 mM of each dNTP (Gibco/BRL, Rockville, Md), 400 nM each of the forward and reverse primers and 1 U Taq DNA polymerase. Primers used in the PCR amplifications of bacterial DNA were the 16S primers U9F (5'-GAGTTTGATYMTGGCTC) (14) and U1406R (5'-ACGGGCGGTGTGTRCA) (27), and the

23S reverse primer LB23R (5'- GCCWAGGYATCCACC). The latter primer was adapted from primer ULR (22) as a bacterial primer. For amplification of cyanobacterial rRNA-ITS, the 16S primer CSIF (5'-GYCACGCCCGAAGTCRTTAC) (22) was used in combination with LB23R. Amplification was performed in a Mastercycler gradient thermocycler (Eppendorf). The thermocycler profile was: one cycle of 4 min at 94°C, 25-40 cycles of 10 s at 95°C, 30 s at 50°C (55°C for cyanobacterial rRNA-ITS) and 60 s at 72°C, followed by 5 min at 72°C. Optimization of PCR was performed for each sample by adjusting the amount of genomic DNA extract used to obtain a strong band on an agarose gel, without visible nonspecific product. The number of PCR thermocycles was dependent on the sample type. For amplification of BBD and dead skeleton (DS) DNA, we performed 25 cycles and for healthy tissue samples (HT and HC) between 30 and 40 cycles.

T-RFLP. For T-RFLP analysis, primers U9F and CSIF were labeled at the 5' end with a blue 6-FAM (phosphoramidite fluorochrome 6-carboxyfluorescein). Primer LB23R was labeled with a green HEX (Hexachlorofluorescein) label. PCR reactions were purified using the Wizard PCR prep kit (Promega, Madison, WI), or, if there was more than one band visible on agarose gel, they were gel-excised and purified using a Qiagen gel extraction kit. Restriction digests were performed independently using the tetrameric enzymes HhaI, MspI, and RsaI, and for some samples also DpnII, HaeIII, AluI and EarI (New England Biolabs). Ten µl of purified PCR product was digested using 20 U of enzyme in 20 µl total reaction volume. Incubation was done at 37°C for 9 h.

The precise lengths of the T-RFLP fragments from the amplified products were determined by multicapillary electrophoresis with a model 3730xl genetic analyzer automated sequencer (Applied Biosystems) at the University of Illinois W. M. Keck Center for Comparative and Functional Genomics (www.biotech.uiuc.edu) and analyzed using Genemapper Analysis

Software Version 3.7 (Applied Biosystems). Sample versus T-RFLP peak data matrices were constructed using peaks above a threshold of 50 units above background. To avoid detection of primers and uncertainties associated with fragment size determination, peaks smaller than 50 base pairs (bp) and larger than 1050 bp were culled from the data set. To account for variation in fragment size determination between samples, peaks were manually aligned and placed into groups. To assure accuracy within one base pair a correction factor based on a 6-Fam labeled sizing ladder was subsequently applied. Abundance data was obtained from the relative peak area following sample standardization (4). The taxonomic identity of T-RFs were assessed by comparison with theoretical digests of various clone library rRNA gene sequences.

Clone libraries. Bacterial clone libraries containing fragments amplified with primers U9F and LB23R (covering the rRNA 16S and ITS) were constructed from BBD mat samples from *D. strigosa* (126 clones), and from BBD mat and healthy tissue (HT) samples from *C. natans* (118 and 39 clones respectively). Bacterial clone libraries from amplified 16S only (primers U9F and U1406R) were constructed from healthy tissue (HT) samples from *D. strigosa* (14 clones), from BBD samples (14 clones) and HC samples (20 clones) from *M. annularis* and from BBD samples (59 clones), infected tissue samples (20 clones) and healthy tissue samples (18 clones) from *G. ventalina*. It was considerably more difficult to obtain clones from healthy tissue samples, especially for the 16S + ITS rRNA gene libraries.

Gel-purified PCR products were cloned into pGEM-T (Promega, Madison, WI), and transformed into calcium chloride competent DH5αMCR E. coli cells using manufacturers instructions and standard techniques. Clones were screened for the presence of the insert and forward orientation by PCR using primers T7 (-26) and U1406R. Useable clones were stored in 0.2 ml 96-well plates filled with Luria broth and 100μg/ml ampicillin (Roche Molecular Biochemicals, Indianapolis, IN) and 15% glycerol. Inoculating, culturing, prepping and sequencing were performed in the

High Throughput Laboratory of the University of Illinois W. M. Keck Center for Comparative and Functional Genomics (www.biotech.uiuc.edu). Sequencing was performed using the T7(-26) primer or M13R primer, depending on the desired sequence information, on an ABI 3730XL capillary sequencer. Sequences were inspected and corrected using Sequencher 4.5 software.

Sequence analyses. The sequences obtained were classified by using the classifier tool of the Ribosomal Database Project II website [Cole et al 2005 uit Jim] and searches for homology with sequences deposited in the GenBank, EMBL, and DDBJ databases were performed by using the program BLAST (2) (www.ncbi.nlm.nih.gov/BLAST) (1). The sequences of the rRNA gene fragments identified in this work are deposited in GenBank under accession numbers XXXXX through YYYYY.

Ordinations of T-RFLP peak abundances from BBD, HT, HC, DS samples. Similarity matrices of T-RFLP peak profiles were calculated using the Bray-Curtis (BC) similarity coefficient . Ordination by non-metric multidimensional scaling (NMDS) [Kruskal 1964] was performed to visually examine differences among samples. This method was chosen because it makes no assumptions about the underlying distribution of data. Each ordination was run with 30 random starting configurations and proceeded through multiple iterations until the fit of a non-parametric regression of d (distances between samples on the NMDS plot) against δ (Bray-Curtis similarities or Euclidean distances) could not be improved. Points closest together on the resulting scatter plot represent samples that are most similar. Ordinations and statistical tests were performed using PRIMER 5 v. 5.2.9 (PRIMER-E, Plymouth, UK) and SPSS 10.0 statistical packages (SPSS Inc., Chicago Ill.)

RESULTS

Infectivity of Black Band Disease (BBD) between coral species

To investigate the extent of coral species specificity in BBD, we performed *in situ* infection experiments. BBD mat biomass was collected at different locations along the west coast of Curaçao, and the infection experiments were carried out at the Water Plant locality, a site with a relatively high disease incidence. Three healthy *D. strigosa* colonies were exposed to BBD mats derived from infected *D. strigosa* under circumstances preventing coral damage. This was done by placing transferred BBD flakes in grooves on the coral surface where they were held in place with patches of transparent plankton nets. Colonies thus exposed to BBD mat flakes without any coral damage showed clear signs of a starting BBD infection after 3 days. The control patches of plankton net without BBD flakes remained free of disease signs for the 10 days of monitoring. After having shown that BBD transmission could be achieved in the absence of coral damage, subsequent infection experiments between coral species were carried out by using sterile needles for attaching the BBD flakes to the coral surface.

BBD mat biomass was collected from the coral species *D. strigosa*, *M. faveolata*, *M. cavernosa*, *C. natans* and *M. meandrites*. Apart from the *M. meandrites* BBD, the mats yielded sufficient biomass to perform duplicate infection experiments on healthy specimens of five species: *D. strigosa*, *M. annularis*, *M. cavernosa*, *C. natans* and *P. porites*. After 8 days, all the exposed corals showed clear signs of infection, i.e. tissue mortality around every needle with BBD flakes. Control needles remained free of tissue mortality (Fig 1E).

Diversity of BBD cyanobacteria between coral species

To investigate whether susceptibility of different coral species was reflected in the cyanobacteria dominating the BBD microbial communities, cyanobacteria infecting different coral species were characterized using a combined approach of terminal restriction fragment length polymorphism

(T-RFLP) and sequencing of clone libraries to taxonomically identify terminal restriction fragments (T-RFs). DNA was extracted from BBD samples collected from infected specimens of 7 coral species from 5 genera: *D. strigosa* (6), *M. annularis* (1), *M. cavernosa* (1), *M. faveolata* (1), *M. meandrites* (2), *C. natans* (2) and the seafan *G. ventalina* (1). BBD samples from the *G. ventalina* included a BBD flake that was peeled off and a tissue sample overgrown with BBD mat. Examples of sampled colonies are given in Fig. 1 A-D. In addition, DNA was extracted from a laboratory strain of *P. corallyticum* (LR-3L), previously isolated from a BBD mat (10, 13).

Highly resolved cyanobacterial community TRFLP profiles were generated by amplification of extracted BBD DNA using a cyanobacteria-specific 16S primer (22) labeled with FAM and a 23S bacterial primer labeled with HEX. This protocol was used to maximize the detection of genotypic variation because the amplified rRNA-ITS region is known to contain more sequence heterogeneity than the more conserved 16S (21), and the dual labeling doubles the detection of fragments. Digestion using 6 different restriction enzymes yielded cyanobacterial T-RFLP profiles that were identical for most BBD samples, but differed clearly from those of *G. ventalina* and of the *P. corallyticum* culture LR-3L (Fig 2A).

Clone libraries covering the full 16S and ITS regions from bacterial rRNA genes were constructed from BBD samples derived from two *D. strigosa* colonies and one *C. natans* colony. Forward (16S) sequences were obtained from 69 cyanobacterial clones (classified by using the classifier tools in RDPII) and 53 of these clones were used to obtain reverse (ITS) sequences as well. Single nucleotide polymorphisms (SNPs) occurred at 45 positions (6%) of the first 750 basepairs from the 16S sequences. Of these SNPs, 37 occurred in only one clone, the remainder in two. Sequences of the 546 basepairs spanning fragment amplified for cyanobacteria-specific rRNA-ITS T-RFLP showed somewhat higher sequence heterogeneity. At 43 positions (8%) there were nucleotide differences between clones. In 23 clones this concerned unique SNPs, 3 SNPs were shared by 2 clones, 1 by 6 clones, and 1 by 9 clones. Interestingly, a consistent sequence

difference was found at nucleotide positions 167-171 bp upstream from the 23S reverse primer. This 6 bp sequence contained an inversion where one sequence was found in all ITS sequences obtained from the *C. natans* BBD and from one *D. strigosa* BBD, and the inverted sequence was found only in the other *D. strigosa* BBD. Based on a theoretical restriction map showing cutsites at this sequence difference for the enzyme EarI, we generated T-RFLP profiles using this enzyme for the different BBD samples described before. As shown in Fig 3, populations of the two closely related cyanobacteria could be distinguished by the length of the HEX labeled reverse primer fragments which was either 170 or 182 bp. The two populations appeared to be differentially distributed over the BBD samples, with *M. annularis*, *M. faveolata*, *M. cavernosa* and *M. meandrities* harboring one species, *C. natans* harbouring the other species, and *D. strigosa* harbouring either one or both (differing between replicates). The *G. ventalina* BBD sample did not contain this cyanobacterial strain. Ordination of all T-RFLP profiles (Fig 2A) illustrates the subtle difference between the cyanobacteria dominating the BBD mats of the two groups of stony corals, and the substantial difference between these groups and the cyanobacteria dominating *G. ventalina* BBD and *P. corallyticum* strain LR3.

Diversity and activity of BBD communities between coral species

To study the identities and relative abundances of the various bacteria involved in BBD infecting different corals, BBD mat communities were characterized by T-RFLP and clone library sequencing. T-RFLP profiles from bacterial communities in BBD mats infecting different coral species were generated by amplification of extracted DNA using labeled Bacteria-specific 16S rRNA primers in combination with universal primers. The taxonomic identities of abundant or important T-RF's were determined by comparison with sequenced clone libraries.

The 16S+ITS rRNA clone libraries obtained from *D. strigosa* and *C. natans* BBD mat samples mentioned above, as well as the 16S library obtained from *M. annularis* BBD samples, were dominated by a cyanobacterial ribotype which was highly similar to the genotype CD1C11

characterized from BBD mats before (10, 13). A theoretical digest of this genotype yielded fragments of 671 bp, 152 bp and 231 bp for HhaI, MspI and RsaI digestion respectively. Table 1 gives the relative peak areas of these T-RFs for the 7 different coral species and replicates investigated. The T-RFs of the CD1C11 genotype formed an abundant fraction of the T-RFLP profiles from BBD mat samples except for that derived from *G. ventalina*. Since multiple species can share a particular T-RF (e.g. several cyanobacterial species share the Hha 671 T-RF), a reliable minimum estimate of the contribution of a particular genotype to the population was based on the lowest peak percentage of any of the three corresponding T-RFs. Considering this, strain CD1C11 constituted between 0% (*G. ventalina*) and 62% (*M. annularis*) of the BBD communities. In replicate samples, the contribution of strain CD1C11 ranged from 15% to 45% between the 8 *D. strigosa* samples and from 2 to 19% between the 2 *C. natans* samples. T-RFs M-152 and R-231, characteristic for genotype CD1C11, were not detected in the *G. ventalina* BBD T-RFLPs (Table 1). A clone library from the *G. ventalina* BBD mat sample showed that other cyanobacterial genotypes were present in these samples. Genotypes SFDC1 and SFDC2 were identified in this clone library, both of which had distinctive T-RFs (Table 1).

Besides cyanobacteria, several bacteria were found to be significant constituents of most BBD mat samples, based on the frequencies of their ribotypes in clone libraries and the contribution of their T-RFs in T-RFLP profiles. The relative abundances of selected T-RFs in the different coral samples are presented in Table 2 (BB columns). The identity of the corresponding bacteria can be derived from Table 3 which displays the most important ribotypes identified from the clone libraries, their theoretical T-RFs sizes and the database entries that are most homologous to these sequences. In cases where sequences were equally similar to several database sequences, the one most relevant for coral associated microbes was displayed. The BBD mat T-RFLP profiles and clone library sequences revealed that the Bacteria that were relatively abundant in BBD mat samples were *α-proteobacteria* from the genus *Rhodobacteraceae*, γ-proteobacteria from the

genus *Vibrionaceae* and *Bacteroidetes*. Other Bacteria that were detected in clone libraries were *Clostridia*, *ε-proteobacteria* and *δ-proteobacteria* from the genera *Desulfovibrionaceae* and *Desulfobacteraceae*. However, their contribution to T-RFLP profiles could not always be confirmed by the presence of all three T-RFs and must thus be interpreted with more caution. Similar to the cyanobacterial T-RFs, the relative abundance of many T-RFs in BBD samples differed between infected coral species. An NMDS ordination of the BBD mat T-RFLP profiles from all coral species and replicates showed differences between the microbial communities inhabiting BBD mats from different coral species (Fig. 2B). This was confirmed by an ANOSIM test for differences between these microbial communities (Global R= 0.519, $p<0.003$). Differences between the samples from several coral species were found to be significant: between *D. strigosa* and *G. ventalina* (r=0.991, $p<0.022$) and between *D. strigosa* and *M. meandrites* (r=0.802, $p<0.022$), and less so between *C. natans* and *G. ventalina* (r= 0.833, $p<0.1$) and between *M. annularis* and *D. strigosa* (r= 0.804, $p< 0.111$). However, in the NMDS ordination, the differences between replicate samples from *D. strigosa*, were not smaller than the differences between most coral species. It is therefore unknown whether analysis of more replicate samples would confirm the differences observed in these samples. The large contribution from cyanobacterial T-RFs to the microbial community profiles is illustrated by the NMDS plot obtained after exclusion of cyanobacterial T-RFs from the analysis (Fig. 2C). In this case the communities were still different (Global R= 0.459, $p<0.016$), but the significance of the differences between microbial communities associated with different corals were less pronounced: *D. strigosa* and *G. ventalina* (r=0.888. $p<0.022$), *D. strigosa* and *M. meandrites* (r=0.599, $p<0.022$), *D. strigosa* and *M. annularis* (r=0.964, $p<0.111$).

To determine if a significant portion of the variation in the BBD community profiles could be attributed to inactive bacteria, and to identify BBD mat components metabolically more active, the microbial community composition based on rRNA genes was compared to that based on

reverse-transcribed rRNA. DNA and RNA was extracted from 9 BBD mat samples from different *D. strigosa* colonies, and T-RFLP profiles were generated from DNA and from cDNA. Corresponding profiles were nearly identical and although a few peaks were slightly bigger in the cDNA profiles compared to the corresponding DNA profiles, these differences were not consistent between the replicate samples.

Differences in microbial communities associated with black band mats, healthy coral tissues and dead skeleton

A potential role of cyanobacteria and other coral associated microbes in BBD pathogenesis could be revealed by differences in the abundance of these organisms between coral tissues in different stages of infection. We compared the relative abundances of microbes in BBD mats (BBD), the healthy tissue of infected colonies (HT), the dead skeleton of infected colonies (DS), and healthy tissue in non-infected distant colonies (HC). A comparison of bacterial communities between BBD and HT samples could point to potential pathogens. In addition, comparison with the microbial communities associated with healthy, non-infected colonies could point to the role of an altered bacterial community in susceptibility for or response to infection. The relative abundances of T-RFs from coral samples from different infection stages and their genotype identification are presented in Tables 2 and 3, respectively.

Shifts in the abundance of particular ribotypes between BBD, HT and HC samples appeared to vary with the coral species under investigation (Tables 1 and 2). Notable differences were found for cyanobacterial genotype CD1C11. This genotype dominated the healthy tissue (HT) samples from *M. annularis*, *M. cavernosa*, *M. faveolata* and *D. strigosa* (Table 1) and the healthy colony (HC) sample from *M. cavernosa*, and was abundant on the healthy coral (HC) sample of *D. strigosa*. In contrast, it was detected but virtually absent from healthy coral (HC) samples from *M. annularis* and *M. faveolata*. This genotype was not detected in either the healthy tissue or healthy colony profiles from *C. natans* or *M. meandrites* (Table 1).

T-RFs corresponding to the *Rhodobactereacea* genotype (*Hha*I-61/ *Msp*I-439/ *Rsa*I-109 or *Rsa*I-423) constituted a larger fraction of the BB and DS microbial communities compared to HT and HC samples in most coral samples. For instance, in the corals *C. natans* and *M. meandrites* the relative abundances of these T-RFs were between 10 to 20 times higher in BB samples compared to HT samples (Table 2). The pattern of relative abundance of *Rhodobactereacea* T-RFs in BB and DS samples was not found in one of the *D. strigosa* replicates, in *M. annularis* and *G. ventalina*. *Vibrio* T-RFs (*Hha*I-385/*Msp*I-507/*Rsa*I-24, *Rsa*I-439 or *Rsa*I-662) were more abundant in BBD and DS samples from *C. natans*, *M. cavernosa* and *M. meandrites*, but were present in equal or higher abundances in the other samples. Other T-RFs which were more dominant in BB and DS samples from several coral species were *Hha*I-96 and *Msp*I-221 in *C. natans*, *D. strigosa*, *M. cavernosa* and *M. meandrina*. For several T-RFs, a significant difference between BBD mats and healthy tissues was found in only one coral species, which makes a general role in BBD disease less likely. These included for example *Hha*I-82 in the *M. faveolata* mat, *Msp*I-164 in *C. natans*, and *Rsa*I-119, *Rsa*I-302 and *Rsa*I-313 in *M. meandrites*. It is possible that the *Hha*I-82 T-RF corresponds to an *α-Proteobacteria* genotype from the clone library, however, the overlap of the other theoretical T-RFs with other genotypes does not allow a confident assignment.

Some T-RFs were relatively more abundant on healthy coral tissues than in BBD mats or dead skeleton. *Oceanospirillales* T-RFs M-145 and R-786 (Tables 2 and 3) were associated with healthy tissues and healthy colonies of both *M. meandrites* colonies and the healthy tissues of one *C. natans* colony. In most coral species, T-RF H-211 was more abundant in the HC samples compared to the HT samples. A similar difference was found for M-505 although not in *D. strigosa* and *M. cavernosa*. Several T-RFs were very abundant in healthy tissue or healthy colony samples, but were restricted to only one or two coral species. Especially the healthy tissues from

C. natans and *M. meandrites* harbored such unique and abundant ribotypes (H85, H91, H715, M146, M452, R58, R131, R231, R700, R786) but their presence was not consistent between replicates, e.g. H-91 in *C. natans* replicates (Table 2).

DISCUSSION

Host specificity and disease transmission of BBD mats

Transfer of BBD infection was possible between various coral species, and even *P. porites* which was thought to be resistant to infection (40) could be infected. Hence, no indication for host specificity of BBD mats has become evident from our in situ infection experiments.

Although BBD is common in areas with little anthropogenic disturbance, a higher frequency of disease has been reported on corals suffering from environmental and physiological stress (10, 40). The Water Plant area where we took most samples and performed most of our experiments can be considered a highly impacted site (23, 24). BBD is also most active late summer at higher seawater temperatures (40). Therefore, the environmental conditions under which the *in situ* infection experiments were carried out may have resulted in the use of corals particularly susceptible to infection. A potential cause for enhanced susceptibility of corals to BBD infection could be a shift in the healthy coral-associated microbial communities. Potential pathogens would be present on healthy corals yet only initiate disease when the normal microbial communities become disturbed (see also below). Provided CD1C11 plays an important role in disease initiation, the detection of a high abundance of these cyanobacteria on apparently healthy corals (24)(Table1) could be used to support this hypothesis.

An alternative or additional factor explaining BBD disease transmission is the direct transfer of BBD bacteria to intact or damaged corals. In our experiments, the presence of BBD microbes rather than mechanical stress initiated the infection of corals. Merely damaging the coral surface by the control needles was not enough to start an infection (even when BBD mat flakes were nearby at about 10 centimeters distance). Moreover, a gentle, non-invasive, exposure of the coral surface to BBD flakes showed that damaging the coral surface is not needed for infection initiation. These findings point to a potential route of disease transmission simply via physical contact. Corals could be inoculated with BBD microbes transported by marine organisms as has

been shown for the Vibrio shiloi/Oculina patagonica coral disease model system (ref Rosenberg) or via seawater after detachment of portions of BBD mats. No consistent clues about the mode of transmission can be derived from the natural BBD distribution as field observations reported of a clumped but also of a random distribution of BBD (5, 11, 26, 31).

Based on our results it seems likely to assume that BBD is also infectious between different coral species by means of contact only, however this was not specifically tested.

Host specificity of BBD mat *Cyanobacteria* in disease progression

The occurrence of species specific associations in the actively migrating BBD mats was studied by analyzing components of the BBD microbial communities in different coral species.

The dominant cyanobacterium microscopically identified as *P.* corallyticum (31, 40) and phylogenetically as a member of the genus *Oscillatoria* (10, 13) is essential for disease progression (31, 40). Notably, BBD mats could be inhibited and disappeared after a few days when shaded from light (18) (unpublished results IJ and JK). High resolution genotypic analysis by using T-RFLP profiles generated from cyanobacterial rRNA-ITS genes showed that the cyanobacteria in most BBD samples were nearly identical, only the seafan *G. ventalina* harbored completely different genotypes (Fig 2A). The *Phormidium corallyticum* strain previously isolated from BBD samples was not the dominant BBD organism (Fig. 2A). This confirmed the conclusion of other authors (10, 13) and is likely due to inherent difficulties of cultivating and identifying marine cyanobacteria.

The different clones from the cyanobacterial genotype CD1C11 which dominated most BBD mats, showed very limited sequence heterogeneity. Similarities of the sequences we obtained from 6 coral species and those obtained by other researchers from Caribbean (10, 13) and Indo-Pacific samples (39) were within the same range (98-99% similarity). Since these samples were obtained in different years and from very different locations, it appears that regional and temporal variability is not greater than local variability for the BBD mat cyanobacteria. The dominant *G.*

ventalina cyanobacteria SFDC1 and SFDC2 were clearly different taxa and had a sequence similarity of only 88-89% with genotype CD1C11. These *G. ventalina* genotypes were more similar to the BBT (95% similarity) and PNG (91%) strains which had been characterized from BBD mats infecting a *D. strigosa* colony in an aquarium and a *Poritis lutea* colony from the Indo-Pacific, respectively (13). Despite its widespread occurrence, cyanobacterium CD1C11 does not seem to have a unique role as its niche in BBD mats may also be occupied by other, quite different cyanobacteria (SFDC1, SFDC2, PNG, BBT). The occurrence of these deviant genotypes only on particular coral species suggested host-specific interactions. Although we found a potential for cross infections between multiple coral species from different genera, these were all massive scleractinian species. It is unknown if a similar cross-infectivity is possible if the *G. ventalina* would be included in the infection scheme. Such interspecies infection experiments between species dominated by different cyanobacterial genotypes could explore the limits to infectivity and host specific interactions.

Monitoring BBD community profiles after such deliberate infection of different coral species would likely yield interesting insights in the role of BBD community bacteria.

We showed that at least two very closely related genotypes occurred in the BBD mats, and that their distribution could be revealed by using a specifically designed T-RFLP analysis. The distribution of these genotypes could suggest species- specific interactions, with one genotype infecting *C. natans* and *D. strigosa*, and the other all investigated species except for *C. natans* and *G. ventalina*. However, the presence of both strains on one *D. strigosa* sample (Fig. 3) and the lack of sufficient replicates for most infected corals make such an assumption highly hypothetical. The possibility to differentiate between closely related cyanobacteria as shown here does not have to be exhaustive. It was based on sequence analysis of the clones of only two BBD samples and it is possible that inclusion of more BBD samples would reveal additional genotypic variation. In addition, ecotypic variation may be missed because it may not be reflected in

sequence variation in the rRNA gene (19). The ecological significance of the observed genotypes could only be derived from thorough studies of multiple different BBDs, from population shifts after interspecific infections, or from ecophysiological studies of isolated strains. The latter option has become realizable by the recent isolation of pure cultures from the dominant BBD cyanobacteria by Sussman *et al.* (39). These authors obtained black and red strains of filamentous cyanobacteria with identical 16S rRNA sequences. The role of these ecotypes could be derived from ecophysiological studies in combination with studies of their distribution between corals and within BBD mats, which may be achieved by differentiation by using rRNA-ITS sequences.

Microbial community diversity of black band disease mats

The extent of the overall microbial diversity in BBD mats yielded contrasting claims in previous studies. DGGE profiles showed clear differences in the microbial diversity in BBD mats obtained from *D. strigosa*, *M. annularis* and *C. natans* (10). However, based on T-RFLP profiles, the microbial communities of BBD mats from 9 *D. strigosa* replicates and 1 *M. annularis* sample were reported to be identical (14), but no information of the extent of variation between these samples was presented in that report. In addition, the bacterial composition of the BBD mat was claimed to depend on the dominant cyanobacterium in BBD mats. The analysis of our samples as pictured by the ordinations of Fig 2B and C showed a significant variation between samples, especially in the relative abundances of particular bacterial groups (Tables 1 and 2). Most T-RFs were found to be present in most coral samples, but their relative abundances varied considerably. Hence, in contrast to the earlier report, clear differences were observed between BBD associated microbial communities, and these differences were significant between several species. In congruence with the earlier finding that the dominant cyanobacterium dictates the community composition, the *G. ventalina* BBD mat microbial communities (dominated by different cyanobacteria) differed clearly from those from other coral species (Fig. 2B and 2C). However, BBD mat communities from other coral species could also be significantly different, and the

differences between some replicate samples of the same species were not smaller than the differences between coral species (Fig 2B and 2C). Particularly the NMDS ordinations of Fig 2C where the dominant cyanobacterial T-RFs were excluded from analysis, showed that the microbial communities in the *G. ventalina* mat were not markedly more distinct than those from the other coral species and replicates. The reason for the contrasting findings in both studies is unknown. Although the dominant BBD cyanobacteria other than CD1C11 differed between both studies, the genotypes in the previous study (PNG and BBT) were more similar to CD1C11 than the genotype from the current study (SFDC).

Microbes associated with BBD mats and with healthy coral tissue

The cyanobacterial genotype CD1C11 dominated most BBD profiles, but its relative abundance varied considerable between samples. This genotype has been detected before in clone libraries (Table 3), but previous studies of its abundance in BBD mats and healthy tissue samples have yielded contrasting records. Using DGGE, Cooney et al (10) found a clear but variable abundance of this genotype in BBD mats, but did not detect it in healthy coral tissues. Frias-Lopez et al (14) detected this strain as a minor proportion in their T-RFLP community profiles of BBD mats, but found it to be dominant in the same samples by using MPN-PCR. They also reported the absence of this strain from healthy coral tisues (10, 13). In contrast, we detected genotype CD1C11 by T-RFLP in all our samples of similar origin (Table 1). Moreover, Klaus et al (24) consistently detected this genotype in 12 healthy *M. annularis* colonies sampled from shallow water. *P. corallyticum* has been identified by microscopy in sediment-filled depressions on the coral surface (32). The reasons for these differences between analyses are unknown. Since replicate samples were analyzed in all these studies, the differences are unlikely due to atypical samples. There was limited annual variation between the studies, but some of the coral species and sampling locations were the same. Another possibility is that technical differences in DNA extraction, PCR or T-RFLP could have resulted in the observed differences between these studies.

The variable abundance of the CD1C11 genotype in some of our BBD samples (e.g. *C. natans* or *D. strigosa* replicates in Table 1) could indicate a non-essential role for the corresponding cyanobacterium. But it is equally possible that different abundances of these cyanobacteria represented BBD mats of different activity, for example at a different stage of infection. This option could be studied by a comparison of BBD mats at different infection stages or moving at different speeds. Likewise, the presence of the dominant BBD cyanobacterium in the microbial communities associated with healthy coral tissues could indicate that this organism can be a normal constituent of a healthy coral and is not specifically associated with infection. On the other hand, it could also mean that the sampled tissue is in the initial stage of disease and will soon be overrun by BBD.

Some T-RFs were found to be more abundant in BBD and DS compared to HT and HC samples samples (Table 2). These organisms are therefore more likely to have an essential role in disease. This was most evident for the species of *Rhodobacteraceae*, *Vibrionaceae*, *Bacteriodetes* and *Desulfovibrionaceae* that were identified (Table 3).

The *Rhodobactereaceal* genotype was especially interesting in that its abundance was higher in BB and DS samples compared to HT and HC samples in the samples from most coral species, including the *G. ventalina* (Table 2). This genotype was 98% similar to the *α-proteobacterial* genotype that had been identified in BBD mats before (10) and was related to the aetological agent of Juvenile Oyster Disease by these authors.

Vibrio species have been implicated in many marine diseases including coral diseases (8, 38, 41). Several of our clone library sequences from BBD mats were 99% similar to *Vibrio* strains that induced yellow band disease in *M. annularis* colonies (8). Other *Vibrio* sequences had a high similarity (97-98%) with *V. shilonii* and *V. coralliilyticus* strains which have been shown to cause heat-dependent coral bleaching in corals (38). In most studies of coral associated microbes, Vibrios were not recognized as a significant component of BBD mats (10, 15) or healthy coral tissue (10, 15, 35, 36). Recently however, members of the *Vibrionaceae* were shown to constitute

a considerable proportion (up to 38% of clone library sequences) of the microbial community of healthy corals (6). Also in our samples, Vibrios constituted a significant yet variable fraction of the microbial communities. They were relatively more abundant in the BBD and DS samples from some species (e.g. *C. natans* and *M. meandrina*), but on other species they were equally present in healthy coral tissues (Table 2). Many Vibrio spp. have been shown to be opportunistic pathogens which are present on the surfaces of marine species but are not toxic until triggered by various stress factors (9). Possibly, the *Vibrios* associated with corals are normal components of the healthy coral microbiota, with environmental triggers such as increased temperature switching on virulence factors to allow infection (38).

Bacteroidetes T-RFs were more abundant in the BBD and DS samples compared to HT and HC samples. Although the characteristic H-96 and M-91 T-RFs were also relatively abundant in the healthy coral samples from *M. annularis* and *M. faveolata*, the Rsa digests were not detected in these samples. The corresponding clone library sequences were 98% similar to uncultured *Bacteroidetes* identified in BBD samples before (Table 3).

Other T-RFs identified in BBD samples corresponded to clone library sequences from strictly anaerobic and sulfate reducing *Desulfovibrio* and *Desulfobacter* species. These were previously identified in the anoxic microenvironment created by BBD by microscopy (16) and in clone libraries (10, 15). One genotype was identified as an important components of BBD mats as well as healthy coral tissue (14). In our samples, only few clones were encountered, and the organisms seemed rare based on the T-RFLP profiles. However, a confident estimate of the abundance of these genotypes was difficult to make since the Hha T-RF (96 or 98) is shared with *Bacteroidetes* which were abundant in BBD mats, and the Msp T-RF (166) with Corynebacteriaceae which were abundant on some healthy tissues. The characteristic Rsa T-RFs from 492 and 497 bp were very low

Differences in microbes associated with healthy tissues of infected and non-infected corals

Differences in the abundances of bacteria associated with healthy tissues of infected and non-infected colonies could reveal a role of these bacteria in disease. When comparing microbial community DGGE profiles from *M. annularis* coral tissue infected with white band disease (WBD) to that of non-infected remote colonies, Pantos et al (29) claimed to have found such differences. Our community profiles from *M. annularis* and from *M. faveolata* clearly showed a much higher relative abundance of the CD1C11 genotype in healthy tissues of infected colonies compared to non-infected colonies (Table 1). The virtual absence of the CD1C11 cyanobacteria from these healthy corals, and their absence from healthy coral tissues of (infected as well as not-infected) *C. natans* and *M. meandrites*, could indicate that some corals actively keep out potential pathogens. The lower incidence of BBD in these coral species would then suggest that keeping the colony tissue devoid of CD1C11 cyanobacteria may prevent BBD infection.

Besides the CD1C11 genotype T-RFs, T-RFs H-211 and M-505 were more abundant in the HC samples compared to the HT samples from the same coral species (Table 2). The corresponding organisms could be normally associated with healthy corals and their lower abundance could be the cause or the result of an infection. Clones retrieved from healthy *M. annularis* clones corresponded to these T-RFs and matched exactly with environmental sequences retrieved previously from *M. annularis* colonies and classified as *Cyanobacteria* (Table 3). These genotypes could be derived from plastids which would point to a relatively lower abundance of these plastids, likely from the symbiotic *Symbiodinium*, in the healthy tissues of infected coral colonies (compared to non-infected coral colonies).

Several T-RFs in healthy tissues samples from *M. meandrina* and *C. natans* colonies (H-211, M-128, M-423, M-486, R647) corresponded to γ-proteobacteria (Table 3), some of which detected previously on healthy tissues obtained from Pacific corals. The presence of unique ribotypes in healthy tissue (e.g. H-85, H-91, H-715, M-145, M-452, R-700, R-786) samples of particular corals underscores the findings of various authors that a coral-specific microbial community lives associated in or on the coral mucus (15, 35, 36). However, the variable abundance between

1 replicate corals of some very abundant T-RFs identified in this study does not suggest an essential
2 role for these particular organims.

REFERENCES

1. **Altschul, S. F., T. L. Madden, A. A. Schaffer, J. H. Zhang, Z. Zhang, W. Miller, and D. J. Lipman.** 1997. Gapped BLAST and PSI-BLAST: a new generation of protein database search programs. Nucleic Acids Research **25:**3389-3402.

2. **Aronson, R. B., and W. F. Precht.** 2001. White-band disease and the changing face of Caribbean coral reefs. Hydrobiologia **460:**25-38.

3. **Ashen, J. B., and L. J. Goff.** 2000. Molecular and ecological evidence for species specificity and coevolution in a group of marine algal-bacterial symbioses. Applied and Environmental Microbiology **66:**3024-3030.

4. **Blackwood, C. B., T. Marsh, S. H. Kim, and E. A. Paul.** 2003. Terminal restriction fragment length polymorphism data analysis for quantitative comparison of microbial communities. Applied and Environmental Microbiology **69:**926-932.

5. **Borger, J. L.** 2003. Three scleractinian coral diseases in Dominica, West Indies: distribution, infection patterns and contribution to coral tissue mortality. Revista De Biologia Tropical **51:**25-38.

6. **Bourne, D. G., and C. B. Munn.** 2005. Diversity of bacteria associated with the coral Pocillopora damicornis from the Great Barrier Reef. Environmental Microbiology **7:**1162-1174.

7. **Carlton, R. G., and L. L. Richardson.** 1995. Oxygen and Sulfide Dynamics in a Horizontally Migrating Cyanobacterial Mat - Black Band Disease of Corals. Fems Microbiology Ecology **18:**155-162.

8. **Cervino, J. M., R. L. Hayes, S. W. Polson, S. C. Polson, T. J. Goreau, R. J. Martinez, and G. W. Smith.** 2004. Relationship of Vibrio species infection and elevated temperatures to yellow blotch/band disease in Caribbean corals. Applied and Environmental Microbiology **70:**6855-6864.

9. **Colwell, R. R.** 1996. Global climate and infectious disease: The cholera paradigm. Science **274:**2025-2031.

10. **Cooney, R. P., O. Pantos, M. D. A. Le Tissier, M. R. Barer, A. G. O'Donnell, and J. C. Bythell.** 2002. Characterization of the bacterial consortium associated with black band disease in coral using molecular microbiological techniques. Environmental Microbiology **4:**401-413.

11. **Edmunds, P. J.** 1991. Extent and Effect of Black Band Disease on a Caribbean Reef. Coral Reefs **10:**161-165.

12. **Ferris, M. J., M. Kuhl, A. Wieland, and D. M. Ward.** 2003. Cyanobacterial ecotypes in different optical microenvironments of a 68 degrees C hot sring mat community revealed by 16S-23S rRNA internal transcribed spacer region variation. Applied and Environmental Microbiology **69:**2893-2898.

13. **Frias-Lopez, J., G. T. Bonheyo, Q. S. Jin, and B. W. Fouke.** 2003. Cyanobacteria associated with coral black band disease in Caribbean and Indo-Pacific Reefs. Applied and Environmental Microbiology **69:**2409-2413.

14. **Frias-Lopez, J., J. S. Klaus, G. T. Bonheyo, and B. W. Fouke.** 2004. Bacterial community associated with black band disease in corals. Applied and Environmental Microbiology **70:**5955-5962.

15. **Frias-Lopez, J., A. L. Zerkle, G. T. Bonheyo, and B. W. Fouke.** 2002. Partitioning of bacterial communities between seawater and healthy, black band diseased, and dead coral surfaces. Applied and Environmental Microbiology **68:**2214-2228.

16. **Garrett, P., and H. Ducklow.** 1975. Coral diseases in Bermuda. Nature **253:**349-350.

17. **Green, E. P., and A. W. Bruckner.** 2000. The significance of coral disease epizootiology for coral reef conservation. Biological Conservation **96:**347-361.

18. **Griffin, S. P.** 1998. The effects of sunlight on the progression of Black Band Disease. Revista De Biologia Tropical **46:**175-179.

19. **Hahn, M. W., and M. Pockl.** 2005. Ecotypes of planktonic Actinobacteria with identical 16S rRNA genes adapted to thermal niches in temperate, subtropical, and tropical freshwater habitats. Applied and Environmental Microbiology **71:**766-773.

20. **Hughes, T. P., A. H. Baird, D. R. Bellwood, M. Card, S. R. Connolly, C. Folke, R. Grosberg, O. Hoegh-Guldberg, J. B. C. Jackson, J. Kleypas, J. M. Lough, P. Marshall, M. Nystrom, S. R. Palumbi, J. M. Pandolfi, B. Rosen, and J. Roughgarden.** 2003. Climate change, human impacts, and the resilience of coral reefs. Science **301:**929-933.

21. **Janse, I., W. E. A. Kardinaal, M. Meima, J. Fastner, P. M. Visser, and G. Zwart.** 2004. Toxic and nontoxic microcystis colonies in natural populations can be differentiated on the basis of rRNA gene internal transcribed spacer diversity. Applied and Environmental Microbiology **70:**3979-3987.

22. **Janse, I., M. Meima, W. E. A. Kardinaal, and G. Zwart.** 2003. High-resolution differentiation of cyanobacteria by using rRNA-internal transcribed spacer denaturing gradient gel electrophoresis. Applied and Environmental Microbiology **69:**6634-6643.

23. **Klaus, J. S., J. Frias-Lopez, G. T. Bonheyo, J. M. Heikoop, and B. W. Fouke.** 2005. Bacterial communities inhabiting the healthy tissues of two Caribbean reef corals: interspecific and spatial variation. Coral Reefs **24:**129-137.

24. **Klaus, J. S., I. Janse, and B. W. Fouke.** 2005. Coral Microbial Communities, Zooxanthellae, and Mucus along Gradients of Seawater Depth and Coastal Pollution. submitted to Environmental Microbiology.

25. **Knowlton, N., and F. Rohwer.** 2003. Multispecies microbial mutualisms on coral reefs: The host as a habitat. American Naturalist **162:**S51-S62.

26. **Kuta, K. G., and L. L. Richardson.** 1996. Abundance and distribution of black band disease on coral reefs in the northern Florida Keys. Coral Reefs **15:**219-223.

27. **Liu, W. T., T. L. Marsh, H. Cheng, and L. J. Forney.** 1997. Characterization of microbial diversity by determining terminal restriction fragment length polymorphisms of genes encoding 16S rRNA. Applied and Environmental Microbiology **63:**4516-4522.

28. **Nomura, M., R. Gourse, and G. Baughman.** 1984. Regulation of the Synthesis of Ribosomes and Ribosomal Components. Annual Review of Biochemistry **53:**75-117.

29. **Pantos, O., R. P. Cooney, M. D. A. Le Tissier, M. R. Barer, A. G. O'Donnell, and J. C. Bythell.** 2003. The bacterial ecology of a plague-like disease affecting the Caribbean coral Montastrea annularis. Environmental Microbiology **5:**370-382.

30. **Porter, J. W., P. Dustan, W. C. Jaap, K. L. Patterson, V. Kosmynin, O. W. Meier, M. E. Patterson, and M. Parsons.** 2001. Patterns of spread of coral disease in the Florida Keys. Hydrobiologia **460:**1-24.

31. **Richardson, L. L.** 1998. Coral diseases: what is really known? Trends in Ecology & Evolution **13:**438-443.

32. **Richardson, L. L.** 1997. Occurrence of the black band disease cyanobacterium on healthy corals of the Florida Keys. Bulletin of Marine Science **61:**485-490.

33. **Ridley, C. P., P. R. Bergquist, M. K. Harper, D. J. Faulkner, J. N. A. Hooper, and M. G. Haygood.** 2005. Speciation and Biosynthetic variation in four dictyoceratid sponges and their cyanobacterial symbiont, oscillatoria spongeliae. Chemistry & Biology **12:**397-406.

34. **Rocap, G., D. L. Distel, J. B. Waterbury, and S. W. Chisholm.** 2002. Resolution of Prochlorococcus and Synechococcus ecotypes by using 16S-23S ribosomal DNA internal transcribed spacer sequences. Applied and Environmental Microbiology **68:**1180-1191.

35. **Rohwer, F., M. Breitbart, J. Jara, F. Azam, and N. Knowlton.** 2001. Diversity of bacteria associated with the Caribbean coral Montastraea franksi. Coral Reefs **20:**85-91.

36. **Rohwer, F., V. Seguritan, F. Azam, and N. Knowlton.** 2002. Diversity and distribution of coral-associated bacteria. Marine Ecology-Progress Series **243:**1-10.

37. **Rosenberg, E., and Y. Ben-Haim.** 2002. Microbial diseases of corals and global warming. Environmental Microbiology **4:**318-326.

38. **Rosenberg, E., and L. Falkovitz.** 2004. The Vibrio shiloi/Oculina patagonica model system of coral bleaching. Annual Review of Microbiology **58:**143-159.

39. **Sussman, M., D. G. Bourne, and B. L. Willis.** 2006. A single cyanobacterial ribotype is associated with both red and black bands on diseased corals from Palau. Diseases of Aquatic Organisms **69:**111-118.

40. **Sutherland, K. P., J. W. Porter, and C. Torres.** 2004. Disease and immunity in Caribbean and Indo-Pacific zooxanthellate corals. Marine Ecology-Progress Series **266:**273-302.

41. **Thompson, J. R., M. A. Randa, L. A. Marcelino, A. Tomita-Mitchell, E. Lim, and M. F. Polz.** 2004. Diversity and dynamics of a north Atlantic coastal Vibrio community. Applied and Environmental Microbiology **70:**4103-4110.

FIG 1

A. Black band disease infecting *Diploria strigosa*

B. Black band disease infecting *Montastraea annularis*

C. Black band disease infecting *Meandrina meandrites*

D. Black band disease infecting *Gorgonia ventalina*

E. Infection of *M. faveolata* with BBD mat flakes derived from *Diploria strigosa* (upper left), *Montastraea faveolata* (lower left), *Montastraea cavernosa* (upper right), *Colpophyllia natans* (lower right). A control needle (middle) contained no BBD flake

FIG 2

A. NMDS ordination of Cyanobacterial communities dominating the BBD mats from the coral species *Colpophyllia natans* (Cn), *Diploria strigosa* (Ds), *Montastraea annularis* (Ma), *Montastraea cavernosa* (Mc), *Montastraea faveolata* (Mf), *Meandrina meandrites* (Mm) and *Gorgonia ventalina* (Gv). Numbers following species code represent replicates. Ordination was based on the Bray-Curtis similarity coefficients generated from T-RFLP profiles from dual-labeled cyanobacterial rRNA-ITS amplicons digested with 7 different enzymes.

B. NMDS ordination of bacterial communities dominating the BBD mats from the coral species *Colpophyllia natans* (Cn), *Diploria strigosa* (Ds), *Montastraea annularis* (Ma), *Montastraea cavernosa* (Mc), *Montastraea faveolata* (Mf), *Meandrina meandrites* (Mm) *and Gorgonia ventalina* (Gv). Numbers following species code represent replicates. Gva is a BBD flake sample and Gvb is a sample from diseased tissue. Ordination was based on the Bray-Curtis similarity coefficients generated from T-RFLP profiles from 16S rRNA amplicons digested with 3 different enzymes.

C. NMDS ordination based on the same T-RFs as 2B, with the exclusion of the Cyanobacterial T-RFs

FIG 3

Section of T-RFLP profiles obtained by EarI digestion of amplified, dual-labeled Cyanobacterial rRNA-ITS. Shown are the fragments that include the HEX labeled LB23R reverse primer from BBD mats infecting *C. natans, D. strigosa* and *M. cavernosa*.

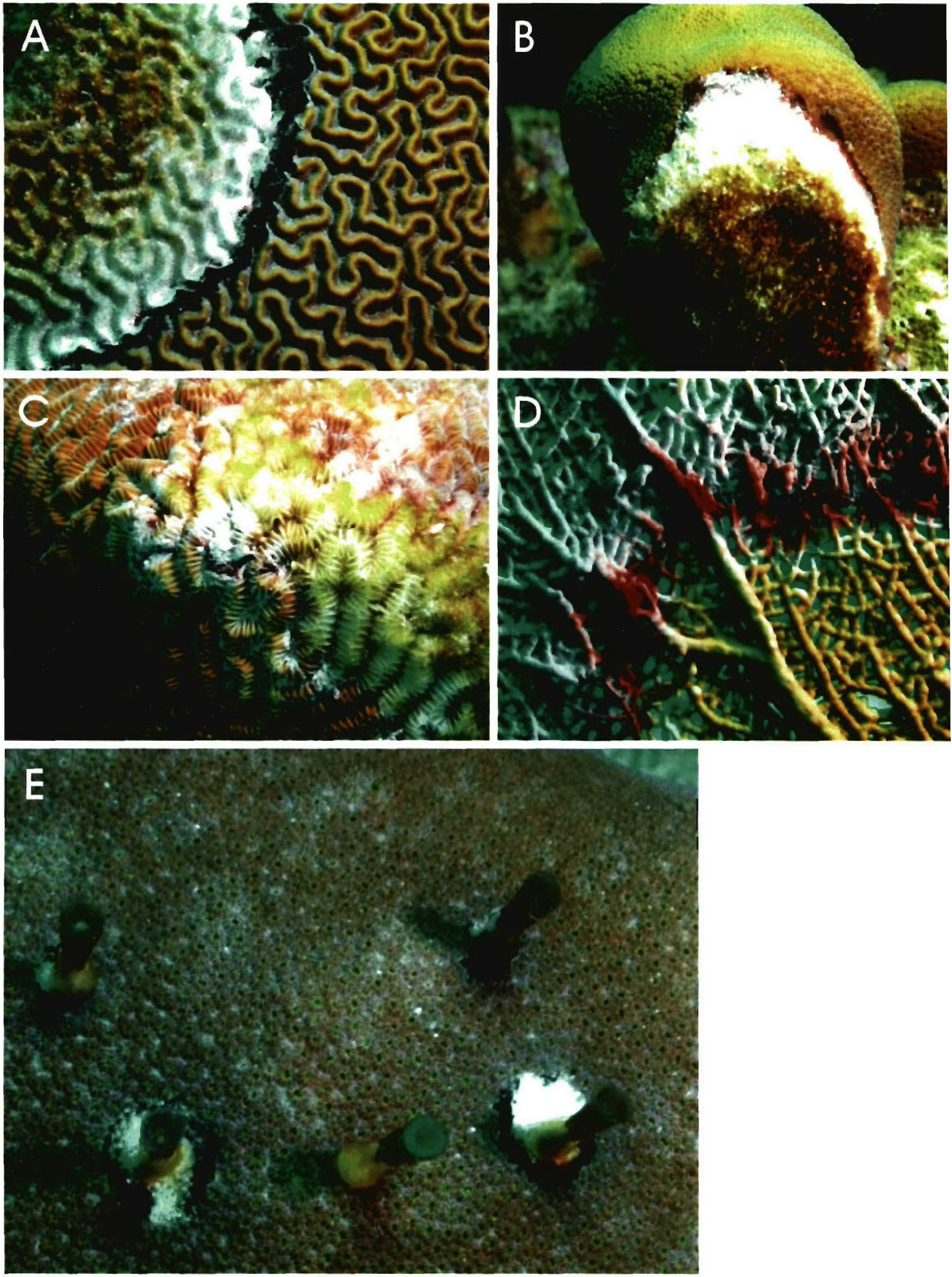
A
B
C
D
E

Fig 2A

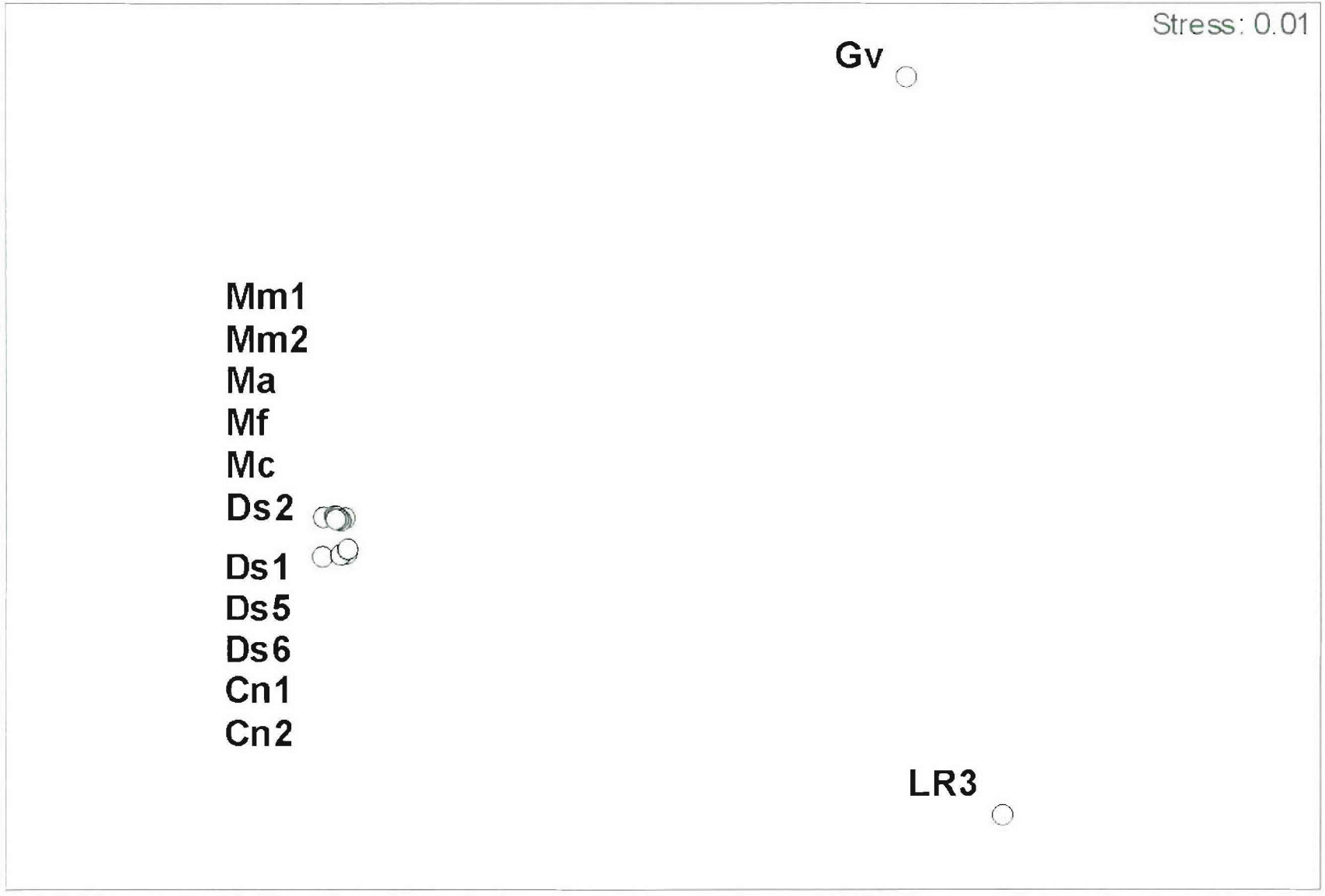

Fig 2B

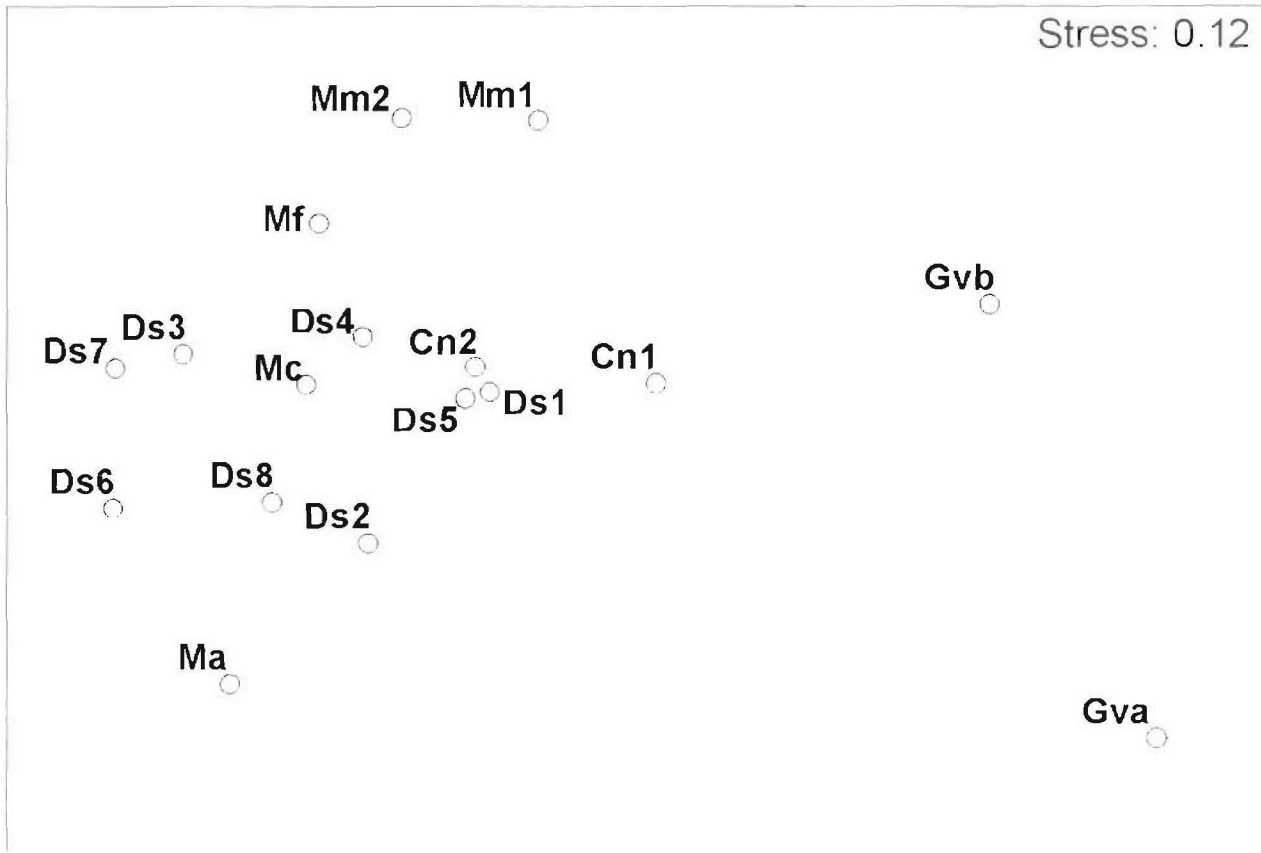
Stress: 0.12
Mm2
Mm1
Mf
Gvb
Ds3
Ds4
Ds7
Cn2
Cn1
Mc
Ds1
Ds5
Ds6
Ds8
Ds2
Ma
Gva

Fig 2C

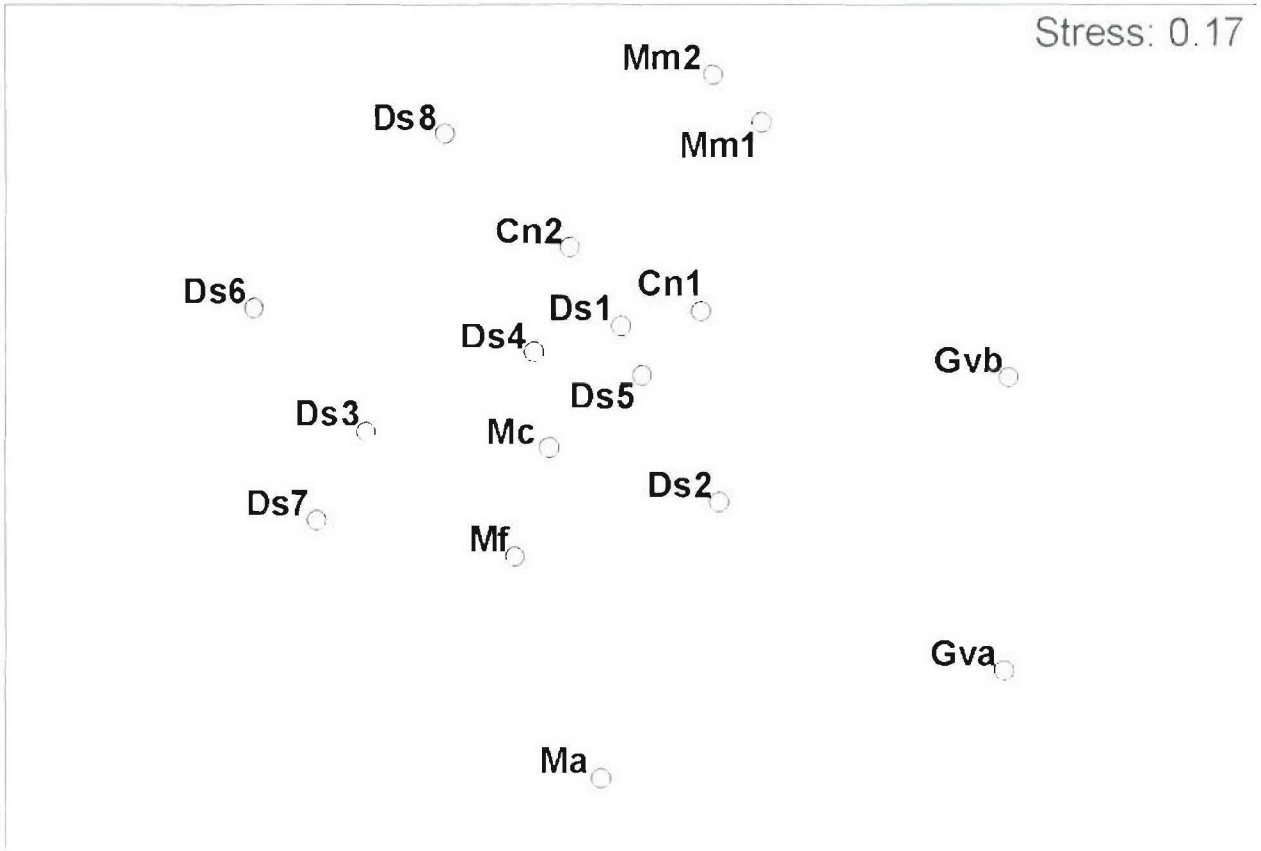
Stress: 0.17
Mm2
Ds8
Mm1
Cn2
Ds6
Cn1
Ds1
Ds4
Gvb
Ds5
Ds3
Mc
Ds2
Ds7
Mf
Gva
Ma

C. natans

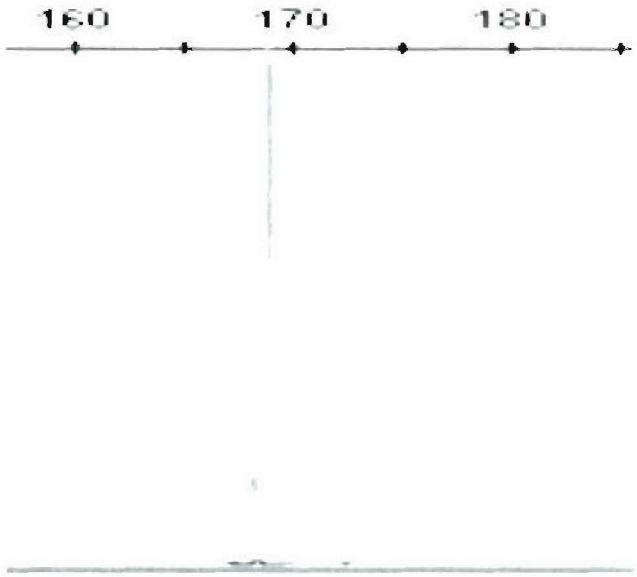

D. strigosa

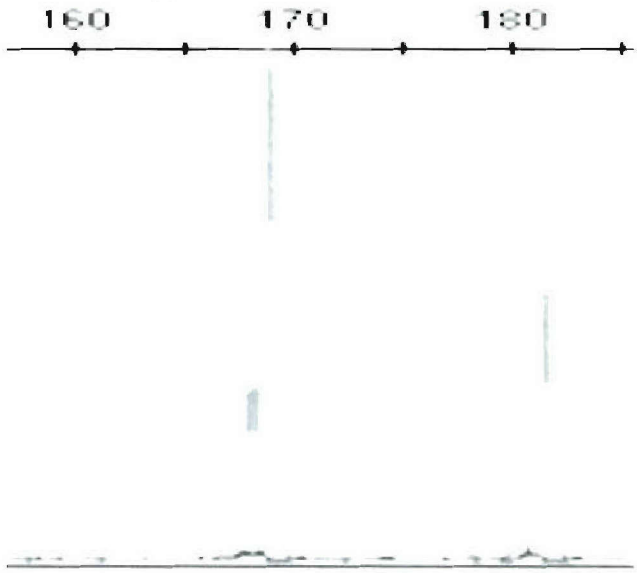

M. cavernosa

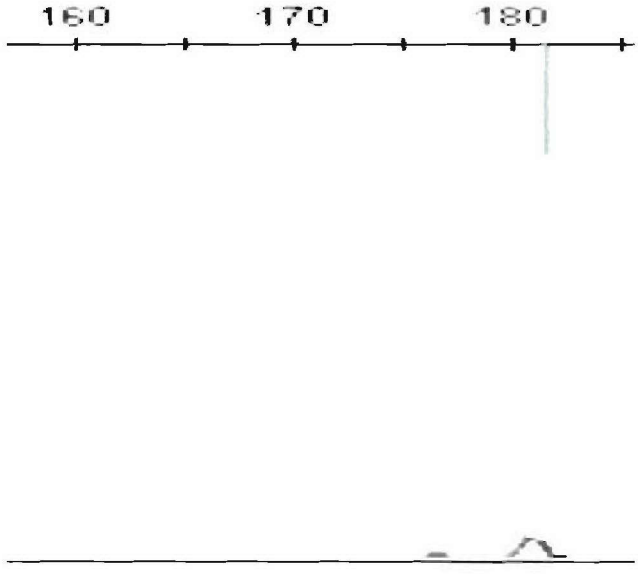

Table 1: Relative abundances of dominant cyanobacteria in the microbial communities of black band disease mats and associated with healthy coral tissues. Values separated by forward slashes are percent peak area of T-RFs in T-RFLP profiles generated with HhaI, MspI and RsaI, respectively. BBD= black band disease mat, HC= healthy tissue infected colony, HT= healthy tissue non-infected remote colony, DS= dead skeleton. nd= not determined

genotype	Coral sample[a]	BBD	HT	HC	DS
CD1C11 (H-671/M-152/R-231)	*C. natans* (1)	2/3/3	0/0/0	1/3/2	0/0/0
	C. natans (2)	20/19/28	0/0/0	0/1/1	5/1/0
	D. strigosa (1)	15/16/21	24/35/44	15/30/48	2/0/1
	D. strigosa (2)	45/43/58	28/30/40	nd	nd
	D. strigosa (3)	38/61/80	20/39/49	nd	nd
	D. strigosa (4)	23/47/57	nd	nd	nd
	D. strigosa (5)	17/35/46	nd	nd	nd
	D. strigosa (6)	26/54/64	nd	nd	nd
	D. strigosa (7)	17/68/78	nd	nd	nd
	D. strigosa (8)	45/48/58	nd	nd	nd
	M. annularis	70/62/70	57/30/42	2/3/0	2/2/1
	M. cavernosa	38/50/64	78/75/89	85/83/96	5/0/0
	M. faveolata	24/30/46	73/71/81	2/1/3	4/0/0
	M. meandrites (1)	10/10/16	0/1/0	0/0/0	0/1/1
	M. meandrites (2)	19/20/28	0/0/0	1/1/0	0/0/0
	G. ventalina	3/0/0	13/22/0	nd	nd
SFDC1 (H-231/M-495/R-425)	*G. ventalina*	9/22/13	0/6/0		
SFDC2 (H-669/M-149/R-190)	*G. ventalina*	17/12/10	7/2/1		

[a]Number between brackets is replicate number

Table 2. Relative abundance of selected T-RFs as measured by % peak area. Only shown are T-RFs that were relatively abundant in at least some coral samples or those that dominated a particular sample. Values from replicate samples are separated by dashes. For *D. strigosa*, the two most different replicates are presented. Empty cells means zero. BB= Black band. HT= Healthy tissue, HT= Healthy colony, DS= Dead Skeleton

	C. natans (1)-(2)				*D. strigosa* (2)-(1)				*M. annularis*				*M. cavernosa*				*M. faveolata*				*M. meandrina* (1)-(2)				*G.ventalina*	
T-RF	**BB**	**HT**	**HC**	**DS**	**BB**	**HT**	**HC**	**DS**	**BB**	**HT**	**HC**	**DS**	**BB**	**HT**	**HC**	**DS**	**BB**	**HT**	**HC**	**DS**	**BB**	**HT**	**HC**	**DS**	**BB**	**HT2**
H-61	11.2-10	0.8-0.6	3.5-3.5	9.2-11	1.8-18	9.6-8.4	6.7	12.2	2.2	1.2	6.3	7.5	7.1	2.8	2.0	20.3	9.4	2.2	0.6	12.1	18-18.8	0.8-1.2	2 1-0.6	15.8-23.9	9.9	12.0
H-82	1-0.3		0 9-1.2	0.4-0.5	0-1 1	0-1.9	1.4	0.8	0.8			1.4	1 6	0.5	0.6	1 5	21.0	0.3			1 8-2	0.5-1.7	0.3-3	0.9-1 7	2.8	2.4
H-85			25.6-9.0										0.3											0.2-0		
H-91			0-36.0		0-0.2		0.9																		0.1	
H-96	5.3-2.5	1-0	1.7-0.8	1.8-0.6	6-8.7	1.7-3.1	2.9	1.5	0.6	0.4	18.2	9.7	6.6	1.6	0.8	2.6	4.1	1.4	9 4	12.3	3.4-5.6	0-0.9		1.1-10.2	7.4	4.5
H-98	3.6-5.7		1.8-0.2	0.5-0.3	3.5-5.2	4.9-8.3	8.2	1.7	0.5		2.7	4.8	7.1	1.0	1.6	2.3	6.8	0.4	0.4		5.8-5.5		0.3-0	3.6-2.2		4.0
H-109		0-11 8				0-0.6																9.6-5.6	5.7-7.1			
H-211	2.6-1.8	8.3-1.9	24.5-15.4	5.8-0.7	0-1 6	2.3-3.8	5.0		1.0		57.5	1.1	2.3		0.5		1.7		7 1		3.9-2.3	2.9-6.5	15.1-1.6	0-1.8	8.5	5.3
H-231				0.1-0									1 3	0.6	0.4		0.5	0.3			2-0.5			0-0.2	8.8	
H-385	7.7-17.3			0-0 1	0-6.4	5.5-2.6	9.0			0 6		27.0	4.8	1.4	0.8			1.2			24 9-9 9			0.3-0.8	0.8	1.6
H-571	1.2-0.8	26.4-0	1 2-0	0-0.2	0-0.5	0.8-1 1						0 1												1.1-0.6	0 7	
H-669																									16.8	7
H-671	1.7-20.1		2.4-0.1	0.2-5.4	45.1-15.4	27.6-24 1	15.1	1 7	69.8	56.7	2.4	1.8	37.1	79.6	84.7	5.0	23.8	72.8	2.1	4.2	10-18.7		0-1.5	0-0.5	2.9	12.6
H-715		0-60.5																				64.1-57 8	51 2-80			
M-91	4.6-2.2	1.3-0	0.7-0	4.9-1.5	2.9-4 9	1.7-2.6	3.2	3 1	0.7		16.1	10.6	4.6	1.4	0.7	1 8	1.7	3	3.9	1.6	2.7-4 9	0-1.2		1.7-2 2	3.6	7
M-127	0.6-0	46.9-1 1	13.5-17.6		7.6-0	0.7-1 9	1.3		1.6		1.2	0.4	2	0.6			0 7	0 9				0 9-0	1-0		4.8	3 7
M-145	0-0.6	0-25.2		2.7-1.2		0-0.4		1.5				0.5				0.6					0.9-0	24.5-16.4	27.1-7	1.3-5.3	1	3.8
M-149																									11.6	2.4
M-152	2 7-19		2.5-3.5	0-0.8	42.6-15.7	29.4-35	30.2		61.5	29.4	3.2	1.5	50.3	75.4	82.6		30.3	70 5	0.6		10.4-19 5	0.5-0	0-0.7	0 5-0	0.5	22.2
M-164	27.3-7.1			0-1 5	3.4-6.5	3 9-0	6.6	0 6	0.7			6.3	1.3				1.1	0.6			0.4-0				1 9	
M-166	1 1-0.5			0-0.7	4.9-3.3	0-1.5			0.6		2		2.7	0.6		1.1	2.6	1.1		7.2	0.5-0			0-8.3	1 3	
M-181		5.9-0											1 4				0.5	0.8	20.6		2-0.5					
M-221	3.2-6.9			0-4.6	0-10.1	1.4-2.3	1 6		0.7				2.5	1.3	0.8		2 3	2.1			1 7-0.6			0.4-0		
M-247			4.6-1.8																25 4							
M-439	16.4-17.3	1.6-0	2 5-1.4	19.6-27 7	2.3-23.5	15.8-14.1	10.4	29.7	9.8		7.7	7.7	10.6	6	3.2	20 1	39.4	6.5		7 6	22.6-27.4	0.5-1 7		19.5-41.5	10.3	6.1
M-452																						58 1-49.9	0-74.2	1 3-0		
M-486	2.4-1.4				4.7-6.5				3.6			0.6	2.5	1.2			1.1	2			0.6-0				3.6	8 3
M-495	5.3-3.1	13.5-0.8	5-2.3	5.3-1.4	0-4.1	1.7-4 3	7.9	5.2				12.1				4.8	2.5		1.8		7-2.8			5.7-3.3	21.3	5.5
M-505		9.4-0.9	13 2-6.3	17.3-0 9							55.1	0.8							2 1	5.7		2-4 1	13.8-0			
M-507	12.6-22 1	5.2-1.1		2.8-4.4	18.6-9.9	9.4-3.1	12.8		2			32.6	6.4	2.4	1.4		0.8	2.9			32-12.1			4.3-2.4	1.8	3.7
R-58	1-0.7	0 9-52.4	4.3-0.9	3.5-1 5	0-0.4	1.6-0	1 6	3.1	2.4			0.9									2.2-1.3	26-17.3	71.4-11 1	3.3-1	0.6	4 1
R-109	3 7-1 5			0.8-1	0-5.9	3.9-5.5	4.4	0 7	0.5			0.6				2 9	1.4				2 1-2.3			0.6-2	1.2	1.3
R-119	2.3-6.8	0.6-0	4 5-0	3.1-4.5	2-2.5	0-3	1.7	4.5	1.4			2.5				3.4	1 6				6.3-10.2			4.6-3.1	1 6	
R-131	1.6-1.3	1.4-0	13.6-9.2	4 6-0.8	0-0.9	0-1.5		2.3				14							12.9						0.5	
R-134											60															
R-190																									10.0	1 3

R-231	3.4-27.7		2.1-0.5	0.4-0	57.9-21.1	39.9-43.9	48	0.5	69.5	42.4		1.3	64.1	89.4	95.5		46.3	80.8	2.6		15.6-28.2			0.7-0			
R-302						2.9-2	2						1.7				5.4	1			4.9-14.5						
R-313	7.9-4			1.5-0	1.8-6	1.3-1.5	2.4	1.2	1.3			1.6	5.2	0.8		2.4	3.7	1.5			7.8-7.7			1.9-1.3	2.0	4
R-423	5.2-6	0.9-0		9.1-9.3	2.2-10.9	8.3-7.5	5.9	6.9	6.7	9.5	16.4	6.6	9.2	5	3.8	7.7	5.9	8.9		25.6	11.9-8.6			6.4-4.1	2.3	2.2
R-425																									12.8	
R-453	37.8-10.1				0-8.5	10.2-4.9	8.9					0.5	2.2				1.4									1.3
R-462			0-16.6																		0-0.8				1.4	
R-469	5.2-9.1				3.3-14.7	1.4-1.5	1.6		3.6			1.2	5.2				4.1	3			1.1-0				4.8	6.2
R-650	2.3-1.8				3.9-1.1	1-2.5	1.8	0.8	2.1			0.9	1.6				1.6				3.4-2.2			0-1.3	8.8	6.9
R-663	5.1-8.7	1.8-0			7.7-4.6	4.2-1.7	2.6					6.7	3.1					1.1			13.8-3.2				0.9	2.7
R-700																							0-49.9			
R-786		0-34.9																				40.3-20.4	14.5-0			

Table 3: Characterization of clone library sequences. Divison level and Genus level classification, theoretical digests and the similarity to database sequences are presented from selected sequences. H= HhaI, M= MspI, R= RsaI digested.

Division level ID	Genus level ID[a]	T-RF (bp)	Accession #	Examples of most homologous sequences [accession #] [b]
Cyano bacteria	Family 3.1 (91-99%)	H671/M152/R231	XX0000	Uncult. BBD cyanobacterium from St. Croix [AF473936] (98-99%); Uncult. BBD cyanobacterium from Curacao [AY038527] (98-99%); Cultured BBD cyanobacterium from Palau [AY839641] (98-99%)
	Family 4.1 (46%)	H671/M152/R423	XX0000	*Spirulina* sp. [AF091109] (97%)
	Family 4.1 (61-72%)	H211/M505	XX0000	Uncult. *Cyanobacterium* from *M. annularis* [AF544885] (100%)
	Family 2.1 (53%)	H230/M495/R425	XX0000	*Limnothrix redekei* [AJ505943] (91%)
	Family 3.1 (61-97%)	H230/M495/R425	XX0000	*Spirulina* sp. [Y18793, AF091109] (91-95%) *Microcoleus* sp. [X70770] (92%)
	Family 1.1 (63-68%)	H669/M149/R190	XX0000	*Spirulina* sp. [Y18792] (92%) *Cyanothece* sp. [AB067581] (91%)
α-Proteo bacteria	*Rhodobacter aceae*	H61/M439/R109	XX0000	*Rhodobacteriaceae* from marine environments, fish farms (94-99%); Uncult. *α-Proteobacterium* from BBD infected D. strigosa and M. annularis corals [AF473920] (95-98%)
		H61/M439/R423	XX0000	
		H61/M439/R824	XX0000	
		H343/M441/R118	XX0000	
	Methylcyst aceae	H342/M87/R689	XX0000	*Oceanospirillum pusillum* [AB006768] (97%)
		H342/M87/R125	XX0000	Uncult. *α-Proteobacterium* A115-18 from *Acropora palmate* corals [AY323137] (97%)
	Sphingomona Daceae	H82/M150/R422	XX0000	*Erythrobacter* sp. AB012062 (99%); *Erythrobacter vulgaris* from marine invertebrates AY706938 (98%)
	Methylocyst aceae (15-58%)	H90/M447/R126	XX0000	Uncult. *α-Proteobacterium* from deap sea [AY354146] (93%)
		H92/M449/R833	XX0000	Uncult. *α-Proteobacterium* from squid [AJ633974] (95%)
		H92/M121/R836	XX0000	*Kopriimonas byunsanensis* from marine biofilm [DQ167245] (93-95%)
	Methylocyst Aceae (33-72%)	H710/M450/R57	XX0000	Uncult. *α-Proteobacterium* A190-6 from healthy *D. strigosa* and *M. annularis* corals [AF473960] (97-100%)
γ-Proteo bacteria	*Vibrionaceae*	H385/M507/R662	XX0000	*Vibrios* FLG2A [AY770830] (99%) and YB3122 [AY770831] (99%) isolated from yellow band disease; *Vibrio parahaemolyticus* [BA000031] (98%); Uncult. *Vibrios* from coral *Pocillopora damicornis* [AY700621] (98%)
		H385/M507/R439	XX0000	*Vibrio shilonii* [AY911392] (98%) *Vibrio coralllyticus* [AJ440004] (97%)
		H385/M507/R24	XX0000	Uncult. *Vibrios* from coral *Pocillopora damicornis* [AY700621] (97%); *Vibrio parahaemolyticus* clone [AF388387] (98%)
	Oceanospirilla ceae	H211/M493/R647	XX0000	Uncult. *γ- Proteobacterium* from healthy or BBD infected corals [AY038408] (99%)
		H211/M127/R647	XX0000	*Oceanospirillum beijerinckii* [AB006760] (92%)
		H567/M493/R647	XX0000	Uncult. *γ-Proteobacterium* from healthy or BBD infected corals [AY038407] (99%)
		H364/M487/R24	XX0000	Uncult. *Oceanospirillum* sp. [AY664230] (96%)
	Alteromonada ceae (51%)	M146 M486	XX0000	*Alteromonadaceae* and *Colwelliaceae* from marine environments (93-96%); Uncult. bacterium from coral *Pocillopora damicornis* (GBR) [AY700607] (96%)
	Hahellaceae (28-77%)	M127/R650	XX0000	Uncult. bacterium from coral *Pocillopora damicornis* (GBR) [AY700601] (95%)
		H223/M127/R765	XX0000	*Spongiobacter nickelotolerans* from marine sponge [AB205011] (97%)
		M145/R786	XX0000	Uncult. bacterium from salmon gills [AY494615] (97%); Uncult. bacterium from coral *Pocillopora damicornis* (GBR) [AY700600] (95-97%)
	Saccharospiril laceae (29-56%)	M127/R650	XX0000	Uncult. *γ-Proteobacterium* from salmon gills [AY494615] (97%)
		M145/R786	XX0000	
Bacteroide	*Rikenellaceae*	H96/M91/R131	XX0000	[AY580708] Uncult. marine *Bacteroidetes* (99%)

	(73-89%)			[AY038398] Uncult. *Flavobacteriaceae* from BBD sample (98%)
tes	*Flammeovirgaceae* (46-55%) *Flavobacteriaceae* (32-50%)	H96/M91/R312	XX0000	Uncultered *Cytophagales* from estuaries [AY337037] (96%) *Flexibacter aggregans* [AB078042] (94%)
δ-Proteobacteria	*Desulfovibrionaceae*	H96/M164/R492	XX0000	*Desulfovibrio aespoeensis* (94%)
	Desulfobacteraceae	H98/M514/R497	XX0000	*Desulfobacter* sp. [U85476] (94%)
		H98/M166/R497	XX0000	Uncult. *Verrucomicrobia* from the Arctic Ocean [AY028221] (96%)
ε-Proteobacteria	*Campylobacteraceae*	H101/M474/R457	XX0000	*Arcobacter* sp. [AF513455] (94%)
Clostridia	*Peptostreptococcaceae*	M222/R872	XX0000	*Clostridium* sp. from marine sediment [AB196728] (96%)
	Peptostreptococcaceae (85-90%)	H385/M484/R467	XX0000	*Fusibacter paucivorans* [AF050099] (94%)
	Clostridiaceae (45%)	M221/R469	XX0000	Uncult. sapropel bacterium [AJ630153] (95%) Uncult. tidal flat bacterium [AJ786046] (96%)
	Lachnospiraceae (37-48%)l	M221/R469	XX0000	Uncult. *Firmicute* from BBD infected corals [AF473925] (99%)
	Lachnospiraceae (76%)l	H531/M221/R469	XX0000	Uncult. sapropel bacterium [AJ630153] (95%) Uncult. intertidal flat bacterium [AJ786046] (96%)

[a] Displayed between brackets is the confidence of assignment as defined in the RDPII classifier tool if below 100%.

[b] Displayed between brackets is the percentage similarity to database sequences